New Methods for the Construction of Fluorinated Cyclic Amines and Amides

Natalie Charlesworth

Thesis submitted to the University of Nottingham for the degree of Doctor of Philosophy

October 2021

Acknowledgements

Firstly, I would like to thank Prof. Ross Denton for the opportunity to do this PhD and to work on such an interesting project. The support and advice over the years has been hugely appreciated and I would not have been able to achieve this without you. I would also like to thank my industrial supervisor, Mark Graham, for his help and support throughout my PhD. This work would also not be possible without the help of the analytical and technical staff, in particular Kevin Butler for his help with quantitative NMR.

Thanks must also go to the past and present members of the Denton Group who I have had the pleasure of sharing the lab with over the years. Thank you for all the helpful ideas and discussions, you have made these four years so enjoyable. A particular mention must go to Emma Stoll and Nick Atkinson who have been a great support. Working with you has been so much fun and I look forward to hopefully having the opportunity to work with you again in the future.

Finally, I would like to thank my partner Dualtagh who has always supported me with my studies, and even moved to Nottingham with me. We wouldn't be without our two dogs, Diego and Hazel, who bring us so much joy on a daily basis. From their enthusiastic greetings after a day in the lab, to their quiet companionship whilst writing this thesis, you have made the last few years so special.

Abstract

In recent years, photoredox catalysis has emerged as a powerful tool for the synthesis of complex building blocks. Fluorine-containing saturated nitrogen heterocycles are desirable structures in medicinal and biological chemistry, as the incorporation of fluorine can be used to influence key properties of a compound such as conformation, basicity and bioavailability. This thesis explores the utilisation of a photoredox-catalysed cyclisation/hydrogen atom transfer reaction of bromodifluoroethylamines, using a modular, two-step approach.

The first chapter provides an introduction to photoredox catalysis, notable developments in the area and relevant examples from the literature of photoredox-mediated radical cyclisation reactions. Following this, the importance of fluorination in drug discovery is discussed, along with traditional methods for the introduction of the geminal difluoro- group.

The second chapter describes a photoredox radical cyclisation protocol using bromodifluoroethylamines, which are prepared through a three-component coupling. The reaction is applicable to a wide range of alkenyl- and alkynyl amines, and the utility of the products are demonstrated. Mechanistic investigations established the role of the tertiary amine base and the additional hydrogen-atom donor in the reactions. The success of the described approach relies on the strongly electron-withdrawing nature of fluorine, which prevents oxidation of the amine substrates and products under the reaction conditions. This eliminates the need for electron-withdrawing protecting groups on nitrogen and promotes cyclisation.

The third chapter builds on the developed photoredox catalysed cyclisation for the mild and efficient synthesis of γ- and δ-lactams. The protocol is applicable to a range of amide substrates, and a mechanism for the reaction is proposed, supported by computational calculations.

Contents

Contents

Abbreviations

1,4-DCB	1,4-Dichlorobenzene
Ac	Acetyl
Acr	Acridinium
AIBN	Azobisisobutyronitrile
API	Active pharmaceutical ingredient
Ar	Aryl
ATR	Attenuated total reflection
ATRC	Atom transfer radical cyclisation
Bn	Benzyl
Boc	*tert*-Butyloxycarbonyl
bpy	2,2'-Bipyridine
bpz	2,2'-Bipyrazyl
calcd	Calculated
Cz	Carbazole
D	Debye
Da	Dalton
dap	2,9-Bis(*para*-anisyl)-1,10-phenanthroline
DAST	Diethylaminosulfur trifluoride
DCE	1,2-Dichloroethane
dF	2,4-Difluorophenyl
DIPEA	Diisopropylethylamine
DMAP	4-Dimethylaminopyridine
DMF	Dimethylformamide
DMPU	*N,N′*-Dimethylpropyleneurea
dpm	2,2,6,6-Tetramethyl-3,5-heptanedionato
dtbbpy	4,4′-Di-*tert*-butyl-2,2′-dipyridyl
equiv.	Equivalents
ESI	Electrospray ionisation

esp	α,α,α′,α′-Tetramethyl-1,3-benzenedipropionic acid
EWG	Electron withdrawing group
F	Fluorescence
FBDD	Fragment-based drug discovery
FDA	U.S. Food and Drug Administration
gem	Geminal
HAT	Hydrogen atom transfer
HMPA	Hexamethylphosphoramide
HOMO	Highest occupied molecular orbital
HRMS	High resolution mass spectrometry
HTS	High-throughput screening
IP	Intellectual property
IPN	Isophthalonitrile
IR	Infrared
ISC	Intersystem crossing
J	Coupling constant
LC-MS	Liquid chromatography–mass spectrometry
LUMO	Lowest unoccupied molecular orbital
m.p.	Melting point
MeCN	Acetonitrile
Mes	Mesityl
MLCT	Metal-to-ligand charge-transfer
MPTP	1-Methyl-4-phenyl-1,2,3,6-tetrahydropyridine
MW	Molecular weight
NFSI	*N*-Fluorobenzenesulfonimide
NMM	*N*-Methyl morpholine
NMR	Nuclear magnetic resonance
Phe	Phenylalanine
phen	Phenanthroline

PMB	*para*-Methoxybenzyl
PMDETA	*N,N,N′,N″,N‴*-Pentamethyldiethylenetriamine
PMI	Principal moments of inertia
PMP	*para*-Methoxyphenyl
ppm	Parts per million
ppy	2-Phenylpyridine
rt	Room temperature
S	Singlet state
SAR	Structure-activity relationship
SCE	Saturated calomel electrode
SET	Single electron transfer
SOMO	Singly occupied molecular orbital
T	Triplet state
T.S.	Transition state
TBAF	Tetrabutylammonium fluoride
TBS	*tert*-Butyldimethylsilyl
TDFA	Trimethylsilyl fluorosulfonyldifluoroacetate
temp	Temperature
Tf	Triflyl
TFA	Trifluoroacetic acid
THF	Tetrahydrofuran
TMS	Trimethylsilyl
TRIP thiol	Triisopropylsilanethiol
Ts	Tosyl
TTMSS	Tris(trimethylsilyl)silane
V	Volts
V_d	Volume of distribution
τ	Lifetime

Chapter One – Part I: Introduction to Photoredox Catalysis

1.1 Visible-light Photoredox Catalysis

In the last 15 years, photoredox catalysis has received considerable attention in organic synthesis, with publications in the area increasing exponentially since late 2008/ early 2009 when MacMillan, Yoon, and Stephenson all published protocols using visible-light photoredox catalysis.[1–3] Prior to this, the area was largely dominated by the environmental and energy sectors with applications such as the harnessing of solar energy[4] and CO_2 reduction.[5] Today, a wide range of photocatalysts are commercially available, making the field more accessible to organic chemists and contributing to its rapid growth. Complexes based on ruthenium(II) or iridium(III) (with low spin $4d^6$ and $5d^6$ electron configurations respectively) are the most commonly used but photocatalysts can be transition metal complexes, organic dyes or inorganic semiconductors. The key properties of these photocatalysts are that they absorb light in the visible region of the electromagnetic spectrum (380-750 nm) and have sufficiently long-lived excited states to facilitate reaction with a substrate. The combined choice of transition metal and ligand can affect the resultant photoredox properties of the complex, and therefore is a useful tool for tuning and optimising reaction conditions. Popular transition metal complexes include $[Ru(bpy)_3]^{2+}$ and *fac*-$[Ir(ppy)_3]$ bearing polypyridyl ligands, while typical organic dye photocatalysts include xanthenes (eosin Y), acridinium salts (Mes-Acr^+) and cyanoarenes (4CzIPN) (Figure 1.1). Whilst the use of scarce metals such as ruthenium and iridium is an economic consideration, photoredox chemistry is a milder and less toxic approach to radical-based organic transformations. It avoids the use and disposal of toxic tin compounds as well as the addition of thermally sensitive radical initiators such as AIBN.

1.1.1 Photocatalyst Properties

Since 2008, photoredox strategies have been used in a wide variety of chemistry ranging from the construction of new C-C and C-H bonds,[6,7] oxidations and cycloaddition reactions.[8,9] Photocatalysis has also been used by process development chemists to shorten synthesis routes to APIs.[10] The redox potentials of a given photocatalyst determine the type of bonds that can be reduced or oxidised. Irradiation wavelength is also a factor, as different

photocatalysts absorb certain wavelengths of visible light more efficiently. Figure 1.1 shows examples of commonly used photocatalysts.

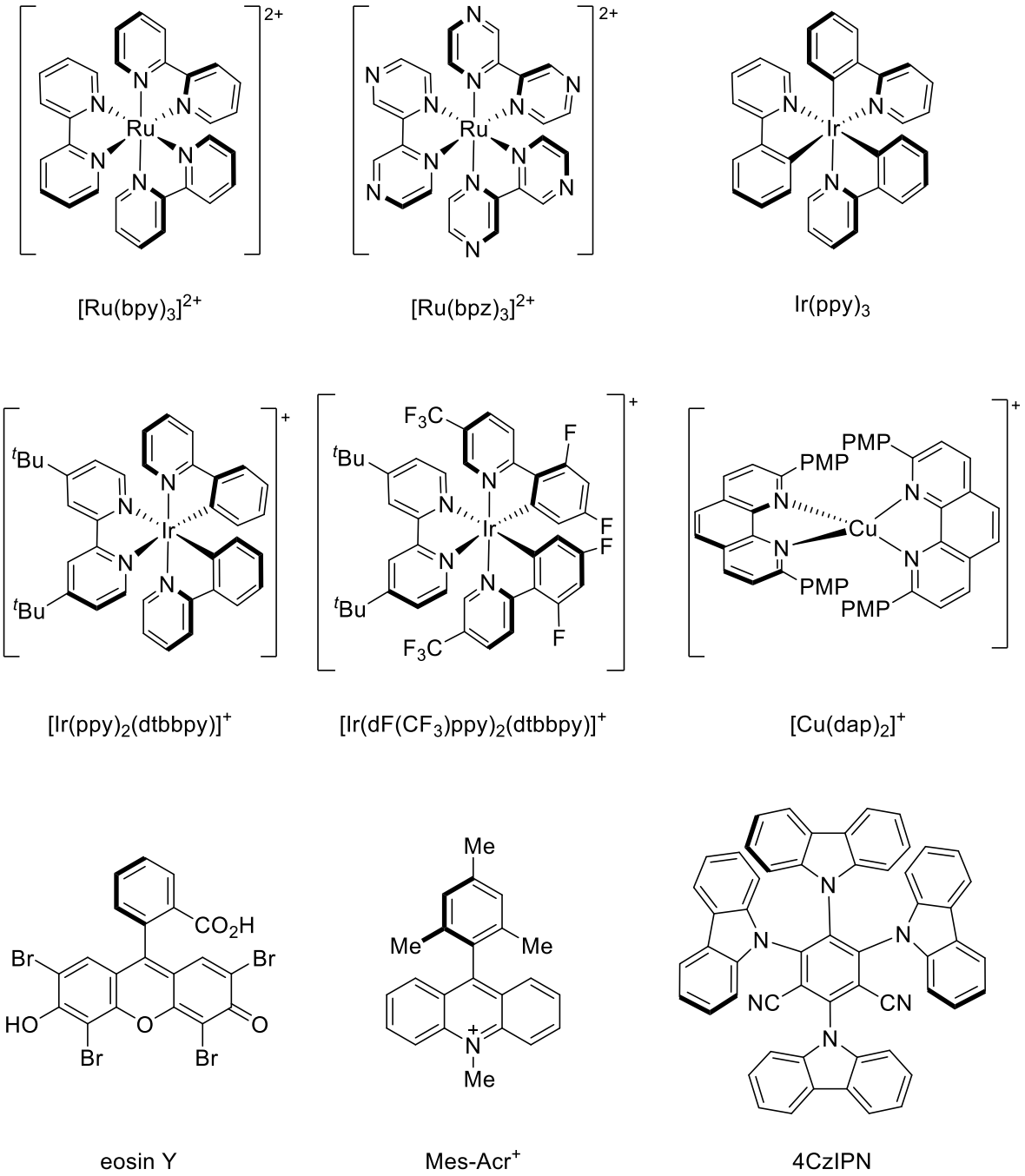

Figure 1.1 Structures of common photocatalysts. Counterions omitted for clarity.

Perhaps the most widely used photocatalyst is $[Ru(bpy)_3]^{2+}$ as its photochemical properties are well known and have been established in fields such as the oxidation and reduction of water and in the manufacture of optical chemical sensors.[11–13] In choosing a photocatalyst, important factors to consider include absorption wavelength maxima, excited state lifetime (τ), ISC yield, how suitably reducing or oxidising the excited species is, ease of preparation and

photostability. In the case of $[Ru(bpy)_3]^{2+}$, the peak absorption wavelength is 452 nm (violet/blue region of the visible-light spectrum) and its excited state lifetime is 1.1 µs. This is sufficient time for single-electron transfer (SET) to or from the substrate to occur. Sacrificial electron donors or acceptors are often used to return the oxidised/reduced catalyst to its original oxidation state, completing the cycle. A general overview of the photophysical and electronic processes involved are shown in Figure 1.2 and Figure 1.3.

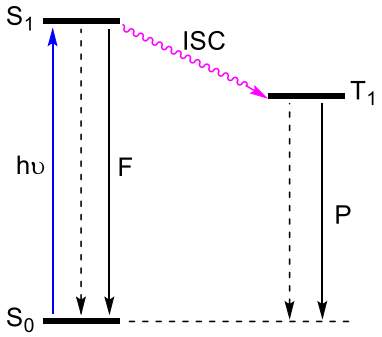

Figure 1.2 Simplified Jablonski diagram.

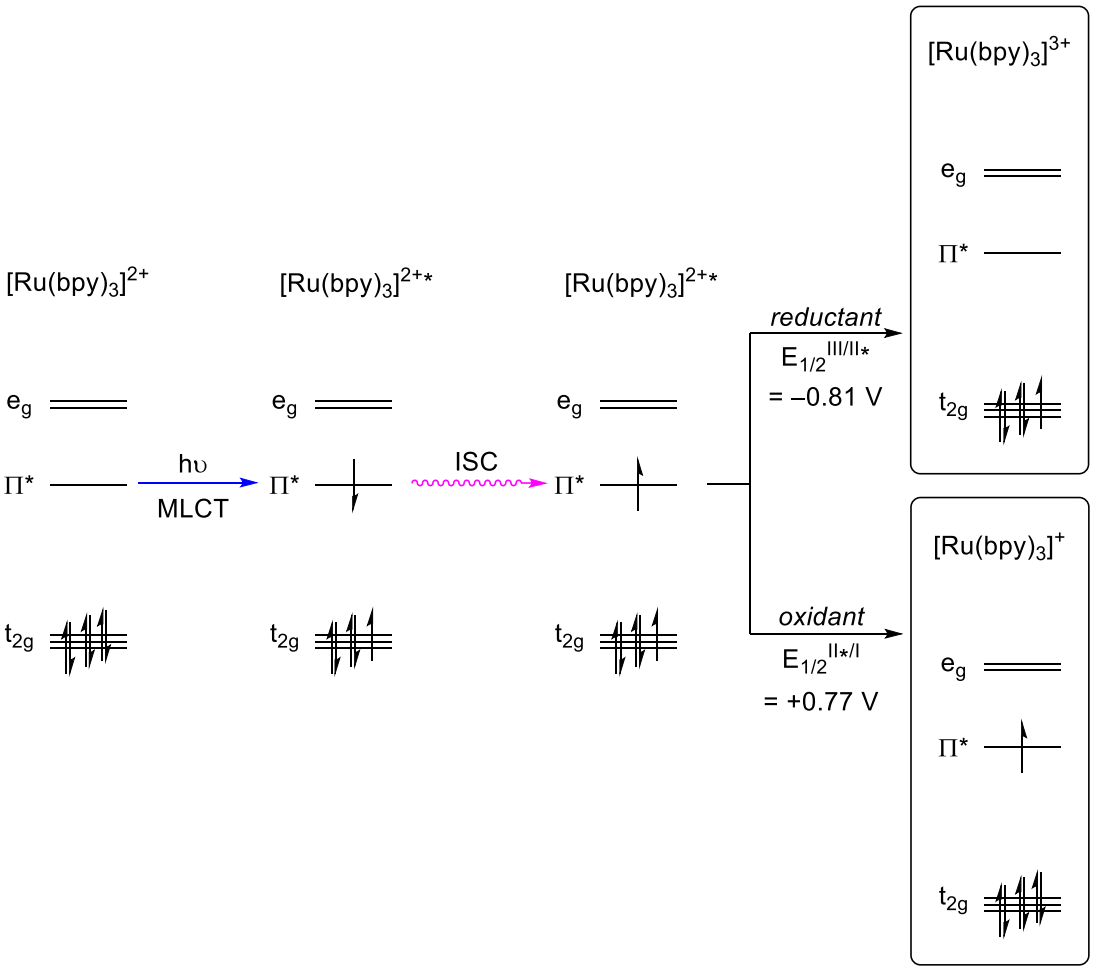

Figure 1.3 Simplified molecular orbital diagram for the excitation and SET of $[Ru(bpy)_3]^{2+}$. Redox potentials stated as V vs SCE. [12]

Irradiation of a photocatalyst with photons of a sufficiently high energy leads to excitation of the catalyst from its ground state (S_0) to a singlet excited state (S_1) (Figure 1.2). An electron is promoted from the highest molecular orbital (HOMO) to the lowest unoccupied molecular orbital (LUMO). As shown in Figure 1.3 using $[Ru(bpy)_3]^{2+}$ as an example, the π * orbitals of the bipyridine ligands are lower in energy than the metal-centred e_g orbital, and so upon absorption of light energy, an electron is promoted from the t_{2g} orbital of ruthenium to the bipyridine π * orbital. This is called metal-to-ligand charge-transfer (MLCT). During excitation, the spin of the promoted electron is unaltered and from this point there are three possibilities: the electron can return to the ground state (S_0) *via* fluorescence (F); the electron can return to the ground state *via* internal conversion (non-radiative process (dotted-line)); the electron can undergo intersystem crossing (ISC), transitioning to the triplet excited state (T_1). In the latter case, the electron's spin is flipped which means relaxation from this state (phosphorescence, P) is spin-forbidden, and as a result, the T_1 excited state is longer-lived than the S_1 excited state. Although SET is possible from both excited states, it is much more likely to occur from a triplet state for this reason. Figure 1.3 shows the T_1 excited state of $[Ru(bpy)_3]^{2+*}$ acting as either an oxidant or a reductant and this concept will be explained in more detail in Section 1.1.2. Organocatalysed photoredox processes happen in much the same way as described above but with the practical advantage that no metals are involved, avoiding any concern over metal contamination of resulting compounds.

$[Ru(bpy)_3]^{2+}$ and $Ir(ppy)_3$ photocatalysts are homoleptic, meaning that the ligands attached to the metal centre are all identical. Electronically this means that electron density is evenly distributed around the complex, stabilising the excited state. However, heteroleptic complexes contain two or more different ligands (e.g. $[Ir(ppy)_2(dtbbpy)]^+$) and in those cases π * orbitals of differing energies are present. This means that there are a greater number of π^* levels into which an excited electron may be promoted. This can be a useful strategy for maximising light absorption,[14] as well as for tuning the redox potentials of the catalyst which are determined by HOMO/LUMO energy gaps.

Table 1.1 shows the excited state lifetimes, τ, and redox potentials of the common photocatalysts drawn in Figure 1.1. $Ir(ppy)_3$ has a reduction potential of -1.73 V *vs* SCE which

is the most negative value listed, making it the strongest reductant. In comparison, $[Ru(bpy)_3]^{2+}$ has a reduction potential of -0.81 V *vs* SCE. Iridium complexes are generally better reductants than their ruthenium counterparts due to the fact that iridium is in group 9 and so must be in the +III oxidation state to achieve a d^6 low spin electron count, whereas ruthenium (group 8) only requires a +II oxidation state for this. Additionally, differences arise from the coordinated ligands. Phenylpyridine has one fewer nitrogen atom than bipyridine making it a less electron-withdrawing ligand. In general, strongly electron-withdrawing ligands lead to a strongly oxidising photocatalyst, whereas strongly electron-donating ligands lead to a strongly reducing complex.

Photocatalyst	**Lifetime, τ/ ns**	**$E_{1/2}$ (M^+/M*) /V**	**$E_{1/2}$ (M*/M^-) /V**
$[Ru(bpy)_3]^{2+}$	1100	-0.81	+0.77
$[Ru(bpz)_3]^{2+}$	740	-0.26	+1.45
$[Ir(ppy)_3]^{3+}$	1900	-1.73	+0.31
$[Ir(ppy)_2(dtbbpy)]^+$	557	-0.96	+0.66
$[Ir(dF(CF_3)ppy)_2(dtbbpy)]^+$	2300	-0.89	+1.21
$[Cu(dap)_2]^+$	270	-1.43	+0.62
eosin Y	2.50	-1.08	+1.23
Mes-Acr^+	37.0	-0.57	+2.08
4CzIPN	2.37	-1.21	+1.35

Table 1.1 Comparison of excited state lifetime and redox potentials for common photocatalysts.[8,9,15,16]

Redox potentials are in V vs SCE.

Of the examples given in Table 1.1, $Ir(ppy)_3$ is the strongest reductant followed by 4CzIPN, and 9-mesityl-10-methylacridinium (Mes-Acr^+) is the strongest oxidant. Although organic dyes generally have shorter excited state lifetimes, they do offer a broad range of redox potentials which are often comparable to the common transition-metal-based photocatalysts.

1.1.2 General Mechanism

A photocatalyst in an excited state is a better oxidant and reductant than its ground state counterpart. Therefore, two catalytic cycles are possible, an oxidative quenching cycle or a reductive quenching cycle, both of which are summarised in Figure 1.4.

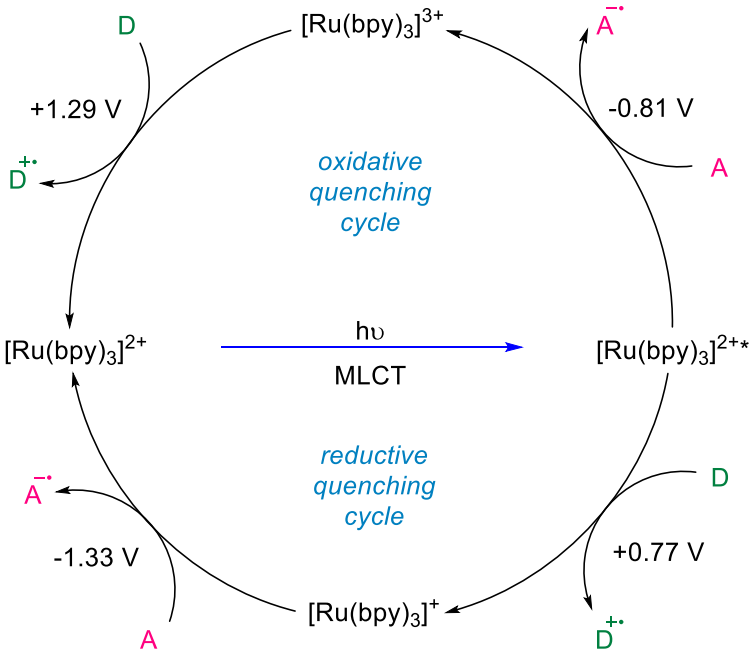

Figure 1.4 Oxidative and reductive photoredox cycles of $[Ru(bpy)_3]^{2+}$.

After excitation, the photocatalyst can donate a single electron to an acceptor (A) to form the oxidised Ru(III) species and the radical anion of the acceptor species. As a result, the Ru(III) species becomes a strong oxidant ($E_{1/2}^{III/II}$ = 1.29 V *vs* SCE) and so can reduce a donor (D), returning the catalyst to its ground state oxidation level while generating the radical cation of the donor. This is an oxidative quenching cycle. Alternatively, in a reductive quenching cycle, the excited photocatalyst first accepts an electron from a donor to generate the reduced Ru(I) species. This is followed by reoxidation to the Ru(II) species by an acceptor to turn over the catalyst, facilitated by the fact that the Ru(I) species is a good reductant ($E_{1/2}^{II/I}$ = −1.33 V *vs* SCE). In both cycles, a donor and an acceptor are required for catalyst turnover. Common reductive quenchers are tertiary amines, and common oxidative quenchers are aryldiazonium salts or dinitrobenzenes.[8] To determine whether an oxidative or reductive quenching mechanism is in action for a given reaction, Stern-Volmer studies must be undertaken.[17]

1.2 Key Developments in Photoredox Catalysis

Photoredox catalysis became an area of rapidly growing interest after 2008, with publications by the MacMillan and Yoon research groups, who developed dehalogenative α-alkylation of aldehydes and intramolecular [2+2] cycloaddition protocols respectively.[1,2] This was closely

followed by the reductive dehalogenation of alkyl halides in 2009 by Stephenson and co-workers (Figure 1.5).[3]

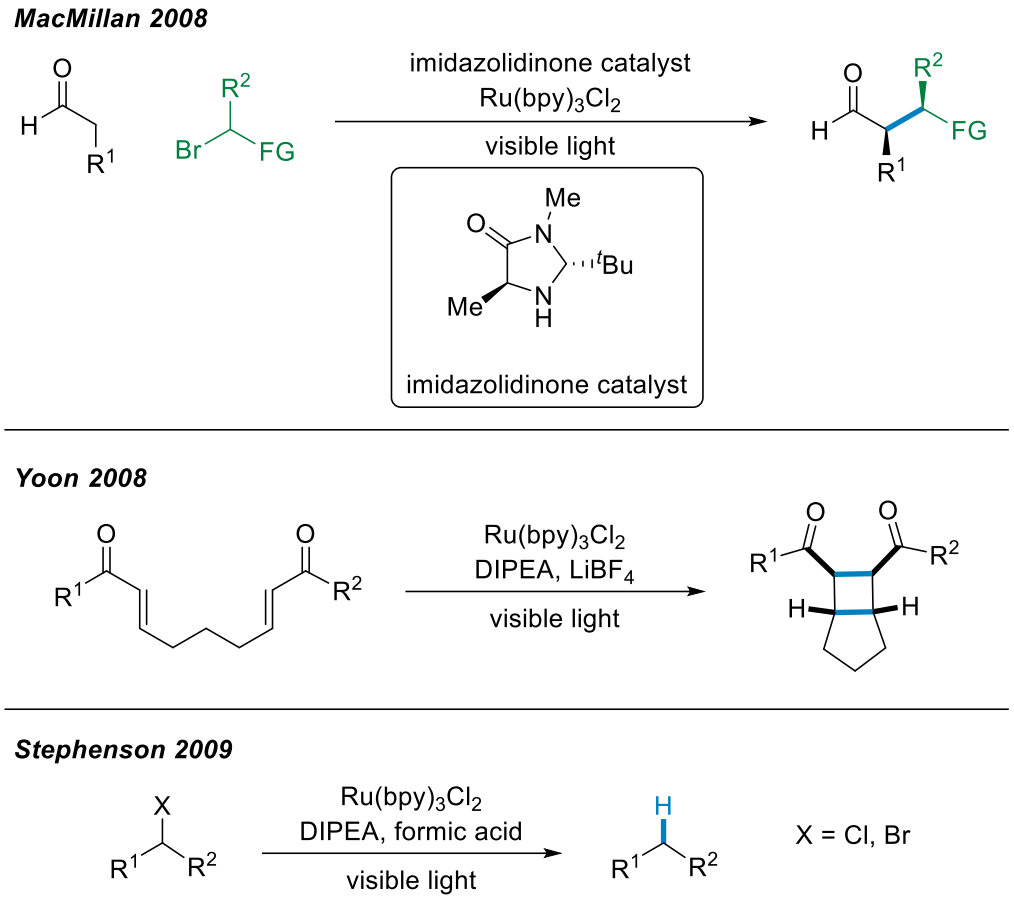

Figure 1.5 Early examples of photoredox catalysis in organic synthesis. Reagents and conditions: MacMillan – aldehyde (2 equiv.), α-bromocarbonyl (1 equiv.), organocatalyst (20 mol%), $Ru(bpy)_3Cl_2$ (0.5 mol%), 2,6-lutidine (2 equiv.), DMF (0.5 M), hv, rt, N_2.. Yoon – enone (1 equiv.), $Ru(bpy)_3Cl_2$ (5 mol%), $LiBF_4$ (2 equiv.), DIPEA (2 equiv.), MeCN (0.1 M), hv, rt, N_2. Stephenson – halide (1 equiv.), $Ru(bpy)_3Cl_2$ (2.5 mol%), DIPEA (10 equiv.) formic acid (10 equiv.), DMF (0.1 M), hv, rt, N_2, 4 h.

MacMillan developed a dual-catalytic system, combining photoredox catalysis with SOMO organocatalysis for the enantioselective α-alkylation of aldehydes, expanding the substrate scope of enamine catalysis to include alkyl halides.[1] Under photocatalytic conditions, the carbon-bromine bond is cleaved to produce an electron-deficient radical, which can add to one face of the enamine formed as part of the organocatalytic cycle. The resultant α-amino radical undergoes a SET process to form an imine whilst regenerating the active ruthenium (I) species, the reductant required for homolytic C-Br bond cleavage. Fully organocatalytic

versions of this chemistry have now been reported, for example by Zeitler who replaced $Ru(bpy)_3Cl_2$ with eosin Y.[18]

Concurrently, Yoon reported the intramolecular [2+2] cycloaddition of dienones, also utilising $Ru(bpy)_3Cl_2$ as the photocatalyst.[2] The protocol was one of the first examples of adapting a known redox-mediated process to a milder and more environmentally friendly photoredox process. The process follows a reductive quenching mechanism and the addition of $LiBF_4$ helps solubilise the catalyst in dry acetonitrile as well as acting as a Lewis acid, activating the enone toward one-electron reduction.[2] DIPEA is used as a terminal reductant to turn over the catalyst. Stephenson and co-workers then reported their reductive dehalogenation protocol in early 2009, using a ruthenium catalyst and DIPEA as the superstoichiometric terminal reductant.[3] Either formic acid or Hantzsch ester are needed as additional hydrogen atom donors to promote the reaction, although labelling studies suggested that DIPEA was the primary source of hydrogen atoms in the reaction. The conditions were applicable to aliphatic chlorides and bromides in the presence of aryl and vinyl halides, however the substrates must be activated (e.g. by an adjacent benzylic or carbonyl group) for the reaction to occur. In a later publication, Stephenson reported the photoredox-mediated reduction of unactivated alkyl, alkenyl and aryl halides using the more strongly reducing $Ir(ppy)_3$ catalyst.[7]

In the examples above, tertiary amines are used as sacrificial reductants, however the α-functionalisation of amines is another prominent area within photoredox catalysis, with amines being an important motif in natural products and biologically active compounds. Nucleophilic α-amino radicals have been utilised in many instances including aza-Henry reactions, the C-H arylation of amines and olefin hydroamination. Scheme 1.1 depicts the photoredox-mediated aza-Henry reaction developed by Stephenson and co-workers.[19] The excited $[Ir(ppy)_2(dtbbpy)]PF_6$ catalyst is capable of oxidising the amine starting material to radical cation **1**. The resulting iridium(II) species that is generated as a result reduces dioxygen, the product of which can then abstract a hydrogen atom α- to the amine functional group to give iminium ion **2**. Nitromethane then adds to this electrophilic iminium ion to yield α-functionalised product **3**. Similar strategies have been implemented using organocatalysts or other nucleophilic coupling partners such as cyanides or malonates.[20–22]

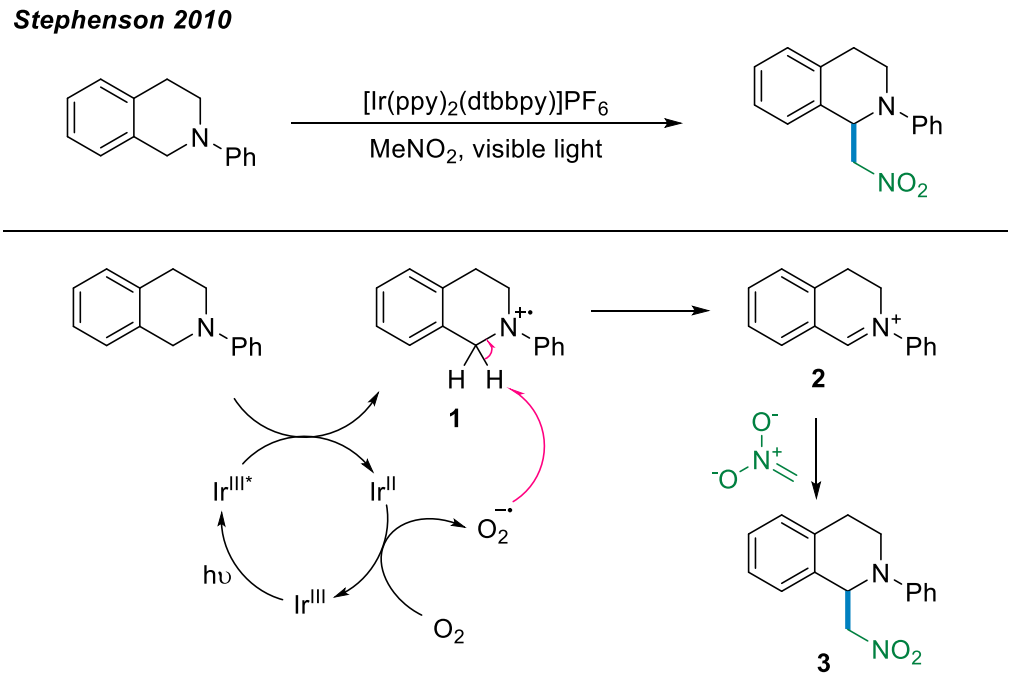

Scheme 1.1 Photoredox aza-Henry reaction. Reagents and conditions: [Ir(ppy)₂(dtbbpy]PF₆ (1 mol%), tetrahydroisoquinoline (1 equiv.), nitromethane (0.25 M), rt, fluorescent lamp.

The C-H arylation of amines reported by MacMillan also makes use of an aminium radical cation but relies on the formation of the radical anion of the aryl coupling partner rather than a separate non-participating oxidant (Scheme 1.2).[23] The strongly reducing $Ir(ppy)_3$ is used and

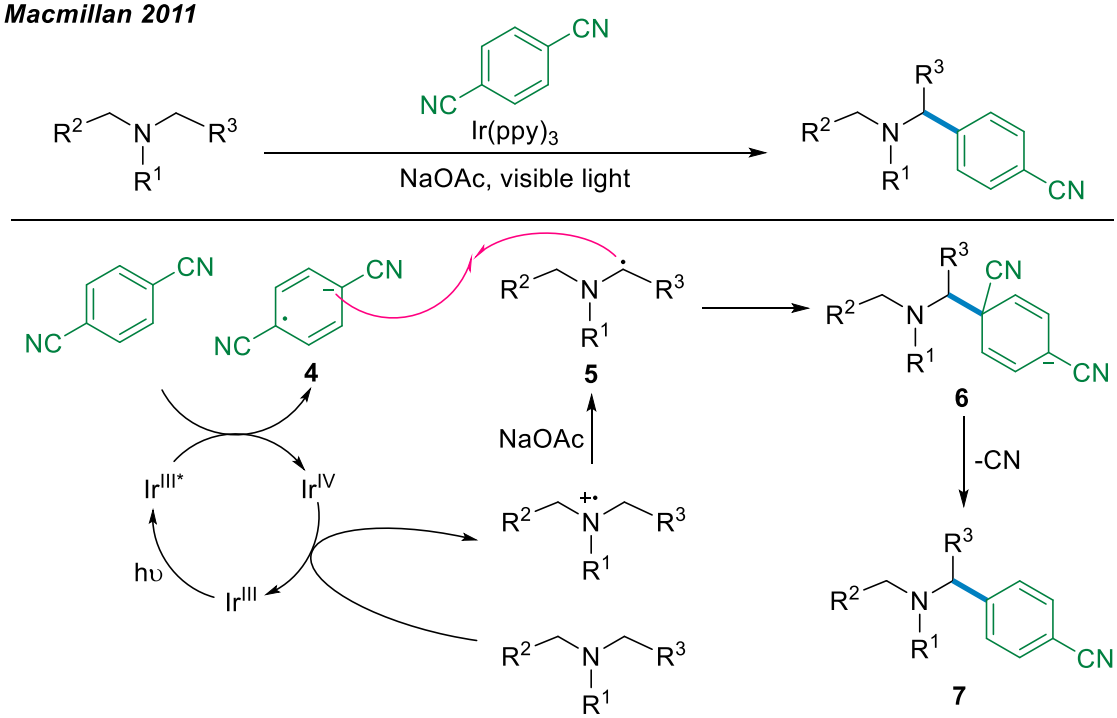

Scheme 1.2 Photoredox C-H arylation reaction. Reagents and conditions: Ir(ppy)₃ (0.5-1 mol%), amine (2.5-3.0 equiv.), arene (1 equiv.), NaOAc (2 equiv.), DMA (0.5 M), visible light, rt, 12-24 h.

thus, an oxidative quenching cycle is proposed. Mechanistically, the excited iridium(III) species donates an electron to the arene ($Ir(ppy)_3^{IV*/III}$ $E_{1/2}$=–1.73 V *vs* 1,4-DCB $E_{1/2}$=–1.61 V) to form the oxidising Ir(IV) species ($E_{1/2}$=+0.77 V) which undergoes single-electron transfer to oxidise the amine substrate. The radical cation formed has a weakened C-H bond α- to the amine, and so sodium acetate is basic enough to deprotonate this position, giving an α-amino radical **5**. Termination of the radical sequence occurs *via* a radical-radical coupling of **4** and **5** to give **6**, followed by elimination of CN^- and aromatisation to give product **7**. The protocol uses low catalyst loadings and mild conditions but is limited by the requirement for electron-deficient arenes and heteroaromatic substrates, as well as selectivity issues if $R^2 \neq R^3$ and both groups have α-C-H groups.

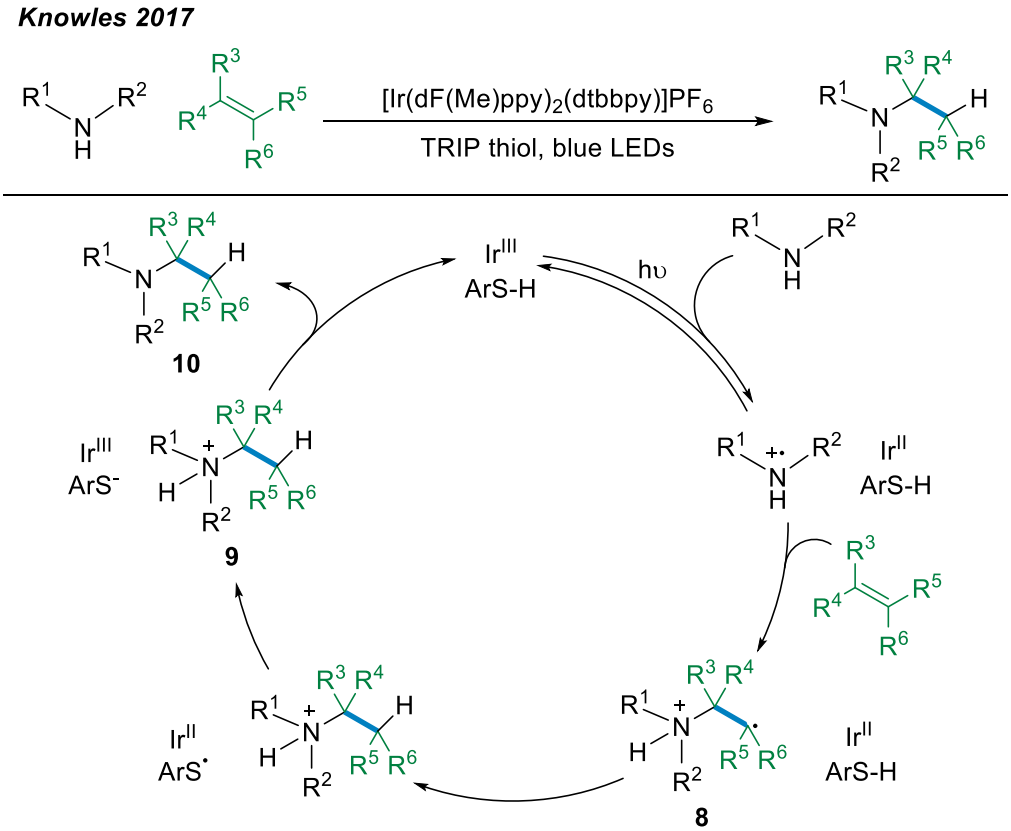

Scheme 1.3 Photoredox anti-Markovnikov hydroamination reaction. Reagents and conditions: [Ir(dF(Me)ppy)₂(dtbbpy)]PF₆ (2 mol%), amine (1 equiv.), alkene (1.5-5 equiv.), TRIP thiol (50 mol%), toluene (0.05 M), rt, blue LEDs.

Whilst the work of Stephenson and MacMillan, among others, have provided useful tools for the construction of functionalised amines, it is limited to the α-position of tertiary amines. Manipulation of the nitrogen atom of an amine is also of significant interest for applications in

C-N bond construction. Using photoredox catalysis, Knowles and co-workers developed an olefin hydroamination protocol using aminium radical cations (Scheme 1.3).[24]

Comparable reactions using traditional metal-catalysts are challenging with unactivated and/or sterically demanding olefins, due to poor metal coordination relative to Lewis-basic amines. Key to the success of the reaction was using an additional HAT donor, in this case 2,4,6-triisopropylbenzenethiol (TRIP thiol). This thiophenol derivative has a weak S-H bond (roughly 79 kcal/mol)[25] and undergoes rapid HAT in the presence of carbon-centred radicals such as **8**. This facilitates the catalytic cycle as the iridium(II) species is not oxidising enough to reduce radical **8** to a carbanion, but it is oxidising enough to reduce the thiyl radical to a thiyl anion.[26] The closed shell ammonium intermediate **9** is then deprotonated by the thiyl anion to give product **10**. The chemistry is applicable to the intermolecular hydroamination of cyclic and acyclic secondary amines with mono-, di-, tri- or tetra-substituted alkenes. Primary amines were not suitable substrates and were inert to the reaction conditions. Intramolecular versions of photoredox-mediated hydroamination reactions have also been developed which will be discussed in more detail in Section 1.3.

1.3 Radical Cyclisation

Radicals are valuable intermediates in chemical synthesis and their applications are far-reaching. For an efficient radical cyclisation to occur, radicals need to be selectively generated, and cyclisation must occur at a faster rate than the quenching of the initially formed radical or faster than any intermolecular side reactions. Radical intermediates are uncharged species, and as a result, reaction conditions are often milder and have greater functional group tolerance than polar reactions. Radical cyclisation to form 5- and 6-membered rings is commonplace, with the cyclisation to form larger rings being increasingly slow. In a typical scenario, a weak C-X bond is broken homolytically to give a carbon-centred radical which can add to a number of radical acceptors such as alkenes, alkynes, aryls, carbonyls and nitriles. In 1976, Baldwin published guidelines predicting the outcome of nucleophilic and radical cyclisation reactions,[27] and in 1980, Beckwith suggested four revisions specifically targeted at

radical cyclisations.[28] A summary of the guidelines for favoured and disfavoured ring closures is shown in Table 1.2.

Type of cyclisation		**Ring size**				
		3	**4**	**5**	**6**	**7**
-tet	*endo-*	–	–	×	×	×
	exo-	✓	✓	✓	✓	✓
-trig	*endo-*	×	×	×	✓	✓
	exo-	✓	✓	✓	✓	✓
-dig	*endo-*	✓	✓	✓	✓	✓
	exo-	×	×	✓	✓	✓

Table 1.2 Baldwin's guidelines for favoured and disfavoured ring closures.

Cyclisation of the hex-1-ene radical (Scheme 1.4) could occur *via* 5-*exo-trig* or 6-*endo-trig* pathways, both of which are allowed under Baldwin's guidelines. Although the 6-*endo-trig* product is a more stable secondary radical than the primary radical produced from 5-*exo-trig* cyclisation, the reaction is under kinetic control and so the 5-*exo* product is favoured. This can be rationalised from the more favourable orbital overlap in the 5-*exo-trig* transition state compared with the 6-*endo-trig* transition state. The 5-*exo-trig* cyclisation is therefore much faster.

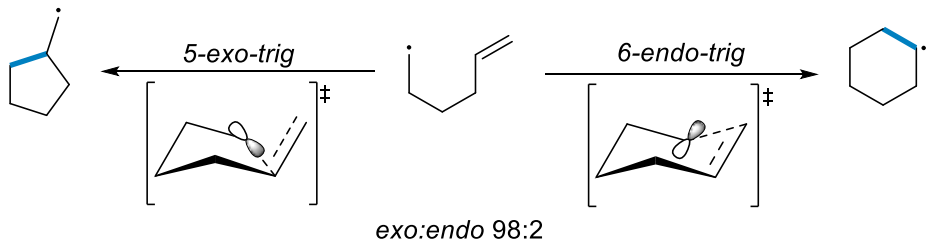

Scheme 1.4 5-exo-trig vs 6-endo-trig radical cyclisations.

Classically, metal hydrides (tin, silicon or mercury hydrides) in combination with an initiator (AIBN or peroxides) are used to generate radicals. Initiators are labelled as such due to having a weak bond present, which can be homolytically cleaved thermally or photochemically to give a source of radicals. This initial radical could then go on to react with a metal hydride to give a metal-centred radical. This in turn would form a strong bond with X, cleaving the C-X bond (Scheme 1.5) and propagating the radical chain. Concerns with this chemistry centre around the toxicity and purification challenges associated with tin and mercury complexes, as

stoichiometric quantities are required. Substrates with weak C-X bonds are typically carbon-bromides, carbon-iodides or carbon-selenides.

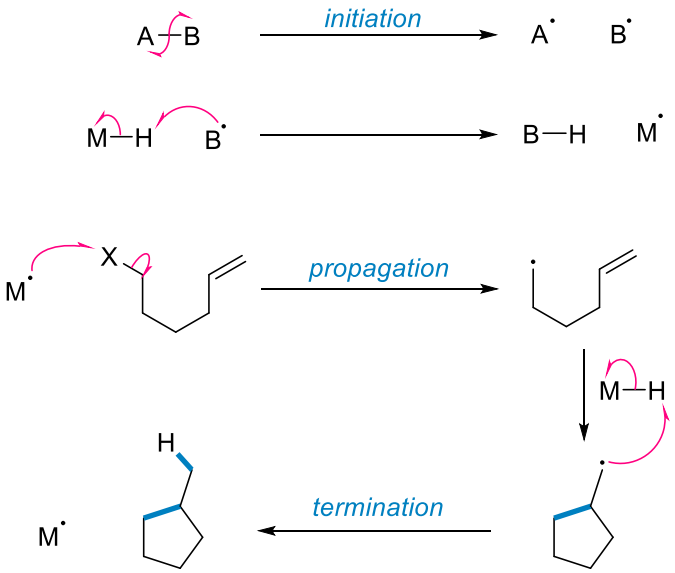

Scheme 1.5 General mechanism for radical cyclisation.

A representative example of a radical 5-*exo-trig* cyclisation was described by Ghelfi using trichloroacetamide substrate **11** and stoichiometric tributyltin hydride (Scheme 1.6).[29] To provide a source of radicals, the initiator AIBN was used which has a half-life of one hour at 81 °C.[30]

Ghelfi 2003

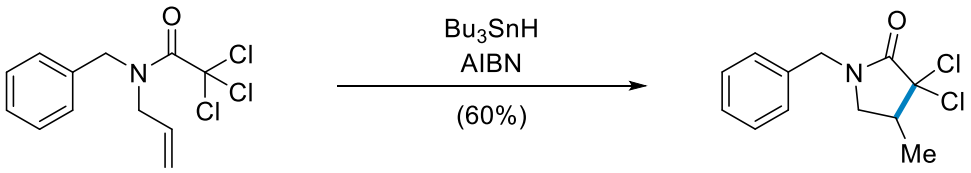

11

*Scheme 1.6 Radical cyclisation of **11** using tributyltin hydride. Reagents and conditions: amide (1 equiv.), Bu_3SnH (1 equiv.), AIBN (10 mol%), toluene, 110 °C, 2 h, 60%.*

Alternatively, atom-transfer radical cyclisation (ATRC) reactions facilitated by metal complexes such as CuBr(bpy) allow similar cyclisations to occur while avoiding tin-based reagents. As is the case in both Scheme 1.6 and Scheme 1.7, amide rotation is necessary in order to place the allyl chain proximal to the carbon-centred radical for cyclisation to occur over reduction. Nagashima demonstrated that electron-withdrawing substituents on the amide nitrogen atom

decreased the energy barrier required for this rotation and increased reaction yields.[31] Single-electron transfer from the copper(I) catalyst to the substrate generates the initial radical and a copper(II) complex (Scheme 1.7). Rapid 5-*exo*-*trig* cyclisation from the *anti*-**13** gives radical **14**. Oxidation of **14** gives the product and regenerates the copper(I) catalyst. Although the use of copper is advantageous over tin, the copper complexes are sparingly soluble in organic solvents, meaning the reactions must be conducted in refluxing chlorinated solvents.[32] The CuBr(bpy) complexes are also air sensitive and therefore special precautions are required when setting up the reactions which undermines practicality, particularly in an industrial context.[32]

Nagashima 2001

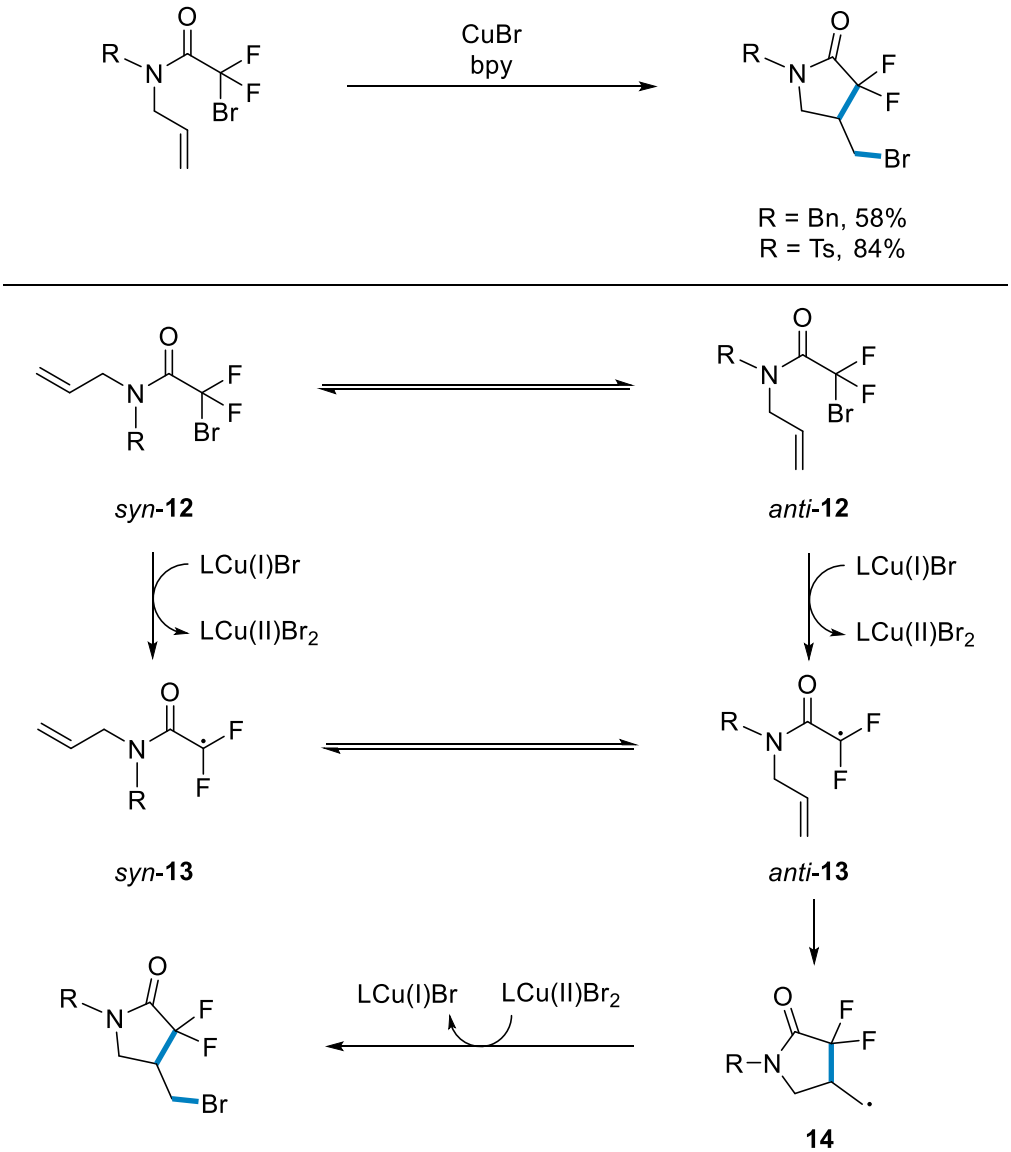

syn-**12** *anti*-**12**

syn-**13** *anti*-**13**

14

Scheme 1.7 ATRC reaction using a copper(I) catalyst. Reagents and conditions: CuBr (30 mol%), bipyridine (30 mol%), DCE, 80 °C, 15 h.

A transition-metal-free cyclisation *via* the same difluoroalkyl radical intermediate was reported by Uneyama using the reduction of diphenyl diselenide with sodium borohydride, and subsequent single-electron transfer to generate the initial radical species (Scheme 1.8).[33] Rotation of the amide bond is again required to give the desired *anti*-**12** rotamer, only avoided if the R group on the nitrogen atom is a second allyl group. The same intermediate as in Scheme 1.7 is formed but here radical **14** is quenched with PhSe$^{\bullet}$ to give selenated products. In the case of R = benzyl, under the reaction conditions, 63% of the desired cyclised product was isolated with the linear dehalogenated side product making up another 34% of the yield. Therefore at 0 °C, amide rotation is sufficiently slowed for radical quenching prior to cyclisation to be competitive. Aside from this limitation to the yield, the use of selenium-based compounds is also not ideal due to their toxicity and stench.

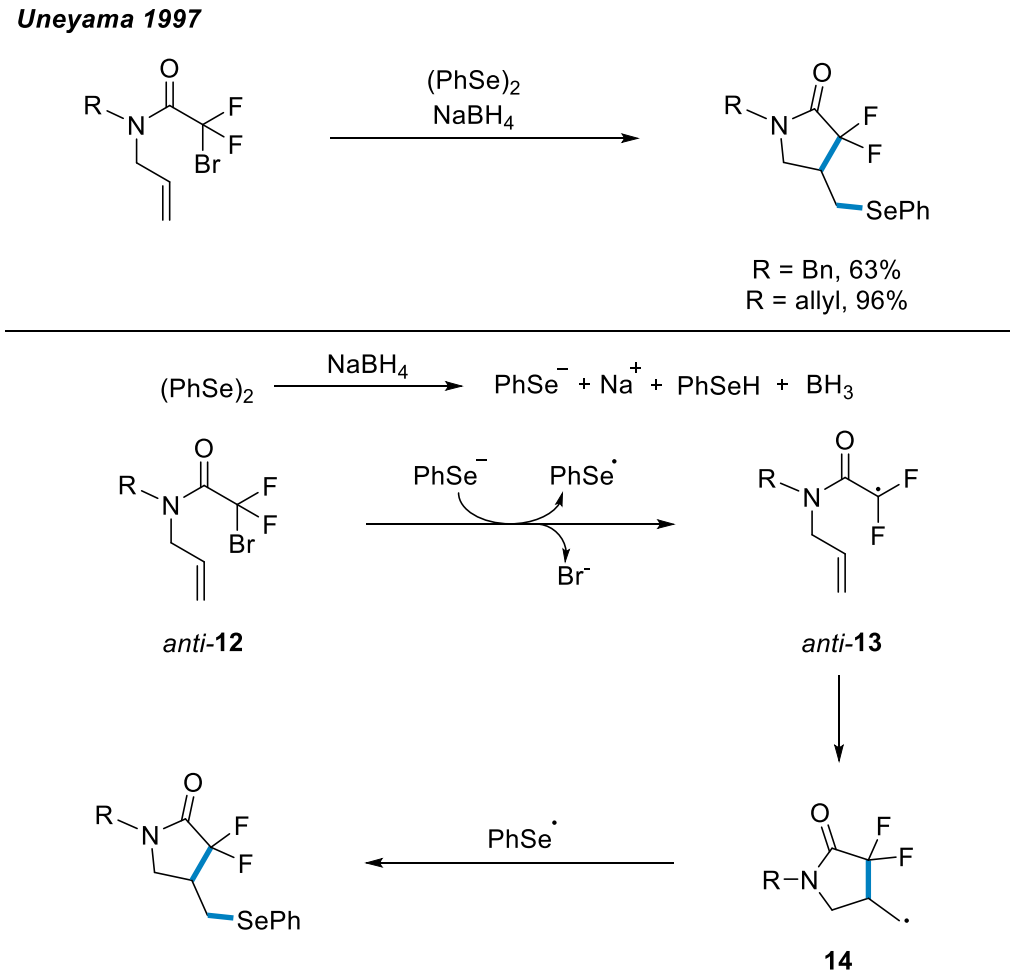

Scheme 1.8 Synthesis of α,α-difluoro-γ-lactams via single-electron transfer from a benzeneselenate anion. Reagents and conditions: amide (1 equiv.), diphenyl diselenide (0.5 equiv.), $NaBH_4$ (1 equiv.), THF/EtOH (4:1, 0.03 M), 0 °C, N_2, 3 h.

1.3.1 Photoredox Radical Cyclisation

With the huge increase in publications in the area of photoredox catalysis, naturally photoredox-mediated radical cyclisation protocols have been developed, rivalling conventional and undesirable organostannane chemistry. Low catalyst loadings and mild reaction conditions are the major advantages of these systems. Notable developments came separately from Stephenson and Lee, both of whom published the cyclisation of unactivated alkyl iodides using iridium catalysts in 2012 (Scheme 1.9).[7,34] Both groups used iridium photocatalysts but Stephenson used the more strongly reducing $Ir(ppy)_3$ catalyst and thus proposed an oxidative quenching cycle. He suggested that the excited photocatalyst was quenched by reductive cleavage of the alkyl iodide substrate, followed by regeneration of the iridium(III) species by oxidation of tributylamine or formate. Lee, on the other hand, proposed a reductive quenching cycle using the less reducing $[Ir(ppy)_2(dtbbpy)]PF_6$ catalyst. In this case, quenching of the excited catalyst to give the Ir(II) species is *via* the tertiary amine base, and reoxidation occurs *via* SET to the alkyl iodide. Both publications use tosyl protecting groups which prevents participation of the amine substrate in oxidative processes, in the same way DIPEA and tributylamine would do. In 2016, Stephenson reported the cyclisation of unactivated alkyl bromides, this time using $[Ir(ppy)_2(dtbbpy)]PF_6$ in combination with DIPEA and tris(trimethylsilyl)silane (TTMSS).[35]

Stephenson 2012 and Lee 2012

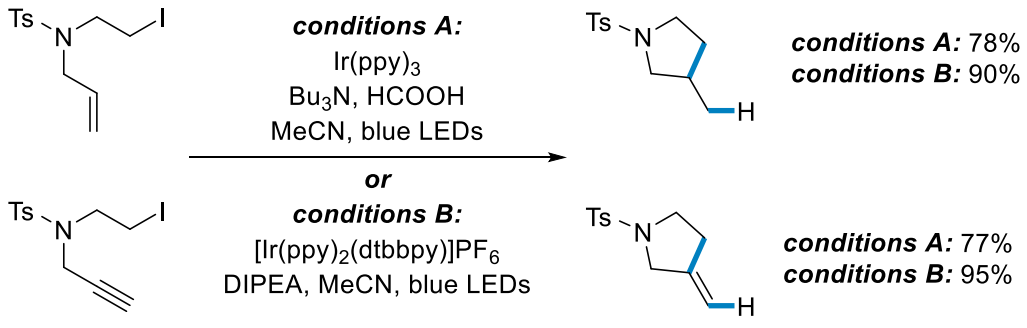

Scheme 1.9 Photoredox radical cyclisation of unactivated alkyl iodides. Reagents and conditions: Conditions A – alkyl iodide (1 equiv.), $Ir(ppy)_3$ (2.5 mol%), Bu_3N (10 equiv.), formic acid (10 equiv.), MeCN (0.1 M), rt, Ar, blue LEDs. Conditions B – alkyl iodide (1 equiv.), $[Ir(ppy)_2(dtbbpy)]PF_6$ (3 mol%), DIPEA (10 equiv.), MeCN (0.1 M), rt, blue LEDs.

Tosyl groups were also utilised in a photoredox-catalysed aminodifluoromethylation protocol, again preventing C-H functionalisation byproduct formation arising from amine oxidation, while still ensuring the sulfonamide was sufficiently nucleophilic to trap the intermediate carbocation (Scheme 1.10).[36] Difluoromethyl radicals are generated by single-electron reduction of difluoromethanesulfonyl chloride by the excited $Cu(dap)_2Cl$ catalyst, which can then add to an alkene, giving radical **15**. Oxidation of the radical regenerates the photocatalyst and gives carbocation **16** which can be trapped by the nucleophilic sulfonamide group giving cyclic pyrrolidine **17**. The reaction does not yield any product when the tosyl group is replaced by a Boc or acetyl protecting group, most likely due to the nitrogen atom being too electron-deficient in those cases. When $Ir(ppy)_3$ was used instead of $Cu(dap)_2Cl$, side product **18** formed, suggesting $[Ir(ppy)_3]^+$ is not an effective reductant of radical **15** despite its greater oxidation

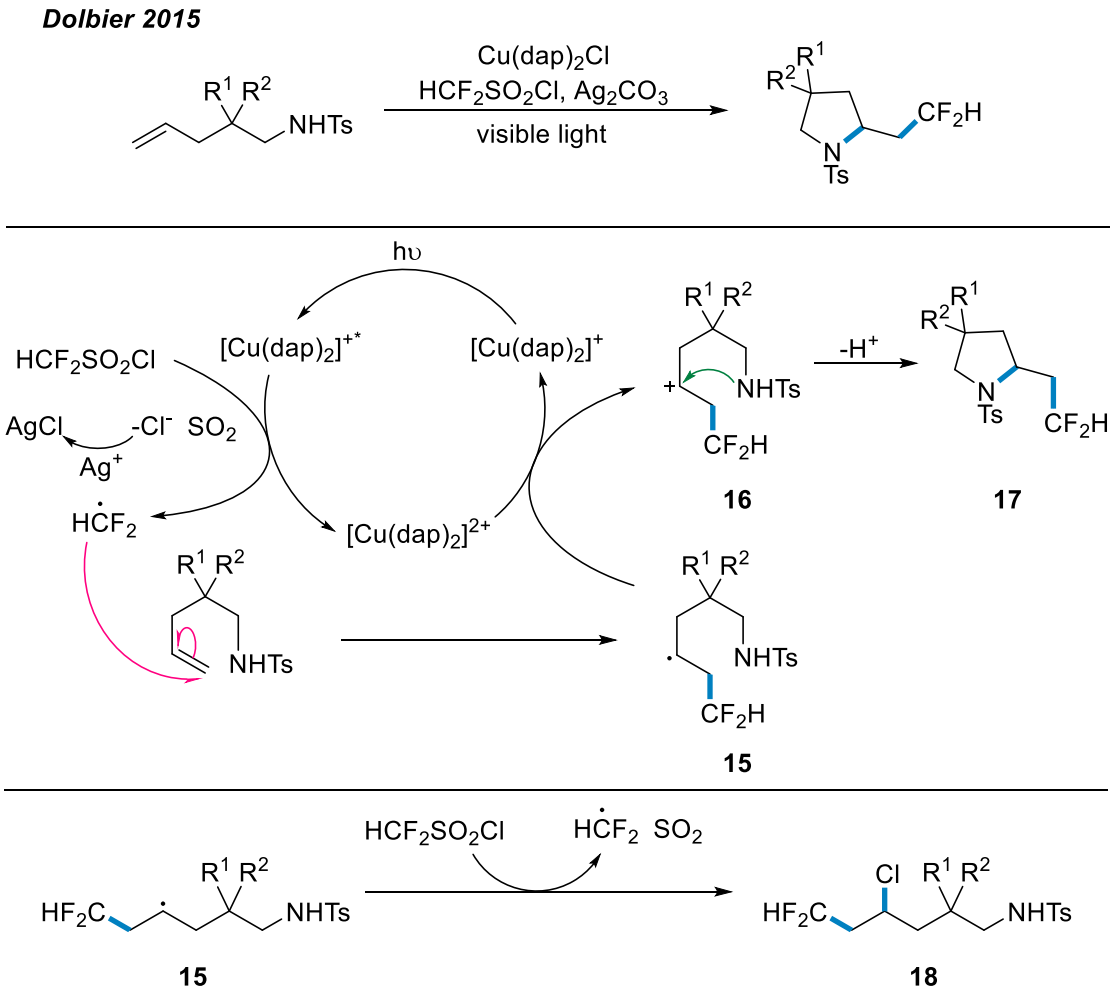

Scheme 1.10 Aminodifluoromethylation procedure using difluoromethyl radicals. Reagents and conditions: alkene (1 equiv.), $Cu(dap)_2Cl$ (1 mol%), HCF_2SO_2Cl (2 equiv.), Ag_2CO_3 (2 equiv.), DCE (0.1 M), 70 °C, 18 h, visible light.

potential. In the absence of oxidation, radical **15** abstracts the chlorine atom from another molecule of difluoromethanesulfonyl chloride, propagating the radical chain. Subjection of **18** to silver carbonate in DCE at 70 °C for 18 hours yielded a small amount of cyclised material, with the remaining material unreacted. Therefore, there are two effective routes to the product in competition; although slow, the pathway *via* **18** is much slower. Silver carbonate addition most likely helps to scavenge chloride ions, thereby suppressing competing chlorine addition reactions.

Knowles 2014

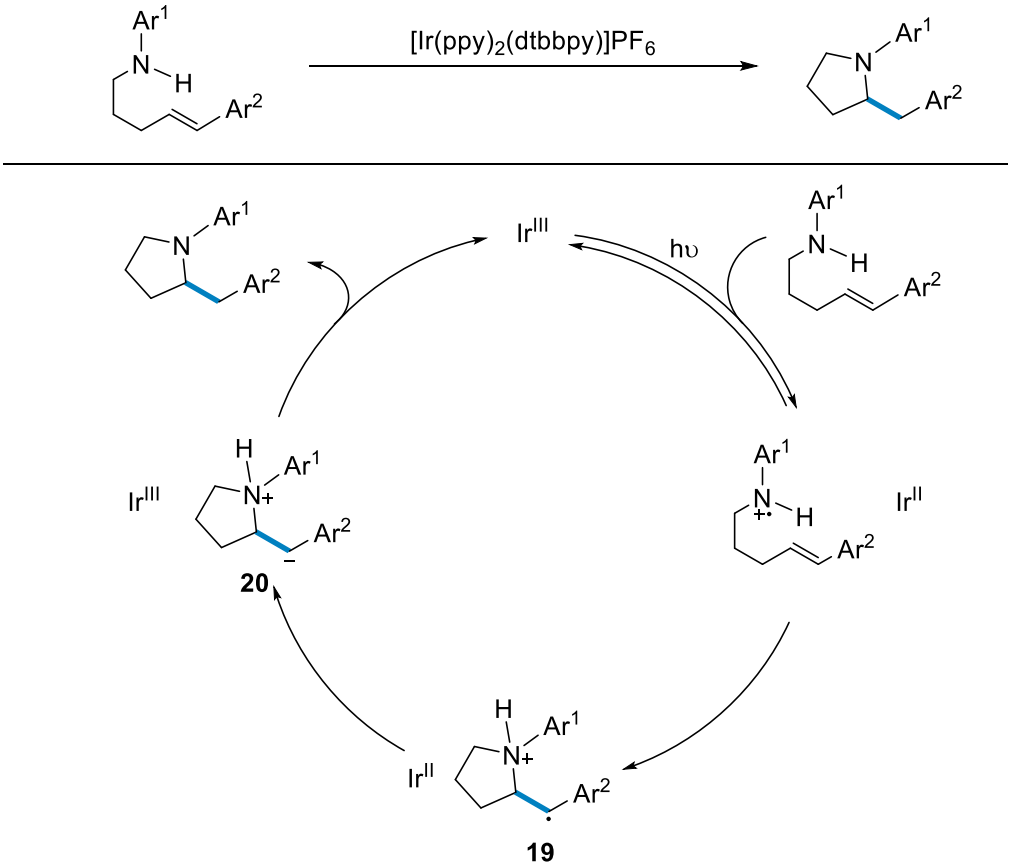

Scheme 1.11 Photoredox-mediated intramolecular olefin hydroamination. Reagents and conditions: aniline (1 equiv.), [Ir(ppy)$_2$(dtbbpy)]PF$_6$ (2 mol%), MeOH (0.05 M), rt, blue LEDs.

Knowles and co-workers' intramolecular olefin hydroamination, in comparison, relies on oxidation of an amine, instead of its deactivation with electron-withdrawing groups. Whilst the protocol was only applicable to substrates containing both aniline-type nitrogen atoms and styrenyl acceptors, thirty-three examples of both 5-*exo-trig* and 6-*exo-trig* cyclisations were reported in good to excellent yield (44-95%).[26,37] Irradiation and excitation of [Ir(ppy)$_2$(dtbbpy)]PF$_6$ facilitates electron transfer from the amine substrate to the photocatalyst

to give an aminium radical cation. In the presence of a styrene group and under sufficiently dilute reaction conditions, *exo-trig* cyclisation is promoted to form distal radical cation **19** (Scheme 1.11). The reduced form of the photocatalyst is reducing enough to act as an electron donor, converting radical **19** into anion **20**. Proton transfer then results in the isolable cyclic product. When the reaction was trialled with $Ru(bpy)_3Cl_2$, only a small amount of product was detected, and instead the major product isolated was from dimerisation of benzylic radical **19**. This result indicated that the oxidation of the Ru(I) species back to Ru(II) was not fast enough to compete with the dimerisation pathway which irreversibly deactivated the catalyst. $[Ir(ppy)_2(dtbbpy)]PF_6$ on the other hand has a less oxidising excited state than $Ru(bpy)_3Cl_2$, but importantly for this reaction has a much more reducing Ir(II) ground state, ensuring fast formation of carbanion **20**. Similar systems have also been developed by Nicewicz.[38,39]

Photoredox catalysis has proven to be a valuable tool to construct complex compounds using unique chemical reactivity. The photocatalysts involved are powerful oxidants and reductants when in their excited forms, and reactions are generally mild and tolerant of a wide variety of functional groups. Photocatalysis has been applied to an astounding range of transformations and will surely remain a formidable tool in organic synthesis for years to come.

Chapter One – Part II: The Relevance of Cyclic Fluorinated Building Blocks

1.4 The Importance of Fluorination in Drug Discovery

In 2018, fluorine-containing compounds represented 50% of blockbuster drugs,[40] and almost 30% of all drugs approved by the FDA in 2019 contained at least one fluorine atom.[41] In the past fluorine has been used as a replacement for hydrogen, due to its ability to block oxidative metabolic pathways in benzylic positions for example.[42] However, in more recent years, fluorine and in particular the *gem*-difluoromethylene unit has also been described as a possible bioisotere of alcohols, carbonyls, ethers and phosphates.[43] In the place of these functional groups, the fluorinated motif can emulate specific properties that would be observed in a biological setting. Unfortunately, the synthetic accessibility of certain fluorinated building blocks is limited. Grygorenko and co-workers conducted a Reaxys database search of *gem*-difluorinated cycloalkanes in 2019 and found that while these compounds were all routinely used in patents to build structure-activity relationships, C2-substituted compounds were less well represented in papers than their C3-substituted counterparts (Figure 1.6).[43] Therefore, it is key to continue development of synthesis routes towards more challenging fluorine-substitution patterns.

As well as its use as a bioisostere, the application of this element in a compound of pharmaceutical interest can further influence physicochemical and pharmacokinetic properties. For example, fluorination can increase a drugs half-life *in vivo* due to altered metabolism, or by modulation of lipophilicity (logP).[44] As fluorine is highly electronegative, it can modify the basicity of nearby functional groups which, in turn, can affect important factors in drug design, including protein binding, membrane permeability and potency.[44,45]

Figure 1.6 Grygorenko and co-workers Reaxys database search results showing the number of papers and patents associated with gem-difluorinated cycloalkanes.

1.4.1 Lipophilicity

Lipophilicity (or logP value) is hugely important in drug design and is a measure of a compound's affinity to lipids/ non-polar solvents. It is determined by the distribution of a given compound between an organic phase (*n*-octanol) and an aqueous phase (water). Lipophilicity plays a role in drug solubility, permeability and distribution around the body, as well as in excretion and so can impact the developability of a drug candidate. Fluorination can often have a significant effect on lipophilicity, and so has applications in the fine-tuning of the physicochemical properties of a given compound. Linclau and co-workers recently conducted a thorough investigation into the effect of fluorination on the lipophilicity of a range of aliphatic alcohols. In all examples, mono- and difluorination led to a decrease in lipophilicity compared to the parent compound (Figure 1.7).[46] This is in contrast to the trend of increased lipophilicities observed upon fluorination of aromatic compounds.[46] Substitution of methyl groups for trifluoromethyl groups gave more varied results, in some cases decreasing lipophilicity and in other compounds increasing it. Therefore, fluorination can be used as a tool to both increase and decrease lipophilicity. Figure 1.7 (a) shows that relative to 1-propanol, the monofluorinated and difluorinated analogues have decreased logP values. The trifluorinated analogue however, has an increased logP value. This change in lipophilicity upon fluorination can be rationalised using a model developed by Müller which is based on dipole moment and hydrophobic volumes.[47] The group assume a perfect tetrahedral geometry is adopted alongside other simplifications to analyse C-F polarity vectors (Table 1.3).

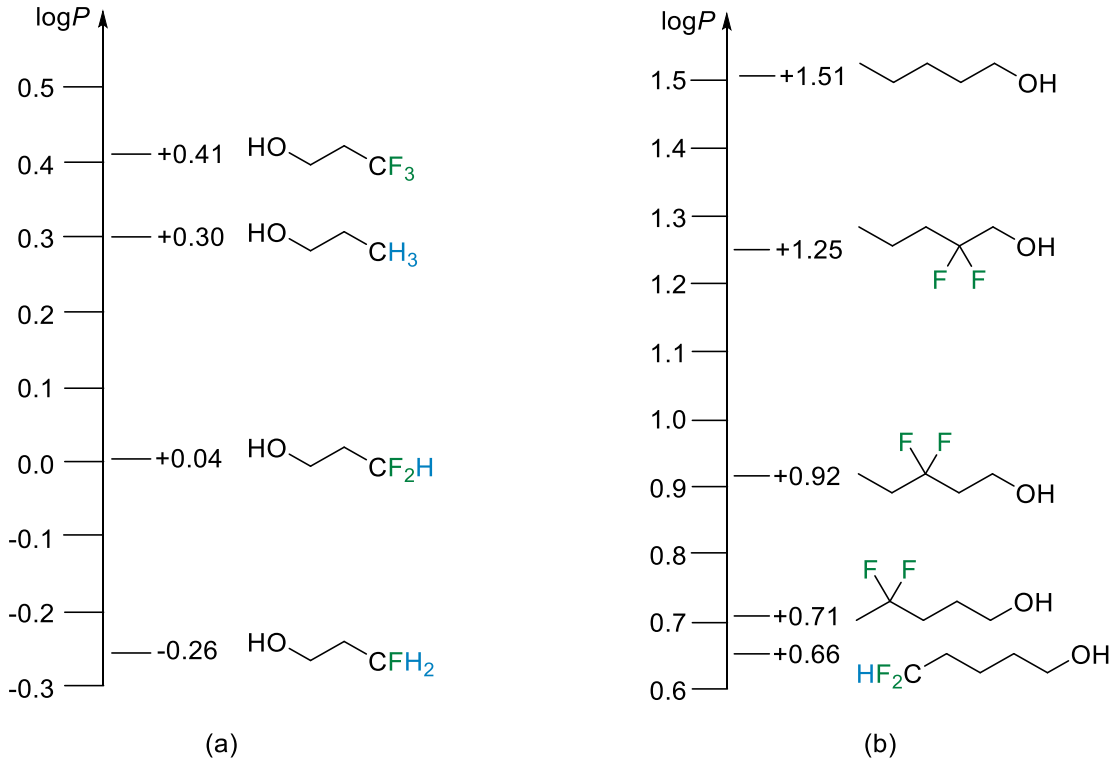

Figure 1.7 (a) The effect of various fluorination patterns on the lipophilicity of 1-propanol. (b) The effect of proximity of the difluoro- group relative to the alcohol functional group in 1-pentanol on lipophilicity.

Fluoromethane has a single C-F bond and so its overall dipole moment is represented by μ_{CF}. Difluoromethane has two C-F bonds but only the vertical component of each vector is taken into consideration (approximately 60% of the total dipole moment), giving an overall dipole approximately 1.2 times greater than that of fluoromethane. Applying the same logic to trifluoromethane, the predicted dipole moment is approximately equal to fluoromethane's.

Dipole, μ	1.85 D $\mu \sim \mu_{CF}$	1.97 D $\mu \sim 1.2\mu_{CF}$	1.65 D $\mu \sim 3 \times 1/3\mu_{CF}$

Table 1.3 C-F polarity vector analysis to understand lipophilicities observed experimentally.

However, in practice the observed dipole moment of trifluoromethane was lower than expected, most likely due to deviations from ideality. An overall increase in dipole moment upon fluorination should translate to a decrease in lipophilicity, but this is balanced by an

increase in hydrophobic surface area which in turn increases lipophilicity. Therefore, the observed lipophilicity is dependent on both of these factors. The decrease in lipophilicity between mono- and difluorinated examples (Figure 1.7 (a)) would be expected to be greater but the increase associated with the larger hydrophobic surface area gives an overall difference of only -0.30 units. The CF_3 analogue has a similar dipole moment to the mono-fluorinated example but has a much larger hydrophobic surface area, leading to an increased logP overall. (Figure 1.7 (b)) shows logP decreasing with distance from the alcohol group. When the difluoro- group is closest to the alcohol, there is potential for the C-O and C-F dipoles be in the antiperiplanar conformation so they counteract. The polarisability of the oxygen lone pairs is also reduced by the negative inductive effect of the fluorine atoms. Both of these factors increase overall lipophilicity and as they have less effect with distance from the alcohol, they will have less of an effect on logP, hence the observed trend.

1.4.2 Acidity and Basicity

Fluorination close to other functional groups such as amines (or alcohols) can affect their pK_a. As amines are often involved in non-covalent interactions, such as the binding of a compound to an active site, modulating the basicity of a drug *via* fluorination represents a powerful tool in medicinal chemistry. In the case of simple aliphatic amines, the addition of a fluorine atom on the β-carbon decreases the basicity, and the effect this has decreases with distance (Table 1.4 and Table 1.5).

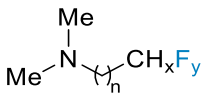

n	ΔpK_aH (H_2O)
1	-1.7 per β-F
2	-0.7 per γ-F
3	-0.3 per δ-F
4	-0.1 per ε-F

Table 1.4 Effect of carbon chain length on fluorinated amine basicity.

The effect is additive and so for each additional β-fluorine a decrease in basicity by 1.7 pK_aH units is observed (Table 1.4).[48] As the carbon chain length increases, the change in pK_aH upon fluorination lessens. The biggest decrease is observed between the β- and γ- positions, and fluorination in the *ε*-position has only a minor impact on amine basicity. This is exemplified with

triethylamine (pK_aH = 10.7), where sequential fluorination decreases the pK_aH by ~1.7 units to 2,2,2-trifluoroethylamine (pK_aH = 5.7) which has a basicity comparable to that of pyridine (Table 1.5(a)). A similar additive effect is seen in cyclic systems but with the added complexity that the electron-withdrawing effect of the fluorine atom(s) are felt down both sides of the ring so the effect is multiplied.[45] For example, 2-fluoropiperidine has one fluorine atom which is both β- and δ- to the amine depending on which way you count around the ring. Therefore, using Table 1.4 the predicted pK_aH would be 11.1 (pK_aH of piperidine) minus 1.7 (1 × β-F) minus 0.3 (1 × δ-F) = 9.1 which is close to the observed value of 9.3 (Table 1.5(b)). As a result, cyclic amines show larger differences in pK_aH upon fluorination than in straight-chain aliphatics.

Amine	pK_aH (H_2O)	ΔpK_aH (H_2O)
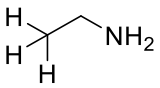	10.7	–
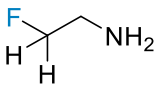	9.0	-1.7
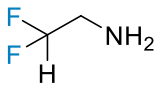	7.3	-3.4
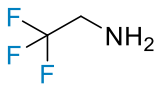	5.7	-5.0

(a)

Amine	pK_aH (H_2O)	ΔpK_aH (H_2O)
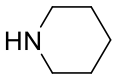	11.1	–
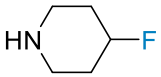	9.4	-1.7
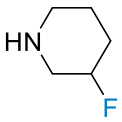	9.3	-1.8
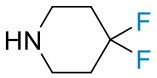	8.5	-2.6

(b)

Table 1.5 (a) Effect of β-fluorine substitution on amine basicity and the difference in pK_a units relative to the non-fluorinated parent compound. (b) Effect of fluorine substitution on cyclic amine basicity and the difference in pK_aH units relative to the non-fluorinated parent compound.

As well as impacting binding ability, changes in pK_a can also affect bioavailability by altering how well a compound is absorbed into the blood stream. This was observed in the development of c-Met inhibitor GEN-890 where the lower pK_aH achieved after fluorination led to improved pharmacologic properties (Table 1.6).[43]

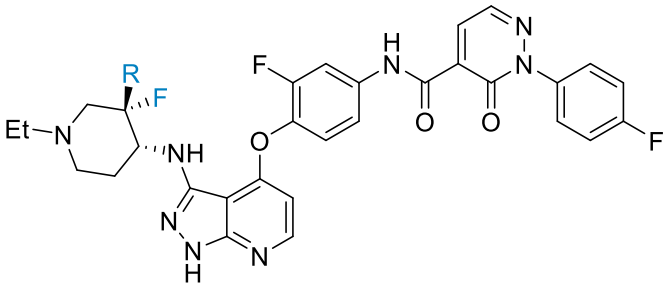

	GEN-203	GEN-890
R	H	F
pK_aH	7.45	5.93
cLogP	4.3	5.2
cMet potency (nM)	35	15
V_d (mL/min/kg)	3.64	0.99

Table 1.6 Mono- vs difluorination in the development of c-Met inhibitor GEN-890.

In comparison to GEN-203 where only one fluorine atom is present, GEN890 has a pK_a 1.48 units lower which crucially led to the compound being 2.3 times more potent, with an approximately 4 times lower volume of distribution.[43] These properties mean a smaller dose of a drug is required to achieve a set plasma concentration level.

1.4.3 Metabolism

The metabolism of a compound is key to its effectiveness and a balance must be drawn. The drug needs to be stable enough *in vivo* for it to be effective, yet needs to be broken down within a reasonable length of time to avoid accumulation in the blood stream. Lipophilic compounds are often metabolised by cytochrome P450 enzymes found in the liver, and so making a compound more polar, perhaps by fluorination, can overcome this. Alternatively, replacement of a hydrogen atom for fluorine is often trialled at a position which may be susceptible to metabolic attack. Often, the reasoning behind this is that the strong C-F bond (116 kcal/mol) is less susceptible to oxidative attack than the weaker C-H bond (99 kcal/mol)[49], thereby extending the half-life of a drug *in vivo*. Fluorine substitution at a site adjacent to the site of oxidation can also affect drug metabolism due to the atom's negative inductive effect.[49]

An example of this concept was illustrated in the development of Ezetimibe, a drug used to control high blood cholesterol levels (Figure 1.8).

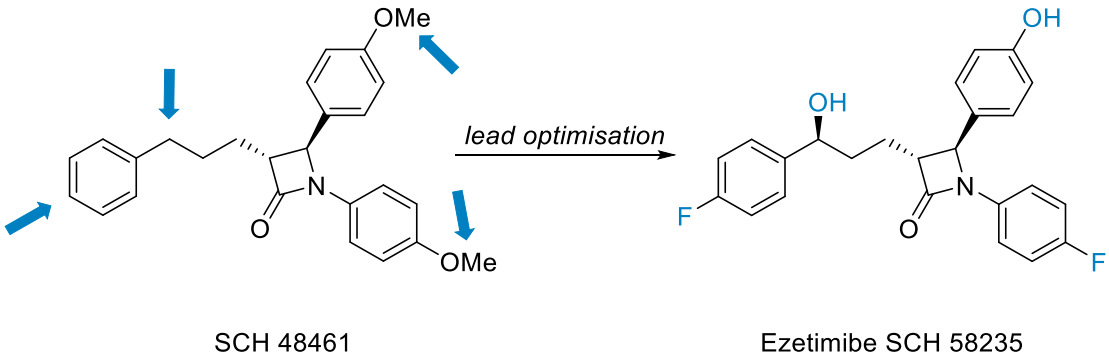

Figure 1.8 Sites of metabolic attack on SCH 48461 and lead optimisation utilising fluorination strategies to give potent Ezetimibe.

Compound SCH 48461 was identified as an intestinal cholesterol absorption inhibitor but was prone to metabolism at four sites (Figure 1.8). Through an SAR study, compound SCH 58235 emerged, with fluorine introduced in two positions which were previously susceptible to hydroxylation and demethylation respectively. These changes blocked oxidation by P450 liver enzymes by deactivating the aromatic rings and, as a result, SCH 58235 was determined to be four-hundred times more potent than SCH 48461 when tested in hamsters.[50]

Ivosidenib was a compound approved in 2018 for the treatment of acute myeloid leukaemia, in patients whose cancer had relapsed or showed resistance to other treatments (Figure 1.9). It has also been used in the treatment of glioma cell cancers and in trials for bile duct cancer.[40]

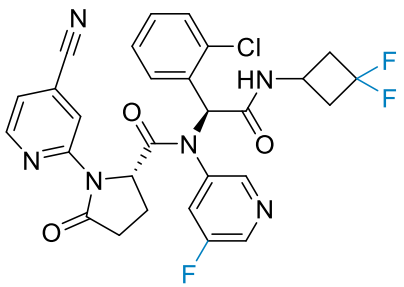

Figure 1.9 Structure of Ivosidenib containing three fluorine atoms.

During optimisation, replacement of a cyclohexyl moiety for a difluorocyclobutyl group led to greater metabolic stability but reduced potency. The largest impact on potency arose from the introduction of the fluoro-pyridine group. Fluorine substitution on this ring increased potency in both enzyme and cell-based assays (6 nM and 1 nM potency respectively), and increased microsomal stability which is an assay used to determine stability to phase I and II enzyme pathways.[51]

1.4.4 Conformation

Fluorine can be used to effect a favourable change in the molecular conformation of a compound. Whilst the steric effect of replacing a fluorine atom for a hydrogen or hydroxyl group is small, the large electronegativity difference and highly polarised C-F bond can allow for conformational control. For example, 1,2-difluoroethane is more stable in a *gauche* rather than *anti* conformation (Figure 1.10).

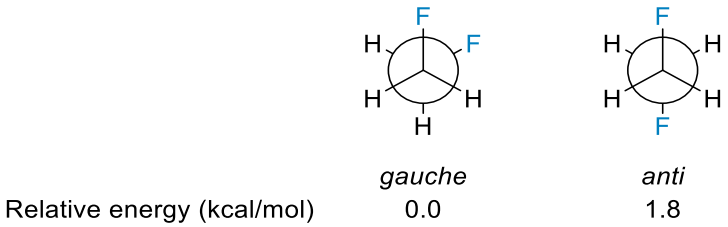

Figure 1.10 Preferred gauche conformation of 1,2-difluoroethane.

This is because the *gauche* conformation places a hydrogen atom antiperiplanar to both fluorines which can each donate electron density from the C-H σ bond into the low-lying C-F σ* orbital *via* hyperconjugation.[45] There are also clear conformational preferences when a fluorine atom is adjacent to functional groups such as carbonyls, amides or alcohols.[45,52] Knowledge of these preferences could be used in the design of drug targets, placing fluorine atoms systematically to yield a desired conformation. This concept was demonstrated by Abell and co-workers where fluorination of a β-peptide led to a difference in secondary structure when folded.[53] They observed that a fluorine atom α to a carbonyl adopted an antiperiplanar conformation, and a fluorine atom β to an amide nitrogen adopted a *gauche* conformation. Further to this, for β-peptides containing less than thirteen residues, the energetic preference for an antiperiplanar conformation between the C-F and C=O bonds of the fluorinated peptide

outweighs the benefits of complete helix formation. Therefore, hydrogen bonds and side-chain interactions that would normally be observed in the helix are disrupted and entirely different secondary structures are seen.[53]

It has also been reported that the multiple fluorination of aromatic rings can lead to a decrease in quadrupole moment which in turn can have large effects on π–π stacking or cation–π stacking.[54] In this way, it is possible to exploit specific interactions between fluorine and the binding site of a target protein. Abbate and co-workers synthesised a perfluorobenzoyl analogue of methazolamide (Figure 1.11), a carbonic anhydrase II inhibitor used in the treatment of glaucoma.[55] It was found that the addition of the perfluorinated aromatic ring led to the compound binding almost ten times more strongly than methazolamide to the enzyme active site (K_I of 1.5 nM *vs* 14 nM).[56]

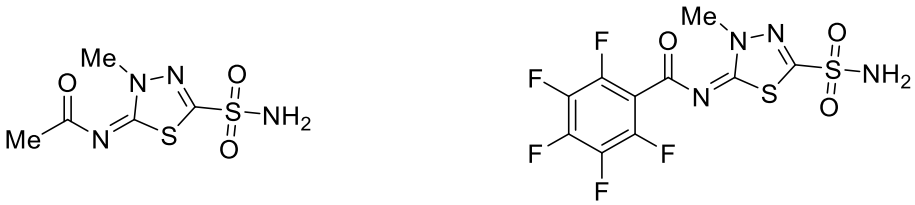

methazolamide perfluorobenzoyl analogue of methazolamide

Figure 1.11 Structures of methazolamide and a perfluorobenzoyl derivative.

This was due a new stacking interaction between the fluorinated aromatic ring in the analogue and the aromatic ring in the Phe131 residue found at the entrance to the active site. The five fluorine atoms are so strongly electron-withdrawing that the electron density of the π aromatic system of the inhibitor is diminished and there is a partial positive charge above and below the ring system (Figure 1.12). This reversal means there are complementary differences between the fluorinated ring and the benzene ring of the phenylalanine residue, meaning they can stack almost parallel (Figure 1.13).

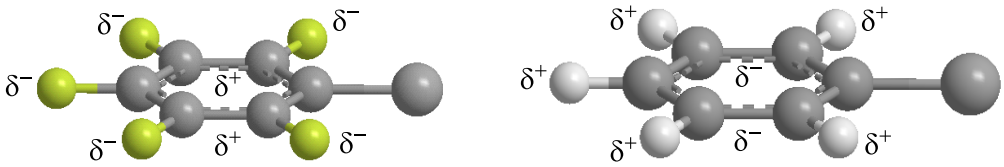

Figure 1.12 Schematic diagram of a polyfluorinated aromatic ring (left) and a non-fluorinated aromatic ring (right) and their regions of partial charges.

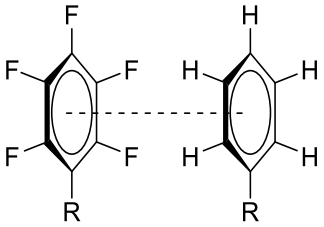

Figure 1.13 The parallel stacking interaction of a fluorinated aromatic ring with a non-fluorinated ring such due to attractive partial charges.

One of the problems limiting medicinal chemists is the lack of access to certain fluorine-containing fragments. Whilst screening of fluorine substitution patterns (a 'fluorine scan') has become commonplace in SAR studies, new methodologies are required for the introduction of fluorine at challenging but desirable positions.[57] The benefits of this research would not just impact the pharmaceutical industry but also the agrochemical industry where 25% of commercial agrochemicals contain at least one fluorine atom.[58]

1.5 The Importance of Expanding Chemical Space

It is well known that the process of bringing a drug to market is fraught with failure, with the success rate of bringing a compound from Phase I to licence application standing at only 10%.[59] Analysis of fragment libraries used for lead generation in pharmaceutical companies has shown that they generally contain a large proportion of two-dimensional and sp^2 rich compounds.[60] Natural products, on the other hand, have highly three-dimensional structures, and when it is considered that protein active sites are also 3D, this seems logical. In recent years, interest has shifted to increasing the shape diversity of compound libraries to explore new chemical space. Another motivator for this is the growing issue of an overcrowded IP space associated with drug molecules containing these 2D features. In 2012 Pfizer reported bicyclo[1.1.1]pentane as a saturated bioisotere of benzene.[61] In the place of a phenyl group in γ-secretase inhibitor BMS-708,163 **21**, used in the treatment of Alzheimer's disease, the analogue **22** (Figure 1.14) showed improved physicochemical properties such as increased solubility, activity and metabolic stability. The aromatic ring was not involved in any enzyme-inhibitor interactions and served mainly to ensure the oxadiazole and sulfonamide groups were

in the desired orientation.[61] At the time the bicyclo[1.1.1]pentane moiety was patent-free and it has since been featured in over 100 patents.[62]

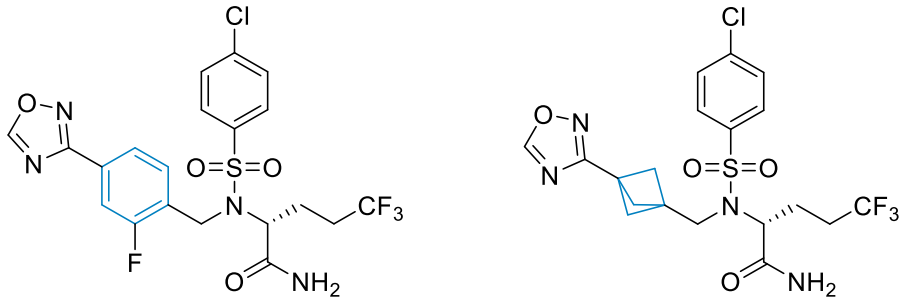

BMS-708,163
21

22

Figure 1.14 Replacement of an aromatic ring in BMS-708,163 with a bicyclo[1.1.1]pentane containing analogue.

The concept of increasing shape diversity was first coined 'Escape from Flatland' by Lovering in 2009, when it was hypothesised that high throughput synthesis methods commonly used in industry had resulted in a disproportionate number of achiral and aromatic compounds in databases.[63] Fragment-based drug discovery (FBDD) has come to the fore in the last 20 years as a method to identify 'lead-like' compounds. Fragments are low molecular weight (MW <300 Da) compounds and generally have higher hit rates and a wider sampling of chemical space than traditional HTS methods. The 'drug developability' of fragments is often determined from a number of factors including the fraction of sp^3 carbons (Fsp^3) present, number of hydrogen bond donors/ acceptors, number of rotatable bonds, molecular weight, lipophilicity and the topological polar surface area. Interestingly, it has been noted that higher Fsp^3 values tend to correlate with higher compound solubilities and reduced toxicities.[64] However, Fsp^3 is not always a good indicator for the true three-dimensionality of a compound and instead, principal moments of inertia (PMI) plots are often used (Figure 1.15). Each vertex of the plot represents an extreme molecular geometry – linear (diacetylene), spherical (adamantane) and disc-like (benzene).[65] The vast majority of pharmaceutical library compounds sit close to the linear/disc-like edge.[66] Compounds (a)-(e) exemplify the difference between Fsp^3 calculations and PMI plots. All five compounds lie close to the linear/disc-like edge, with (a)-(c) closer to being linear

and (d) and (e) being more disc-like. None of the compounds are close to the spherical vertex. However, the Fsp^3 values of these compounds range from zero to one. Imidazole (b) has an Fsp^3 value of 0 suggesting little 3D shape and its position is on the edge of the PMI plot. Therefore, these two pieces of information correlate well. In contrast, morpholine (d) has an Fsp^3 value of 1 which would indicate a highly 3D structure but the PMI plot shows this compound is instead very disc-like. Ibuprofen (a), 2-methoxyacetic acid (c), and Simvastatin (e) have Fsp^3 values of 0.46, 0.67 and 0.76 respectively suggesting some degree of three-dimensionality, but in reality are quite flat.

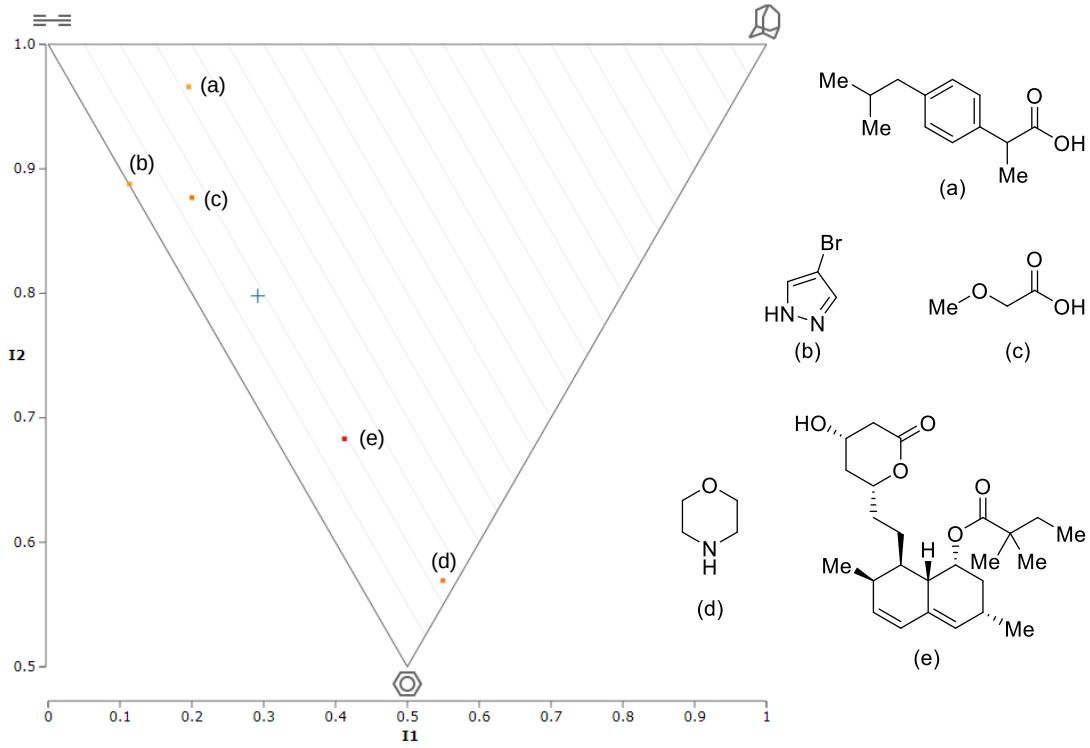

Figure 1.15 PMI plot for compounds (a)-(e) generated using LLAMA.[65]

It is important to develop reactions that install more structural complexity in three-dimensional chemical space, bearing in mind that compounds which appear 3D on paper do not necessarily have 3D shapes in reality. Fluorine can be utilised to tune the conformation of a compound (Section 1.4.4) and so it is possible it can be put to use in the exploration of new pharmaceutic space.

1.6 Fluorination Methods in Aliphatics

Traditionally, compounds containing fluorine were synthesised using fluorinating reagents such as HF, F_2, KF, or SF_4, but the reactions can suffer from poor selectivities and/or harsh conditions.[67–69] There have been many developments of milder and more selective fluorination strategies and these new reagents broadly fall under one of two categories – nucleophilic or electrophilic fluorinating reagents.[70] There is a vastly growing demand for fluorine-containing compounds and so many are now available in commercial catalogues.

Nucleophilic fluorination is limited by the high solvation energy of the fluoride anion and its strong hydrogen bonding ability (Figure 1.16),[71] the stabilisation from which leads to the anion being only weakly nucleophilic. Challenges also arise from its second role as a strong base which often leads to unwanted side reactions occurring.[72] Common nucleophilic fluorinating reagents include fluoride salts (KF, CsF, AgF, TBAF), HF.amine complexes, DAST, Deoxo-Fluor, PhenoFluor and many more. A number of review articles have been published detailing the developments in this area.[72–74]

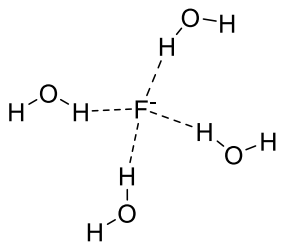

$\Delta G_{hyd}(F^-) = -111$ kcal/mol

Figure 1.16 Gibbs free energy change upon fluoride anion solvation in water.

Electrophilic fluorination on the other hand, uses F^+ equivalents, and common reagents include SelectFluor, NFSI and *N*-fluoropyridinium salts for monofluorination, and Togni's reagent or Umemoto's reagent for trifluoromethylation. These reagents are typically difficult to synthesise and their reactions are inefficient in terms of atom economy.[74] As fluorine is so strongly electronegative, the electrophilic nature of these compounds arises from the fluorine being bonded to other electronegative heteroatoms such as nitrogen, oxygen or hypervalent iodine. This causes the electron density of the fluorine atom to decrease. Methods to introduce both

one or three fluorine atoms are widely documented,[75–77] but there are fewer methods to produce geminal difluoro- substitution patterns. This area will be the main focus of this thesis.

1.6.1 *Gem*-difluorination Strategies

One of the most frequently used methods to introduce the *gem*-difluoro- group is to convert a carbonyl using DAST in a deoxofluorination reaction (Scheme 1.12). This example from the patent literature generates a cyclic β-fluorinated amine in 74% yield,[78] however, one of the limitations associated with DAST is its limited functional group tolerance.[79] Extensive protection and deprotection strategies are required to limit side-reactions with alcohols, carboxylic acids or other aldehydes/ketones present in a substrate. Elimination, fluorodesulfurisation and fluorodesilylation reactions can also occur.[80] DAST is thermally unstable and heating to 70 °C or higher for an extended amount of time presents safety concerns. Detonation has been reported during its preparation and use, with the decomposition occurring in two stages – evolution of sulfur tetrafluoride initially, followed by an explosion upon further heating.[81] Deoxo-Fluor was developed as a more thermally stable alternative, but both fluorinating reagents produce highly corrosive and toxic HF gas, react violently with water and cannot be used with standard laboratory glassware. Other deoxofluorinating reagents have been developed such as XtalFluor-E and XtalFluor-M which are more stable and more easily handled as they are crystalline, but they still react with a wide range of functional groups and often need to be used in conjunction with an exogenous fluoride source.[80]

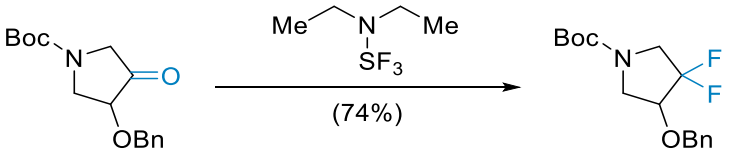

Scheme 1.12 Deoxodifluorination of ketones using DAST. Reagents and conditions: DAST (2.8 equiv.), DCE, 70 °C, 4 h, 74%.

There are many commercially available reagents containing difluoro- groups, and so this represents a large proportion of syntheses towards difluorinated target compounds. An example of such a reagent is ethyl bromodifluoroacetate, which was used in the synthesis of fluorinated derivatives of the proneurotoxin MPTP (Scheme 1.13).[82] Introduction of the difluoro- group is achieved using Reformatsky chemistry with samarium iodide and ethyl bromodifluoroacetate. However, synthesis of the benzyl-protected amino ketone starting material is required, adding multiple steps to the sequence, only to later remove this benzyl group *via* hydrogenolysis. Formation of the secondary amine leads to spontaneous ring closure (or lactamisation), facilitated by the activation of the ester carbonyl by the *gem*-difluoro group, to yield lactam **23**. The amide is then reduced to amine **24** using sodium borohydride and TFA, before chlorination and elimination to give the final product **25**. As drawn, the route is four steps but has a poor overall yield of only 8% and is not well suited for generating a diverse range of products. Protection/deprotection strategies are inefficient as are performing redox steps, particularly with the huge number of sodium borohydride equivalents required in this example.

Rimoldi 2003

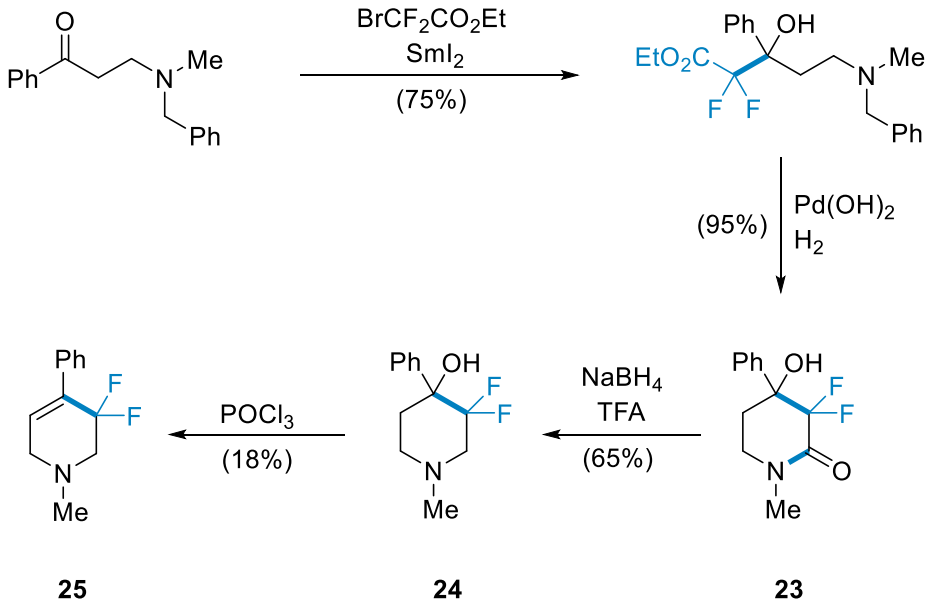

*Scheme 1.13 Synthesis of tetrahydropyridine **25**. Reagents and conditions: a) amino ketone (1 equiv.), ethyl bromodifluoroacetate (1.1 equiv.), SmI_2 (0.1 M in THF, 2 equiv.), THF (1 M), rt, 15 min. b) $Pd(OH)_2$ (10% w/w), H_2 (1 atm), MeOH (0.1 M), rt, 24 h. c) $NaBH_4$ (10 equiv.), TFA (10 equiv.), dioxane (0.25 M), 0-100 °C, 24 h. d) $POCl_3$ (1 equiv.), pyridine (0.1 M), 0 °C, 2 h.*

Another strategy involves the use of difluorocarbene to install a difluoromethylene group. Difluorocarbene is an electrophilic species and can react with alkenes and alkynes to give *gem*-difluorocyclopropanes or *gem*-difluorocyclopropenes respectively. First developed difluorocarbene precursors were toxic to the environment as they depleted ozone (HCF_2Cl or HCF_2Br), or were toxic to humans (CF_3HgI or Me_3SnCF_3), but today there are many more non-toxic and efficient difluorocarbene sources.[83] Difluorocarbene generation is initiated through thermolysis or by dehydrohalogenation using alkoxides or alkyllithiums. Mykhailiuk and co-workers reported the difluorocyclopropanation of *N*-Boc protected enamides, using either sodium chlorodifluoroacetate or Dolbier's reagent (trimethylsilyl 2-(fluorosulfonyl)-2,2-difluoroacetate, TFDA) as the fluorine source (Scheme 1.14).[84]

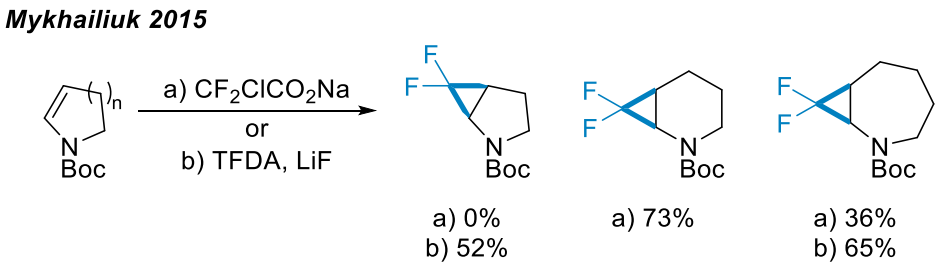

Scheme 1.14 Difluorocyclopropanation reaction using chlorodifluoroacetate or TFDA. Reagents and conditions: a) CF_2ClCO_2Na (10 equiv.), diglyme, reflux. b) TFDA (1.6-1.8 equiv.), LiF (5 mol%), toluene, reflux.

Ten equivalents of chlorodifluoroacetate were required, alongside extremely harsh reflux conditions to observe full starting material consumption, however, use of TFDA gave improved yields with a more modest number of reagent equivalents. Upon Boc group deprotection the free amines proved to be unstable to fragmentation, but the 6- and 7-membered rings could be stabilised as salts for a short time before conversion to isolable amides or carbamates. The group later reported the addition of difluorocarbene to bicyclo[1.1.0]butanes to give fluorinated bicyclo[1.1.1]pentanes.[62] Dibromo- and dichlorocarbenes were already known to react with the central electron-rich C-C bond of bicyclo[1.1.0]butanes,[85,86] and difluorocarbene is yet more electrophilic in nature. Optimisation of the reaction revealed the Ruppert-Prakash reagent (CF_3TMS) and sodium iodide as the best combination of reagents for the transformation (Scheme 1.15). The use of difluorocarbenes generated *via* the Ruppert-Prakash reagent

represents an atom-economical approach to installing the difluoro- group. The reagent is also non-toxic and easy to handle.

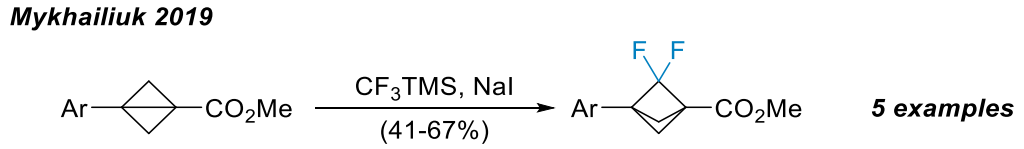

Scheme 1.15 Difluorocarbene addition to bicyclo[1.1.0]butanes. Reagents and conditions: CF_3TMS (3 equiv.), NaI (0.5 equiv.), THF (0.3 M), 65 °C, 4 h.

Possibly the most common occurrence of the *gem*-difluoro- moiety is as a terminal difluoromethyl group, a bioisotere of the hydroxyl group. It can act as a more lipophilic hydrogen bond donor, which in turn can positively effect membrane permeability.[87] Publications in this area have largely focused on difluoromethyl arenes, but there are a number of publications with this functional group present in aliphatic compounds. For example, Radchenko and co-workers utilised $TMSCF_2H$, made from the reduction of $TMSCF_3$ with sodium borohydride, in a nucleophilic addition reaction to ketones, including enolisable ketones (Scheme 1.16).[87]

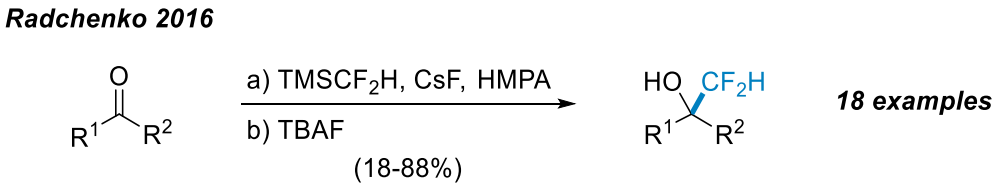

Scheme 1.16 Synthesis of difluoromethyl alcohols using $TMSCF_2H$. Reagents and conditions: a) $TMSCF_2H$ (2 equiv.), CsF (0.3 equiv.), HMPA (5 equiv.), THF, rt, 24 h. b) TBAF (1 M in THF, 1 equiv.), rt, 1 h.

Of the eighteen examples, acyclic and 5-7 membered cyclic ketones performed well, as did aryl ketones. Halide, cyano, ester and tertiary amine functional groups were tolerated, however, no yield was observed in the reactions of cyclobutanones or enones. The group proposed that a low concentration of F^- anions on the surface of the insoluble caesium fluoride was maintained throughout the slow reaction, which minimises aldol side reactions from ketone enolates occurring but allowed for activation of $TMSCF_2H$.[87] The hypothesised role of

HMPA was to form a reactive hypervalent silicon species, but the reagent is highly toxic and so to use five equivalents is undesirable. It was possible to use DMPU as a safer alternative, but significantly lower yields were observed (57% *vs* 76% yield for 4-phenylcyclohexanone substrate).

Difluorodiazoethane is a useful difluoromethylation reagent, and it was only successfully synthesised as recently as 2015, despite efforts dating back to 1971. Formed *in situ* by the reaction of acetic acid and *t*-butyl nitrite, NO^+ is released which then reacts with difluoroethylamine in a diazotisation reaction (Scheme 1.17).[88] Unlike the analogous trifluorodiazoethane, difluorodiazoethane is unstable and can only be synthesised under rigorously dry conditions.

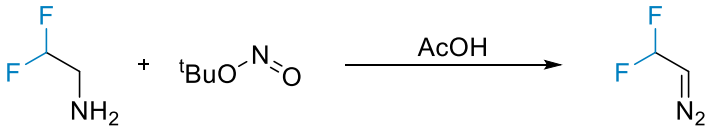

Scheme 1.17 Synthesis of difluorodiazoethane. Reagents and conditions: AcOH (5-10 mol%), $CHCl_3$, reflux, 10 mins.

Applications of this diazo compound are wide-ranging, with it being used in 1,3-dipolar cycloadditions, carbene reactions and esterification reactions (Scheme 1.18).[88,89] The diazo species is formed *in situ*, and the cycloaddition reaction extends to the use of alkenes or alkynes to give difluoromethylated pyrazolines or pyrazoles respectively, as long as an electron-withdrawing group is present. The difluoromethyl carbene was first used in a cyclopropanation reaction in 2016 by Koenigs and co-workers, with the products finding applications in various agrochemicals.[90]

Traditional choices for transition metal-catalysed cyclopropanations include iron/ rhodium porphyrins, Co(salen), Cu(I) or Ru(III) complexes but none of the desired product was formed when these were used. Limited success was found with Ru(II) complexes, but in particular the

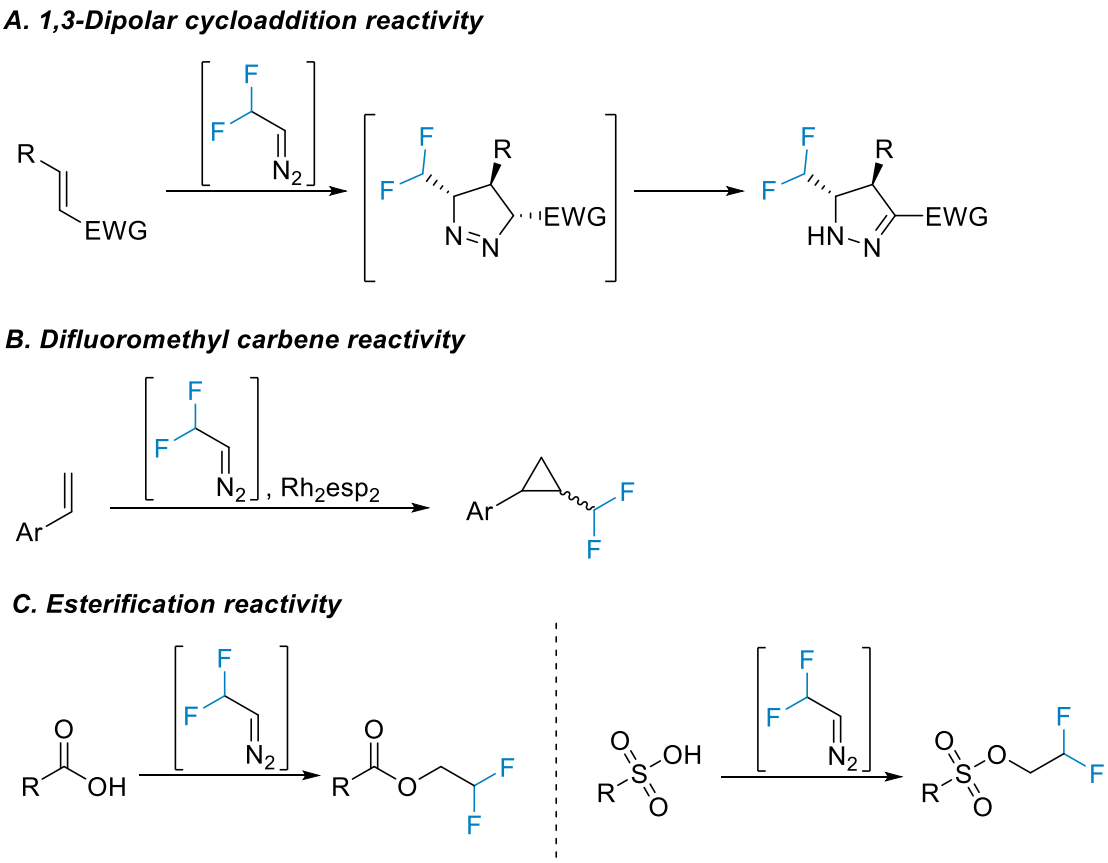

Scheme 1.18 Example applications of difluorodiazoethane.

highly sterically hindered Ru_2esp_2 catalyst gave the best results. This was proposed to be due to its steric bulk minimising the rate of β-hydride elimination from the intermediate metal-carbene.[90] The method is applicable to electron-rich or deficient styrenes as well as substituted styrenes, and does not lead to any diastereoselectivity in the products. Unlike trifluorodiazoethane which does not react with carboxylic acids, difluorodiazoethane readily undergoes esterification (Scheme 1.18).[88,91] Esterification reactions are common in the pharmaceutical industry, for example in prodrug design. With the positive pharmacological effects of fluorination, this could be a useful combination.

As has been shown, there are numerous methods for introducing the terminal difluoromethyl group, but fewer methods exist for the introduction of internal difluoro- groups. The use of nucleophilic fluorinating reagents such as DAST is typical, but reactions using these reagents suffer from low selectivity and low functional group tolerance. New methods overcoming the challenges described in this Section would be a great contribution to the field.

Chapter Two: Photoredox Radical Cyclisation of Fluorinated Amines

2.1 Introduction

2.1.1 The Occurrence and Utility of Pyrrolidines and Piperidines

Small cyclic amines are ubiquitous in organic chemistry and are found in many natural products, pharmaceuticals and agrochemicals.[92–95] Pyrrolidines and piperidines, like other amines, are basic and nucleophilic, and these chemical properties contribute to their broad biological properties and their utility in synthesis. For example, proline is a naturally occurring amino acid which is biosynthesised from L-glutamate (Figure 2.1).[96] It has been shown to act as a weak agonist of the glycine receptor, but its main application is in organic synthesis as an inexpensive chiral pool building block. The pyrrolidine ring is also present in many alkaloids such as nicotine. Likewise, piperidine based alkaloids are very common, such as piperine which gives black pepper its flavour. Morphine is an abundant opiate found in poppy seeds

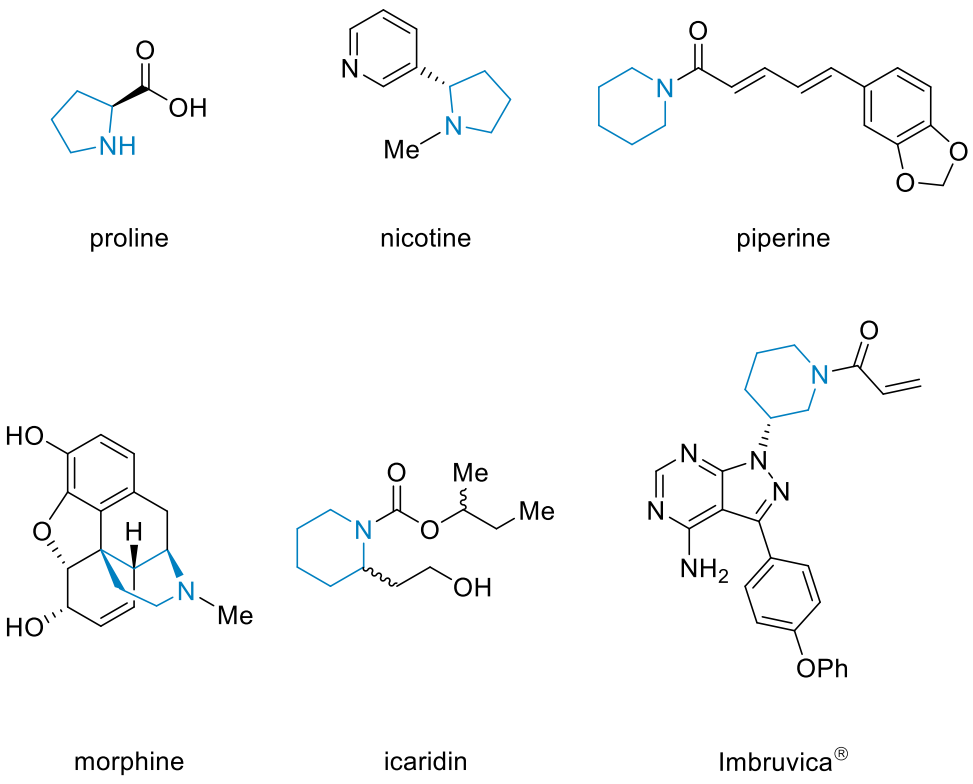

Figure 2.1 Examples of pyrrolidine and piperidine containing compounds.

and is used in a medical setting as a strong analgesic, although the substance is addictive and is prone to abuse.[97] Icaridin is an insect repellent effective against mosquitos, ticks, fleas and gnats. Finally, Imbruvica is a drug for mantle cell lymphoma which generates in excess of eight billion dollars every year.[95] It works by blocking the Bruton tyrosine kinase enzyme, helping to stop cancerous B lymphocytes from surviving and migrating around the body.

Sections 1.4 and 1.5 explored how fluorination of amines has been used to effect biological changes in compounds of pharmaceutical interest, as well as the relevance of conformationally restricted amines in this context. For these reasons and the fact that small cyclic amines are such omnipresent motifs, practical methods for the synthesis of fluorinated analogues are of significant interest to the chemical industry.

2.1.2 Aims

The project aims to deliver new methods for the construction of three-dimensional fluorinated amine building blocks for applications in drug discovery. Synthesis methods for these small, functionalised rings currently rely on hazardous fluorinating reagents such as DAST, or lengthy routes with numerous redox and protection steps (Scheme 1.12 and Scheme 1.13, Section 1.6.1),[78,82] which are not conducive for generating a diverse range of products. A more concise method to synthesise these complex structures would be a valuable addition to the field.

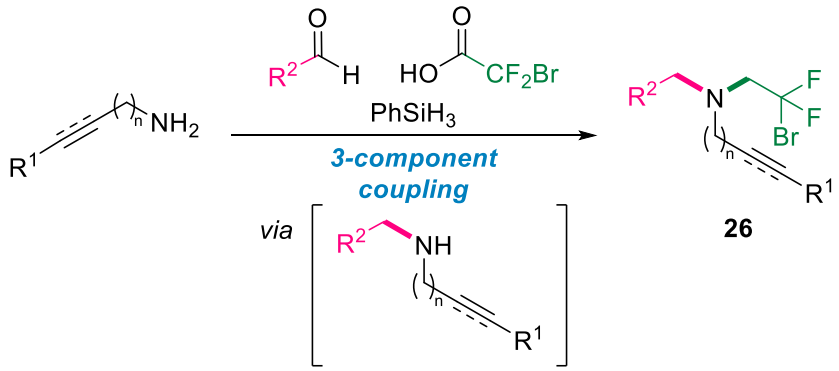

Scheme 2.1 Proposed three-component coupling using bromodifluoroacetic acid as an abundant source of fluorine.

Given the above, we envisaged a two-step strategy, utilising a method previously published by the Denton group,[98] and photoredox catalysis. Firstly, an adaptation of the trifluoroethylation of amines is proposed, using readily available primary amines, aldehydes and bromodifluoroacetic acid. This modular three-component coupling builds complex tertiary amines **26** bearing the β-difluoroethyl group in a single step (Scheme 2.1).

Secondly, from these bromodifluoroalkyl amines, we planned to develop a photoredox cyclisation protocol (Scheme 2.2). Homolytic cleavage of the carbon-bromine bond should give a carbon-centred radical ideally suited to intramolecular cyclisation. Free rotation of the amine bonds should facilitate fast cyclisation to form cyclic fluorinated amine products **27** of high value.

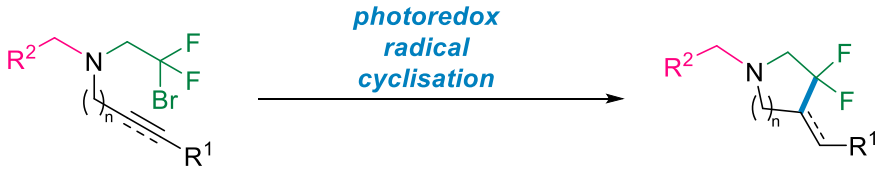

26 **27**

Scheme 2.2 Proposed photoredox radical cyclisation of bromodifluoroethyl amines.

To the best of our knowledge, photoredox cyclisations of this type have not been previously described. In photoredox systems, tertiary amines are most commonly used as sacrificial reductants, owing to the ease in which they are oxidised. This attribute has been utilised in chemistry where oxidation of an amine substrate to a radical cation triggers a C-H functionalisation or cyclisation reaction adjacent to nitrogen.[99] However, in cases where amine oxidation is undesired, researchers have circumvented the problem by using redox inert sulfonamides[7,35] or amides[100–103] as cyclisation substrates. This deactivation of the amine nitrogen atom adds additional steps to a synthesis, as subsequent deprotection or redox adjustments are required to access the amine products. We envisaged that, by making use of β-bromodifluoroethylamines **26** as cyclisation substrates, the strongly negative inductive effect of the two fluorine atoms would sufficiently deactivate the amine nitrogen towards the typical C-H functionalisation processes. As a result, the desired cyclisation pathway would be promoted, thereby giving access to valuable cyclic fluorinated amines **27** without the need for a separate amine protection/deprotection strategy.

2.2 Results and Discussion

2.2.1 Synthesis of Tertiary β-Fluoroalkylamines

With conditions for the previously published two-component and three-component trifluoroethylation of secondary and primary amines respectively in hand,[98] we set out to develop the related bromodifluoroethylation reaction. Denton and co-workers reported the successful reductive alkylation of *N*-methylbenzylamine using TFA and other strong acids such as trichloroacetic acid and difluoroacetic acid (Scheme 2.3).

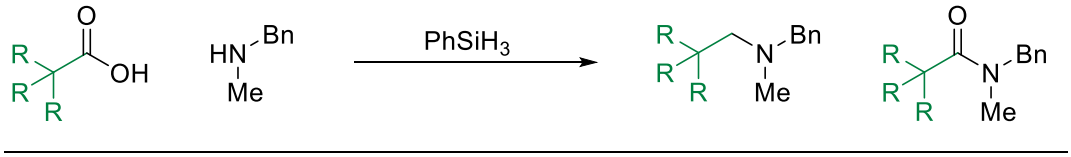

F, F, F	Cl, Cl, Cl	F, F, H	Cl, H, H
67% 85:9	60% 62:9	44% 60:30	17% 30:60

Scheme 2.3 Comparison of amine:amide ratio using different acids by Denton and co-workers. Isolated yield of amine. Ratio is conversion to amine:amide. Reagents and conditions: N-methylbenzylamine (1 equiv.), acid (2 equiv.), THF (1 M), 60 °C, 3 h.

Lower yields are observed for acids weaker than TFA.[98]. For this reason, the reaction with the strong acid, bromodifluoroacetic acid, was expected to be high yielding. Based on the mechanism suggested by Denton and co-workers, we proposed the following analogous mechanism using bromodifluoroacetic acid (Scheme 2.4). Silyl ester **28** is formed *via* amine-catalysed dehydrogenation and can then either follow a pathway generating an amide or a pathway generating the desired amine. If the concentration of acid is low, the relative concentration of free amine is high and the electrophilic silyl ester intermediate functions as an activated acid which leads to the amide product. However, when excess acid is used, the concentration of free amine is low and reduction of the silyl ester occurs to yield silyl acetal **29**. Under the acidic conditions, iminium ion **30** is generated. Phenylsilane then reduces this reactive iminium ion to give the amine product.

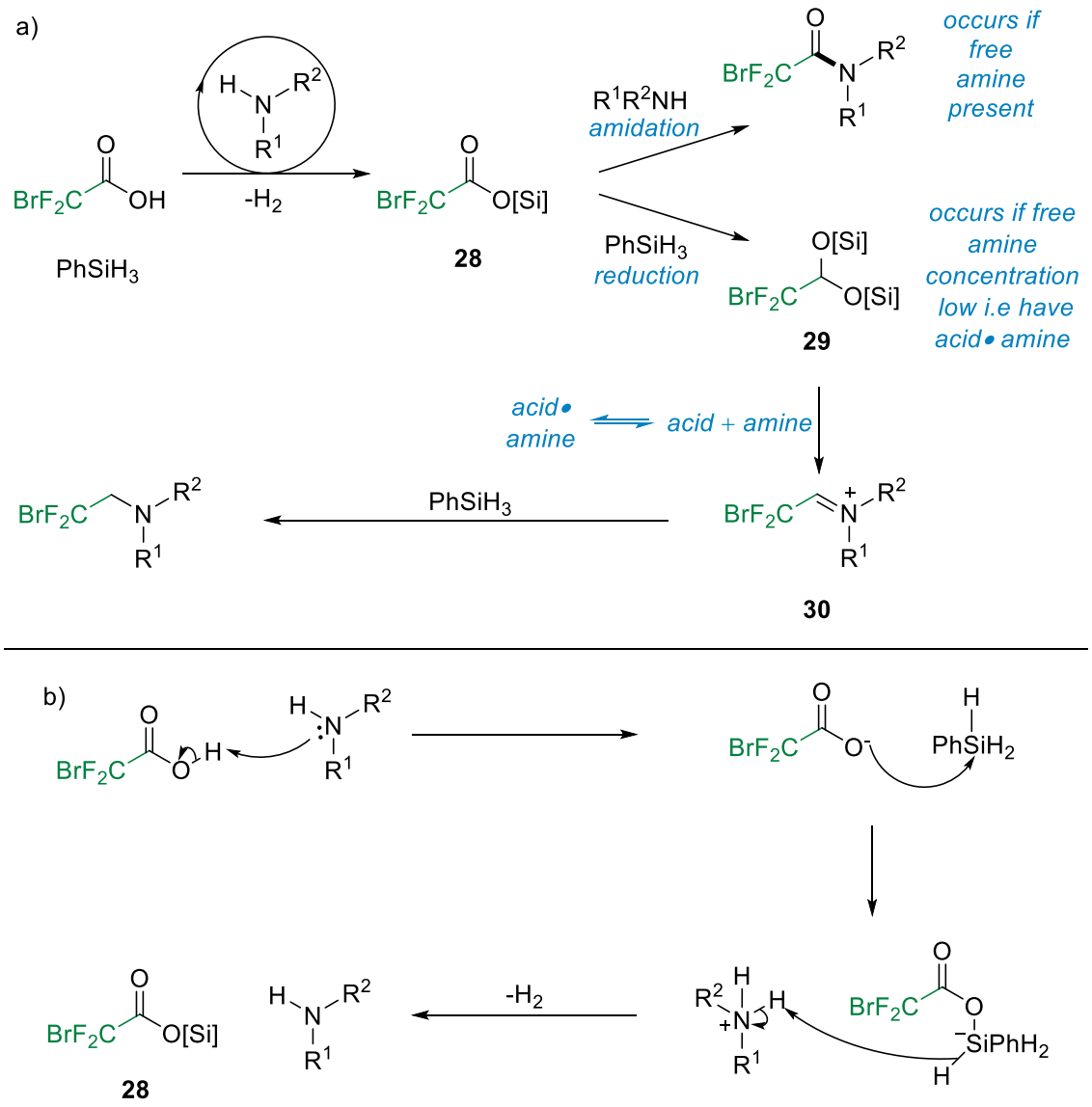

Scheme 2.4 a) Proposed mechanism for the bromodifluoroethylation reaction based on the reported trifluoroethylation pathway. b) Proposed mechanism for silyl ester formation via amine-catalysed dehydrogenation.

An exploration of the conditions was performed and optimised conditions using this acid were obtained using *N*-methylbenzylamine as a model substrate (Table 2.1). The most widely used method for the trifluoroethylation of amines involves reduction of trifluoromethylamides (made *via* trifluoroacetic anhydride) with lithium aluminium hydride or borane.[104,105] Not only is this a two-step procedure but these reagents are pyrophoric and substrates containing other reducible functional groups are precluded. We are also able to avoid unnecessary and uneconomical redox steps with this one-step alternative strategy.

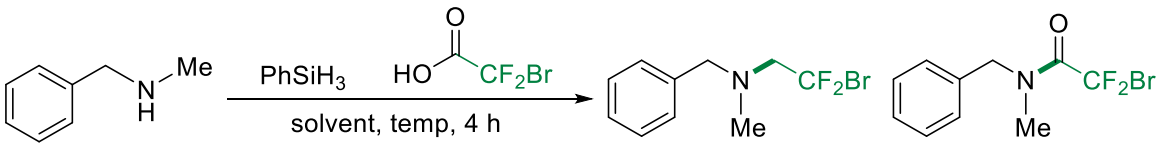

31 **32**

entry	$PhSiH_3$ (equiv.)	acid (equiv.)	solvent	temp /°C	yield /%	ratio amine:amide
1	2	2	THF	70	76	99:1
2	2	3	THF	70	79	99:1
3	4	2	THF	70	83	93:7
4	8	2	THF	70	69	85:15
5	2	1	THF	70	58	85:15
6	4	2	toluene	110	83	96:4
7	4	2	MeCN	82	69	99:1
8	3	2	THF	70	89	99:1
9	4	2	MeCN	70	82	99:1

Table 2.1 Optimisation of bromodifluoroethylation reaction. Yields determined by ^{19}F NMR spectroscopy using trifluorotoluene as an internal standard.

From the originally published conditions (entry 1,Table 2.1), increasing the equivalents of acid from two to three (entry 2) showed a 3% increase in yield, whereas decreasing the equivalents to one (entry 5) gave a decrease in yield to 58% along with a higher proportion of amide by-product **32**. This result is in keeping with the proposed mechanistic pathway. It was decided that the increase in yield associated with an extra equivalent of bromodifluoroacetic acid was insignificant. Instead, increasing the equivalents of phenylsilane from two to eight incrementally (entries 1, 3, 4 and 8) showed an increase in yield up to three equivalents (89%), then a decrease to 83% (four equivalents) and 69% (eight equivalents). It is likely that beyond three equivalents, phenylsilane participates in more off-cycle activity, lowering the yield of **31**. Different solvents at reflux were explored including THF, toluene and MeCN (entries 3, 6 and 7), with THF and toluene proving to be equally high yielding. Interestingly, when using MeCN, lowering the temperature from 82 °C to 70 °C showed an increase in yield from 69% to 82% (entry 7 *vs* 9). The optimum conditions were chosen based on entry 8. THF was a preferred solvent choice over toluene based on toxicity and ease of handling in the work-up.

Using either the two-component protocol with a secondary amine, or the three-component protocol (Scheme 2.1) with a primary amine and aldehyde, tertiary amines **33**–**40** were synthesised (Scheme 2.5 and Scheme 2.6). In the three-component protocol, the primary amine and aldehyde are first heated with phenylsilane in a reductive amination reaction, forming a secondary amine *in situ* which then goes on to react with bromodifluoroacetic acid, as is the case in the two-component protocol. Advantageously, a complex, bespoke, β-fluorinated amine core is generated without the need for pre-functionalisation of the amine precursor, therefore saving on step count.

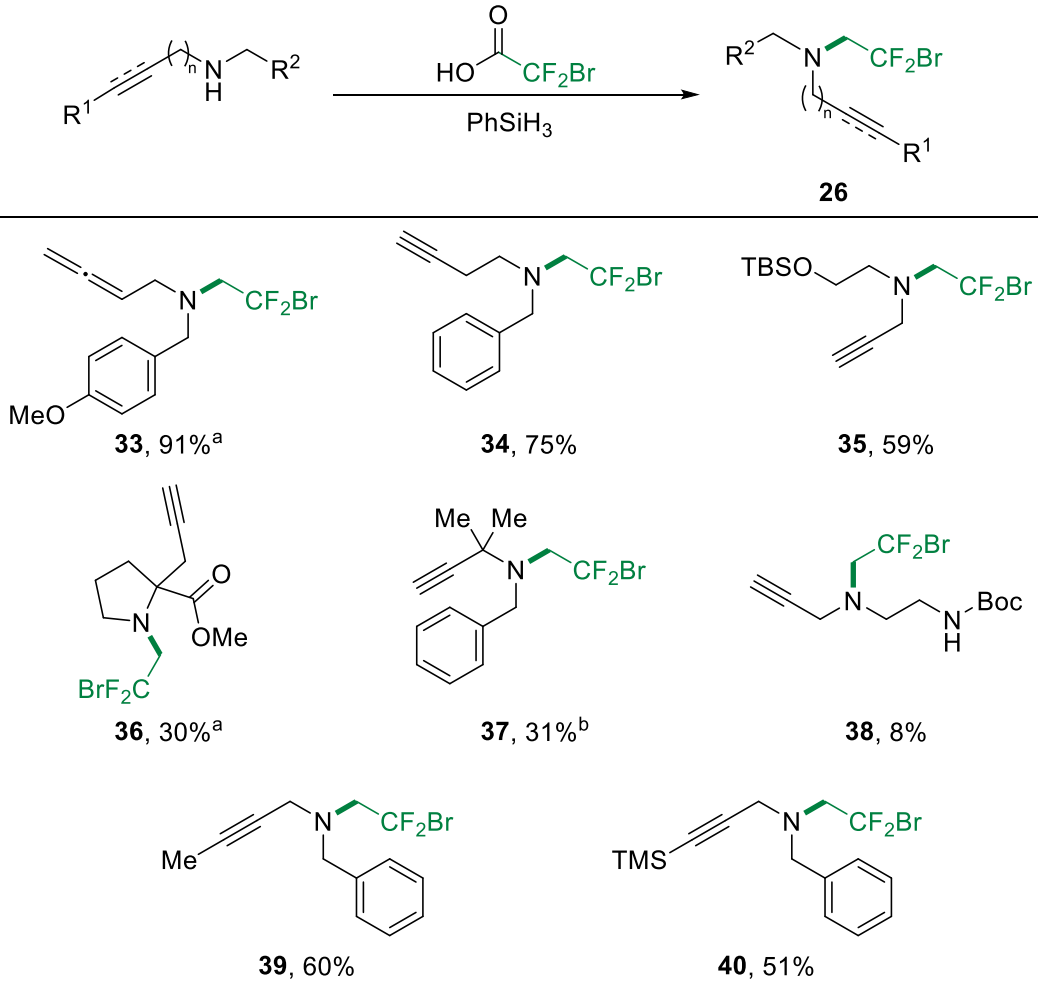

Scheme 2.5 Scope of the two-component bromodifluoroethylation reaction. Reagents and conditions: secondary amine (1 equiv.), $PhSiH_3$ (3 equiv.), bromodifluoroacetic acid (2 equiv.), THF (1.0 M), 70 °C. [a]Et_3N (1 equiv.) added. [b]Reaction charged with further $PhSiH_3$ (3 equiv.), bromodifluoroacetic acid (2 equiv.) after 16 h.

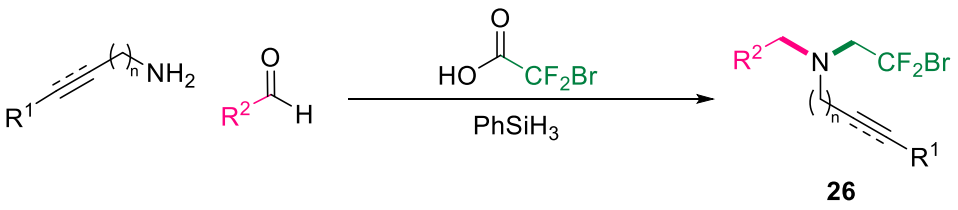

26

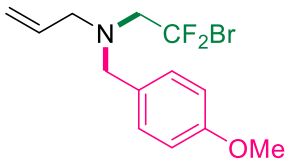

41, 52%

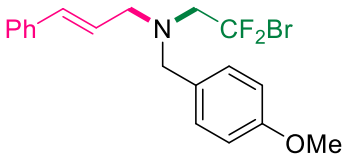

42, 57%

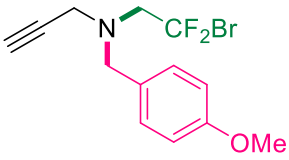

43, 56%

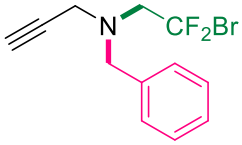

44, 38%

Scheme 2.6 Scope of the three-component bromodifluoroethylation reaction. Reagents and conditions: primary amine (1 equiv.), aldehyde (1 equiv.), $PhSiH_3$ (0.5 equiv.), THF (1.0 M), 70 °C, 10 min, then $PhSiH_3$ (3 equiv.), bromodifluoroacetic acid (2 equiv.), 70 °C.

Beginning with the two-component reaction (Scheme 2.5), it can be seen that amines bearing electron-donating groups such as PMB give products in higher yield. Allene **33** in particular was generated in high yield due to the amine being very electron rich. This promotes reaction of the amine with the silyl acetal species formed *in situ* to give an iminium species. Secondary amine starting materials giving products **34**, **35**, **39** and **40** are also reasonably electron-rich and are isolated in modest yield. Conversely, products **36** and **38** bearing electron-withdrawing ester and carbamate groups respectively are isolated in much lower yield. In the case of proline derivative **36**, steric hindrance may also play a role in the low yield observed, with the approach of the fluorinated silyl acetal species being more limited in this example. In the same way, geminally disubstituted substrate **37** has significant steric bulk adjacent to the amine nitrogen which may be detrimental to the success of the reaction. In the cases of **33** and **36**, an equivalent of triethylamine was added to the reaction mixture. This is because the hydrochloride salt of the secondary amine was used. Similar trends are observed in the three-component version of the reaction, with PMB-substituted products generally achieving higher yields over benzyl-substituted examples (**43** *vs* **44**, Scheme 2.6). Reductively labile functional

groups are compatible in the reaction including alkenes, alkynes, esters and carbamates, with no reduction products detected. In addition, the off-cycle amide by-product was not detected in any of the above examples. Retention of the alkene or alkyne functionality is key to our photoredox catalysis reaction design and therefore this method is a powerful tool for building these functionalised β-bromodifluoroethyl tertiary amine cores.

2.2.2 Photoredox Radical Cyclisation Reaction Optimisation

We began our studies by reviewing the literature for suitable starting conditions. The work most closely related was conducted by Stephenson (Scheme 1.9, Section 1.3.1) on the cyclisation of unactivated alkyl iodides.[7] Stephenson and co-workers used $Ir(ppy)_3$ as the photocatalyst, a tertiary amine sacrificial reductant, and formic acid as an additional hydrogen atom donor. However, the group only used tosyl-protected amines which prevents the amine from participating in oxidative processes by ensuring it is redox inert. In our proposed cyclisation system, the β-bromodifluoroethylamines synthesised previously would theoretically deactivate the amine sufficiently to prevent the alternative C-H functionalisation manifold from occurring, without the need for a separate protection/deprotection strategy. To test this hypothesis and develop optimal conditions for the process, alkynyl amine **35** was used as a model substrate.

We opted to use the strongly reducing $Ir(ppy)_3$ catalyst ($E_{1/2}^{Ir^{III*}/Ir^{IV}}$ = -1.73 V *vs* SCE) as a starting point and, gratifyingly, the desired cyclised product **45** was detected and no products arising from oxidation of the substrate or product were observed (entry 1, Table 2.2). We then surveyed tertiary amine bases (entries 1-3) and found triethylamine gave the highest product yield. Reactions using DMAP and potassium carbonate (entries 4 and 5) did not proceed, suggesting a tertiary amine base is required for catalyst turnover. Similarly, reactions with fewer than ten equivalents of triethylamine gave inferior yields (entries 6-8). Next, solvent choice was examined, but neither MeCN:MeOH (1:1) nor toluene (entries 9 and 10) improved the yield relative to the equivalent reaction with MeCN. Additional hydrogen atom sources were then surveyed and, while the Hantzsch ester (entry 11) and tris(trimethylsilyl)silane

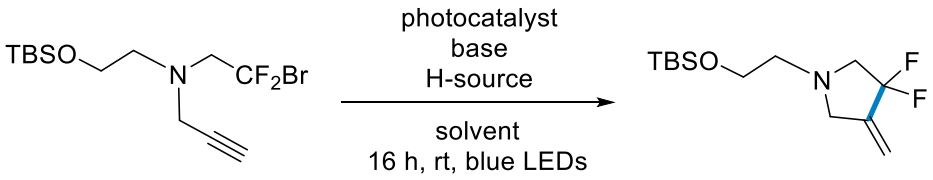

35 **45**

entry	catalyst (mol%)	base (equiv.)	H-source (equiv.)	solvent	conc /M	product yield[a] /%	starting material yield[a] /%
1	$Ir(ppy)_3$ (1)	DIPEA (10)	none	MeCN	0.01	44	0
2	$Ir(ppy)_3$ (1)	Et_3N (10)	none	MeCN	0.01	56	0
3	$Ir(ppy)_3$ (1)	Bu_3N (10)	none	MeCN	0.01	25	0
4	$Ir(ppy)_3$ (1)	DMAP (10)	none	MeCN	0.01	0	100
5	$Ir(ppy)_3$ (1)	K_2CO_3 (10)	none	MeCN	0.01	0	100
6	$Ir(ppy)_3$ (1)	Et_3N (1.5)	none	MeCN	0.01	0	70
7	$Ir(ppy)_3$ (1)	Et_3N (3)	none	MeCN	0.01	0	33
8	$Ir(ppy)_3$ (1)	Et_3N (5)	none	MeCN	0.01	34	17
9	$Ir(ppy)_3$ (1)	Et_3N (10)	none	MeCN:MeOH 1:1	0.01	18	0
10	$Ir(ppy)_3$ (1)	Et_3N (10)	none	toluene	0.01	8	100
11	$Ir(ppy)_3$ (1)	Et_3N (10)	Hantzsch ester (1.5)	MeCN	0.01	7	0
12	$Ir(ppy)_3$ (1)	Et_3N (10)	HCOOH (1.5)	MeCN	0.01	71	0
13	$Ir(ppy)_3$ (1)	Et_3N (10)	TTMSS (1.5)	MeCN	0.01	12	0
14	$Ir(ppy)_3$ (1)	Et_3N (10)	HCOOH (3)	MeCN	0.01	72	0
15	$Ir(ppy)_3$ (1)	Et_3N (10)	HCOOH (5)	MeCN	0.01	77	0
16	$Ir(ppy)_3$ (1)	Et_3N (10)	HCOOH (10)	MeCN	0.01	5	93
17	$Ir(ppy)_3$ (1)	none	HCOOH (1.5)	MeCN	0.01	0	93
18	$Ir(ppy)_3$ (1)	Et_3N (5)	HCOOH (3)	MeCN	0.01	60	0
19	$Ir(ppy)_3$ (1)	Et_3N (5)	HCOOH (5)	MeCN	0.01	5	62
20	$Ir(ppy)_3$ (1)	Et_3N (5)	Et_3N.HI salt (5)	MeCN	0.01	20	92
21	$Ir(ppy)_3$ (1)	Et_3N (10)	CH_3COOH (5)	MeCN	0.01	88	4
22	$Ir(ppy)_3$ (1)	Et_3N (10)	C_6H_5COOH (5)	MeCN	0.01	0	100
23	$Ir(ppy)_3$ (1)	Et_3N (10)	NaOAc (5)	MeCN	0.01	70	0
24	$Ir(ppy)_3$ (1)	Et_3N (10)	CH_3COOH (5)	MeCN	0.1	26	60
25	$Ir(ppy)_3$ (1)	Et_3N (10)	CH_3COOH (5)	MeCN	0.005	90	0
26	eosin Y (1)	Et_3N (10)	CH_3COOH (5)	MeCN	0.01	13	83
27	eosin Y (5)	Et_3N (10)	CH_3COOH (5)	MeCN	0.01	25	58
28	4CzIPN (1)	Et_3N (10)	CH_3COOH (5)	MeCN	0.01	29	63
29	4CzIPN (5)	Et_3N (10)	CH_3COOH (5)	MeCN	0.01	75	3

entry	catalyst (mol%)	base (equiv.)	H-source (equiv.)	solvent	conc /M	product yield[a] /%	starting material yield[a] /%
30	$Ir(ppy)_3$ (0.5)	Et_3N (10)	CH_3COOH (5)	MeCN	0.01	69	0
31	$Ir(ppy)_3$ (3)	Et_3N (10)	CH_3COOH (5)	MeCN	0.01	46	0
32	$[Ir(dtbbpy)(ppy)_2]PF_6$ (1)	Et_3N (10)	CH_3COOH (5)	MeCN	0.01	54	0
33	[9-Mesityl-10-methyl acridinium]BF_4 (5)	Et_3N (10)	CH_3COOH (5)	MeCN	0.01	5	95
34	$Cu(dap)_2Cl$ (1)	Et_3N (10)	CH_3COOH (5)	MeCN	0.01	0	97
35	$Ru(bpy)_3Cl_2$ (1)	Et_3N (10)	CH_3COOH (5)	MeCN	0.01	7	92

Table 2.2 Optimisation of alkynyl amine photoredox-mediated radical cyclisation. [a]Yields were determined by ^1H NMR using 1,3-benzodioxole as an internal standard.

(TTMSS) (entry 13) were found to be poor, formic acid (entries 12 and 15) and acetic acid (entry 21) were superior and gave a substantial increase in yield. When the number of equivalents of triethylamine matched the number of equivalents of formic acid (entry 16), reactivity of **35** halted. This again suggests a quantity of free amine is required in the system for a successful reaction. This was also corroborated when 0% yield was obtained for the reaction with no base added (entry 17). The weak acid benzoic acid was also trialled in the place of acetic and formic acid but did not yield any product (entry 22). Investigation of the reaction concentration revealed that 0.01 M was optimal (entry 21 *vs* 24 *vs* 25). A concentration of 0.1 M slowed down the reaction, with 60% of the starting material remaining after 16 hours. This concentration may also have promoted intermolecular reactions over the desired intramolecular cyclisation. Dilution of the reaction to 0.005 M gave a marginal improvement in yield but this was within error and was not deemed worthwhile considering the impact this would have on the practicality of the set-up. Finally, the choice of photocatalyst was explored with $Ir(ppy)_3$ being superior. Lower and higher catalyst loadings were trialled (entries 30 and 31) but 1 mol% loading proved optimal. Whilst other metal photocatalysts such as $[Ir(dtbbpy)(ppy)_2]PF_6$, $Cu(dap)_2Cl$ and $Ru(bpy)_3Cl_2$ were examined (entries 21, 34, 35), none rivalled $Ir(ppy)_3$, most likely as a result of their sub-optimal redox potential windows for this reaction. Reactions with organocatalysts eosin Y and 4CzIPN (entries 26-29) did yield product **45** but did not reach completion within 16 hours. Increasing the catalyst loading of 4CzIPN to 5 mol% was beneficial and led to a product yield of 75% with only 3% starting

material remaining. This loading increase would be considered satisfactory as organocatalysts are much cheaper and are more sustainable choices than metal-based photocatalysts. No by-products of the reaction were isolated and any mass balance discrepancies were attributed to the presence numerous unidentifiable baseline compounds by NMR. Based on Table 2.2, the conditions shown in entry 21 were chosen as optimal and taken forward to investigate the substrate scope of the reaction.

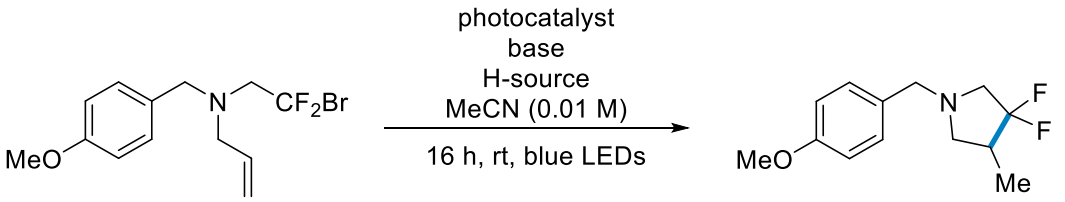

41 **46**

entry	catalyst (mol%)	base (equiv.)	H-source (equiv.)	product yield[a] /%	starting material yield[a] /%
1	$Ir(ppy)_3$ (1)	DIPEA (10)	none	44	0
2	$Ir(ppy)_3$ (1)	Et_3N (10)	none	38	0
3	$Ir(ppy)_3$ (1)	Et_3N (10)	CH_3COOH (5)	10	51
4	$Ir(ppy)_3$ (1)	DIPEA (10)	HCOOH (5)	49	13
5	$Ir(ppy)_3$ (1)	DIPEA (10)	TTMSS (5)	97	0
6	4CzIPN (5)	DIPEA (10)	none	48	0
7	$Ir(ppy)_3$ (1)	DIPEA (5)	TTMSS (5)	95	0
8	$Ir(ppy)_3$ (1)	DIPEA (10)	TTMSS (10)	94	0
9	$Ir(ppy)_3$ (1)	DMAP (10)	TTMSS (10)	93	0
10	$Ir(ppy)_3$ (5)	DIPEA (10)	none	55	0
11	$Ir(ppy)_3$ (1)	none	TTMSS (5)	0	0
12	$Ir(ppy)_3$ (1)	DIPEA (5)	TTMSS (2)	85	0
13	$Ir(ppy)_3$ (1)	DIPEA (2)	TTMSS (2)	53	0
14	$Ir(ppy)_3$ (1)	DIPEA (10)	TTMSS (2)	73	0
15	$Ir(ppy)_3$ (1)	DIPEA (5)	TTMSS (1)	37	0
16	$Ir(ppy)_3$ (1)	DIPEA (20)	TTMSS (2)	93	0
17	$Ir(ppy)_3$ (1)	DIPEA (10)	triethylsilane (5)	21	14
18	$Ir(ppy)_3$ (1)	DIPEA (10)	triethoxysilane (5)	35	9
19	$Ir(ppy)_3$ (1)	DIPEA (10)	triisopropylsilanethiol (5)	77	0
20	4CzIPN (5)	DIPEA (10)	TTMSS (5)	97	0

Table 2.3 Optimisation of alkenyl amine photoredox-mediated radical cyclisation. [a]Yields were determined by ^{19}F NMR using trifluorotoluene as an internal standard.

It was later found that alkenyl amines gave markedly lower yields than alkynyl amines using the optimised reaction conditions above. For this reason, a separate screening of conditions was conducted for this class of substrates using model substrate **41** (Table 2.3).

Using the conditions optimised for alkynyl amines (entry 3), only 10% yield of **46** was observed when using alkenyl amine **41**, while 51% yield of unreacted starting material remained after 16 hours. It appeared that the addition of acetic acid was hindering the reaction, as when it was removed (entry 2), full conversion of starting material was observed. For this substrate, DIPEA was found to be a better choice of terminal reductant than triethylamine (entry 1 *vs* 2). The reaction does proceed in the absence of an additional hydrogen atom donor but does not without an amine base additive (entry 10), again suggesting this reagent is key to catalyst turnover. While acetic acid and formic acid were poor H-donors, the use of TTMSS gave a significant increase in yield (entry 5). The number of equivalents of amine and TTMSS were altered to find the optimal combination (entries 7-9, 12-16) and it was found that reducing the equivalents of TTMSS to less than five was detrimental to the yield, whereas increasing the number of equivalents to ten had little impact on the yield. Considering cost and yield, a balance of ten equivalents of DIPEA and five equivalents of TTMSS were decided upon. Three other silanes were trialled (entries 17-19) but were inferior to TTMSS. Finally, the use of 4CzIPN at 5 mol% loading was explored (entry 22) which gave a product yield of 97%, comparable to the yield observed with 1 mol% $Ir(ppy)_3$ (entry 5). Conditions using $Ir(ppy)_3$ were chosen as optimal based on visualisation of the crude NMR spectra and ease of product isolation by column chromatography.

2.2.3 Substrate Scope

Following the optimisation of both alkynyl and alkenyl amine cyclisation procedures, we next sought to explore the scope and functional group tolerance of the photoredox reaction. Starting with alkynyl amines, on a 0.25 mmol scale, model substrate **45** was isolated in 56% yield (Scheme 2.7). Not only are silyl-protected alcohols tolerated, but free hydroxyl groups are also stable (**53**) so there is no requirement for prior protection of these groups. This would not be the case if nucleophilic fluorinating reagents were used. Carbamates (**52**) and esters (**50**) are

also tolerated, clearly demonstrating the numerous advantages of this method over using reagents such as DAST. 5-*Exo-dig* and 6-*exo-dig* cyclisations were possible using the developed protocol with no *endo* cyclisation products detected. Conformational restriction in the proline-derived substrate and resulting favourable orbital interactions promoted the desired cyclisation to give indolizidine **50** in 92% NMR yield. Substrates **45**-**53** arose from cyclisation

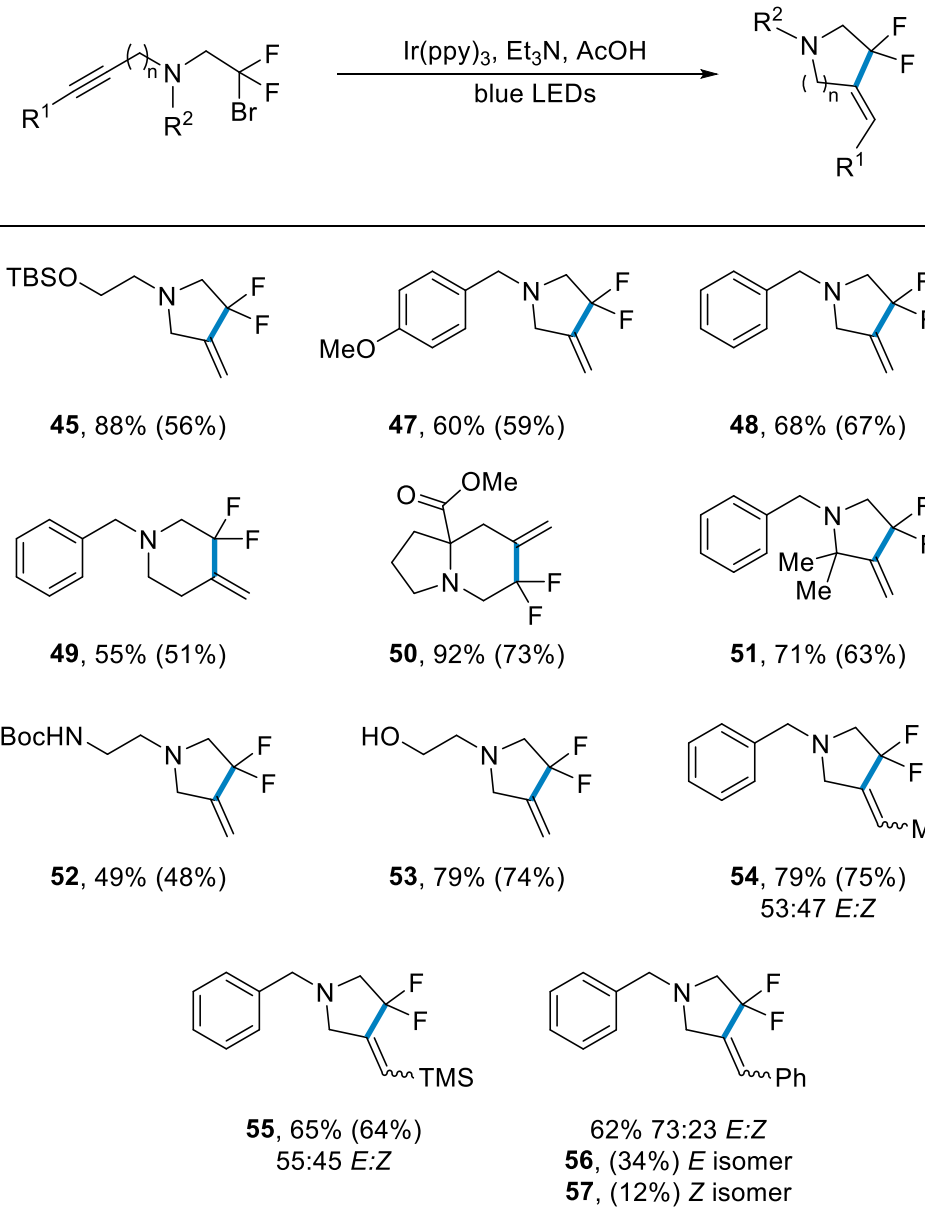

Scheme 2.7 Scope of the photoredox radical cyclisation of alkynyl amines. Reagents and conditions: amine (1 equiv.), Ir(ppy)$_3$ (1 mol%), Et$_3$N (10 equiv.), acetic acid (5 equiv.), MeCN (0.01 M), rt, 16-88 h, blue LED irradiation. Yields were determined by ^{1}H NMR spectroscopy vs internal standard (1,3-benzodioxole). Yields of isolated material are given in parentheses.

of a radical onto a terminal alkyne, whereas **54**-**57** were derived from internal alkynes. We predicted that additional stabilisation of the radical formed after cyclisation with these three substrates would lead to improved yields, but the yields were found to be relatively comparable between terminal and internal alkyne substrates. Additionally, cyclisation of these internal alkynes predictably led to a mixture of *E* and *Z* isomers. In the cases of **54** and **55**, the mixtures of isomers were inseparable and the *E:Z* ratios for each were close to 50:50. Compound **56** was separable from compound **57**, but isolation proved challenging, hence the loss in isolated yield from the calculated NMR yield. The observed 73:23 *E*:*Z* ratio was attributed to steric hindrance between the bulky phenyl group and the difluoro- group, favouring formation of the *E* isomer.

Following on from the cyclisation of alkynyl amines, the scope of the cyclisation of alkenyl amines was investigated (Scheme 2.8). Particularly high yields were observed for products **58** and **59** where the cyclic radical intermediates are stabilised by electron-withdrawing ester and ketone groups respectively. The starting materials for these cyclisations were synthesised *via* cross metathesis with ethyl acrylate and methyl vinyl ketone respectively (see Section 4.4.3). This additional stabilisation, however, was not crucial as product **46**, derived from a terminal alkene, was isolated in an excellent yield. Endocyclic alkenes were also effective substrates, giving the novel spirocyclic amine **60**. Both 5-*exo*-*trig* and 6-*exo*-*trig* cyclisations are demonstrated. A slightly modified procedure was utilised for the cyclisation of the allene substrate to give alkene product **61**. Under the standard reaction conditions, a silylated by-product was generated (see Section 2.2.5). This indicates that TTMSS likely acts as a hydrogen donor in the reaction, producing a silyl radical which was then able to attack the alkene within **61** to eventually form the observed by-product. For this reason, high yielding conditions that used fewer equivalents of TTMSS from the screening reactions conducted previously were chosen (entry 16, Table 2.3). Under these modified conditions, **61** was generated in 90% NMR yield.

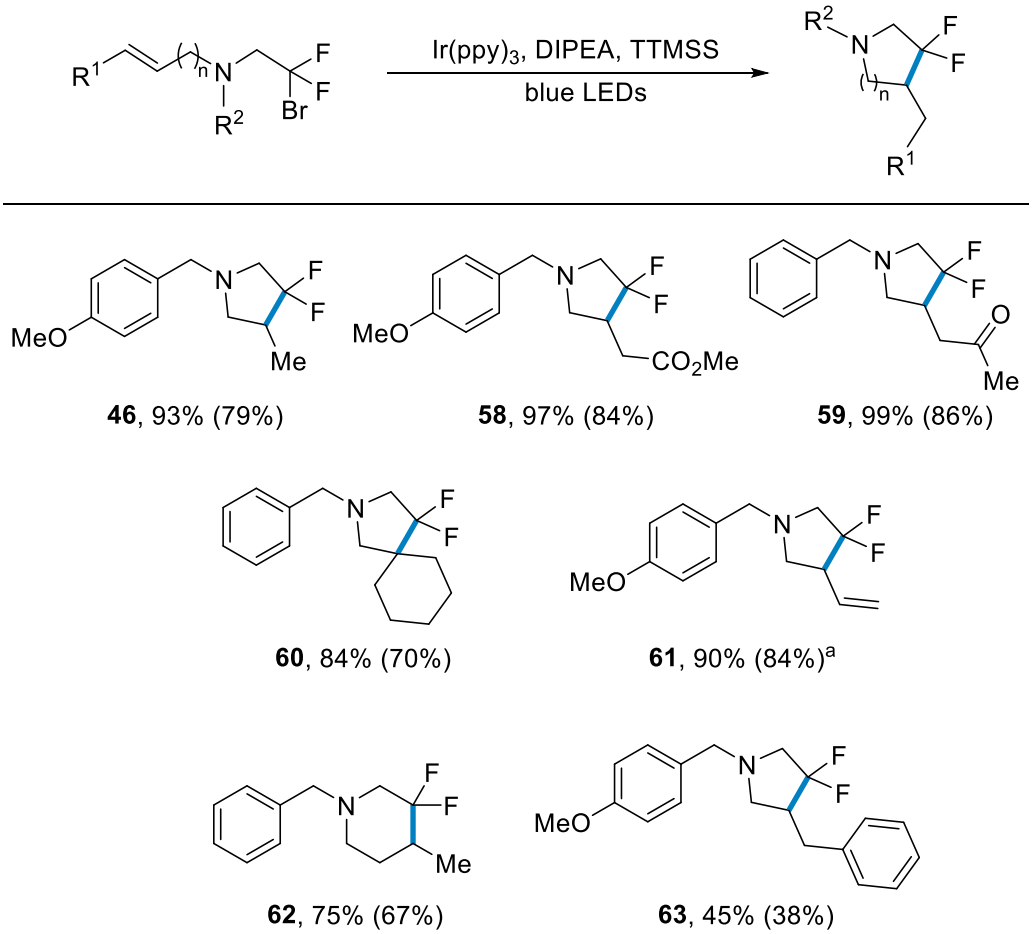

Scheme 2.8 Scope of the photoredox radical cyclisation of alkenyl amines. Reagents and conditions: amine (1 equiv.) Ir(ppy)$_3$ (1 mol%), DIPEA (10 equiv.), TTMSS (5 equiv.), MeCN (0.01 M), rt, 4.5-16 h, blue LED irradiation. Yields were determined by ^{1}H or ^{19}F NMR spectroscopy vs internal standard (1,3-benzodioxole or trifluorotoluene). Yields of isolated material are given in parentheses. [a]DIPEA (20 equiv.), TTMSS (2 equiv.).

2.2.4 Reaction Scalability and Product Derivatisation

Following investigation of the substrate scope, we next sought to explore the practicality of the reaction and one of our main considerations was carrying out the reaction on a larger scale. Pleasingly, we were able to scale up the batch reaction for the synthesis of **47** from 0.25 mmol to 2.00 mmol with no detriment to the yield (Scheme 2.9).

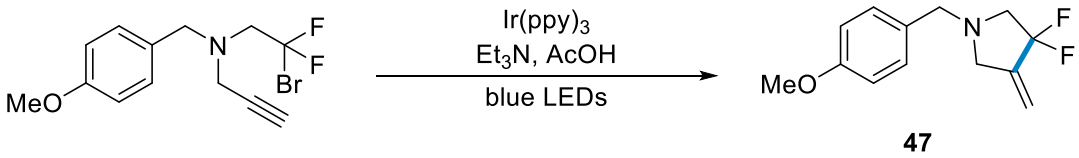

47

0.25 mmol scale, 59%
2.00 mmol scale, 63%

Scheme 2.9 Scale-up of batch photoredox radical cyclisation procedure. Reagents and conditions: $Ir(ppy)_3$ (1 mol%), Et_3N (10 equiv.), acetic acid (5 equiv.), MeCN (0.01 M), rt, blue LED irradiation.

The batch photoredox radical cyclisation reaction is limited by the requirement for thin walled culture tubes and low concentrations of the substrate in the solvent. For effective light penetration, the surface area being irradiated must be also be maximised. This eight-fold increase in scale without compromising yield was promising, but efforts to increase the reaction scale beyond 2 mmol have not been possible due to the above limitations. In the long term, we believe the developed reaction would be amenable to a photoredox flow system. This could allow for continuous product formation (if desired) and possibly a lower catalyst loading. Stephenson and co-workers trialled their reductive deiodination reaction in a flow reactor and reported faster reaction times and lower catalyst loadings without any loss of efficiency.[7] This group, among others, also designed their own flow reactor using non-specialist equipment,[106–108] but commercial flow reactors are also available.

Given that several of the products contain a PMB group we next explored deprotection to access the free secondary amine. Using **47**, this was achieved using 1-chloroethyl chloroformate in 69% yield giving fluorinated pyrrolidine **64** as the hydrochloride salt. The structure of **64** was confirmed by x-ray crystallography. Our two-step protocol represents a very efficient method to access this pyrrolidine analogue, which could be a useful building block for drug discovery. pK_aH calculations performed by Prof. Ross Denton and logP prediction software suggested that **64** has a pK_aH value of 15.1 in acetonitrile and a logP value of 1.20. This is in comparison with pyrrolidine (pK_aH = 19.5 (MeCN), logP = 0.77).[109] These figures signify the impact that fluorine can have on key properties which then can, in principle, modulate biological activity and metabolic stability.

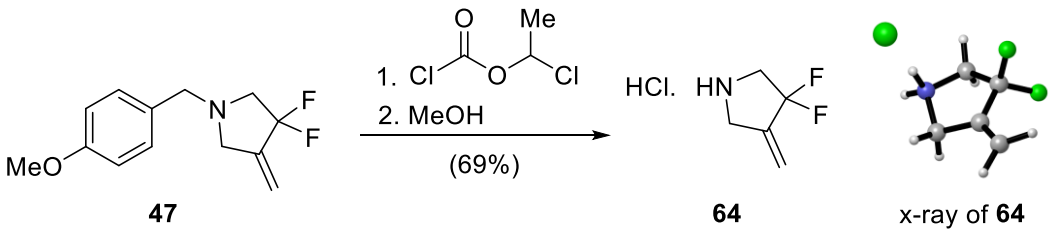

*Scheme 2.10 PMB deprotection to access pyrrolidine **64**. Reagents and conditions: amine (1 equiv.), 1-chloroethyl chloroformate (1.1 equiv.), DCE (0.4 M), 90 °C, 2 h, then MeOH (1.0 M), 75 °C, 1 h.*

Finally, the alkene in product **47** was functionalised using Mukaiyama hydration conditions, which gave tertiary alcohol **65** in 67% yield, demonstrating the versatility of the alkene handle and providing a new method to access the difluorohydrin motif previously generated through Reformatsky chemistry (**24**, Scheme 1.13).

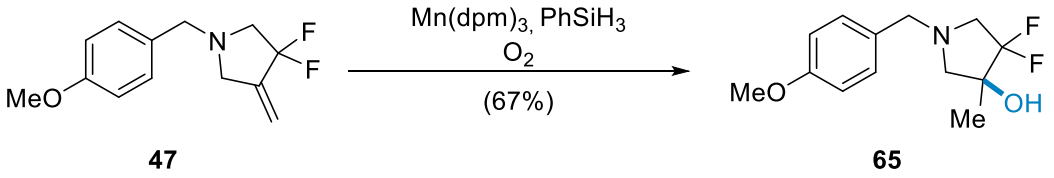

*Scheme 2.11 Derivatisation of cyclic fluorinated amine **47** using Mukaiyama hydration conditions. Reagents and conditions: amine (1 equiv.), $Mn(dpm)_3$ (5 mol%), $PhSiH_3$ (2 equiv.), O_2 (1 atm), THF (0.2 M), rt, 24 h.*

2.2.5 Mechanistic Investigations

Having explored the scope and utility of the photoredox catalysed cyclisation system, we next delved into the mechanism of the amine cyclisation/hydrogen atom transfer reactions. Given that $Ir(ppy)_3$ has a reduction potential of -1.73 V *vs* SCE ($E_{1/2}^{Ir^{III*}/Ir^{IV}}$) and taking into account mechanistic investigations into cyclisations of unactivated alkyl iodides,[7] an oxidative quenching cycle is likely to be operating (Figure 2.2). We propose that irradiation of the catalyst forms the excited Ir(III)* complex which then reduces the bromodifluoroalkyl starting material **26** by single-electron transfer to give radical **66** and the corresponding Ir(IV) species. Intramolecular radical addition to the alkyne is favoured under our dilute conditions to give

radical intermediate **67**, which is then able to participate in hydrogen atom transfer with multiple donors. Turnover of the photocatalyst is then achieved by oxidation of triethylamine

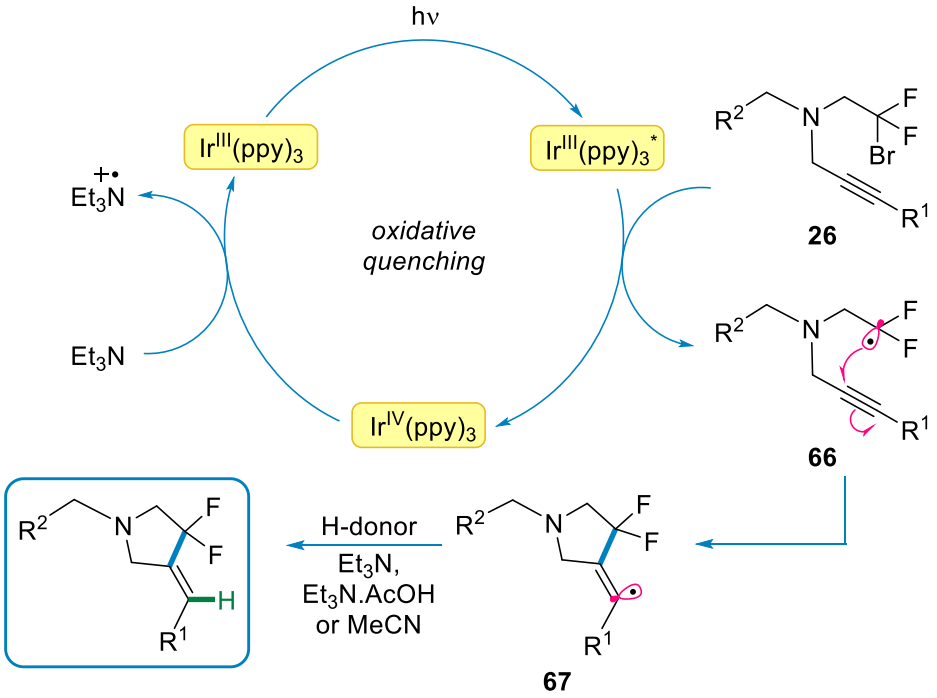

Figure 2.2 Proposed mechanism for the photoredox radical cyclisation reaction.

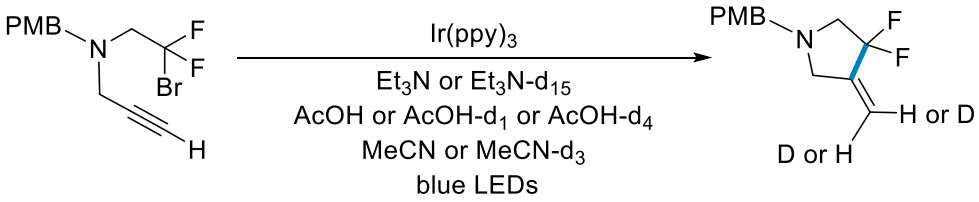

entry	source of deuterium	^{2}H incorporation
1	none	0%
2	AcOH-d_1	45%
3	AcOH-d_4	45%
4	Et_3N-d_{15}	36%
5	MeCN-d_3	17%
6	Et_3N-d_{15}, AcOH-d_4 and MeCN-d_3	85%

Table 2.4 Deuterium-labelling experiments to investigate the hydrogen atom donor species. Reagents and conditions: Amine (1 equiv.), Ir(ppy)$_3$ (1 mol%), Et$_3$N or Et$_3$N-d$_{15}$ (10 equiv.), AcOH, AcOH-d$_1$ or AcOH-d$_4$ (5 equiv.), MeCN or MeCN-d$_3$ (0.01 M), rt, 16 h, blue LED irradiation.

to a radical cation. A series of deuterium-labelling studies were conducted to help elucidate the source of the hydrogen atom. These reactions revealed that triethylamine, acetic acid and acetonitrile were all competent hydrogen atom donors (Table 2.4) in the intermolecular hydrogen atom transfer process and so the provenance of the hydrogen in the product is complicated in the case of the *N*-alkynyl substrates.

As expected, when no labelled reagents were used (entry 1, Table 2.4), there was no incorporation of deuterium into the cyclised product. Integration of ^{1}H NMR signals was used to calculate deuterium incorporation, and ^{2}H NMR analysis was also used to corroborate deuterium presence. Use of either acetic acid-d_1 or acetic acid-d_4 (entries 2 and 3) led to 45% labelled product. This result shows that acetic acid is a hydrogen-atom donor in the reaction but is not the only source. More specifically, the hydrogen atom is donated from the acidic position and not from one of the methyl group hydrogens. Separately, when fully labelled triethylamine (entry 4) or acetonitrile (entry 5) were used in the reaction, 36% and 17%

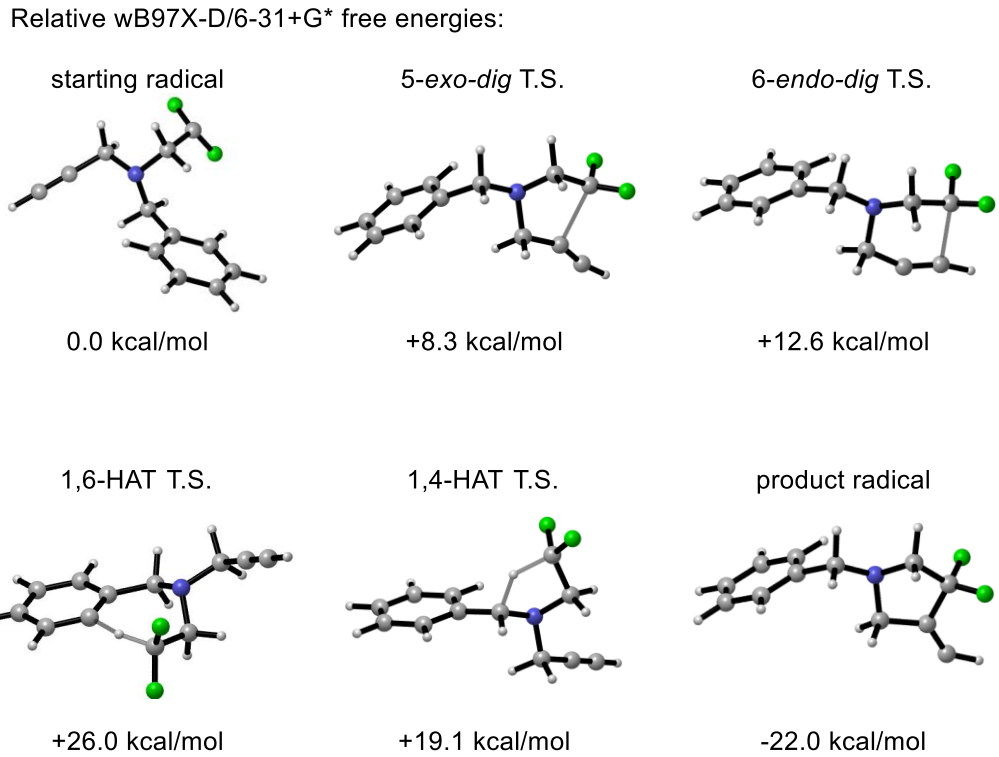

Figure 2.3 Computational investigation of the radical cyclisation and related hydrogen atom transfer processes.

deuterium incorporation was observed respectively. Again this suggests that both components are effective hydrogen atom donors. Any further analysis is complicated by the use of both an acid and base, as the exact speciation under the reaction conditions is not known.

In order to probe other competing reactions of radical **66**, computational studies using the wB97X-D/6-31G* theoretical model were carried out by Prof. Ross Denton. Large barriers were obtained for the potentially competitive 1,4-HAT and 1,6-HAT pathways as well as for the alternative *endo*-cyclisation, while the *exo*-cyclisation had a barrier of 8.3 kcal/mol (Figure 2.3) which is consistent with related processes.[110] These computational findings are in line with experimental observations in which cyclisation occurs readily at room temperature and products arising from the hydrogen atom transfer pathways are not observed. Products arising from oxidation of either the amine substrate or product were also absent. This is due to the negative inductive effect of the β-difluoro group which must substantially alter the redox potential of both compounds as well as the acidity of the potential radical cations derived from oxidation.

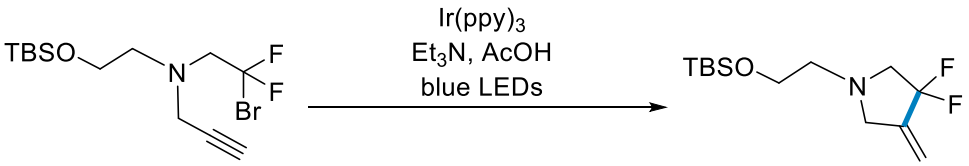

entry	variable(s) changed	product yield /%	starting material yield /%
1	none	88	4
2	no AcOH	56	0
3	no Et_3N	0	100
4	no visible-light irradiation	0	100

Table 2.5 Control experiments for alkynyl amine cyclisation reaction. Standard reagents and conditions: amine (1 equiv.), $Ir(ppy)_3$ (1 mol%), Et_3N (10 equiv.), AcOH (5 equiv.), MeCN (0.01 M), rt, 16 h, blue LED irradiation. Yields were determined by ^1H NMR spectroscopy vs internal standard (1,3-benzodioxole).

Control experiments confirmed that the reaction does not proceed in the absence of light irradiation, nor in the absence of tertiary amine base (Table 2.5). The reaction does proceed (albeit in lower yield) in the absence of acetic acid, which in combination with our mechanistic

investigation suggests that triethylamine can act as both an electron and hydrogen atom donor, whereas acetic acid cannot.

Circumstantial evidence for the hydrogen atom source in the alkenyl amine cyclisation was provided during the cyclisation of allene **33** (Scheme 2.12). Under the standard reaction conditions, a significant amount of **68** was isolated. Therefore, it is likely that TTMSS acts as a hydrogen atom donor in the reaction, producing a silyl radical which is then able to react with the remaining alkene of **61**, eventually giving product **68**. As was described in Section 2.2.3, modification of the conditions minimised by-product formation, allowing isolation of **61** in 84% yield (Scheme 2.8).

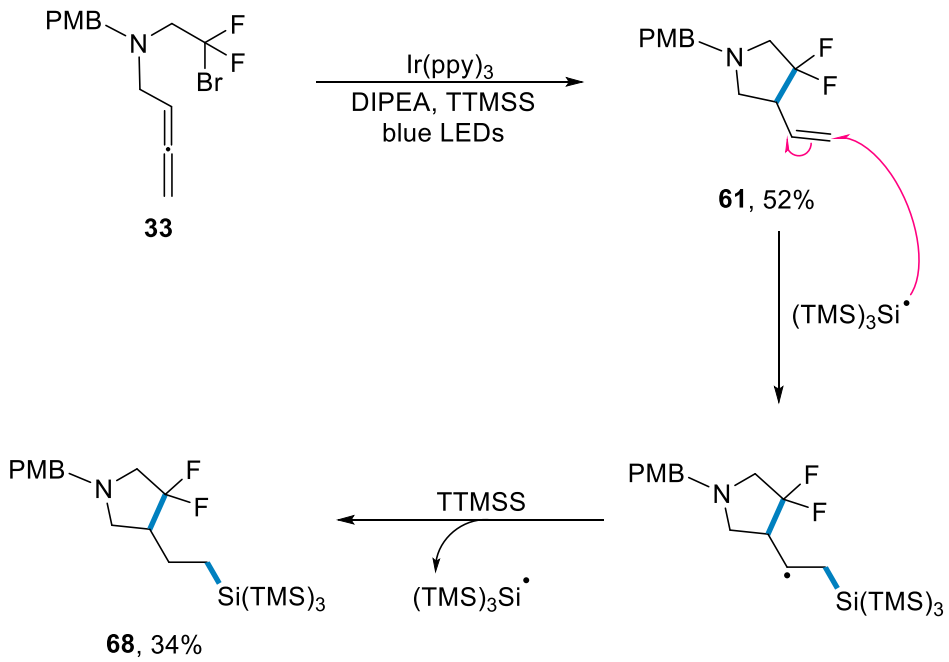

*Scheme 2.12 Formation of by-product **68**, providing evidence of a radical pathway. Reagents and conditions: Ir(ppy)₃ (1 mol%), DIPEA (10 equiv.), TTMSS (5 equiv.), MeCN (0.01 M), rt, blue LED irradiation.*

2.2.6 Conclusions

In conclusion, a mild and efficient visible-light-mediated intramolecular cyclisation reaction of unactivated bromodifluoroalkyl amines has been developed. Using a readily available and abundant source of fluorine, the bromodifluoro- group was installed with high selectivity for the amine product over the amide by-product. The strongly acidic nature of bromodifluoroacetic acid accounts for this observed selectivity, and the method is both air and moisture stable. Photoredox catalysis has been shown to produce carbon-centred radicals under mild and tuneable conditions, and here, a procedure for the synthesis of complex fluorinated nitrogen-containing heterocycles has been developed, utilising the cyclisation of radicals generated under photocatalytic conditions. The cyclic amine products are β-difluorinated and are expected to be of value to a wide range of researchers as fluorine-containing amines exhibit decreased basicities and altered pharmacological properties. The incorporation of fluorine in this strategy deactivated the amine through the strong negative inductive effects of the fluorine atoms, rendering the amine redox inert. This disfavoured any oxidative processes from occurring and promoted the desired intramolecular cyclisation reaction, and avoided the typical protection/deprotection steps of other related photoredox systems. Finally, mechanistic investigations helped establish the role of the tertiary amine base and the additional hydrogen-atom donor in the reactions. Future work should focus on transferring the photoredox process to a flow system with the long-term goal of producing small, fluorinated building blocks on a large scale.

Chapter Three: Photoredox Radical Cyclisation of Fluorinated Amides

3.1 Introduction

3.1.1 The Utility and Synthesis of 3,3-Difluoro-γ-lactams

γ-Lactams are prevalent in a range natural products and pharmaceuticals, and they can exhibit antibacterial, antifungal and anticancer activities. Given the impact that fluorination can have on biological properties, the introduction of a difluoro- group could lead to the generation of new APIs. These α,α-difluorinated analogues have received considerable attention in recent years.[111–113] Most commonly, 3,3-difluoro-γ-lactams are synthesised by nucleophilic deoxodifluorination of α-ketoamides,[114] but the method suffers serious drawbacks in terms of its low functional group tolerance and the limited availability or difficult syntheses of the starting material. Chapter One: Part I discussed the intramolecular cyclisation reactions developed by Nagashima and Uneyama utilising copper(I) bromide and $NaBH_4$/ diphenyl diselenide respectively to make 3,3-difluoro-γ-lactams.[31,33] Several groups have also developed conditions for an intermolecular aminodifluoroalkylation reaction using *N*-aryl halodifluoroacetamides and alkenes to make these fluorinated lactams (Scheme 3.1).[113,115–117]

These systems all involve the radical-mediated 1,2-functionalisation of alkenes, where a radical is generated from the *N*-aryl halodifluoroacetamide substrate, which then adds to the alkene radical trap before ring closure. These methods can only produce 5-substituted 3,3-difluoro-γ-lactams and are also limited either by the use of strong base, elevated temperatures or expensive catalysts. While a variety of alkenes are tolerated, only aryl-substituted acetamide substrates can be utilised. Other groups have reported the intramolecular radical cyclisation of similar compounds which can be used to generate 4-substituted 3,3-difluoro-γ-lactams (Figure 3.2). Mai and co-workers disclosed a nickel-catalysed intramolecular radical cyclisation reaction in tandem with an intramolecular arylation reaction.[118] The following year, Sun and co-workers developed a copper-catalysed radical selenodifluoromethylation

protocol.[119] However, aryl-substituted acetamides are still required, the choice of boronic acid coupling partner is limited, and the use of selenides is undesirable.

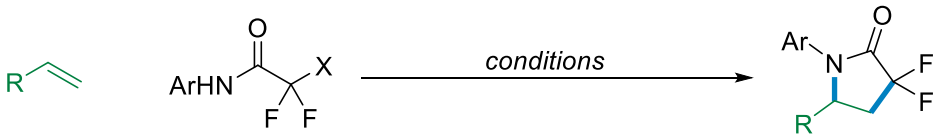

Chen	$Na_2S_2O_4$/NaOH	X = I	R = alkyl, benzyl, TMS
Wang	CuI, PMDETA	X = Br	R = Ar, benzyl, alkyl, ester, amide
Lv	CuI, phen, K_2CO_3	X = Br	R = Ar, benzyl, alkyl, amide, ether, TMS
Zhu	$Ir(ppy)_3$, NaOAc, NaI, blue LEDs	X = Br	R = aryl, alkyl, ether

Zhu

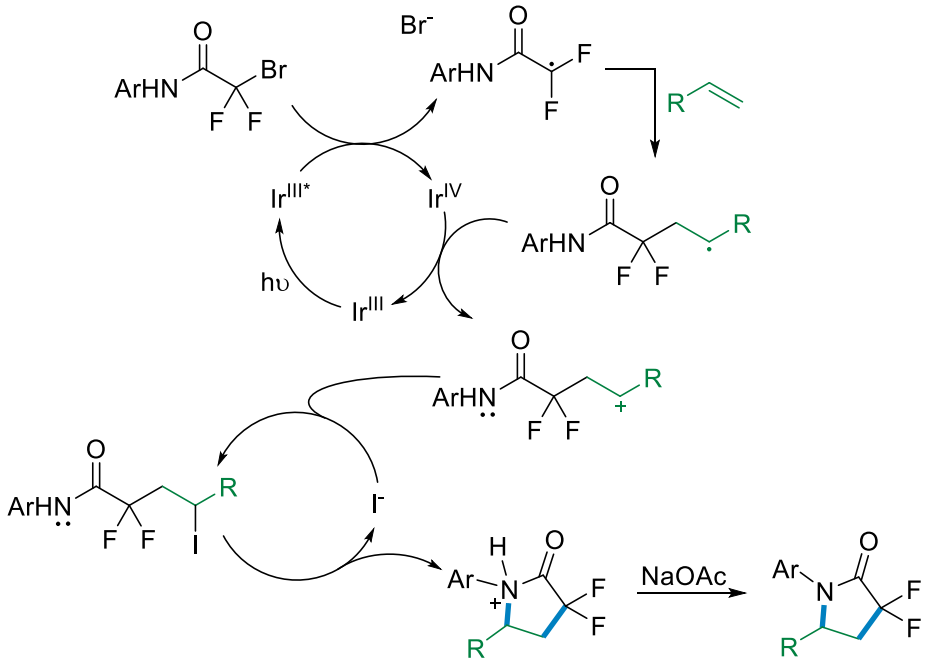

Figure 3.1 Intermolecular aminodifluoroalkylation reactions. Reagents and conditions: Chen – acetamide (1 equiv.), alkene (2 equiv.), $Na_2S_2O_4$ (1.5 equiv.), NaOH (1.5 equiv.) H_2O (0.33 M), MeCN (0.2 M), N_2, 10-15 °C, 30 min. Wang - acetamide (1 equiv.), alkene (2 equiv.), CuI (10 mol%), PMDETA (1.5 equiv.), MeCN (0.5 M), 80 °C, 10 h. Lv - acetamide (1 equiv.), alkene (1.2 equiv.), CuI (10 mol%), Phen (10 mol%), K_2CO_3 (2 equiv.), MeCN (0.1 M), 110 °C, 2 h. Zhu - acetamide (1 equiv.), alkene (1.5 equiv.), $Ir(ppy)_3$ (2 mol%), NaOAc (2 equiv.), NaI (20 mol%), DMF (0.1 M), rt, blue LEDs, 30-48 h.

Mai 2018

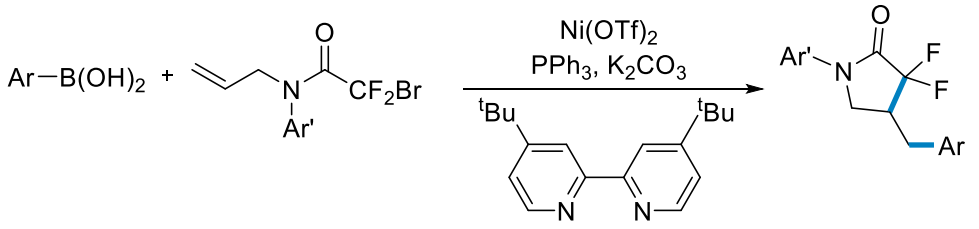

Sun 2019

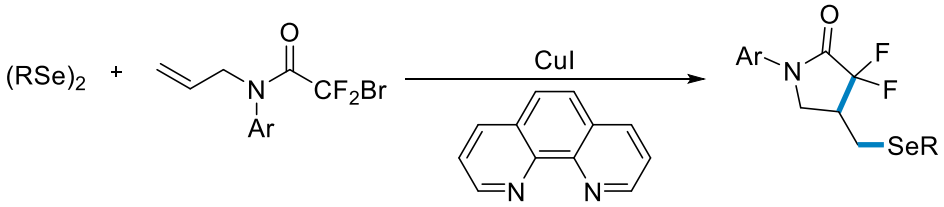

Figure 3.2 Intramolecular radical cyclisation and intermolecular functionalisation reactions. Reagents and conditions: Mai – boronic acid (2 equiv.), alkene (1 equiv.), $Ni(OTf)_2$ (7.5 mol%), K_2CO_3 (3 equiv.), ligand (7.5 mol%), PPh_3 (15 mol%), dioxane (0.17 M), 80 °C, 8 h. Sun – alkene (1 equiv.), $(RSe)_2$ (1.1 equiv.), CuI (10 mol%), phen (10 mol%), DCE (0.1 M), 120 °C.

In 2021, Su and co-workers reported a metal-free photoredox-catalysed cyclisation reaction with a wider substrate scope than the above methods. Alkenes and alkynes are suitable substrates and γ- and δ-lactams (5- and 6-membered rings) are both successfully generated (Scheme 3.1).[103] δ-lactams are also of significant interest to medicinal chemists. Advantages of this protocol include the use of an inexpensive organocatalyst over metal-based photocatalysts and mild reaction conditions.

Su 2021

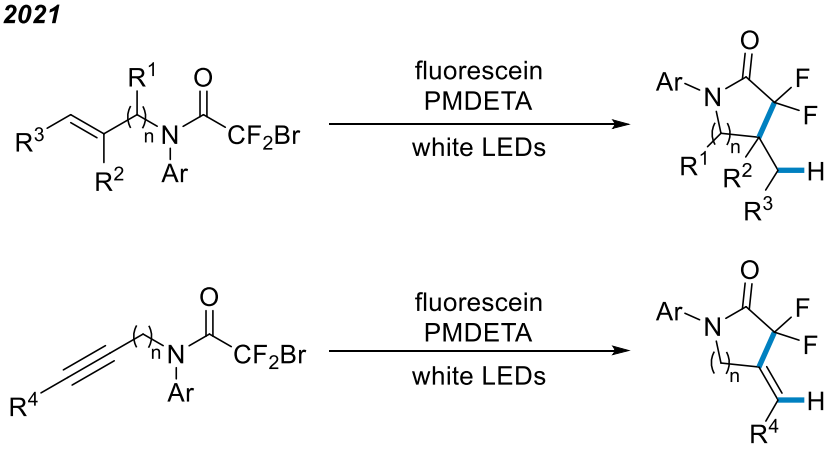

Scheme 3.1 Photoredox radical cyclisation reaction. Reagents and conditions: alkene or alkyne (1 equiv.), fluorescein (10 mol%), PMDETA (2 equiv.), DCE (0.25 M), white LEDs, N_2, rt, 10-24 h. n = 1 or 2.

Thirty-three alkene substrates with yields ranging from 39-83%, and twelve alkyne substrates with yields ranging from 42-89% are reported. Substitution at all of the ring positions was possible, demonstrating the scope of the process. However, as with previous methods, only *N*-aryl amides were used which is a key limitation of all the current literature protocols. The use of DCE is also undesirable due to its toxicity.

3.1.2 Aims

Based on the current methods available, we believe that new practical methods to construct these fluorinated γ- and δ-lactams would be valuable additions to the field. Therefore, we sought to adapt our protocol for the photoredox-mediated cyclisation of amines to amide substrates in order to access these building blocks. We hoped that our simple and practical system would lead to a greater scope than has previously been defined. As with the amine substrates described in Chapter Two, homolytic cleavage of the carbon-bromine bond of **69** should give a carbon-centred radical. Advantageously, with amide substrates this radical should be well stabilised by the adjacent carbonyl group *via* resonance. However, in this system, the energy barrier for amide bond rotation must be overcome under the reaction conditions in order to place the double or triple bond close to the difluoro- radical. If this energy barrier is not exceeded, then reductive debromination products are expected. However, once in the desired conformation, fast cyclisation to form cyclic fluorinated amide products **70** should occur.

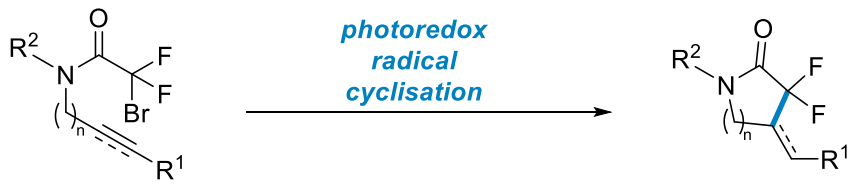

69 **70**

Scheme 3.2 Proposed photoredox radical cyclisation of bromodifluoroacetamides.

3.2 Results and Discussion

3.2.1 Photoredox Radical Cyclisation Reaction Optimisation

We began our studies by surveying reaction conditions and chose **71** as a model substrate (Table 3.1). Factors that significantly affected product yield during the optimisation of alkenyl amine and alkynyl amine cyclisations were concentration, solvent choice and tertiary amine base equivalents. Fortunately, at concentrations <0.02 M, product **72** was observed by ^{1}H and ^{19}F NMR analysis with 0.01 M concentration being optimal (entry 2). MeCN was the preferred solvent over DMF due to the higher yields and ease of work-up associated with using MeCN.

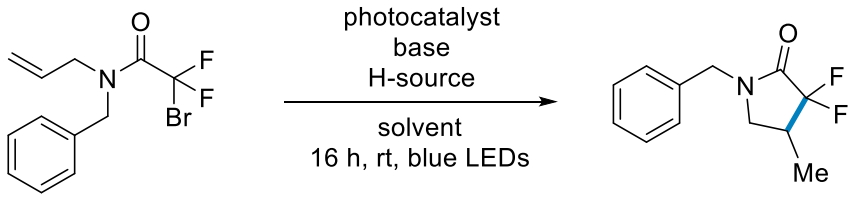

71 **72**

entry	catalyst (mol%)	base (equiv.)	H-source (equiv.)	solvent	concentration /M	product yield[a] /%
1	$Ir(ppy)_3$ (1)	Et_3N (2)	none	MeCN	0.02	31
2	$Ir(ppy)_3$ (1)	Et_3N (2)	none	MeCN	0.01	32
3	$Ir(ppy)_3$ (1)	Et_3N (2)	none	MeCN	0.005	25
4	$Ir(ppy)_3$ (1)	Et_3N (10)	none	MeCN	0.01	42
5	$Ir(ppy)_3$ (1)	DIPEA (2)	none	MeCN	0.01	40
6	$Ir(ppy)_3$ (1)	DIPEA (10)	none	MeCN	0.01	47
7	$Ir(ppy)_3$ (1)	Bu_3N (10)	none	MeCN	0.01	38
8	$Ir(ppy)_3$ (1)	DIPEA (10)	none	DMF	0.01	36
9	$Ir(ppy)_3$ (1)	DIPEA (10)	none	DMF:^{t}AmOH	0.01	33
10	$Ir(ppy)_3$ (1)	DIPEA (10)	HCOOH (10)	MeCN	0.01	51
11	$Ir(ppy)_3$ (1)	DIPEA (10)	Hantzsch ester (2)	MeCN	0.01	45
12	$Ru(bpy)_3Cl_2$ (1)	Et_3N (10)	none	MeCN	0.01	45
13	$Ru(bpy)_3Cl_2$ (1)	DIPEA (10)	none	MeCN	0.01	42

Table 3.1 Optimisation of amide photoredox-mediated radical cyclisation. [a]Yields were determined by ^{1}H NMR using 1,3-benzodioxole as an internal standard.

A 1:1 ratio of DMF:^{t}AmOH (entry 9) was trialled as Rovis and co-workers reported improved yields under this solvent system, however under these conditions, the yield was inferior.[120] Three tertiary amine bases were compared (entries 4, 6 and 7), with DIPEA giving the highest yield by ^{1}H NMR. The stoichiometry of the amine base was also investigated (entries 2 *vs* 4, or 5 *vs* 6). It was found that using ten equivalents gave higher yields. Next, the effect of an additional hydrogen atom source was considered. Comparing the reactions with no additive, formic acid (10 equiv.) and Hantzsch ester (2 equiv.) (entries 6, 10 and 11), the use of additives had only a small effect on the yield. The benefit of using formic acid did not outweigh the need for ten equivalents, with the additional expense and more complex reaction mixtures associated. When comparing iridium and ruthenium catalysts (entries 6 *vs* 12 and 13), $Ru(bpy)_3Cl_2$ gave comparable yields by NMR. However, there were a larger number of impurities as indicated by LC-MS, ^{1}H and ^{19}F NMR analysis. The optimal conditions (entry 6) were chosen based on the NMR yield, visualisation of the crude NMR spectra and the practicality of set-up and purification.

3.2.2 Substrate Scope

Following the optimisation of the amide photoredox radical cyclisation procedure, we next sought to explore the scope and functional group tolerance of the reaction (Table 3.2). The single set of conditions was implemented successfully for the cyclisation of both alkene- and alkyne-containing substrates.

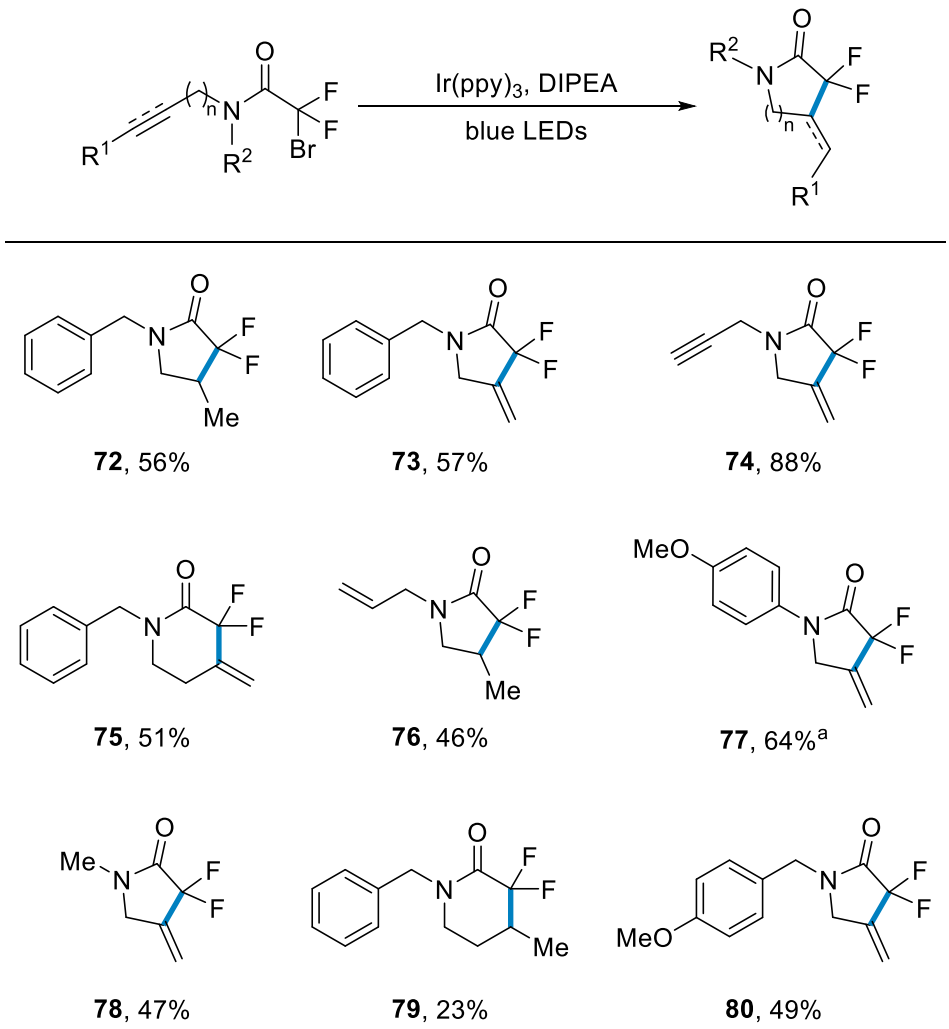

Table 3.2 Scope of the photoredox radical cyclisation of amides. Reagents and conditions: amide (1 equiv.) Ir(ppy)₃ (1 mol%), DIPEA (10 equiv.), MeCN (0.01 M), rt, 2-22 h, blue LED irradiation. [a]DIPEA (2 equiv.)

In common with the amine cyclisations, 5- and 6- membered ring formation was possible. Dipropargyl and diallyl substrates (**74** and **76**) were tolerated without observation of subsequent intermolecular reactions of the products. Under the standard reaction conditions, cyclisation of the PMP-substituted substrate led to significant reductive debromination. To minimise this, the number of equivalents of DIPEA used were reduced, which allowed isolation of **77** in 64% yield. This is comparable to the 66% yield reported by Su and co-workers for the same substrate.[103] This confirms that our protocol can, like most other literature protocols, be applied to aryl acetamides. However, unlike the methods reported by Su or any of the

publications discussed in Section 3.1.1, our system can also be applied to benzyl- or alkyl-substituted amides.

Following investigation of the substrate scope, we next sought to explore the practicality of the reaction by increasing the scale. Pleasingly, we were able to scale up the batch reaction for the synthesis of **79** from 0.25 mmol to 1.40 mmol with no detriment to the yield (Scheme 3.3). As was the case with the scale-up of the amine substrates, the requirement for thin walled culture tubes and low concentrations of the substrate in the solvent limit the general applicability of this reaction, and a flow-system would be preferred.

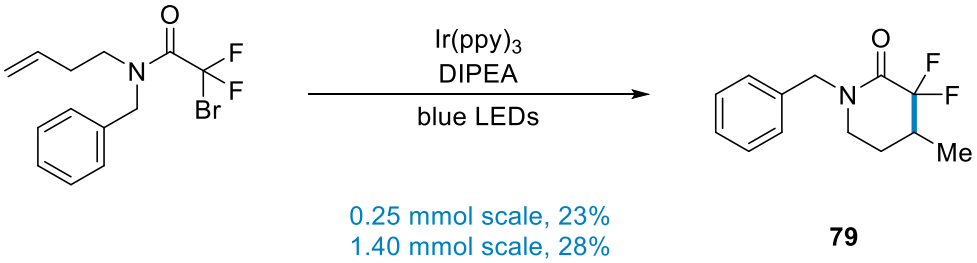

Scheme 3.3 Scale-up of batch photoredox radical cyclisation procedure. Reagents and conditions: $Ir(ppy)_3$ (1 mol%), DIPEA (10 equiv.), MeCN (0.01 M), rt, 3 h, blue LED irradiation.

We next explored amide reduction to access the corresponding amine product. Amide reduction conditions previously reported in the Denton group, using phenylsilane and zinc acetate, were used.[121] Fortunately under the reaction conditions, product **47** was formed in 42% yield. Whilst a good option to have in hand, straightforward synthesis of amine **47** using the two-step modular approach described in Chapter Two is significantly more efficient.

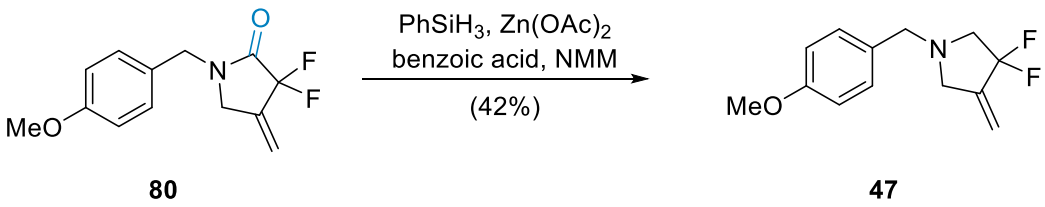

*Scheme 3.4 Reduction of amide **80** to amine **47**. Reagents and conditions: amide (1 equiv.), $PhSiH_3$ (2 equiv.), $Zn(OAc)_2$ (10 mol%), benzoic acid (0.5 equiv.), NMM (10 mol%), toluene, 110 °C, 19 h, 42%.*

3.2.3 Mechanistic Investigations

Having explored the scope of the photoredox catalysed amide cyclisation reaction, we next proposed a mechanism for the process (Figure 3.3). Based on our investigation into the mechanism of the amine cyclisation and hydrogen atom transfer reactions (Chapter Two), we propose a similar pathway. The strong reduction potential of $Ir(ppy)_3$ (-1.73 V *vs* SCE ($E_{1/2}^{Ir^{III*}/Ir^{IV}}$)) suggests an oxidative quenching mechanism is likely in action. In this case, upon irradiation, the catalyst forms the excited Ir(III)* complex which then reduces bromodifluoroacetamide **69** to give radical **81** and the corresponding Ir(IV) species. The Ir(IV) species is reduced back to Ir(III) by oxidation of the tertiary amine base to a radical cation. Intramolecular cyclisation should be rapid from the desired amide conformation to give **82**. Finally, as no additional sacrificial hydrogen atom donors are added to the reaction mixture, the radical cation of DIPEA is the most likely source of hydrogen atoms to quench the reaction. In the amine cyclisation system, deuterium-labelling studies revealed that acetonitrile was a competent hydrogen atom donor, responsible for a small proportion of hydrogen atom incorporation. Therefore, it is possible that some hydrogen atoms come from acetonitrile as well as from DIPEA in this system too.

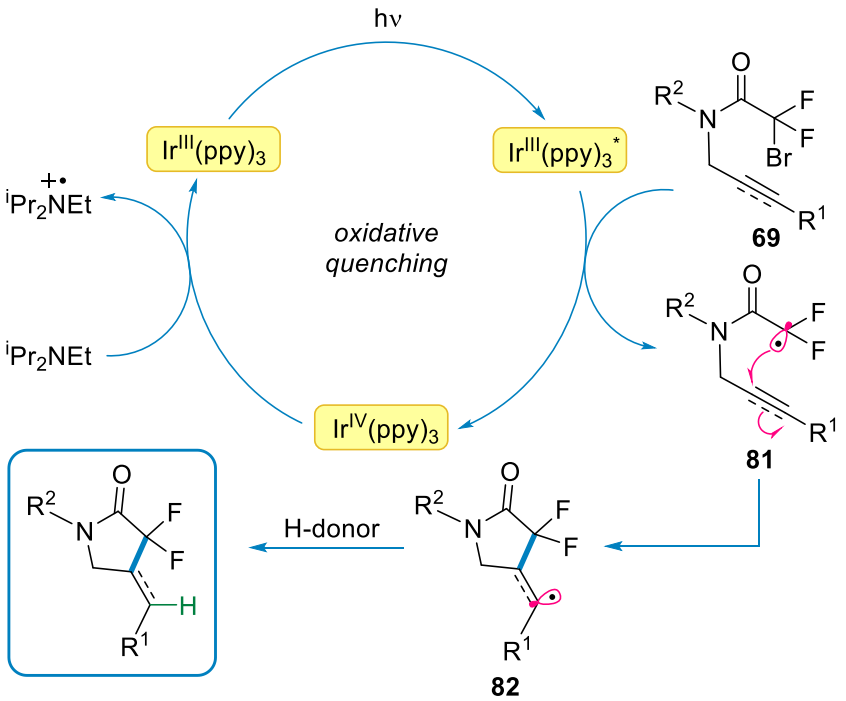

Figure 3.3 Proposed mechanism for the photoredox radical cyclisation of amides.

Control experiments confirmed that the reaction does not proceed in the absence of LED irradiation. Using blue LEDs as the source of irradiation led to a significantly higher yield of product **72** compared to the use of white LEDs, suggesting that the blue LEDs emit light of the correct wavelength for the catalyst to absorb, whereas the white LEDs emit fewer photons with this wavelength.

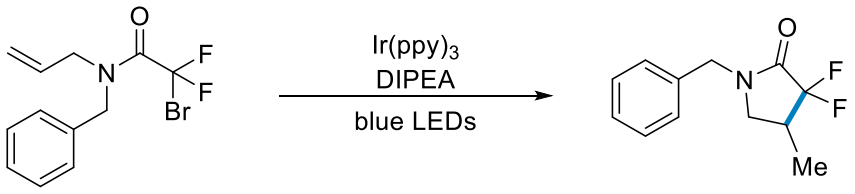

71 **72**

entry	variable(s) changed	product yield /%	starting material yield /%
1	none	55	0
2	white LEDs	23	0
3	no visible-light irradiation	0	100

Table 3.3 Control experiments for the amide cyclisation reaction. Standard reagents and conditions: amide (1 equiv.), Ir(ppy)$_3$ (1 mol%), DIPEA (10 equiv.), MeCN (0.01 M), rt, 16 h, blue LED irradiation. Yields were determined by ^{19}F NMR spectroscopy using trifluorotoluene as an internal standard.

To gain further insight into the possible mechanism, computational modelling was carried out by Prof. Ross Denton. Energy barriers associated with amide bond rotation and the transition states for 5-*exo-trig* and 6-*endo-trig* cyclisations were calculated (Figure 3.4). From these transition states, the equilibrium geometry for the nearest energy minimum was calculated. The calculations were modelled on the simple *N*-allyl-*N*-methyl radical substrate, and it was found that rotation of the amide bond (energy barrier +11.0 kcal/mol) was achievable at 298 K. This was also confirmed by the ^{1}H NMR spectrum of the amide starting material having time-averaged signals. The energy barrier for 5-*exo-trig* cyclisation is also very small (+6.1 kcal/mol), suggesting this process occurs readily from the reactive amide bond conformation. It is therefore predicted that dimerisation reactions or quenching of the linear radical prior to cyclisation should be limited. The 6-*endo-trig* cyclisation product was not expected to form in the reaction, as the energy barrier (+12.8 kcal/mol) for this transition state is too high relative to that of the 5-*exo-trig* transition state. This is a case of kinetic control as the 6-*endo-trig*

cyclisation is slower than the 5-*exo-trig* cyclisation. These computational findings are in line with experimental observations in which cyclisation occurs readily at room temperature and products arising from 6-*endo-trig* cyclisation, starting material dimerisation or quenching of the initally formed radical are not observed.

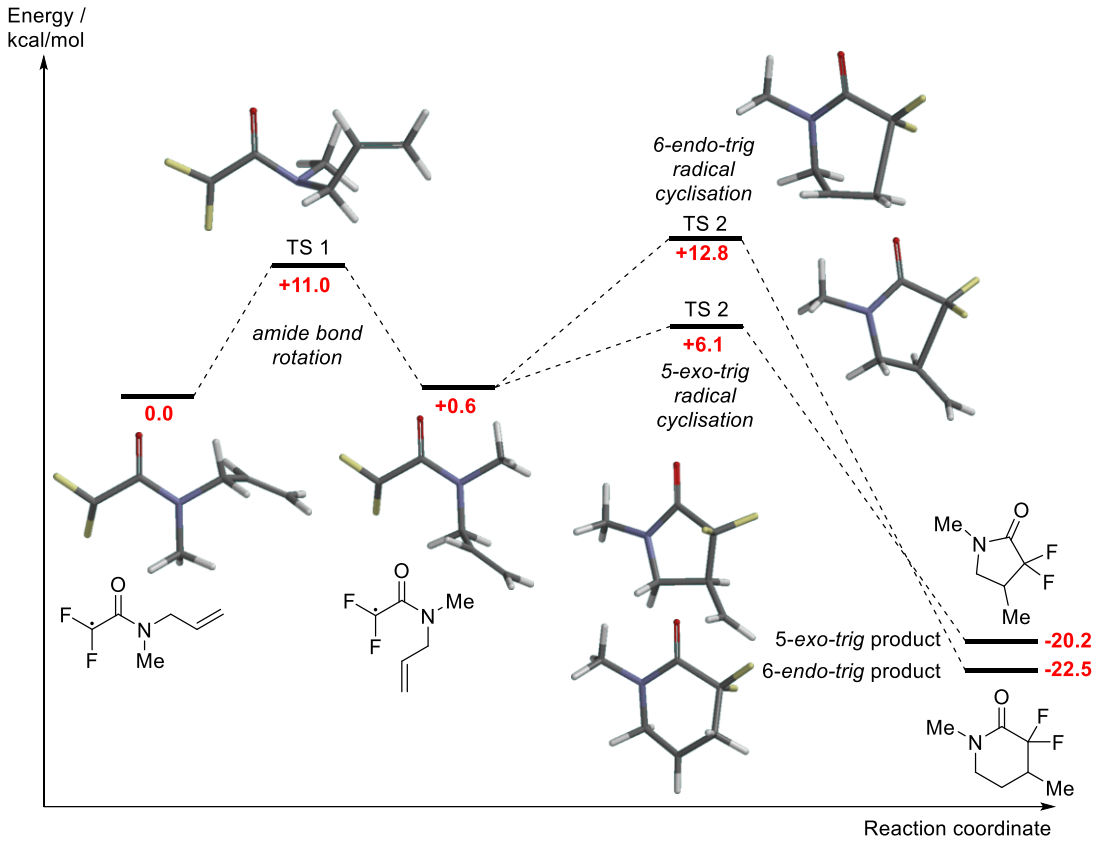

Figure 3.4 Relative energies calculated for amide bond rotation and radical cyclisation at 298 K.

3.2.4 Conclusions

In conclusion, we have extended our mild and efficient visible-light-mediated intramolecular cyclisation reaction from unactivated bromodifluoroalkyl amines to include bromodifluoroacetamides, generating complex and valuable γ- and δ-lactam products. The reaction was optimised, and nine lactams were isolated containing varying functional group patterns. As well as aryl acetamide substrates, benzyl and alkyl group substitution at the amide nitrogen atom was tolerated, expanding the current scope of the radical cyclisations used to make these lactams reported in the literature. A plausible mechanism for the cyclisation was proposed, and computational calculations helped to validate our experimental observations. These fluorinated lactam products are expected to be of value to the pharmaceutical and agrochemical industries.

Experimental

4.1 General Experimental

Reagents were purchased from commercial suppliers and used directly without further purification. Unless indicated, technical grade solvents were purchased from commercial suppliers and used without further purification, except THF which was dried over sodium wire and obtained from a solvent tower, where degassed solvent was passed through two columns of activated alumina and 7-micron filter under a 4-bar pressure. Petrol refers to the fraction of petroleum ether boiling between 40–60 °C. All water was deionised before use and all reactions are conducted under an Ar atmosphere unless otherwise stated.

Analytical Thin Layer Chromatography (TLC) was performed on Merck aluminium-backed silica-gel plates 60 F254 plates and visualized by ultraviolet (UV) irradiation (254 nm) or by staining with a solution of potassium permanganate. Column chromatography was carried out using Fluorochem silica gel 60 Å (40-63 mesh). Melting points were obtained using a Stuart SMP3 and Fourier Transform Infrared Spectrometry (IR) was carried out using a Bruker Tensor 27 using an Attenuated Total Reflection (ATR) attachment and peaks are reported in terms of frequency of absorption (cm^{-1}). High Resolution Mass Spectrometry (HRMS) were measured on a Bruker microTOF II with Electron Spray Ionisation (ESI). NMR spectra were recorded on either a Bruker AV 400, AV(III) 400HD or AV(III) 500HD in $CDCl_3$, DMSO-d_6 or MeOH-d_4. ^1H NMR chemical shifts (δ) were reported in parts per million (ppm) and coupling constants (*J*) are given in Hertz (Hz), with residual protic solvent as the internal reference ($CDCl_3$ δ = 7.26 ppm, DMSO-d_6 δ = 2.50 ppm, MeOH-d_4 δ = 3.31 ppm). The proton spectra are reported as follows: δ (multiplicity, coupling constant J, number of protons). Abbreviations used include s – singlet, d – doublet, t – triplet, q – quartet, sept – septet, m – multiplet, br – broad, app. – apparent. ^{13}C chemical shifts (δ) were reported in ppm relative to the ^{13}C signals in the solvent (central peak of $CDCl_3$ δ = 77.16 ppm, DMSO δ = 39.52 ppm, MeOH-d_4 δ = 49.03 ppm) and coupling constants (*J*) are given in Hertz (Hz). All ^{13}C NMR are reported as proton decoupled spectra. ^{19}F NMR were recorded on a 376 MHz spectrometer, chemical shifts (δ) were reported in ppm relative to $CFCl_3$ at 0.00 ppm and are reported as proton

decoupled spectra. Where appropriate, COSY, HMQC and HMBC experiments were performed to aid assignment. All photoredox reactions were conducted in borosilicate glass disposable culture tubes (approximate wall thickness 0.6 mm), or in a 250 mL borosilicate glass measuring cylinder.

4.2 Reaction Optimisation

Optimisation of alkynyl amine cyclisation

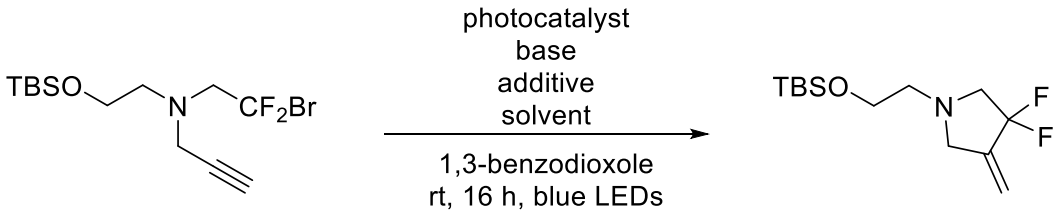

To a 10 mL culture tube was added *N*-(2-bromo-2,2-difluoroethyl)-*N*-(2-((*tert*-butyldimethylsilyl)oxy)ethyl)prop-2-yn-1-amine (0.05 mmol), photocatalyst (equiv. as in Table 2.2), base (equiv. as in Table 2.2), H-source additive (equiv. as in Table 2.2) and solvent (see Table 2.2). The culture tube was sealed and the mixture was sparged with Ar for 15 minutes. The blue LEDs were switched on and the reaction was stirred at room temperature for 16 hours. 1,3-Benzodioxole (1 equiv.) was added and the mixture was stirred at room temperature for 5 minutes, then analysed by ^{1}H NMR.

Optimisation of alkenyl amine cyclisation

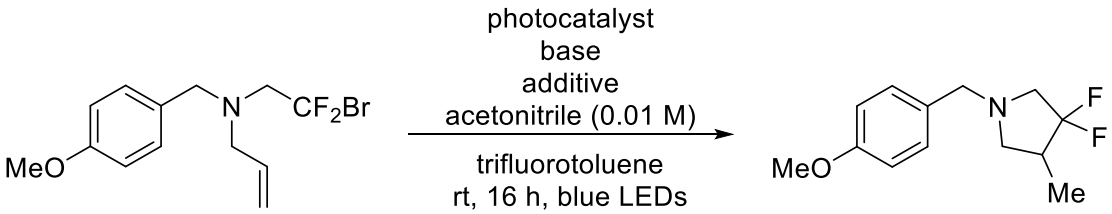

To a 10 mL culture tube was added *N*-(2-bromo-2,2-difluoroethyl)-*N*-(4-methoxybenzyl)prop-2-en-1-amine (0.05 mmol), photocatalyst (equiv. as in Table 2.3), base (equiv. as in Table 2.3), H-source additive (equiv. as in Table 2.3) and acetonitrile (100 mL/mmol). The culture tube was sealed and the mixture was sparged with Ar for 15 minutes. The blue LEDs were

switched on and the reaction was stirred at room temperature for 16 hours. Trifluorotoluene (1 equiv.) was added and the mixture was stirred at room temperature for 5 minutes, then analysed by ^{19}F NMR.

Optimisation of amide cyclisation

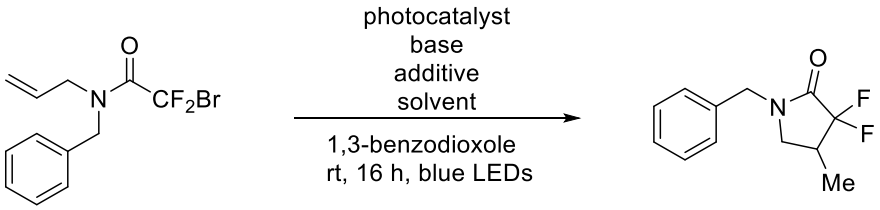

To a 50 mL culture tube was added *N*-allyl-*N*-benzyl-2-bromo-2,2-difluoroacetamide (0.25 mmol), photocatalyst (equiv. as in Table 3.1), base (equiv. as in Table 3.1), H-source additive (equiv. as in Table 3.1) and solvent (see Table 3.1). The culture tube was sealed and the mixture was sparged with Ar for 15 minutes. The blue LEDs were switched on and the reaction was stirred at room temperature for 16 hours. 1,3-Benzodioxole (1 equiv.) was added and the mixture was stirred at room temperature for 5 minutes, then analysed by ^{1}H NMR.

4.3 General Procedures

1. Amidation reaction using ethyl bromodifluoroacetate

To ethyl bromodifluoroacetate (1.1 equiv.) at 0°C was added the appropriate amine (1 equiv.) dropwise over 10 minutes. The flask was purged with Ar and stirred at room temperature for 16 hours. To the reaction mixture was added ethyl acetate (20 mL/g), water (10 mL/g), HCl (5 mL/g of a 1 M aq. solution), $NaHCO_3$ (5 mL/g of a sat. aq. solution) and brine (5 mL/g of a sat. aq. solution) and the mixture was extracted with ethyl acetate (3 × 20 mL/g). The combined organics were dried over magnesium sulfate and concentrated to give a residue which was used in the next step without further purification.

2. Two-Component Bromodifluoroalkylation Reaction

To an oven-dried flask fitted with a water condenser under an argon atmosphere was added the appropriate secondary amine (1 equiv.), and THF (0.5 mL/mmol). $PhSiH_3$ (3 equiv.) and bromodifluoroacetic acid (2 equiv.) in THF (0.5 mL/mmol) were added at 70 °C and the reaction mixture was heated at 70 °C until TLC analysis indicated complete secondary amine consumption. The reaction mixture was cooled to room temperature and $NaHCO_3$ (10 mL/g of a sat. aq. solution) was added. The mixture was extracted with diethyl ether (3 × 10 mL/g). The combined organics were dried ($MgSO_4$) and concentrated to ~2 mL volume, then purified as specified.

3. Three-Component Bromodifluoroalkylation Reaction

To an oven-dried flask fitted with a water condenser under an argon atmosphere was added the appropriate primary amine (1 equiv.), aldehyde (1 equiv.) and THF (0.5 mL/mmol), followed by $PhSiH_3$ (0.5 equiv.). The reaction was stirred at 70 °C for 10 minutes. Further $PhSiH_3$ (3 equiv.) and bromodifluoroacetic acid (2 equiv.) in THF (0.5 mL/mmol) were added and the reaction mixture was heated at 70 °C until TLC analysis indicated complete consumption of starting material. The reaction mixture was cooled to room temperature and $NaHCO_3$ (10 mL/g of a sat. aq. solution) was added. The mixture was extracted with diethyl ether (3 × 10 mL/g). The combined organics were dried ($MgSO_4$) and concentrated to ~2 mL volume, then purified as specified.

4. Photoredox Radical Cyclisation Reaction of Amides

To a culture tube was added the appropriate amide (1 equiv.), $Ir(ppy)_3$ (1 mol%) and acetonitrile (100 mL/mmol). The culture tube was sealed and the mixture was sparged with Ar for 20 minutes. To the reaction mixture was added DIPEA (10 equiv.). The blue LEDs were switched on and the reaction was stirred at room temperature until complete amide consumption was observed, and then concentrated. The crude material was purified as specified.

5. Photoredox Radical Cyclisation Reaction of Alkynyl Amines

To a culture tube was added the appropriate amine (1 equiv.), $Ir(ppy)_3$ (1 mol%), Et_3N (10 equiv.), AcOH (5 equiv.) and acetonitrile (100 mL/mmol). The culture tube was sealed and the mixture was sparged with Ar for 20 minutes. The blue LEDs were switched on and the reaction was stirred at room temperature until complete amine consumption was observed, and then concentrated. The crude material was purified as specified.

6. Photoredox Radical Cyclisation Reaction of Alkenyl Amines

To a culture tube was added the appropriate amine (1 equiv.), $Ir(ppy)_3$ (1 mol%), DIPEA (10 equiv.), TTMSS (5 equiv.) and acetonitrile (100 mL/mmol). The culture tube was sealed and the mixture was sparged with Ar for 20 minutes. The blue LEDs were switched on and the reaction was stirred at room temperature until complete amine consumption was observed. KF on alumina (40 wt%, 6 g/mmol) was added and the mixture was stirred at room temperature for 15 minutes, then filtered and concentrated. The crude material was purified as specified.

4.4 Experimental Procedures

4.4.1 Synthesis of Tertiary Amine Starting Materials

_N_-(2-Bromo-2,2-difluoroethyl)-_N_-(4-methoxybenzyl)prop-2-en-1-amine 41

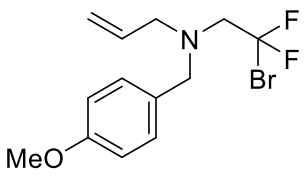

Allylamine (75.0 µL, 1.00 mmol) and *p*-anisaldehyde (120 µL, 1.00 mmol) were subjected to General Procedure 3, stirring for 16 hours. The crude material was purified by flash column chromatography (SiO_2, eluting with 0-5% diethyl ether in petroleum ether) to give **41** (165 mg, 517 µmol, 52% yield) as a colourless oil.

R_f (98:2 petroleum ether: ethyl acetate) = 0.26; **ν_{max}** (thin film)/cm^{-1} 3076, 3002, 2935, 2909, 2835, 1612, 1510; **δ_H** (500 MHz, $CDCl_3$) 7.28 – 7.23 (m, 2H, Ar*H*), 6.89 – 6.85 (m, 2H, Ar*H*), 5.84 (ddt, *J* = 17.7, 9.7, 6.5 Hz, 1H, *H*C=CH_2), 5.21 – 5.19 (m, 1H, HC=C*H*$_2$), 5.19 – 5.16 (m, 1H, HC=C*H*$_2$), 3.81 (s, 3H, OC*H*$_3$), 3.79 (s, 2H, NC*H*$_2$Ar), 3.32 (t, *J* = 13.4 Hz, 2H, NC*H*$_2$$CF_2Br$), 3.26 (d, *J* = 6.5 Hz, 2H, NC*H*$_2$CH); **δ_C** (126 MHz, $CDCl_3$) 159.0 (Ar*C*(OCH_3)), 134.9 (H*C*=CH_2), 130.5 (Ar*C*q), 130.2 (Ar*C*H), 124.2 (t, *J* = 310.3 Hz, *C*F_2Br), 118.6 (HC=*C*H$_2$), 113.9 (Ar*C*H), 62.0 (t, *J* = 22.0 Hz, N*C*$H_2$$CF_2Br$), 58.0 (N*C*H$_2$Ar), 56.7 (N*C*$H_2$CH), 55.4 (O*C*$H_3$); **$\delta_F$** (376 MHz, $CDCl_3$) –49.55; **HRMS** (ESI) m/z: $[M+H]^+$ calcd for $C_{13}H_{16}{}^{79}BrF_2NO$ 320.0456; found 320.0457 (+0.40 ppm).

Methyl (*E*)-4-((2-bromo-2,2-difluoroethyl)(4-methoxybenzyl)amino)but-2-enoate 83

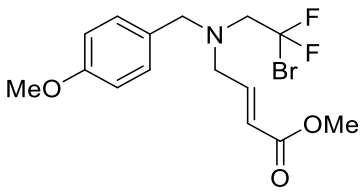

To a stirred solution of *N*-(2-bromo-2,2-difluoroethyl)-*N*-(4-methoxybenzyl)prop-2-en-1-amine (265 mg, 827 µmol) and methyl acrylate (0.37 mL, 4.14 mmol) in DCM (1.6 mL) was added (1,3-dimesitylimidazolidin-2-ylidene)dichloro(2-isopropoxy-5-nitrobenzylidene)ruthenium(II) (11.1 mg, 16.5 µmol). The mixture was stirred at room temperature for 72 hours. The crude material was purified by flash column chromatography (SiO_2, eluting with 0-20% diethyl ether in pentane) to give **83** (166 mg, 438 µmol, 53% yield) as a colourless oil.

R_f (80:20 petroleum ether: diethyl ether) = 0.30; **ν_{max}** (thin film)/cm^{-1} 3000, 2952, 2907, 2837, 1721; **δ_H** (400 MHz, $CDCl_3$) 7.24 (d, *J* = 8.5 Hz, 2H, ArC*H*), 6.92 (dt, *J* = 15.8, 6.2 Hz, 1H, NH_2CC(*H*)=CH), 6.87 (d, *J* = 8.5 Hz, 2H, ArC*H*), 6.00 (dt, *J* = 15.8, 1.5 Hz, 1H, H_2CC(H)=C*H*), 3.81 (br s, 5H, NCH_2Ar and ArC(OC*H*$_3$)), 3.75 (s, 2H, OC*H*$_3$, ester), 3.43 (d, *J* = 6.2 Hz, 2H, NC*H*$_2$C(H)=CH), 3.34 (t, *J* = 13.3 Hz, 2H, NC*H*$_2$$CF_2Br$); **$\delta_C$** (101 MHz, $CDCl_3$) 166.6 (*C*=O), 159.2 (Ar*C*(OCH_3)), 145.0 (NCH_2*C*(H)=CH), 130.1 (Ar*C*), 129.8 (Ar*C*q), 123.7 (t, *J* = 310.0 Hz, CF_2Br), 123.4 (HC=*C*(H)C=O), 114.0 (Ar*C*H), 62.6 (t, *J* = 22.4 Hz, NCH_2CF_2Br), 58.2 (NCH_2Ar), 55.4 (ArC(O*C*H_3)), 54.4 (N*C*H_2C(H)=CH), 51.8 (O*C*H_3, ester); **δ_F** (376 MHz, $CDCl_3$)

–49.96; **HRMS** (ESI) m/z: $[M+Na]^+$ calcd for $C_{15}H_{18}{}^{79}BrF_2NO_3$ 400.0330; found 400.0331 (+0.10 ppm).

(*E*)-5-(Benzyl(2-bromo-2,2-difluoroethyl)amino)pent-3-en-2-one 84

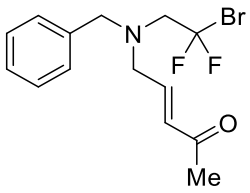

To a stirred solution of *N*-benzyl-*N*-(2-bromo-2,2-difluoroethyl)prop-2-en-1-amine (232 mg, 800 µmol) and methyl vinyl ketone (0.33 mL, 4.00 mmol) in DCM (1.6 mL) was added (1,3-Dimesitylimidazolidin-2-ylidene)dichloro(2-isopropoxy-5-nitrobenzylidene) ruthenium(II) (10.7 mg, 16.0 µmol). The mixture was stirred at 40 °C for 23 hours. The crude material was purified by flash column chromatography (SiO_2, eluting with 10-20% diethyl ether in pentane) to give **84** (161 mg, 483 µmol, 61% yield) as a colourless oil.

R_f (90:10) petroleum ether: diethyl ether) = 0.13; **ν_{max}** (thin film)/cm^{-1} 3087, 3063, 3030, 3006, 2924, 2834, 1698, 1675, 1631; **δ_H** (400 MHz, $CDCl_3$) 7.39 – 7.31 (m, 4H, Ar*H*), 7.34 – 7.25 (m, 1H, Ar*H*), 6.71 (dt, *J* = 16.1, 6.1 Hz, 1H, *H*C=CHC(O)CH_3), 6.18 (d, *J* = 16.1 Hz, 1H, HC=C*H*C(O)CH_3), 3.90 (s, 2H, NCH_2Ar), 3.47 (d, *J* = 6.1 Hz, 1H, NCH_2C(H)=C), 3.38 (t, *J* = 13.2 Hz, 2H, NCH_2CF_2Br), 2.24 (s, 3H, CH_3); **δ_C** (101 MHz, $CDCl_3$) 198.3 (*C*=O), 143.9 (H*C*=CHC(O)CH_3), 137.9 (Ar*C*q), 132.8 (HC=*C*HC(O)CH_3), 128.9 (Ar*C*H), 128.6 (Ar*C*H), 127.7 (Ar*C*H), 123.5 (t, *J* = 309.8 Hz, *C*F_2Br), 63.1 (t, *J* = 22.4 Hz, *C*H_2CF_2Br), 59.3 (N*C*H_2Ar), 55.2 (N*C*H_2C(H)=C), 27.1 (*C*H_3); **δ_F** (376 MHz, $CDCl_3$) –0.22; **HRMS** (ESI) m/z: $[M+H]^+$ calcd for $C_{14}H_{16}{}^{79}BrF_2NO$ 332.0456; found 332.0460 (+1.00 ppm).

_N_-Benzyl-2-bromo-_N_-(cyclohex-1-en-1-ylmethyl)-2,2-difluoroethan-1-amine 85

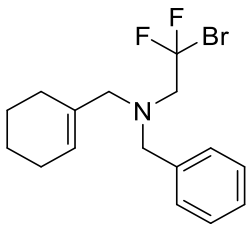

To a stirred solution of cyclohexene-1-carboxylic acid (1.00 g, 7.93 mmol) and benzylamine (580 µL, 5.28 mmol) in toluene (5.3 mL) at 110 °C was added phenylsilane (490 µL, 3.96 mmol). The reaction mixture was stirred at 110 °C for 16 hours, then $Zn(OAc)_2$ (970 µg, 528 µmol) and further phenylsilane (1.95 mL, 15.8 mmol) were added. The reaction mixture was stirred at 110 °C for 8 hours, then cooled to room temperature. Ethyl acetate (20 mL) was added and the mixture was extracted with HCl (3 × 10 mL of a 3 M aq. solution) The combined aqueous layers were basified until pH 12 with NaOH (6 M aq. solution). The mixture was extracted with dichloromethane (3 × 15 mL). The combined organics were dried over magnesium sulfate and concentrated. The resulting residue was purified by flash column chromatography (SiO_2, eluting with 10% methanol in dichloromethane) to give a yellow oil which was dissolved in THF (0.9 mL) and heated to 70 °C. $PhSiH_3$ (655 µL, 5.31 mmol) was added, followed by bromodifluoroacetic acid (619 mg, 3.54 mmol) in THF (0.9 mL). The reaction mixture was stirred at 70 °C for 21 hours then cooled to room temperature. $NaHCO_3$ (20 mL of a sat. aq. solution) was added and the mixture was extracted with diethyl ether (3 × 20 mL). The combined organics were dried over magnesium sulfate and concentrated to ~2 mL volume. The material was purified by flash column chromatography (SiO_2, eluting with 0-2% diethyl ether in petroleum ether). The mixed fractions were repurified by flash column chromatography (SiO_2, eluting with 0-2% diethyl ether in pentane) to give **85** (314 mg, 912 µmol, 12% yield) as a colourless oil.

R_f (pentane) = 0.53; **ν_{max}** (thin film)/cm^{-1} 3087, 3064, 3028, 2998, 2926, 2856, 2808, 1668, 1603; **δ_H** (400 MHz, $CDCl_3$) 7.38 – 7.26 (m, 5H, Ar*H*), 5.60 (app s, 1H, C*H*, alkene), 3.79 (s, 2H, NCH_2), 3.30 (t, *J* = 13.7 Hz, 2H, NCH_2CF_2Br), 3.09 (s, 2H, NCH_2), 2.06 – 1.93 (m, 4H, C$H_2CH_2CH_2CH_2$), 1.67 – 1.49 (m, 4H, $CH_2CH_2CH_2CH_2$); **δ_C** (101 MHz, $CDCl_3$) 138.9 (*C*,

alkene), 135.4 (Ar*C*, quaternary), 129.0 (Ar*C*), 128.4 (Ar*C*), 127.4 (Ar*C*), 126.2 (*C*H, alkene), 124.3 (t, *J* = 310.8 Hz, *C*F_2Br), 62.3 (t, *J* = 21.7 Hz, N*C*$H_2$$CF_2$Br), 61.8 (N*C*$H_2$), 58.6 (t, *J* = 1.7 Hz, N*C*H_2Ar), 26.9 (HC=C-*C*H_2), 25.4 (C=CH-*C*H_2), 22.8 (CH_2*C*$H_2$$CH_2$$CH_2$), 22.6 ($CH_2$$CH_2$*C*$H_2$$CH_2$); **$\delta_F$** (376 MHz, $CDCl_3$) –48.56; **HRMS** (ESI) m/z: $[M+H]^+$ calcd for $C_{16}H_{20}{}^{79}BrF_2N$ 344.0820; found 344.0822 (+0.70 ppm).

tert-Butyl (4-methoxybenzyl)(prop-2-yn-1-yl)carbamate 86

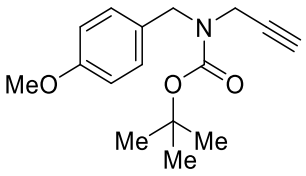

To a 0 °C solution of 4-methoxybenzylamine (2.87 mL, 22.0 mmol) in dichloromethane (60 mL) was added Boc_2O (4.36 g, 20.0 mmol). The mixture was stirred at room temperature for 16 hours. Water (15 mL) was added and the mixture was extracted with dichloromethane (3 × 20 mL). The combined organics were dried over magnesium sulfate and concentrated to give a residue which was dissolved in DMF (5 mL) and added dropwise over 20 minutes to a 0 °C suspension of NaH (960 mg, 24.0 mmol of a 60% dispersion in mineral oil) in DMF (15 mL). The mixture was stirred at 0 °C for 30 minutes. To the mixture was added propargyl bromide (2.67 mL, 24.0 mmol of 80% w/w solution in toluene) dropwise over 10 minutes. The reaction mixture was stirred at room temperature for 16 hours. To the reaction mixture was added water (100 mL) and brine (50 mL of a sat. aq. solution) and the mixture was extracted with diethyl ether (3 × 30 mL). The combined organics were dried over magnesium sulfate and concentrated. The resulting residue was purified by flash column chromatography (SiO_2, eluting with 5-10% diethyl ether in pentane) to give **86** (3.53 g, 12.8 mmol, 64% yield) as a yellow oil.

R_f (90:10 petroleum ether: diethyl ether) = 0.46; **ν_{max}** (thin film)/cm^{-1} 3291, 3262, 3002, 2976, 2933, 2873, 2837, 1689; **δ_H** (400 MHz, $CDCl_3$) 7.18 (d, *J* = 8.1 Hz, 2H, Ar*H*), 6.83 (d, *J* = 8.1 Hz, 2H, Ar*H*), 4.46 (s, 2H, NCH_2Ar), 4.12 – 3.82 (m, 2H, NCH_2, propargyl), 3.75 (s, 3H, OCH_3), 2.21 (t, *J* = 2.5 Hz, 1H, C*H*, alkyne), 1.47 (s, 9H, (C(CH_3)$_3$)); **δ_C** (101 MHz, $CDCl_3$) 159.0

(Ar*C*(OMe)), 154.9 (*C*=O), 129.4 (Ar*C*H), 129.1 (Ar*C*q), 113.9 (Ar*C*H), 80.4 (*C*(CH_3)$_3$), 79.4 (*C*q, alkyne), 71.7 (*C*H, alkyne), 55.1 (O*C*H_3), 48.4 (N*C*H_2Ar), 34.9 (N*C*H_2, propargyl), 28.3 (C(*C*H_3)$_3$); **HRMS** (ESI) m/z: $[M+H]^+$ calcd for $C_{16}H_{21}NO_3$ 276.1594; found 276.1589 (+1.90 ppm).

***tert*-Butyl buta-2,3-dien-1-yl(4-methoxybenzyl)carbamate 87**

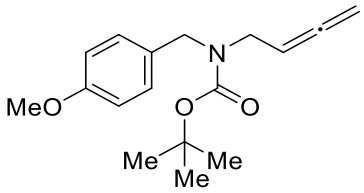

tert-Butyl (4-methoxybenzyl)(prop-2-yn-1-yl)carbamate (135 mg, 0.491 mmol), CuI (46.8 mg, 0.246 mmol) and $(CHO)_n$ (73.9 mg, 2.46 mmol) were dissolved in 1,4-dioxane (2.5 mL). Diisopropylamine (140 µL, 0.982 mmol) was added and the reaction mixture stirred at 110 °C for 16 h. The reaction mixture was cooled to room temperature, diluted with ethyl acetate (5 mL) and filtered through a silica plug, washing with ethyl acetate (50 mL) and the solvent was evaporated under reduced pressure. The resulting residue was purified by flash column chromatography (SiO_2, eluting with 10% diethyl ether in pentane) to give **87** (136 mg, 0.470 mmol, 96% yield) as a pale yellow oil.

R_f (90:10 petroleum ether: diethyl ether) = 0.18; **ν_{max}** (thin film)/cm^{-1} 3062, 3032, 2975, 2932, 2871, 2836, 1955, 1687, 1612; **δ_H** (400 MHz, $CDCl_3$) 7.17 (d, *J* = 8.5 Hz, 2H, Ar*H*), 6.84 (d, *J* = 8.5 Hz, 2H, Ar*H*), 5.08 (d, *J* = 19.2 Hz, 1H, *H*C=C=CH_2), 4.74 (d, *J* = 3.9 Hz, 2H, HC=C=C*H*$_2$), 4.37 (s, 2H, NC*H*$_2$Ar), 3.90 – 3.63 (m, 5H, OC*H*$_3$ and NC*H*$_2$C(H)=C), 1.48 (s, 9H, C(C*H*$_3$)$_3$); **δ_C** (101 MHz, $CDCl_3$) 209.1 (HC=*C*=CH_2), 158.9 (Ar*C*(OMe)), 155.6 (*C*=O), 130.3 (Ar*C*H), 129.4 (Ar*C*q), 113.9 (Ar*C*H), 87.0 (H*C*=C=CH_2), 79.8 (*C*(CH_3)$_3$), 76.2 (HC=C=*C*H_2), 55.2 (O*C*H_3), 48.9 (N*C*H_2Ar), 44.7 (N*C*H_2C(H)=C), 28.5 (C(*C*H_3)$_3$); **HRMS** (ESI) m/z: $[M+H]^+$ calcd for $C_{17}H_{23}NO_3$ 290.1751; found 290.1741 (+3.50 ppm).

_N_-(4-Methoxybenzyl)buta-2,3-dien-1-amine hydrochloride 88

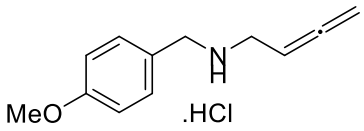

To a 0 °C solution of *tert*-butyl buta-2,3-dien-1-yl(4-methoxybenzyl)carbamate (128 mg, 0.441 mmol) in dioxane (0.62 mL) was added HCl (0.53 mL of a 4 M solution in dioxane). The mixture was warmed to room temperature and stirred for 18 hours. The reaction mixture was filtered, washing with diethyl ether to give **88** (69.5 mg, 0.308 mmol, 70%) as a white solid.

m.p. 145–148 °C; $\boldsymbol{\nu_{max}}$ (thin film)/cm^{-1} 3065, 2990, 2956, 2936, 2911, 2856, 2836, 2790, 2759, 2717, 2650, 2623, 2480, 1949, 1742, 1614; $\boldsymbol{\delta_H}$ (500 MHz, MeOH-d_4) 7.50 – 7.40 (m, 2H, Ar*H*), 7.07 – 6.96 (m, 2H, Ar*H*), 5.38 (tt, *J* = 7.0, 7.0 Hz, 1H, *H*C=C=CH$_2$), 5.07 (dt, *J* = 7.0, 2.5 Hz, 2H, HC=C=C*H*$_2$), 4.18 (s, 2H, NHC*H*$_2$Ar), 3.83 (s, 3H, OC*H*$_3$), 3.65 (dt, *J* = 7.0, 2.5 Hz, 2H, NC*H*$_2$C(H)=C); $\boldsymbol{\delta_C}$ (126 MHz, MeOH-d_4) 211.7 (HC=*C*=CH$_2$), 162.2 (Ar*C*(OMe)), 132.6 (Ar*C*H), 124.1 (Ar*C*q), 115.6 (Ar*C*H), 83.1 (H*C*=C=CH$_2$), 78.1 (HC=C=*C*H$_2$), 55.9 (O*C*H$_3$), 51.1 (NH*C*H$_2$Ar), 46.6 (NH*C*H$_2$C(H)=C); **HRMS** (ESI) m/z: [M+H]$^+$ calcd for $C_{12}H_{15}NO$ 190.1226; found 190.1223 (+1.60 ppm).

_N_-(2-bromo-2,2-difluoroethyl)-_N_-(4-methoxybenzyl)buta-2,3-dien-1-amine 33

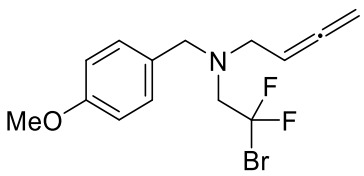

N-(4-Methoxybenzyl)buta-2,3-dien-1-amine hydrochloride (162 mg, 0.719 mmol) and Et$_3$N (100 µL, 0.719 mmol) were subjected to General Procedure 2, stirring at 70 °C for 14 hours. The crude material was purified by flash column chromatography (SiO$_2$, eluting with 0-2% diethyl ether in petroleum ether) to give **33** (218 mg, 0.656 mmol, 91% yield) as a colourless oil.

R_f (95:5 petroleum ether: diethyl ether) = 0.41; **ν_{max}** (thin film)/cm^{-1} 3063, 3034, 2997, 2955, 2935, 2909, 2836, 1953, 1612; **δ_H** (400 MHz, $CDCl_3$) 7.29 (d, *J* = 8.6 Hz, 2H, Ar*H*), 6.89 (d, *J* = 8.6 Hz, 2H, Ar*H*), 5.15 (tt, *J* = 6.7, 5.0 Hz, 1H, *H*C=C=CH_2), 4.77 (dt, *J* = 6.7, 2.5 Hz, 2H, HC=C=CH_2), 3.85 (s, 2H, NCH_2Ar), 3.82 (s, 3H, OCH_3), 3.39 (t, *J* = 13.3 Hz, 2H, NCH_2CF_2Br), 3.36 – 3.29 (m, 2H, NCH_2C(H)=C); **δ_C** (101 MHz, $CDCl_3$) 209.9 (HC=*C*=CH_2), 159.1 (Ar*C*(OMe)), 130.3 (Ar*C*q), 130.2 (Ar*C*H), 124.0 (t, *J* = 309.7 Hz, *C*F_2Br), 113.8 (Ar*C*H), 86.0 (H*C*=C=CH_2), 75.3 (HC=C=*C*H_2), 62.1 (t, *J* = 22.5 Hz, N*C*H_2CF_2Br), 57.7 (N*C*H_2Ar), 55.3 (O*C*H_3), 52.3 (NH*C*H_2C(H)=C); **δ_F** (376 MHz, $CDCl_3$) –9.94; **HRMS** (ESI) m/z: $[M+H]^+$ calcd for $C_{14}H_{16}{}^{79}BrF_2NO$ 332.0456; found 332.0455 (+0.40 ppm).

_N_-Benzylbut-3-yn-1-amine 89

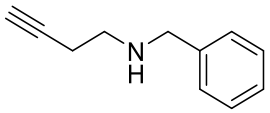

To a 0 °C suspension of 3-butyn-1-ol (1.50 mL, 20.0 mmol) and Et_3N (5.58 mL, 40.0 mmol) in dichloromethane (100 mL) was added methane sulfonylchloride (3.10 mL, 40.0 mmol) dropwise over 10 minutes. The mixture was stirred at room temperature for 4 hours, then water (20 mL) was added dropwise over 5 minutes. Dichloromethane (50 mL), water (20 mL) and $NaHCO_3$ (30 mL of a sat. aq. solution) were added and the mixture was extracted with dichloromethane (2 × 50 mL). The combined organics were dried over magnesium sulfate and concentrated. The resultant residue was added to a stirred solution of Et_3N (5.60 mL, 40.0 mmol), benzylamine (4.40 mL, 40.0 mmol) in THF (100 mL). The mixture was stirred at 70 °C for 21 hours. The reaction mixture was cooled to room temperature and ethyl acetate (50 mL), water (30 mL) and brine (20 mL of a sat. aq. solution) were added. The mixture was extracted with ethyl acetate (2 × 50 mL). The combined organics were dried over magnesium sulfate and concentrated. The resultant residue was purified by flash column chromatography (SiO_2, eluting with 20-80% ethyl acetate in petroleum ether, then 2-5% methanol in dichloromethane). The mixed fractions were purified again by flash column chromatography (SiO_2, eluting with 0-10% methanol in dichloromethane). The residues were combined to give **89** (1.36 g, 8.55 mmol, 43% yield) as a yellow/orange oil.

R_f (95:5 dichloromethane/methanol) = 0.42; **ν_{max}** (thin film)/cm^{-1} 3293, 3085, 6062, 3027, 2915, 2835, 2117; **δ_H** (400 MHz, $CDCl_3$) 7.39 – 7.21 (m, 5H, Ar*H*), 3.82 (s, 2H, NCH_2Ar), 2.81 (t, *J* = 6.6 Hz, 2H, NCH_2CH_2), 2.42 (td, *J* = 6.6, 2.7 Hz, 2H, NCH_2CH_2), 1.99 (t, *J* = 2.7 Hz, 1H, CH, alkyne); **δ_C** (101 MHz, $CDCl_3$) 140.1 (Ar*C*q), 128.4 (Ar*C*H), 128.1 (Ar*C*H), 127.0 (Ar*C*H), 82.5 (*C*q, alkyne), 69.6 (*C*H, alkyne), 53.3 (N*C*H_2), 47.3 (N*C*H_2), 19.5 (H_2C-C≡CH); **HRMS** (ESI) m/z: $[M+H]^+$ calcd for $C_{11}H_{13}N$ 160.1121; found 160.1123 (+1.40 ppm).

Data are consistent with the literature.[122]

***N*-Benzyl-*N*-(2-bromo-2,2-difluoroethyl)but-3-yn-1-amine 34**

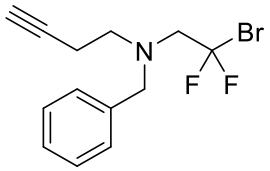

N-Benzylbut-3-yn-1-amine (0.203 g, 1.27 mmol) was subjected to General Procedure 2, stirring at 70 °C for 17 hours. The crude material was purified by flash column chromatography (SiO_2, eluting with 0-2% diethyl ether in petroleum ether) to give **34** (290 mg, 961 µmol, 75% yield) as a colourless oil.

R_f (98:2 petroleum ether: diethyl ether) = 0.47; **ν_{max}** (thin film)/cm^{-1} 3305, 3087, 3065, 3030, 2919, 2834; **δ_H** (400 MHz, $CDCl_3$) 7.39 – 7.27 (m, 5H, Ar*H*), 3.93 (s, 2H, NCH_2Ar), 3.46 (t, *J* = 13.3 Hz, 2H, N*C*$H_2$$CF_2$Br), 2.94 (t, *J* = 7.3 Hz, 2H, N*C*H_2*C*H_2), 2.35 (td, *J* = 7.3, 2.6 Hz, 2H, NCH_2*C*H_2), 1.97 (t, *J* = 2.6 Hz, 1H, C*H*, alkyne); **δ_C** (101 MHz, $CDCl_3$) 138.4 (Ar*C*q), 128.7 (Ar*C*H), 128.6 (Ar*C*H), 127.6 (Ar*C*H), 123.9 (t, *J* = 310.4 Hz, *C*F_2Br), 82.4 (*C*q, alkyne), 69.7 (*C*H, alkyne), 63.6 (t, *J* = 22.2 Hz, *C*$H_2$$CF_2$Br), 58.7 (N*C*$H_2$Ar), 52.8 (N*C*$H_2$$CH_2$), 17.7 (NC$H_2$*C*$H_2$); **$\delta_F$** (376 MHz, $CDCl_3$) –50.56; **HRMS** (ESI) m/z: $[M+H]^+$ calcd for $C_{13}H_{14}{}^{79}BrF_2N$ 302.0347; found 302.0350 (+1.20 ppm).

_N_-Benzyl-_N_-(2-bromo-2,2-difluoroethyl)but-3-en-1-amine 90

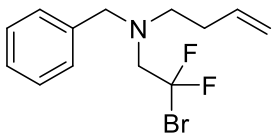

A solution of *N*-benzyl-*N*-(2-bromo-2,2-difluoroethyl)but-3-yn-1-amine (278 mg, 0.919 mmol) and Lindlar's catalyst (5 wt% Pd, 391 mg, 0.184 mmol) in THF (1.8 mL) was placed under a H_2 atmosphere. The reaction mixture was stirred at room temperature for 23 hours, then filtered through a silica plug, washing with diethyl ether and concentrated. The crude material was purified by flash column chromatography (SiO_2, eluting with 0-2% diethyl ether in pentane) to give **90** (158 mg, 0.519 mmol, 56% yield) as a yellow oil.

R_f (90:10 petroleum ether: diethyl ether) = 0.57; **ν_{max}** (thin film)/cm^{-1} 3309, 3079, 3065, 3030, 3002, 2977, 2945, 2926, 2831; **δ_H** (400 MHz, $CDCl_3$) 7.43 – 7.27 (m, 5H, Ar*H*), 5.78 (ddt, *J* = 17.1, 10.1, 6.7 Hz, 1H, *H*C=CH_2), 5.17 – 4.93 (m, 2H, HC=CH_2), 3.90 (s, 2H, NCH_2Ar), 3.40 (t, *J* = 13.6 Hz, 2H, NCH_2CF_2Br), 2.78 (t, *J* = 7.5 Hz, 2H, NCH_2CH_2), 2.28 (dt, *J* = 7.5, 7.5 Hz, 2H, NCH_2CH_2); **δ_C** (101 MHz, $CDCl_3$) 138.7 (Ar*C*q), 136.2 (H*C*=CH_2), 128.8 (Ar*C*H), 128.5 (Ar*C*H), 127.4 (Ar*C*H), 124.1 (t, *J* = 311.4 Hz, *C*F_2Br), 116.1 (HC=*C*H_2), 63.3 (t, *J* = 21.9 Hz, N*C*H_2CF_2Br), 58.9 (N*C*H_2Ar), 53.7 (N*C*H_2CH_2), 32.0 (NCH_2*C*H_2); **δ_F** (376 MHz, $CDCl_3$) –49.79; **HRMS** (ESI) m/z: $[M+H]^+$ calcd for $C_{13}H_{16}{}^{79}BrF_2N$ 304.0512; found 304.0458 (+17.7 ppm).

(*E*)-*N*-(2-Bromo-2,2-difluoroethyl)-*N*-(4-methoxybenzyl)-3-phenylprop-2-en-1-amine 42

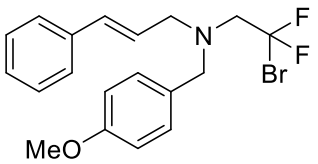

4-Methoxybenzylamine (260 µL, 2.00 mmol) and cinnamaldehyde (250 µL, 2.00 mmol) were subjected to General Procedure 3, stirring for 16 hours. The crude material was purified by flash column chromatography (SiO_2, eluting with 2-5% ethyl acetate in petroleum ether) to give **42** (451 mg, 1.14 mmol, 57% yield) as a pale yellow oil.

R_f (95:5 petroleum ether: ethyl acetate) = 0.43; **ν_{max}** (thin film)/cm^{-1} 3103, 3081, 3060, 3026, 3003, 2954, 2933, 2909, 2835, 1611; **δ_H** (400 MHz, $CDCl_3$) 7.42 – 7.22 (m, 7H, Ar*H*), 6.94 – 6.84 (m, 2H, Ar*H*), 6.52 (d, *J* = 15.8 Hz, 1H, *H*C=CH(CH_2)), 6.31 – 6.18 (m, 1H, HC=C*H*(CH_2)), 3.86 (d, *J* = 2.5 Hz, 2H, NC*H*$_2$), 3.82 (app d, *J* = 1.9 Hz, 3H, OC*H*$_3$), 3.44 (d, *J* = 6.7 Hz, 2H, NC*H*$_2$), 3.38 (td, *J* = 13.4, 2.5 Hz, 2H, C*H*$_2$$CF_2$Br); **$\delta_C$** (101 MHz, $CDCl_3$) 159.16 (Ar*C*(OCH_3)), 137.0 (Ar*C*q), 133.5 (H*C*=CH(CH_2)), 130.5 (Ar*C*q), 130.2 (Ar*C*H), 128.7 (Ar*C*H), 127.8 (Ar*C*H), 126.5 (Ar*C*H), 126.4 (HC=*C*H(CH_2)), 124.2 (t, *J* = 310.3 Hz, *C*F_2Br), 113.9 (Ar*C*H), 62.1 (t, *J* = 22.1 Hz, *C*$H_2$$CF_2$Br), 58.2 (N*C*$H_2$), 56.1 (N*C*$H_2$), 55.4 (O*C*$H_3$); **$\delta_F$** (376 MHz, $CDCl_3$) –9.47; **HRMS** (ESI) m/z: $[M+H]^+$ calcd for $C_{19}H_{20}{}^{79}BrF_2NO$ 396.0769; found 396.0767 (+0.60 ppm).

***N*-(2-((*tert*-Butyldimethylsilyl)oxy)ethyl)prop-2-yn-1-amine 91**

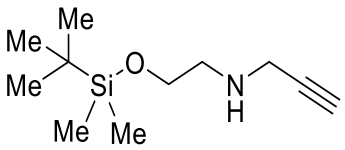

To a solution of ethanolamine (0.60 mL, 10.0 mmol) and imidazole (1.02 g, 15.0 mmol) in dichloromethane (5 mL) was added a solution of TBSCl (1.81 g, 12.0 mmol) in dichloromethane (10 mL) dropwise over 5 minutes. The reaction mixture was stirred at room temperature for 17 hours. The reaction mixture was poured into water (20 mL). The mixture was extracted with dichloromethane (3 × 20 mL). The combined organics were dried over magnesium sulfate and concentrated. To the resultant residue was added DIPEA (1.2 mL, 6.67 mmol) and dichloromethane (50 mL). Propargyl bromide (0.74 mL, 6.67 mmol of an 80% w/w solution in toluene) was added dropwise at 0 °C over 2 hours. The reaction mixture was stirred at room temperature for a further 3 hours. The reaction mixture was poured into $NaHCO_3$ (30 mL of a sat. aq. solution). The mixture was extracted with dichloromethane (3 × 30 mL). The combined organics were dried over magnesium sulfate and concentrated. The resultant residue was purified by flash column chromatography (SiO_2, eluting with 20-50% ethyl acetate in petroleum ether) to give **91** (523 mg, 2.45 mmol, 37% yield) as a yellow oil.

R_f (80:20 petroleum ether: ethyl acetate) = 0.28; **ν_{max}** (thin film)/cm^{-1} 3311, 2954, 2929, 2886, 2857, 1462; **δ_H** (400 MHz, $CDCl_3$) 3.74 (t, *J* = 5.2 Hz, 2H, OC*H*$_2$), 3.46 (d, *J* = 2.4 Hz, 2H,

NC*H*$_2$C≡CH), 2.79 (t, *J* = 5.2 Hz, 2H, NC*H*$_2$CH$_2$), 2.21 (t, *J* = 2.4 Hz, 1H, C*H*, alkyne), 0.90 (s, 9H, SiC(C*H*$_3$)$_3$), 0.06 (s, 6H, Si(C*H*$_3$)$_2$); **δ$_C$** (101 MHz, $CDCl_3$) 82.3 (*C*q, alkyne), 71.4 (*C*H, alkyne), 62.5 (O*C*H$_2$), 50.7 (N*C*H$_2$CH$_2$), 38.3 (N*C*H$_2$C≡CH), 26.0 (SiC(*C*H$_3$)$_3$), 18.4 (Si*C*(CH$_3$)$_3$), –5.2 Si(*C*H$_3$)$_2$; **HRMS** (ESI) m/z: [M+H]+ calcd for $C_{11}H_{23}NOSi$ 214.1622; found 214.1620 (+0.60 ppm).

Data are consistent with the literature.[123]

***N*-(2-Bromo-2,2-difluoroethyl)-*N*-(2-((*tert*-butyldimethylsilyl)oxy)ethyl)prop-2-yn-1-amine 35**

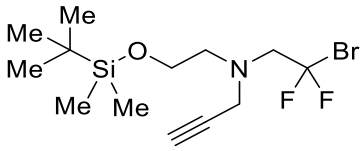

N-(2-((*tert*-Butyldimethylsilyl)oxy)ethyl)prop-2-yn-1-amine (1.72 g, 8.07 mmol) was subjected to General Procedure 2, stirring at 70 °C for 15 hours. The crude material was purified by flash column chromatography (SiO_2, eluting with 0-2% diethyl ether in petroleum ether) to give **35** (1.68 g, 4.73 mmol, 59% yield) as a colourless oil.

R$_f$ (98:2 petroleum ether: ethyl acetate) = 0.41; **ν$_{max}$** (thin film)/cm^{-1} 3309, 2954, 2930, 2897, 2886, 2858, 1472; **δ$_H$** (400 MHz, $CDCl_3$) 3.76 (t, *J* = 5.9 Hz, 2H, OC*H*$_2$), 3.58 (d, *J* = 2.4 Hz, 2H, C*H*$_2$C≡CH), 3.45 (t, *J* = 13.0 Hz, 2H, NC*H*$_2$CF$_2$Br), 2.86 (t, *J* = 5.9 Hz, 2H, NC*H*$_2$CH$_2$), 2.23 (t, *J* = 2.4 Hz, 1H, C*H*, alkyne), 0.90 (s, 9H, SiC(C*H*$_3$)$_3$), 0.06 (s, 6H, Si(C*H*$_3$)$_2$); **δ$_C$** (101 MHz, $CDCl_3$) 123.4 (t, *J* = 307.8 Hz, *C*F$_2$Br), 79.1 (*C*q, alkyne), 73.1 (*C*H, alkyne), 63.8 (t, *J* = 22.8 Hz, N*C*H$_2$CF$_2$Br), 62.5 (O*C*H$_2$), 57.2 (N*C*H$_2$CH$_2$), 44.8 (t, *J* = 1.6 Hz, N*C*H$_2$C≡CH), 26.0 (SiC(*C*H$_3$)$_3$), 18.4 (Si*C*(CH$_3$)$_3$), –5.3 (Si(*C*H$_3$)$_2$); **δ$_F$** (376 MHz, $CDCl_3$) –51.63; **HRMS** (ESI) m/z: [M+H]$^+$ calcd for $C_{13}H_{24}{}^{79}BrF_2NOSi$ 356.0851; found 356.0847 (+1.10 ppm).

_N_-(2-Bromo-2,2-difluoroethyl)-_N_-(4-methoxybenzyl)prop-2-yn-1-amine 43

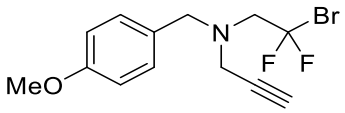

Propargylamine (0.45 mL, 7.00 mmol) and *p*-anisaldehyde (0.85 mL, 7.00 mmol) were subjected to General Procedure 3, stirring for 16 hours. The crude material was purified by flash column chromatography (SiO_2, eluting with 2-5% ethyl acetate in petroleum ether) to give **43** (1.26 g, 3.96 mmol, 56% yield) as a colourless oil.

R_f (90:10 petroleum ether: ethyl acetate) = 0.40; **ν_{max}** (thin film)/cm^{-1} 3299, 3000, 2956, 2935, 2908, 2836; **δ_H** (500 MHz, $CDCl_3$) 7.35 – 7.31 (m, 2H, Ar*H*), 6.92 – 6.87 (m, 2H, Ar*H*), 3.83 (s, 2H, NCH_2Ar), 3.82 (s, 3H, OCH_3), 3.42 (d, *J* = 2.5 Hz, 2H, NCH_2), 3.39 (t, *J* = 12.6 Hz, 2H, CH_2CF_2Br), 2.29 (t, *J* = 2.5 Hz, 1H, C*H*, alkyne); **δ_C** (126 MHz, $CDCl_3$) 159.2 (Ar*C*(OCH_3)), 130.4 (Ar*C*H), 129.7 (Ar*C*q), 123.4 (t, *J* = 307.8 Hz, *C*F_2Br), 113.9 (Ar*C*H), 78.3 (*C*q, alkyne), 73.6 (*C*H, alkyne), 62.6 (t, *J* = 23.3 Hz, *C*H_2CF_2Br), 58.2 (N*C*H_2Ar), 55.3 (O*C*H_3), 42.3 (N*C*H_2); **δ_F** (376 MHz, $CDCl_3$) –50.69; **HRMS** (ESI) m/z: $[M+H]^+$ calcd for $C_{13}H_{14}{}^{79}BrF_2NO$ 318.0300; found 318.0295 (+1.30 ppm).

_N_-Benzyl-_N_-(2-bromo-2,2-difluoroethyl)prop-2-yn-1-amine 44

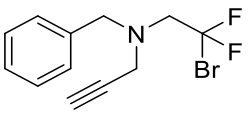

Propargylamine (320 µL, 5.00 mmol) and benzaldehyde (510 µL, 5.00 mmol) were subjected to General Procedure 3, stirring for 14 hours. The crude material was purified by flash column chromatography (SiO_2, eluting with 0-2% diethyl ether in pentane). The mixed fractions were repurified by flash column chromatography (SiO_2, eluting with 0-0.5% diethyl ether in pentane). The residues were combined to give **44** (546 mg, 1.89 mmol, 38% yield) as a colourless oil.

R_f (98:2 petroleum ether: ethyl acetate) = 0.39; **ν_{max}** (thin film)/cm^{-1} 3303, 3088, 3065, 2932, 2897, 2843; **δ_H** (400 MHz, $CDCl_3$) 7.43 – 7.37 (m, 2H, Ar*H*), 7.37 – 7.31 (m, 2H, Ar*H*), 7.31 –

7.27 (m, 1H, Ar*H*), 3.88 (s, 2H, NCH_2Ar), 3.41 (d, *J* = 2.5 Hz, 2H, NCH_2), 3.39 (t, *J* = 12.5 Hz, 2H, C$H_2$$CF_2$Br), 2.27 (t, *J* = 2.5 Hz, 1H, C*H*, alkyne); **δ_C** (101 MHz, $CDCl_3$) 137.7 (Ar*C*q), 129.2 (Ar*C*H), 128.6 (Ar*C*H), 127.8 (Ar*C*H), 123.4 (t, *J* = 307.8 Hz, *C*F_2Br), 78.3 (*C*q, alkyne), 73.6 (*C*H, alkyne), 62.8 (t, *J* = 23.4 Hz, *C*$H_2$$CF_2$Br), 58.9 (N*C*$H_2$), 42.5 (t, *J* = 1.7 Hz, N*C*H_2); **δ_F** (376 MHz, $CDCl_3$) –50.77; **HRMS** (ESI) m/z: $[M+H]^+$ calcd for $C_{12}H_{12}{}^{79}BrF_2N$ 288.0194; found 288.0184 (+3.40 ppm).

Methyl 2-(prop-2-yn-1-yl)pyrrolidine-2-carboxylate hydrochloride 92

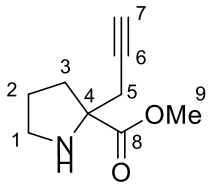

.HCl

To a -78 °C solution of diisopropylamine (2.25 mL, 16.0 mmol) in THF (15 mL) was added *n*-BuLi (6.8 mL, 15.0 mmol of a 2.2 M solution in hexanes) dropwise over 15 minutes. The mixture was stirred at -78 °C for 30 minutes after which time a solution of *N*-Boc proline methyl ester (2.29 g, 10.0 mmol) in THF (5 mL) was added dropwise over 10 minutes. The mixture was stirred at -78 °C for 30 minutes, then a solution of propargyl bromide (2.0 mL, 18 mmol of an 80% w/w solution in toluene) was added dropwise over 10 minutes. The mixture was stirred at -78 °C for 4 hours. Isopropanol (1.90 mL, 25.0 mmol) was added and the mixture was warmed to room temperature. NH_4Cl (20 mL of a sat. aq. solution) was added and the mixture was extracted with diethyl ether (3 × 20 mL). The combined organics were dried over magnesium sulfate and concentrated. The resultant residue was purified by flash column chromatography (SiO_2, eluting with 5-10% ethyl acetate in pentane) to give a residue which was dissolved in dioxane (10 mL). HCl (8.9 mL of a 4 M solution in dioxane) was added at 0 °C. The mixture was warmed to room temperature and stirred for 23 hours. The reaction mixture was filtered, then triturated with diethyl ether to give **92** (1.29 g, 6.33 mmol, 63%) as a light brown solid.

m.p. 172–174 °C (literature m.p. 180 °C); **ν_{max}** (thin film)/cm^{-1} 3171, 2999, 2945, 2917, 2877, 2848, 2779, 2742, 2676, 2649, 2594, 2528, 2471, 2413, 2393, 1757, 1561; **δ_H** (500 MHz, methanol-d_4) 3.91 (s, 3H, *H*-9), 3.48 (dd, *J* = 8.0, 5.7 Hz, 2H, *H*-1), 3.15 (dd, *J* = 17.6, 2.7 Hz,

1H, *H*-5), 2.93 (app ddd, *J* = 17.6, 2.7, 2.7 Hz, 1H, *H*-5), 2.74 (dd, *J* = 2.7, 2.7 Hz, 1H, *H*-7), 2.51 – 2.41 (m, 1H, *H*-3), 2.28 – 2.09 (m, 2H, *H*-3 and *H*-2), 2.09 – 1.98 (m, 1H, *H*-2); **δ_C** (126 MHz, MeOD) 171.1 (*C*-8), 77.2 (*C*-6), 75.2 (*C*-7), 72.9 (*C*-4), 54.7 (*C*-9), 47.6 (*C*-1), 35.5 (*C*-3), 26.2 (*C*-5), 24.2 (*C*-2); **HRMS** (ESI) m/z: $[M+Na]^+$ calcd for $C_9H_{13}NO_2$ 190.0838; found 190.0836 (+1.10 ppm).

Data are consistent with the literature.[124]

Methyl 1-(2-bromo-2,2-difluoroethyl)-2-(prop-2-yn-1-yl)pyrrolidine-2-carboxylate 36

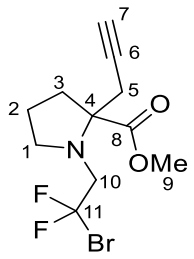

Methyl 2-(prop-2-yn-1-yl)pyrrolidine-2-carboxylate hydrochloride (407 mg, 2.00 mmol) and Et_3N (280 µL, 2.00 mmol) were subjected to General Procedure 2, stirring at 70 °C for 16 hours. The crude material was purified by flash column chromatography (SiO_2, eluting with 2% diethyl ether in pentane) to give **36** (188 mg, 606 µmol, 30% yield) as a colourless oil.

R_f (95:5 petroleum ether: diethyl ether) = 0.26; **ν_{max}** (thin film)/cm^{-1} 3306, 2954, 2917, 2871, 2841, 1729; **δ_H** (400 MHz, $CDCl_3$) 3.78 – 3.65 (m, 4H, *H*-9 and *H*-10), 3.46 – 3.35 (m, 2H, *H*-1 and *H*-10), 2.95 (ddd, *J* = 8.5, 8.5, 6.7 Hz, 1H, *H*-1), 2.72 – 2.61 (m, 2H, *H*-5), 2.26 (ddd, *J* = 12.9, 7.9, 5.2 Hz, 1H, *H*-3), 2.09 – 1.98 (m, 2H, *H*-3 and *H*-7), 1.94 – 1.82 (m, 2H, *H*-2); **δ_C** (101 MHz, $CDCl_3$) 174.0 (*C*-8), 123.5 (t, *J* = 308.2 Hz, *C*-11), 80.4 (*C*-8), 70.9 (*C*-7), 70.7 (*C*-4), 60.7 (t, *J* = 23.7 Hz, *C*-10), 54.7 (*C*-1), 52.1 (*C*-9), 35.8 (*C*-3), 26.9 (*C*-5), 22.2 (*C*-2); **δ_F** (376 MHz, $CDCl_3$) –51.04, –51.08; **HRMS** (ESI) m/z: $[M+H]^+$ calcd for $C_{11}H_{15}{}^{79}BrF_2NO_2$ 310.0249; found 310.0250 (+0.30 ppm).

_N_-Benzyl-2-methylbut-3-yn-2-amine 93

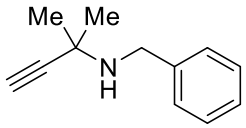

To a solution at 0 °C of 1,1-dimethyl prop-2-ynylamine (2.10 mL, 20.0 mmol) was added DIPEA (350 µL, 5.00 mmol) and dichloromethane (30 mL). was added a solution of benzyl bromide (600 µL, 5.00 mmol) in dichloromethane (5 mL) was added dropwise over 1 hour. The mixture was stirred at room temperature for 21 hours. The reaction mixture was poured into $NaHCO_3$ (20 mL of a sat. aq. solution) and extracted with dichloromethane (3 × 20 mL). The combined organics were dried over magnesium sulfate and concentrated. The resultant residue was purified by flash column chromatography (SiO_2, eluting with 10-20% diethyl ether in pentane) to give **93** (506 mg, 2.92 mmol, 58%) as a colourless solid.

R_f (90:10 petroleum ether: diethyl ether) = 0.21; **m.p.** 42–44 °C; **ν_{max}** (thin film)/cm^{-1} 3302, 3121, 3031, 2980, 2911, 2860, 2832, 2080; **δ_H** (400 MHz, $CDCl_3$) 7.39 – 7.22 (m, 5H, Ar*H*), 3.88 (s, 2H, NCH_2), 2.36 (s, 1H, C*H*, alkyne), 1.43 (s, 6H, C(CH_3)$_2$); **δ_C** (101 MHz, $CDCl_3$) 140.7 (Ar*C*q), 128.6 (Ar*C*H), 128.5 (Ar*C*H), 127.1 (Ar*C*H), 89.1 (*C*q, alkyne), 70.0 (*C*H, alkyne), 50.1 (*C*(CH$_3$)$_2$), 49.1 (N*C*H$_2$), 29.7 (C(*C*H$_3$)$_2$); **HRMS** (ESI) m/z: $[M+H]^+$ calcd for $C_{12}H_{15}N$ 174.1277; found 174.1266 (+6.70 ppm).

Data are consistent with the literature.[125]

_N_-Benzyl-_N_-(2-bromo-2,2-difluoroethyl)-2-methylbut-3-yn-2-amine 37

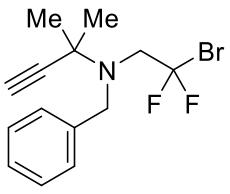

To an oven-dried flask fitted with a water condenser under an argon atmosphere was added *N*-benzyl-2-methylbut-3-yn-2-amine (436 mg, 2.52 mmol) and THF (1.25 mL). Then

bromodifluoroacetic acid (881 mg, 5.04 mmol) in THF (1.25 mL) and $PhSiH_3$ (930 µL, 7.56 mmol) were added at 70 °C and the reaction was heated at 70 °C for 16 hours. The reaction mixture was charged with further bromodifluoroacetic acid (881 mg, 5.04 mmol) and $PhSiH_3$ (930 µL, 7.56 mmol) and stirred at 70 °C for 86 hours. The reaction mixture was cooled to room temperature. Diethyl ether (15 mL) and $NaHCO_3$ (15 mL of a sat. aq. solution) were added. The mixture was extracted with diethyl ether (3 × 15 mL). The combined organics were dried ($MgSO_4$) and concentrated to ~2 mL volume. The crude material was purified by flash column chromatography (SiO_2, eluting with 0-2% diethyl ether in pentane) to give **37** (245 mg, 774 µmol, 31% yield) as a colourless oil.

R_f (98:2 petroleum ether: diethyl ether) = 0.70; **ν_{max}** (thin film)/cm^{-1} 3301, 3088, 3064, 3028, 2987, 2938, 2855; **δ_H** (400 MHz, $CDCl_3$) 7.42 – 7.37 (m, 2H, Ar*H*), 7.33 – 7.27 (m, 2H, Ar*H*), 7.24 – 7.17 (m, 1H, Ar*H*), 4.06 (s, 2H, NC*H*$_2$Ar), 3.54 (t, *J* = 13.6 Hz, 2H, NC*H*$_2$CF$_2$Br), 2.32 (s, 1H, C*H*, alkyne), 1.36 (s, 6H, C(C*H*$_3$)$_2$); **δ_C** (101 MHz, $CDCl_3$) 141.5 (Ar*C*q), 128.3 (Ar*C*H), 127.5 (Ar*C*H), 126.7 (Ar*C*H), 123.5 (t, *J* = 309.0 Hz, *C*F$_2$Br), 86.7 (*C*q, alkyne), 70.6 (*C*H, alkyne), 62.9 (t, *J* = 21.7 Hz, *C*H$_2$CF$_2$Br), 57.9 (NCH$_2$Ar), 56.0 (*C*(CH$_3$)$_2$), 29.9 (C(*C*H$_3$)$_2$); **δ_F** (376 MHz, $CDCl_3$) –50.52; **HRMS** (ESI) m/z: $[M+H]^+$ calcd for $C_{14}H_{16}{}^{79}BrF_2N$ 316.0507; found 316.0504 (+0.90 ppm).

***tert*-Butyl (2-(prop-2-yn-1-ylamino)ethyl)carbamate 94**

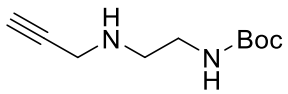

To a 0 °C solution of ethylene diamine (6.70 mL, 10.0 mmol) in dichloromethane (12 mL) was added a solution of Boc_2O (2.18 g, 10.0 mmol) in dichloromethane (6 mL). The mixture was stirred at room temperature for 17 hours after which water (20 mL) was added and the mixture was extracted with dichloromethane (3 × 20 mL). The combined organics were dried over magnesium sulfate and concentrated. To the residue was dissolved in dichloromethane (16 mL) and to this solution was added DIPEA (530 µL, 3.03 mmol). At 0 °C, a solution of propargyl bromide (340 µL, 3.03 mmol of an 80% w/w solution in toluene) in dichloromethane (5 mL)

was added dropwise over 1.5 hours. The mixture was stirred at room temperature for 6 hours. The reaction mixture was poured into $NaHCO_3$ (20 mL of a sat. aq. solution) and extracted with dichloromethane (3 × 20 mL). The combined organics were dried over magnesium sulfate and concentrated. The resultant residue was purified by flash column chromatography (SiO_2, eluting with 70-100% ethyl acetate in pentane) to give **94** (290 mg, 1.46 mmol, 48%) as a yellow oil.

R_f (70:30 petroleum ether: ethyl acetate) = 0.13; **ν_{max}** (thin film)/cm^{-1} 3303, 3254, 2975, 2931, 2853, 2836, 1688; **δ_H** (400 MHz, $CDCl_3$) 4.98 (s, 1H, N*H,* amine), 3.40 (d, *J* = 2.4 Hz, 2H, NHC*H*$_2$C), 3.21 (dt, *J* = 5.8, 5.8 Hz, 2H, NHC*H*$_2$CH$_2$NHBoc), 2.79 (t, *J* = 5.8 Hz, 2H, NHCH$_2$C*H*$_2$NHBoc), 2.20 (t, *J* = 2.4 Hz, 1H, C*H,* alkyne), 1.42 (s, 9H, C(C*H*$_3$)$_3$); **δ_C** (101 MHz, $CDCl_3$) 156.2 (*C*=O), 82.1 (*C*q, alkyne), 79.3 (*C*(CH$_3$)$_3$), 71.6 (*C*H, alkyne), 48.0 (NHCH$_2$*C*H$_2$NHBoc), 40.1 (NH*C*H$_2$CH$_2$NHBoc), 37.9 (NH*C*H$_2$C), 28.5 (C(*C*H$_3$)$_3$); **HRMS** (ESI) m/z: $[M+H]^+$ calcd for $C_{10}H_{18}N_2O_2$ 199.1441; found 199.1443 (+0.80 ppm).

***tert*-Butyl (2-((2-bromo-2,2-difluoroethyl)(prop-2-yn-1-yl)amino)ethyl)carbamate 38**

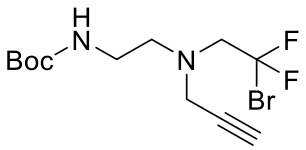

tert-Butyl (2-(prop-2-yn-1-ylamino)ethyl)carbamate (0.290 g, 1.46 mmol) was subjected to General Procedure 2, stirring at 70 °C for 16 hours. The crude material was purified by flash column chromatography (SiO_2, eluting with 5-10% diethyl ether in pentane). The material was purified again by flash column chromatography (SiO_2, eluting with 2-15% diethyl ether in pentane) to give **38** (37.7 mg, 110 µmol, 8% yield) as a colourless oil.

R_f (80:20 petroleum ether: diethyl ether) = 0.40; **ν_{max}** (thin film)/cm^{-1} 3434, 3306, 2978, 2932, 2850, 1697, 1503; **δ_H** (400 MHz, $CDCl_3$) 4.94 (br s, 1H, N*H*, carbamate), 3.52 (d, *J* = 2.4 Hz, 2H, C*H*$_2$, propargyl), 3.31 (t, *J* = 12.6 Hz, 2H, C*H*CF$_2$Br), 3.21 (dt, *J* = 5.8, 5.8 Hz, 2H, BocHNC*H*$_2$CH$_2$), 2.82 (t, *J* = 5.8 Hz, 2H, BocHNCH$_2$C*H*$_2$), 2.23 (t, *J* = 2.4 Hz, 1H, C*H*, alkyne), 1.43 (s, 9H, C(C*H*$_3$)$_3$); **δ_C** (101 MHz, $CDCl_3$) 156.1 (*C*=O), 123.2 (t, *J* = 307.5 Hz, *C*F$_2$Br), 79.4

(*C*(CH_3)$_3$), 78.1 (*C*q, alkyne), 73.6 (*C*H, alkyne), 63.3 (t, *J* = 23.4 Hz, *C*H_2CF_2Br), 54.7 (BocHNCH$_2$*C*H$_2$), 43.5 (*C*H$_2$, propargyl), 38.3 (BocHN*C*H$_2$CH$_2$), 28.5 (C(*C*H$_3$)$_3$); **δ_F** (376 MHz, $CDCl_3$) –51.42; **HRMS** (ESI) m/z: $[M+H]^+$ calcd for $C_{12}H_{19}{}^{79}BrF_2N_2O_2$ 341.0671; found 341.0674 (+1.00 ppm).

2-((2-Bromo-2,2-difluoroethyl)(prop-2-yn-1-yl)amino)ethan-1-ol 95

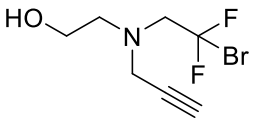

N-(2-Bromo-2,2-difluoroethyl)-*N*-(2-((*tert*-butyldimethylsilyl)oxy)ethyl)prop-2-yn-1-amine was dissolved in dioxane (2.8 mL). HCl (2.4 mL of a 4 M solution in dioxane) was added at 0 °C. The mixture was warmed to room temperature and stirred for 16 hours. The reaction mixture was poured into $NaHCO_3$ (20 mL of a sat. aq. solution) and extracted with ethyl acetate (3 × 10 mL). The combined organics were dried over sodium sulfate and concentrated. The resultant residue was purified by flash column chromatography (SiO_2, eluting with 5-20% ethyl acetate in pentane) to give **95** (365 mg, 1.51 mmol, 75%) as a colourless oil.

R_f (50:50 petroleum ether: ethyl acetate) = 0.54; **ν_{max}** (thin film)/cm^{-1} 3424, 3302, 2946, 2883, 2847; **δ_H** (400 MHz, $CDCl_3$) 3.62 (t, *J* = 5.2 Hz, 2H, C*H*$_2$OH), 3.55 (d, *J* = 2.4 Hz, 2H, NC*H*$_2$, propargyl), 3.34 (t, *J* = 12.5 Hz, 2H, NC*H*$_2CF_2Br$), 2.88 (t, *J* = 5.2 Hz, 2H, C*H*$_2$CH$_2$OH), 2.43 (br s, 1H, O*H*), 2.25 (t, *J* = 2.4 Hz, 1H, C*H*, alkyne); **δ_C** (101 MHz, $CDCl_3$) 123.1 (t, *J* = 307.2 Hz, *C*F_2Br), 78.1 (*C*q, alkyne), 73.7 (*C*H, alkyne), 63.1 (t, *J* = 23.5 Hz, NCH$_2CF_2Br$), 59.2 (*C*H$_2$OH), 57.2 (*C*H$_2$CH$_2$OH), 43.8 (t, *J* = 1.4 Hz, NCH$_2$, propargyl); **δ_F** (376 MHz, $CDCl_3$) –51.29; **HRMS** (ESI) m/z: $[M+Na]^+$ calcd for $C_7H_{10}{}^{79}BrF_2NO$ 241.9987; found 241.9985 (+0.50 ppm).

_N_-Benzylbut-2-yn-1-amine 96

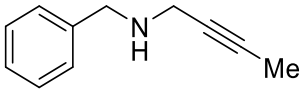

To a solution at 0 °C of benzylamine (5.5 mL, 50.0 mmol), DIPEA (1.75 mL, 10.0 mmol) and dichloromethane (40 mL) was added a solution of 1-bromo-2-butyne (1.33 g, 10.0 mmol) in dichloromethane (10 mL) dropwise over 20 minutes. The mixture was stirred at room temperature for 8 hours. The reaction mixture was poured into $NaHCO_3$ (20 mL of a sat. aq. solution) and extracted with dichloromethane (3 × 20 mL). The combined organics were dried over magnesium sulfate and concentrated. The resultant residue was purified by flash column chromatography (SiO_2, eluting with 20-50% ethyl acetate in pentane) to give **96** (1.04 g, 6.53 mmol, 65%) as a pale yellow oil.

R_f (80:20 petroleum ether: ethyl acetate) = 0.10; **ν_{max}** (thin film)/cm^{-1} 3315, 3085, 3062, 3027, 2918, 2840, 2809; **δ_H** (400 MHz, $CDCl_3$) 7.42 – 7.20 (m, 5H, Ar*H*), 3.86 (s, 2H, NHC*H*$_2$Ar), 3.38 (q, *J* = 2.4 Hz, 2H, NHC*H*$_2$), 1.85 (t, *J* = 2.4 Hz, 3H, C*H*$_3$); **δ_C** (101 MHz, $CDCl_3$) 139.8 (Ar*C*q), 128.5 (Ar*C*H), 128.5 (Ar*C*H), 127.2 (Ar*C*H), 79.4 (*C*q, alkyne), 77.4 (*C*q, alkyne), 52.6 (NH*C*H$_2$Ar), 38.0 (NH*C*H$_2$), 3.7 (*C*H$_3$); **HRMS** (ESI) m/z: $[M+H]^+$ calcd for $C_{11}H_{13}N$ 160.1121; found 160.1116 (+3.10 ppm).

Data are consistent with the literature.[126]

_N_-Benzyl-_N_-(2-bromo-2,2-difluoroethyl)but-2-yn-1-amine 39

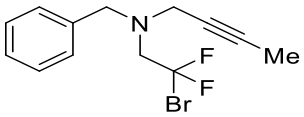

N-Benzyl-2-methylbut-3-yn-2-amine (638 mg, 4.00 mmol) was subjected to General Procedure 2, stirring at 70 °C for 20 hours. The crude material was purified by flash column chromatography (SiO_2, eluting with 0-2% diethyl ether in pentane) to give **39** (721 mg, 2.38 mmol, 60% yield) as a yellow oil.

R_f (98:2 petroleum ether: diethyl ether) = 0.29; **ν_{max}** (thin film)/cm^{-1} 3088, 3064, 3031, 2922, 2895, 2842; **δ_H** (400 MHz, $CDCl_3$) 7.43 – 7.37 (m, 2H, Ar*H*), 7.37 – 7.30 (m, 2H, Ar*H*), 7.30 – 7.27 (m, 1H, Ar*H*), 3.85 (s, 2H, NC*H*$_2$Ar), 3.53 – 3.16 (m, 4H, NC*H*$_2$ and NC*H*$_2$), 1.88 (t, *J* = 2.3 Hz, 3H, C*H*$_3$); **δ_C** (101 MHz, $CDCl_3$) 138.1 (Ar*C*q), 129.2 (ArC*H*), 128.5 (ArC*H*), 127.6 (ArC*H*), 123.6 (t, *J* = 308.0 Hz, *C*F_2Br), 81.3 (*C*q, alkyne), 73.5 (*C*q, alkyne), 62.9 (t, *J* = 23.1 Hz, NC$H_2$$CF_2$Br), 59.0 (N*C*$H_2$Ar), 43.1 (t, *J* = 1.7 Hz, N*C*H_2), 3.6 (*C*H_3); **δ_F** (376 MHz, $CDCl_3$) –50.50; **HRMS** (ESI) m/z: $[M+H]^+$ calcd for $C_{13}H_{14}{}^{79}BrF_2N$ 302.0350; found 302.0352 (+0.40 ppm).

***N*-Benzyl-3-(trimethylsilyl)prop-2-yn-1-amine 97**

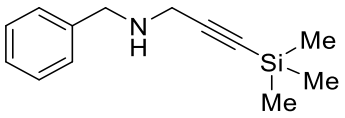

To a solution at 0 °C of benzylamine (5.5 mL, 50.0 mmol), DIPEA (1.75 mL, 10.0 mmol) and dichloromethane (40 mL) was added a solution of 3-bromo-1-(trimethylsilyl)-1-propyne (1.91 g, 10.0 mmol) in dichloromethane (10 mL) dropwise over 20 minutes. The mixture was stirred at room temperature for 8 hours. The reaction mixture was poured into $NaHCO_3$ (20 mL of a sat. aq. solution) and extracted with dichloromethane (3 × 20 mL). The combined organics were dried over magnesium sulfate and concentrated. The resultant residue was purified by flash column chromatography (SiO_2, eluting with 10-20% ethyl acetate in pentane) to give **97** (1.65 g, 7.62 mmol, 76%) as a pale yellow oil.

R_f (80:20 petroleum ether: ethyl acetate) = 0.22; **ν_{max}** (thin film)/cm^{-1} 3067, 3028, 2959, 2899, 2838, 2164; **δ_H** (400 MHz, $CDCl_3$) 7.42 – 7.16 (m, 5H, Ar*H*), 3.88 (s, 2H, NHC*H*$_2$Ar), 3.44 (s, 2H, NHC*H*$_2$), 0.19 (s, 9H, Si(C*H*$_3$)$_3$); **δ_C** (101 MHz, $CDCl_3$) 139.5 (Ar*C*q), 128.6 (Ar*C*H), 128.6 (Ar*C*H), 127.3 (Ar*C*H), 104.3 (*C*q, alkyne), 88.5 (*C*q, alkyne), 52.5 (NH*C*H_2Ar), 38.6 (NH*C*H_2), 0.2 (Si(*C*H_3)$_3$); **HRMS** (ESI) m/z: $[M+H]^+$ calcd for $C_{13}H_{19}NSi$ 218.1360; found 218.1364 (+2.10 ppm).

_N_-Benzyl-_N_-(2-bromo-2,2-difluoroethyl)-3-(trimethylsilyl)prop-2-yn-1-amine 40

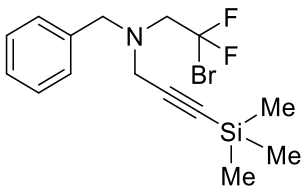

_N_-Benzyl-3-(trimethylsilyl)prop-2-yn-1-amine (870 mg, 4.00 mmol) was subjected to General Procedure 2, stirring at 70 °C for 20 hours. The crude material was purified by flash column chromatography (SiO_2, eluting with 0-2% diethyl ether in pentane) to give **40** (732 mg, 2.03 mmol, 51% yield) as a yellow oil.

R_f (98:2 petroleum ether: diethyl ether) = 0.33; **ν_{max}** (thin film)/cm^{-1} 3088, 3065, 3031, 2960, 2927, 2899, 2841; **δ_H** (400 MHz, $CDCl_3$) 7.41 – 7.37 (m, 2H, Ar*H*), 7.36 – 7.31 (m, 2H, Ar*H*), 7.31 – 7.27 (m, 1H, Ar*H*), 3.86 (s, 2H, NC*H*$_2$Ar), 3.40 (s, 2H, NC*H*$_2$C≡C), 3.37 (t, *J* = 12.4 Hz, 2H, NC*H*$_2$$CF_2Br$), 0.21 (s, 9H, Si(C*H*$_3$)$_3$); **$\delta_C$** (101 MHz, $CDCl_3$) 137.8 (Ar*C*q), 129.2 (Ar*C*H), 128.6 (Ar*C*H), 127.7 (Ar*C*H), 123.5 (t, *J* = 307.9 Hz, *C*F_2Br), 100.4 (*C*q, alkyne), 90.7 (*C*q, alkyne), 62.9 (t, *J* = 23.3 Hz, N*C*H_2CF_2Br), 58.9 (N*C*H_2Ar), 43.6 (N*C*H_2C≡C), 0.2 (Si(*C*H_3)$_3$); **δ_F** (376 MHz, $CDCl_3$) –50.59; **HRMS** (ESI) m/z: $[M+H]^+$ calcd for $C_{15}H_{20}{}^{79}BrF_2NSi$ 360.0589; found 360.0577 (+3.30 ppm).

_N_-Benzyl-_N_-(2-bromo-2,2-difluoroethyl)-3-phenylprop-2-yn-1-amine 98

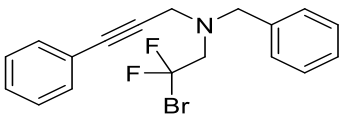

To a solution of 3-phenyl-2-propyn-1-ol (902 mg, 6.82 mmol) and Et_3N (1.90 mL, 13.6 mmol) in dichloromethane (35 mL) was added MsCl (1.1 mL, 13.6 mmol). The mixture was stirred at room temperature for 16 hours. $NaHCO_3$ (15 mL of a sat. aq. solution) was added. The mixture was extracted with dichloromethane (3 × 15 mL). The combined organics were dried ($MgSO_4$) and concentrated. To the residue was added benzylamine (3.72 mL, 34.1 mmol), Et_3N (1.90 mL, 13.6 mmol) and THF (35 mL). The mixture was stirred at room temperature for 16 hours.

$NaHCO_3$ (20 mL of a sat. aq. solution) was added. The mixture was extracted with diethyl ether (3 × 20 mL). The combined organics were dried ($MgSO_4$) and concentrated. The material was purified by flash column chromatography (SiO_2, eluting with 10-50% diethyl ether in pentane) to give a yellow residue (1.02 g). To a portion of the residue (448 mg) in THF (1 mL) was added bromodifluoroacetic acid (700 mg, 4.00 mmol) in THF (1 mL) and $PhSiH_3$ (740 µL, 6.00 mmol) were added at 70 °C and the reaction was heated at 70 °C for 16 hours. The reaction mixture was cooled to room temperature. $NaHCO_3$ (15 mL of a sat. aq. solution) was added. The mixture was extracted with diethyl ether (3 × 15 mL). The combined organics were dried ($MgSO_4$) and concentrated to ~2 mL volume. The crude material was purified by flash column chromatography (SiO_2, eluting with 0-2% diethyl ether in pentane) to give **98** (363 mg, 996 µmol, 34% yield) as a colourless oil.

R_f (95:5 petroleum ether: diethyl ether) = 0.50; **ν_{max}** (thin film)/cm^{-1} 3084, 3062, 3031, 2992, 2926, 2897, 2840; **δ_H** (400 MHz, $CDCl_3$) 7.52 – 7.41 (m, 4H, Ar*H*), 7.39 – 7.27 (m, 6H, Ar*H*), 3.97 (s, 2H, NCH_2C≡C), 3.65 (s, 2H, NCH_2Ar), 3.48 (t, *J* = 12.6 Hz, 2H, NC$H_2$$CF_2$Br); **$\delta_C$** (101 MHz, $CDCl_3$) 137.7 (Ar*C*q), 132.0 (Ar*C*H), 129.3 (Ar*C*H), 128.6 (Ar*C*H), 128.5 (Ar*C*H), 127.8 (Ar*C*H), 125.7 (Ar*C*q), 123.3 (t, *J* = 307.8 Hz, *C*F_2Br), 123.0 (Ar*C*H), 86.0 (*C*q, alkyne), 83.7 (*C*q, alkyne), 62.9 (t, *J* = 23.4 Hz, N*C*$H_2$$CF_2$Br), 59.1 (N*C*$H_2$C≡C), 43.5 (N*C*$H_2$Ar); **$\delta_F$** (376 MHz, $CDCl_3$) –50.52; **HRMS** (ESI) m/z: $[M+H]^+$ calcd for $C_{18}H_{16}{}^{79}BrF_2N$ 364.0507; found 364.0505 (+0.50 ppm).

4.4.2 Cyclised Alkynyl Amines

1-(2-((*tert*-Butyldimethylsilyl)oxy)ethyl)-3,3-difluoro-4-methylenepyrrolidine 45

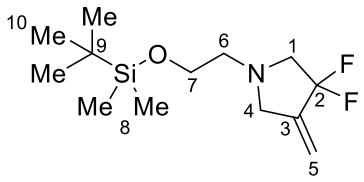

N-(2-Bromo-2,2-difluoroethyl)-*N*-(2-((*tert*-butyldimethylsilyl)oxy)ethyl)prop-2-yn-1-amine **35** (89.8 mg, 250 µmol) was subjected to General Procedure 5, stirring at room temperature for

16 hours. The resultant residue was purified by flash column chromatography (SiO_2, eluting with 0-5% diethyl ether in pentane) to give **45** (39.4 mg, 142 µmol, 56% yield) as a colourless oil.

R_f (90:10 petroleum ether: ethyl acetate) = 0.43; **ν_{max}** (thin film)/cm^{-1} 2955, 2929, 2907, 2887, 2857, 2812, 2777, 2714; **δ_H** (400 MHz, $CDCl_3$) 5.58 (dt, *J* = 5.5, 2.8 Hz, 1H, *H*-5), 5.30 (dt, *J* = 5.5, 2.8 Hz, 1H, *H*-5), 3.76 (t, *J* = 5.9 Hz, 2H, *H*-7), 3.44 (m, 2H, *H*-4), 3.08 (t, *J* = 11.4 Hz, 2H, *H*-1), 2.65 (t, *J* = 5.9 Hz, 2H, *H*-6), 0.89 (s, 9H, *H*-10), 0.06 (s, 6H, *H*-8); **δ_C** (101 MHz, $CDCl_3$) 142.9 (t, *J* = 20.9 Hz, *C*-3), 122.8 (t, *J* = 246.0 Hz, *C*-2), 112.0 (t, *J* = 2.1 Hz, *C*-5), 62.2 (*C*-7), 62.1 (t, *J* = 27.0 Hz, *C*-1), 57.9 (*C*-6), 57.8 (t, *J* = 3.1 Hz, *C*-4), 26.0 (*C*-10), 18.4 (*C*-9), –5.3 (*C*-8); **δ_F** (376 MHz, $CDCl_3$) –98.23; **HRMS** (ESI) m/z: $[M+Na]^+$ calcd for $C_{13}H_{25}F_2NOSi$ 300.1566; found 300.1564 (+0.40 ppm).

3,3-Difluoro-1-(4-methoxybenzyl)-4-methylenepyrrolidine 47

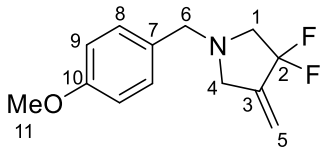

Photoredox conditions: *N*-(2-Bromo-2,2-difluoroethyl)-*N*-(4-methoxybenzyl)prop-2-yn-1-amine **43** (80.2 mg, 252 µmol) was subjected to General Procedure 5, stirring at room temperature for 16 hours. The resultant residue after concentration was purified by flash column chromatography (SiO_2, eluting with 80:20 pentane/diethyl ether) to give **47** (35.4 mg, 148 µmol, 59% yield) as a colourless oil.

Amide reduction conditions: To 3,3-difluoro-1-(4-methoxybenzyl)-4-methylenepyrrolidin-2-one (29 mg, 110 mmol), benzoic acid (7.0 mg, 57 µmol) and $Zn(OAc)_2$ (2 mg, 11 µmol) in toluene (0.2 mL) at 110 °C was added *N*-Me morpholine (1.5 µL, 11 µmol) and $PhSiH_3$ (30 µL, 230 µmol). The reaction mixture was stirred at 110 °C for 19 hours, then cooled to room temperature. Dichloromethane (3 mL) was added, then silica (0.5 g). The mixture was stirred for 30 minutes, then concentrated and purified by flash column chromatography (SiO_2, eluting

with 0-10% ethyl acetate in petroleum ether) to give **47** (11 mg, 48 µmol, 42% yield) as a colourless oil.

R_f (80:20 petroleum ether:ethyl acetate) = 0.49; **ν_{max}** (thin film)/cm^{-1} 2924, 2837, 2808, 1512; **δ_H** (400 MHz, $CDCl_3$) 7.35 – 7.18 (m, 2H, Ar*H*), 6.94 – 6.81 (m, 2H, Ar*H*), 5.59 (m, 1H, *H*-5), 5.29 (m, 1H, *H*-5), 3.82 (s, 3H, *H*-11), 3.62 (s, 2H, *H*-6), 3.34 (t, *J* = 2.2 Hz, 2H, *H*-4), 2.99 (t, *J* = 12.0 Hz, 2H, *H*-1); **δ_C** (101 MHz, $CDCl_3$) 159.1 (*C*-10), 143.1 (t, *J* = 20.9 Hz, *C*-3), 130.1 (Ar*C*H), 129.5 (*C*-5), 122.8 (t, *J* = 246.5 Hz, *C*-2), 113.9 (Ar*C*H), 112.1 (t, *J* = 2.4 Hz, *C*-5), 61.0 (t, *J* = 27.0 Hz, *C*-1), 59.4 (*C*-6), 56.60 (t, *J* = 3.1 Hz, *C*-4), 55.4 (*C*-11); **δ_F**(376 MHz, $CDCl_3$) –97.63; **HRMS** (ESI) m/z: $[M+H]^+$ calcd for $C_{13}H_{15}F_2NO$ 240.1194; found 2440.1192 (+1.10 ppm).

1-Benzyl-3,3-difluoro-4-methylenepyrrolidine 48

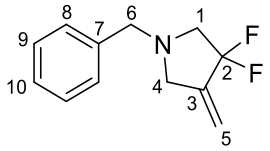

N-Benzyl-*N*-(2-bromo-2,2-difluoroethyl)prop-2-yn-1-amine **44** (72.0 mg, 250 µmol) was subjected to General Procedure 5, stirring at room temperature for 24 hours. The resultant residue was purified by flash column chromatography (SiO_2, eluting with 0-5% diethyl ether in pentane) to give **48** (35.4 mg, 169 µmol, 67% yield) as a colourless oil.

R_f (95:5 petroleum ether: diethyl ether) = 0.48; **ν_{max}** (thin film)/cm^{-1} 3107, 3064, 2957, 2923, 2805; **δ_H** (400 MHz, $CDCl_3$) 7.37 – 7.26 (m, 5H, Ar*H*), 5.59 (m, 1H, *H*-5), 5.29 (m, 1H, *H*-5), 3.67 (s, 2H, *H*-6), 3.36 (t, *J* = 2.0 Hz, 2H, *H*-4), 3.01 (t, *J* = 11.3 Hz, 2H, *H*-1); **δ_C** (101 MHz, $CDCl_3$) 143.1 (t, *J* = 21.0 Hz, *C*-3), 137.4 (Ar*C*H), 128.9 (Ar*C*H), 128.6 (Ar*C*H), 127.6 (Ar*C*q), 122.8 (t, *J* = 246.5 Hz, *C*-2), 112.1 (t, *J* = 2.5 Hz, *C*-5), 61.1 (t, *J* = 27.1 Hz, *C*-1), 60.0 (*C*-6), 56.7 (t, *J* = 3.1 Hz, *C*-4); **δ_F** (376 MHz, $CDCl_3$) –97.69; **HRMS** (ESI) m/z: $[M+H]^+$ calcd for $C_{12}H_{13}F_2N$ 210.1089; found 210.1087 (+0.70 ppm).

1-Benzyl-3,3-difluoro-4-methylenepiperidine 49

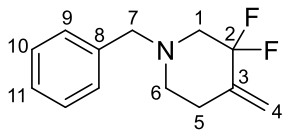

N-Benzyl-*N*-(2-bromo-2,2-difluoroethyl)but-3-yn-1-amine **34** (75.6 mg, 250 µmol) was subjected to General Procedure 5, stirring at room temperature for 17.5 hours. The resultant residue after concentration was purified by flash column chromatography (SiO_2, eluting with 0-5% diethyl ether in pentane) to give **49** (28.3 mg, 0.127 µmol, 51% yield) as a colourless oil.

R_f (95:5 petroleum ether: diethyl ether) = 0.43; **ν_{max}** (thin film)/cm^{-1} 3088, 3064, 3029, 3004, 2951, 2917, 2879, 2813, 2773, 2743; **δ_H** (400 MHz, $CDCl_3$) 7.40 – 7.33 (m, 4H, Ar*H*), 7.31 (t, *J* = 4.3 Hz, 1H, Ar*H*), 5.40 (d, *J* = 1.0 Hz, 1H, *H*-4), 5.09 (d, *J* = 1.0 Hz, 1H, *H*-4), 3.66 (s, 2H, *H*-7), 2.77 (t, *J* = 11.1 Hz, 2H, *H*-1), 2.58 (t, *J* = 5.7 Hz, 2H, *H*-6), 2.50 (t, *J* = 5.7 Hz, 2H, *H*-5); **δ_C** (101 MHz, $CDCl_3$) 140.2 (t, *J* = 20.7 Hz, *C*-3), 137.3 (Ar*C*q), 129.0 (Ar*C*H), 128.4 (Ar*C*H), 127.4 (Ar*C*H), 117.2 (t, *J* = 242.6 Hz, *C*-2), 111.5 (t, *J* = 7.4 Hz, *C*-4), 61.6 (*C*-7), 59.5 (t, *J* = 28.7 Hz, *C*-1), 53.3 (*C*-6), 31.9 (t, *J* = 2.2 Hz, *C*-5); **δ_F** (376 MHz, $CDCl_3$) –105.54; **HRMS** (ESI) m/z: $[M+H]^+$ calcd for $C_{13}H_{15}F_2N$ 224.1245; found 224.1245 (+0.10 ppm).

Methyl 6,6-difluoro-7-methylenehexahydroindolizine-8a(1H)-carboxylate 50

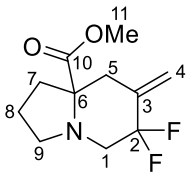

Methyl 1-(2-bromo-2,2-difluoroethyl)-2-(prop-2-yn-1-yl)pyrrolidine-2-carboxylate **36** (78.7 mg, 254 µmol) was subjected to General Procedure 5, stirring at room temperature for 17 hours. The resultant residue was purified by flash column chromatography (SiO_2, eluting with 5-10% diethyl ether in pentane) to give **50** (43.1 mg, 186 µmol, 73% yield) as a colourless oil.

R_f (90:10 petroleum ether: diethyl ether) = 0.20; **ν_{max}** (thin film)/cm^{-1} 2953, 2916, 2884, 2854, 1730; **δ_H** (400 MHz, $CDCl_3$) 5.40 – 5.36 (m, 1H, *H*-4), 5.11 – 5.07 (m, 1H, *H*-4), 3.68 (s, 3H, *H*-11), 3.32 – 3.22 (m, 2H, *H*-1), 3.21 – 3.09 (m, 2H, *H*-9), 2.93 (dd, *J* = 13.3, 3.8 Hz, 1H, *H*-5), 2.46 (ddddd, *J* = 13.3, 1.9, 1.9, 1.9, 1.9 Hz, 1H, *H*-5), 2.18 – 2.07 (m, 1H, *H*-7), 2.00 – 1.91 (m, 1H, *H*-8), 1.91 – 1.77 (m, 2H, *H*-7 and *H*-8); **δ_C** (101 MHz, $CDCl_3$) 174.1 (*C*-10), 138.3 (dd, *J* = 23.1, 19.8 Hz, *C*-3), 117.8 (dd, *J* = 249.8, 241.7 Hz, *C*-2), 113.8 (dd, *J* = 9.2, 6.0 Hz, *C*-4), 69.0 (*C*-6), 53.1 (dd, *J* = 31.9, 25.6 Hz, *C*-1), 51.9 (*C*-11), 50.4 (*C*-9), 39.2 (d, *J* = 4.1 Hz, *C*-5), 36.4 (d, *J* = 1.3 Hz, *C*-7), 21.9 (*C*-8); **δ_F** (376 MHz, $CDCl_3$) –95.30 (d, *J* = 240.4 Hz), –115.57 (d, *J* = 240.4 Hz); **HRMS** (ESI) m/z: $[M+Na]^+$ calcd for $C_{11}H_{15}F_2NO_2$ 254.0963; found 254.0962 (+0.30 ppm).

1-Benzyl-4,4-difluoro-2,2-dimethyl-3-methylenepyrrolidine 51

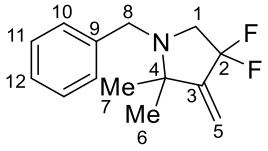

N-Benzyl-*N*-(2-bromo-2,2-difluoroethyl)-2-methylbut-3-yn-2-amine **37** (79.0 mg, 250 µmol) was subjected to General Procedure 5, stirring at room temperature for 24 hours. The resultant residue was purified by flash column chromatography (SiO_2, eluting with 0-2% diethyl ether in pentane) to give **51** (37.3 mg, 157 µmol, 63% yield) as a colourless solid.

R_f (95:5 petroleum ether: ethyl acetate) = 0.56; **m.p.** 55–57 °C; **ν_{max}** (thin film)/cm^{-1} 3088, 3067, 3033, 2989, 2971, 2928, 2901, 2870, 2847, 2814, 2712; **δ_H** (400 MHz, $CDCl_3$) 7.46 – 7.17 (m, 5H, Ar*H*), 5.63 – 5.57 (m, 1H, *H*-5), 5.33 – 5.22 (m, 1H, *H*-5), 3.64 (s, 2H, *H*-8), 2.99 (tt, *J* = 11.9, 1.7 Hz, 2H, *H*-1), 1.30 (s, 3H, *H*-6), 1.29 (s, 3H, *H*-7); **δ_C** (101 MHz, $CDCl_3$) 153.6 (t, *J* = 19.6 Hz, *C*-3), 139.0 (*C*-9), 128.5 (Ar*C*H), 128.4 (Ar*C*H), 127.2 (*C*-12), 122.6 (t, *J* = 245.0 Hz, *C*-2), 110.8 (t, *J* = 2.7 Hz, *C*-5), 62.8 (t, *J* = 2.9 Hz, *C*-4), 56.8 (t, *J* = 27.5 Hz, *C*-1), 51.6 (*C*-8), 23.6 (*C*-6 and *C*-7); **δ_F** (376 MHz, $CDCl_3$) –96.22; **HRMS** (ESI) m/z: $[M+H]^+$ calcd for $C_{14}H_{17}F_2N$ 238.1402; found 238.1404 (+1.00 ppm).

tert-Butyl (2-(3,3-difluoro-4-methylenepyrrolidin-1-yl)ethyl)carbamate 52

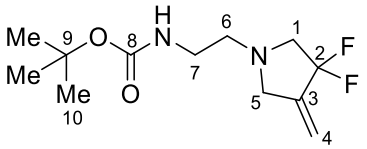

tert-Butyl (2-((2-bromo-2,2-difluoroethyl)(prop-2-yn-1-yl)amino)ethyl)carbamate **38** (30.0 mg, 87.9 µmol) was subjected to General Procedure 5, stirring at room temperature for 17 hours. The resultant residue after concentration was purified by flash column chromatography (SiO_2, eluting with 20-50% diethyl ether in pentane) to give **52** (11.2 mg, 42.7 µmol, 48% yield) as a yellow oil.

R_f (50:50 petroleum ether: diethyl ether) = 0.31; **ν_{max}** (thin film)/cm^{-1} 3434, 3350, 2976, 2932, 2814, 1698, 1503; **δ_H** (400 MHz, $CDCl_3$) 5.73 – 5.58 (m, 1H, *H*-4), 5.43 – 5.27 (m, 1H, *H*-4), 3.42 (t, *J* = 2.1 Hz, 2H, *H*-5), 3.27 (dt, *J* = 5.9, 5.1 Hz, 2H, *H*-7), 3.05 (t, *J* = 11.3 Hz, 2H, *H*-1), 2.65 (t, *J* = 5.9 Hz, 2H, *H*-6), 1.47 (s, 9H, *H*-10); **δ_C** (101 MHz, $CDCl_3$) 156.0 (*C*-8), 142.3 (t, *J* = 21.0 Hz, *C*-3), 122.4 (t, *J* = 246.4 Hz, *C*-2), 112.3 (t, *J* = 2.3 Hz, *C*-4), 79.4, 61.0 (t, *J* = 27.3 Hz, *C*-9), 56.5 (t, *J* = 3.1 Hz, *C*-5), 54.9 (*C*-6), 38.1 (*C*-7), 28.4 (*C*-10); **δ_F** (376 MHz, $CDCl_3$) – 97.89; **HRMS** (ESI) m/z: $[M+H]^+$ calcd for $C_{12}H_{20}F_2N_2O_2$ 263.1566; found 263.1569 (+1.20 ppm).

2-(3,3-Difluoro-4-methylenepyrrolidin-1-yl)ethan-1-ol 53

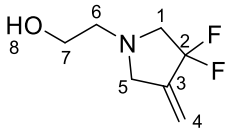

2-((2-Bromo-2,2-difluoroethyl)(prop-2-yn-1-yl)amino)ethan-1-ol **95** (60.6 mg, 250 µmol) was subjected to General Procedure 5, stirring at room temperature for 16 hours. The resultant residue was purified by flash column chromatography (SiO_2, eluting with 10-20% acetone in pentane) to give **53** (30.2 mg, 185 µmol, 74% yield) as a yellow oil.

R_f (80:20 petroleum ether: acetone) = 0.15; **ν_{max}** (thin film)/cm^{-1} 3362, 2930, 2883, 2810; **δ_H** (400 MHz, $CDCl_3$) 5.72 – 5.51 (m, 1H, *H*-4), 5.39 – 5.14 (m, 1H, *H*-4), 3.65 (t, *J* = 5.3 Hz, 2H, *H*-7), 3.44 (s, 2H, *H*-5), 3.27 (br s, 1H, *H*-8), 3.07 (t, *J* = 11.3 Hz, 2H, *H*-1), 2.69 (t, *J* = 5.3 Hz, 2H, *H*-6); **δ_C** (101 MHz, $CDCl_3$) 142.4 (t, *J* = 21.0 Hz, *C*-3), 122.5 (t, *J* = 246.5 Hz, *C*-2), 112.5 (t, *J* = 2.5 Hz, *C*-4), 61.2 (t, *J* = 27.3 Hz, *C*-1), 59.4 (*C*-7), 57.4 (*C*-6), 56.8 (t, *J* = 3.1 Hz, *C*-5); **δ_F** (376 MHz, $CDCl_3$) –97.97; **HRMS** (ESI) m/z: $[M+Na]^+$ calcd for $C_7H_{11}F_2NO$ 164.0881; found 164.0878 (+1.90 ppm).

1-Benzyl-4-ethylidene-3,3-difluoropyrrolidine 54

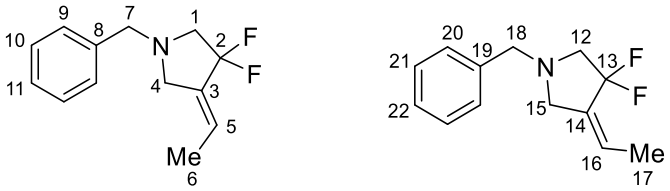

N-Benzyl-*N*-(2-bromo-2,2-difluoroethyl)but-2-yn-1-amine **39** (75.5 mg, 250 µmol) was subjected to General Procedure 5, stirring at room temperature for 16 hours. The resultant residue after concentration was purified by flash column chromatography (SiO_2, eluting with 2-5% diethyl ether in pentane) to give **54** (421 µg, 189 µmol, 75% yield, 53:47 *E:Z*) as a colourless oil. The following data is for the 53:47 mixture of *E* and *Z* products. The stereochemistry of each component was determined by NOESY interactions. The *E* stereochemistry was assigned on the basis of a NOESY interaction between *H*-6 and *H*-4. The *Z* stereochemistry was assigned on the basis of a NOESY interaction between *H*-15 and *H*-16.

R_f (90:10 petroleum ether: diethyl ether) = 0.31; **ν_{max}** (thin film)/cm^{-1} 3087, 3064, 3030, 2921, 2804, 2765; **δ_H** (400 MHz, $CDCl_3$) 7.39 – 7.25 (m, 10H, Ar*H*), 6.11 – 5.99 (m, 1H, *H*-5), 5.80 – 5.69 (m, 1H, *H*-16), 3.70 (s, 2H, *H*-7), 3.63 (s, 2H, *H*-18), 3.41 – 3.31 (m, 2H, *H*-4), 3.31 – 3.17 (m, 2H, *H*-15), 3.00 (app t, *J* = 11.2 Hz, 4H, *H*-1 and *H*-12), 1.92 – 1.84 (m, 3H, *H*-17), 1.72 – 1.63 (m, 3H, *H*-6); **δ_C** (101 MHz, $CDCl_3$) 137.6 (Ar*C*q), 137.5 (Ar*C*q), 135.2 (t, *J* = 20.5 Hz, *C*-3), 133.6 (t, *J* = 19.2 Hz, *C*-14), 128.9 (Ar*C*H), 128.9 (Ar*C*H), 128.6 (Ar*C*H), 128.5 (Ar*C*H), 127.5 (Ar*C*H), 127.5 (Ar*C*H), 126.3 (*C*-16), 124.6 (t, *J* = 246.0 Hz, *C*-13), 123.8 (t, *J* = 2.5 Hz,

C-5), 123.2 (t, *J* = 244.9 Hz, *C*-2), 62.7 (t, *J* = 27.7 Hz, *C*-12), 61.3 (t, *J* = 27.3 Hz, *C*-1), 60.2 (*C*-7), 60.0 (*C*-18), 57.9 (t, *J* = 3.8 Hz, *C*-15), 54.3 (t, *J* = 3.2 Hz, *C*-4), 14.7 (t, *J* = 2.1 Hz, *C*-6), 13.9 (*C*-17); δ_F (376 MHz, $CDCl_3$) –96.12, –96.58; **HRMS** (ESI) m/z: $[M+H]^+$ calcd for $C_{13}H_{15}F_2N$ 224.1245; found 224.1243 (+1.20 ppm).

1-Benzyl-3,3-difluoro-4-((trimethylsilyl)methylene)pyrrolidine 55

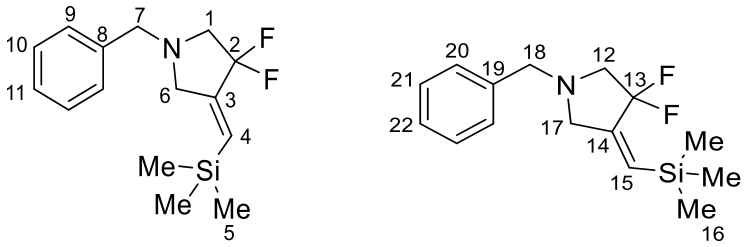

N-Benzyl-*N*-(2-bromo-2,2-difluoroethyl)-3-(trimethylsilyl)prop-2-yn-1-amine **40** (90.1 mg, 250 µmol) was subjected to General Procedure 5, stirring at room temperature for 88 hours. The resultant residue after concentration was purified by flash column chromatography (SiO_2, eluting with 2-5% diethyl ether in pentane) to give **55** (450 µg, 160 µmol, 64% yield, 55:45 *E:Z*) as a pale yellow oil. The following data is for the 55:45 mixture of *E* and *Z* products. The stereochemistry of each component was determined by NOESY interactions. The *Z* stereochemistry was assigned on the basis of a NOESY interaction between *H*-15 and *H*-17.

$\mathbf{R_f}$ (95:5 petroleum ether: diethyl ether) = 0.35; $\boldsymbol{\nu_{max}}$ (thin film)/cm^{-1} 3088, 3065, 3030, 2956, 2922, 2900, 2802, 2760, 2701; δ_H (400 MHz, $CDCl_3$) 7.38 – 7.27 (m, 10H, Ar*H*), 6.16 (tt, *J* = 2.7, 2.7 Hz, 1H, *H*-4), 5.86 (tt, *J* = 2.7, 2.4 Hz, 1H, *H*-15), 3.70 (s, 2H, *H*-7), 3.64 (s, 2H, *H*-18), 3.41 (d, *J* = 2.7 Hz, 2H, *H*-6), 3.35 (d, *J* = 2.7 Hz, 2H, *H*-17), 3.01 (t, *J* = 11.5 Hz, 2H, *H*-12), 2.94 (t, *J* = 11.1 Hz, 2H, *H*-1), 0.17 (s, 9H, *H*-16), 0.13 (s, 9H, *H*-5); δ_C (101 MHz, $CDCl_3$) 149.4 (t, *J* = 21.1 Hz, *C*-3), 148.6 (t, *J* = 21.1 Hz, *C*-14), 137.4 (*C*-19), 137.4 (*C*-8), 130.5 (*C*-15), 129.0 (Ar*C*H), 128.9 (Ar*C*H), 128.6 (Ar*C*H), 128.6 (Ar*C*H), 127.6 (*C*-11), 127.6 (*C*-22), 126.9 (t, *J* = 2.0 Hz, *C*-4), 123.1 (t, *J* = 247.5 Hz, *C*-13), 122.1 (t, *J* = 246.6 Hz, *C*-2), 62.1 (t, *J* = 27.8 Hz, *C*-12), 60.4 (t, *J* = 3.9 Hz, *C*-17), 60.1 (*C*-7), 60.1 (*C*-18), 60.0 (t, *J* = 27.2 Hz, *C*-1), 56.7 (t, *J* = 2.9 Hz, *C*-6), -0.2 (t, *J* = 2.4 Hz, *C*-16), -0.90 (*C*-5); δ_F (376 MHz, $CDCl_3$) –94.50, –97.55; **HRMS** (ESI) m/z: $[M+H]^+$ calcd for $C_{15}H_{21}F_2NSi$ 282.1484; found 282.1487 (+0.90 ppm).

(*E*)-1-Benzyl-4-benzylidene-3,3-difluoropyrrolidine 56 and (*Z*)-1-Benzyl-4-benzylidene-3,3-difluoropyrrolidine 57

N-Benzyl-*N*-(2-bromo-2,2-difluoroethyl)-3-phenylprop-2-yn-1-amine **98** (91.5 mg, 251 µmol) was subjected to General Procedure 5, stirring at room temperature for 16 hours. The resultant residue after concentration was purified by flash column chromatography (SiO_2, eluting with 1-3% diethyl ether in pentane) to give **56** (24.4 mg, 85.5 µmol, 34% yield) as a colourless oil and **57** (8.47 mg, 29.7 µmol, 12% yield) as a colourless oil. The *E* stereochemistry was assigned on the basis of a NOESY interaction between *H*-7 and *H*-4. The *Z* stereochemistry was assigned on the basis of a NOE interaction between *H*-5 and *H*-4.

(*E*)-1-Benzyl-4-benzylidene-3,3-difluoropyrrolidine 56:

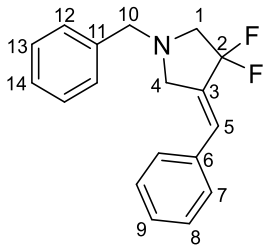

R_f (90:10 petroleum ether: diethyl ether) = 0.16; **ν_{max}** (thin film)/cm^{-1} 3129, 3106, 3087, 3061, 3029, 2958, 2923, 2884, 2804; **δ_H** (400 MHz, $CDCl_3$) 7.46 – 7.22 (m, 10H, Ar*H*), 6.92 (t, *J* = 2.8 Hz, 1H, *H*-5), 3.78 (s, 2H, *H*-10), 3.75 – 3.70 (m, 2H, *H*-4), 3.08 (t, *J* = 10.8 Hz, 2H, *H*-1); **δ_C** (101 MHz, $CDCl_3$) 137.4 (*C*-11), 135.5 (t, *J* = 2.4 Hz, (*C*-6), 134.4 (t, *J* = 20.0 Hz, *C*-3), 129.0 (Ar*C*H), 128.9 (Ar*C*H), 128.8 (Ar*C*H), 128.7 (Ar*C*H), 128.5 (Ar*C*H), 127.6 (Ar*C*H), 127.4 (t, *J* = 2.9 Hz, *C*-5), 124.4 (t, *J* = 246.2 Hz, *C*-2), 60.3 (d, *J* = 27.1 Hz, *C*-1), 60.0 (*C*-10), 56.1 (t, *J* = 2.9 Hz, *C*-4); **δ_F** (376 MHz, $CDCl_3$) –95.66; **HRMS** (ESI) m/z: $[M+H]^+$ calcd for $C_{18}H_{17}F_2N$ 286.1402; found 286.1399 (+1.10 ppm).

(*Z*)-1-Benzyl-4-benzylidene-3,3-difluoropyrrolidine 57:

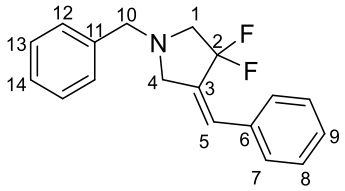

R_f (90:10 petroleum ether: diethyl ether) = 0.10; **ν_{max}** (thin film)/cm^{-1} 3090, 3063, 3032, 2962, 2936, 2922, 2884, 2854, 2828, 1795; **δ_H** (400 MHz, $CDCl_3$) 7.54 (d, *J* = 7.2 Hz, 2H, Ar*H*), 7.42 – 7.26 (m, 8H, Ar*H*), 6.60 (t, *J* = 2.6 Hz, 1H, *H*-5), 3.70 (s, 2H, *H*-10), 3.51 (s, 2H, *H*-4), 3.11 (t, *J* = 11.7 Hz, 2H, *H*-1); **δ_C** (126 MHz, $CDCl_3$) 137.2 (*C*-6), 134.3 (*C*-11), 130.1 (*C*-5), 129.4 (t, *J* = 4.1 Hz, *C*-3), 129.1 (Ar*C*H), 128.7 (Ar*C*H), 128.5 (Ar*C*H), 128.4 (Ar*C*H), 127.7 (Ar*C*H), 125.7 (Ar*C*H), 123.6 (t, *J* = 247.1 Hz, *C*-2), 62.9 (t, *J* = 28.4 Hz, *C*-1), 60.0 (*C*-10), 59.6 (t, *J* = 4.2 Hz, *C*-4); **δ_F** (376 MHz, $CDCl_3$) –95.35; **HRMS** (ESI) m/z: $[M+H]^+$ calcd for $C_{18}H_{17}F_2N$ 286.1402; found 286.1403 (+0.50 ppm).

4.4.3 Cyclised Alkenyl Amines

Methyl 2-(4,4-difluoro-1-(4-methoxybenzyl)pyrrolidin-3-yl)acetate 58

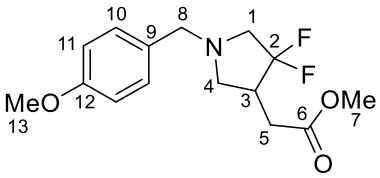

Methyl (*E*)-4-((2-bromo-2,2-difluoroethyl)(4-methoxybenzyl)amino)but-2-enoate **83** (94.5 mg, 250 µmol) was subjected to General Procedure 6, stirring at room temperature for 16 hours. The resultant residue after concentration was purified by flash column chromatography (SiO_2, eluting with 10-20% diethyl ether in pentane) to give **58** (62.7 mg, 209 µmol, 84% yield) as a yellow oil.

R_f (80:20 petroleum ether: diethyl ether) = 0.29; **ν_{max}** (thin film)/cm^{-1} 3067, 3033, 2998, 2955, 2913, 2836, 2807, 1737, 1613; **δ_H** (400 MHz, $CDCl_3$) 7.20 (d, *J* = 8.5 Hz, 2H, *H*-11), 6.85 (d, *J*

= 8.5 Hz, 2H, *H*-10), 3.80 (s, 3H, *H*-13), 3.68 (s, 3H, *H*-7), 3.61 – 3.48 (m, 2H, *H*-8), 3.16 – 3.02 (m, 2H, *H*-1 and *H*-4), 2.97 – 2.78 (m, 1H, *H*-3), 2.79 – 2.61 (m, 2H, *H*-1 and *H*-5), 2.39 (dddd, *J* = 16.8, 9.5, 1.4, 1.4 Hz, 1H, *H*-5), 2.30 (app t, *J* = 8.7 Hz, 1H, *H*-4); **δ_C** (101 MHz, $CDCl_3$) 172.2 (dd, *J* = 1.4, 1.4 Hz, *C*-6), 159.0 (*C*-12), 129.9 (*C*-11), 129.7 (*C*-9), 128.8 (dd, *J* = 252.3, 252.3 Hz, *C*-2), 113.9 (*C*-10), 61.5 (dd, *J* = 28.9, 28.9 Hz, *C*-1), 59.1 (*C*-8), 58.0 (d, *J* = 5.5 Hz, *C*-4), 55.4 (*C*-13), 52.0 (*C*-7), 42.5 (dd, *J* = 25.3, 19.9 Hz, *C*-3), 31.8 (d, *J* = 9.9 Hz, *C*-5); **δ_F** (376 MHz, $CDCl_3$) –93.53 (d, *J* = 230.9 Hz), –104.76 (d, *J* = 230.9 Hz); **HRMS** (ESI) m/z: $[M+H]^+$ calcd for $C_{15}H_{19}F_2NO_3$ 300.1406; found 300.1407 (+0.50 ppm).

1-(1-Benzyl-4,4-difluoropyrrolidin-3-yl)propan-2-one 59

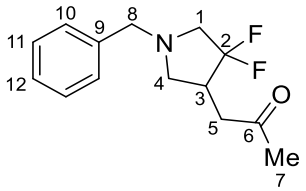

(*E*)-5-(Benzyl(2-bromo-2,2-difluoroethyl)amino)pent-3-en-2-one **84** (83.0 mg, 250 µmol) was subjected to General Procedure 6, stirring at room temperature for 16 hours. The resultant residue after concentration was purified by flash column chromatography (SiO_2, eluting with 20% diethyl ether in pentane) to give **59** (54.9 mg, 217 µmol, 86% yield) as a yellow oil.

R_f (80:20 petroleum ether: diethyl ether) = 0.13; **ν_{max}** (thin film)/cm^{-1} 3088, 3064, 3029, 3006, 2964, 2914, 2804, 1718; **δ_H** (400 MHz, $CDCl_3$) 7.36 – 7.23 (m, 5H, Ar*H*), 3.67 – 3.52 (m, 2H, *H*-8), 3.20 – 3.01 (m, 2H, *H*-4 and *H*-1), 2.99 – 2.81 (m, 2H, *H*-3 and *H*-5), 2.74 (ddd, *J* = 17.6, 11.6, 11.6 Hz, 1H, *H*-1), 2.50 (dddd, *J* = 18.2, 9.4, 2.4, 2.4 Hz, 1H, *H*-5), 2.24 (dd, *J* = 8.4, 8.4 Hz, 1H, *H*-4), 2.17 (s, 3H, *H*-7); **δ_C** (101 MHz, $CDCl_3$) 206.2 (*C*-6), 137.7 (*C*-9), 129.3 (dd, *J* = 252.0, 252.0 Hz, *C*-2), 128.8 (Ar*C*H), 128.5 (Ar*C*H), 127.5 (*C*-12), 61.5 (dd, *J* = 29.1, 29.1 Hz, *C*-1), 59.8 (*C*-8), 58.3 (dd, *J* = 5.5, 1.5 Hz, *C*-4), 41.5 (dd, *J* = 24.9, 20.0 Hz, *C*-3), 41.1 (dd, *J* = 7.7 Hz, *C*-5), 30.2 (*C*-7); **δ_F** (376 MHz, $CDCl_3$) –93.72 (d, *J* = 230.3 Hz), –103.90 (d, *J* = 230.3 Hz); **HRMS** (ESI) m/z: $[M+H]^+$ calcd for $C_{14}H_{17}F_2NO$ 254.1351; found 254.1353 (+0.60 ppm).

2-Benzyl-4,4-difluoro-2-azaspiro[4.5]decane 60

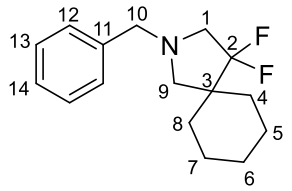

N-Benzyl-2-bromo-*N*-(cyclohex-1-en-1-ylmethyl)-2,2-difluoroethan-1-amine **85** (86.6 mg, 252 µmol) was subjected to General Procedure 6, stirring at room temperature for 16 hours. The resultant residue after concentration was purified by flash column chromatography (SiO_2, eluting with 0-1% diethyl ether in pentane) to give **60** (46.7 mg, 176 µmol, 70% yield) as a pale yellow oil.

R_f (95:5 petroleum ether: diethyl ether) = 0.33; **ν_{max}** (thin film)/cm^{-1} 3087, 3064, 3029, 2933, 2859, 2798, 2753; **δ_H** (400 MHz, $CDCl_3$) 7.42 – 7.16 (m, 5H, Ar*H*), 3.63 (s, 2H, *H*-10), 2.96 (dd, *J* = 14.2, 14.2 Hz, 2H, *H*-1), 2.66 (s, 2H, *H*-9), 1.84 – 1.52 (m, 7H, CH_2, cyclohexane), 1.39 – 1.09 (m, 3H, CH_2, cyclohexane); **δ_C** (101 MHz, $CDCl_3$) 138.4 (*C*-11), 129.7 (t, *J* = 254.4 Hz, *C*-2), 128.6 (Ar*C*H), 128.5 (Ar*C*H), 127.3 (Ar*C*H), 62.5 (*C*-9), 61.1 (t, *J* = 29.5 Hz, *C*-1), 60.1 (*C*-10), 47.0 (t, *J* = 19.6 Hz, *C*-3), 30.0 (t, *J* = 5.7 Hz, *H*-4 and *H*-8), 25.9 (*H*-6), 23.1 (t, *J* = 1.6 Hz, *H*-5 and *H*-7); **δ_F** (376 MHz, $CDCl_3$) –107.39; **HRMS** (ESI) m/z: $[M+H]^+$ calcd for $C_{16}H_{21}F_2N$ 266.1715; found 266.1723 (+3.00 ppm).

3,3-Difluoro-1-(4-methoxybenzyl)-4-vinylpyrrolidine 61

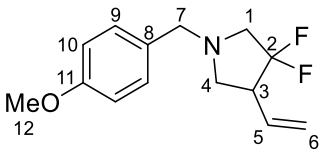

To a 50 mL culture tube was added *N*-(2-bromo-2,2-difluoroethyl)-*N*-(4-methoxybenzyl)buta-2,3-dien-1-amine **33** (82.5 mg, 248 mmol), $Ir(ppy)_3$ (1.64 mg, 2.50 µmol), DIPEA (0.90 mL, 5.00 mmol), TTMSS (150 µL, 500 µmol) and acetonitrile (25 mL). The culture tube was sealed and the mixture was sparged with Ar for 20 minutes. The blue LEDs were switched on and the

reaction was stirred at room temperature for 4.5 hours. KF on alumina (40 wt%, 1.5 g) was added and the mixture was stirred for 20 minutes, then filtered and concentrated. The resultant residue was purified by flash column chromatography (SiO_2, eluting with 5-10% diethyl ether in pentane) to give **61** (528 mg, 209 µmol, 84% yield) as a yellow oil.

R_f (90:10 petroleum ether: diethyl ether) = 0.17; **ν_{max}** (thin film)/cm^{-1} 3082, 3034, 2997, 2957, 2937, 2912, 2835, 2810, 2751; **δ_H** (400 MHz, $CDCl_3$) 7.23 (d, *J* = 8.6 Hz, 2H, Ar*H*), 6.87 (d, *J* = 8.6 Hz, 2H, Ar*H*), 5.89 – 5.71 (m, 1H, *H*-5), 5.25 – 5.13 (m, 2H, *H*-6), 3.81 (s, 3H, *H*-12), 3.66 – 3.50 (m, 2H, *H*-7), 3.20 (ddd, *J* = 13.5, 11.2, 11.0 Hz, 1H, *H*-1), 3.14 – 2.95 (m, 2H, *H*-3 and *H*-4), 2.72 (ddd, *J* = 19.1, 12.9, 11.2 Hz, 1H, *H*-1), 2.51 – 2.37 (m, 1H, *H*-4); **δ_C** (101 MHz, $CDCl_3$) 159.1 (*C*-11), 131.4 (d, *J* = 8.6 Hz, *C*-5), 130.0 (Ar*C*H), 129.9 (Ar*C*q), 128.6 (dd, *J* = 253.4, 250.3 Hz, *C*-2), 119.1 (*C*-6), 113.9 (Ar*C*H), 61.7 (dd, *J* = 29.0, 29.0 Hz, *C*-1), 59.3 (*C*-7), 57.6 (d, *J* = 5.9 Hz, *C*-4), 55.4 (*C*-12), 50.8 (dd, *J* = 24.7, 20.7 Hz, *C*-3); **δ_F** (376 MHz, $CDCl_3$) –93.68 (d, *J* = 230.7 Hz), –102.27 (d, *J* = 230.7 Hz); **HRMS** (ESI) m/z: $[M+H]^+$ calcd for $C_{14}H_{17}F_2NO$ 254.1351; found 254.1351 (+0.20 ppm).

1-Benzyl-3,3-difluoro-4-methylpiperidine 62

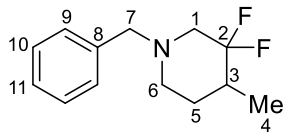

N-Benzyl-*N*-(2-bromo-2,2-difluoroethyl)but-3-en-1-amine **90** (76.2 mg, 251 µmol) was subjected to General Procedure 6, stirring at room temperature for 16 hours. The resultant residue after concentration was purified by flash column chromatography (SiO_2, eluting with 0-4% diethyl ether in pentane) to give **62** (37.8 mg, 168 µmol, 67% yield) as a colourless oil.

R_f (90:10 petroleum ether: diethyl ether) = 0.32; **ν_{max}** (thin film)/cm^{-1} 3087, 3064, 3029, 2975, 2943, 2926, 2885, 2858, 2813, 2772, 2937, 2682; **δ_H** (400 MHz, $CDCl_3$) 7.52 – 7.10 (m, 5H, Ar*H*), 3.69 – 3.50 (m, 2H, *H*-7), 3.06 (dddd, *J* = 11.7, 9.8, 5.8, 1.6 Hz, 1H, *H*-1), 2.86 (ddd, *J* = 11.5, 3.1, 2.6 Hz, 1H, *H*-6), 2.21 (ddd, *J* = 27.6, 11.8, 2.4 Hz, 1H, *H*-1), 2.11 (ddd, *J* = 11.6, 2.9, 1.7 Hz, 1H, *H*-6), 1.90 – 1.73 (m, 1H, *H*-3), 1.73 – 1.51 (m, 2H, *H*-5), 1.07 (d, *J* = 6.7 Hz,

3H, *H*-4); **δ_C** (101 MHz, $CDCl_3$) 137.5 (*C*-8), 129.1 (Ar*C*H), 128.5 (Ar*C*H), 127.4 (Ar*C*H), 121.3 (dd, *J* = 247.7, 240.4 Hz, *C*-2), 62.2 (*C*-7), 58.3 (dd, *J* = 31.1, 25.0 Hz, *C*-1), 52.2 (*C*-6), 37.1 (dd, *J* = 23.2, 21.1 Hz, *C*-3), 30.5 (d, *J* = 8.4 Hz, *C*-5), 12.2 (dd, *J* = 4.9, 2.4 Hz, *C*-4); **δ_F** (376 MHz, $CDCl_3$) –105.13 (d, *J* = 239.2 Hz), –117.38 (d, *J* = 241.9 Hz); **HRMS** (ESI) m/z: $[M+H]^+$ calcd for $C_{13}H_{17}F_2N$ 226.1402; found 226.1407 (+2.20 ppm).

4-Benzyl-3,3-difluoro-1-(4-methoxybenzyl)pyrrolidine 63

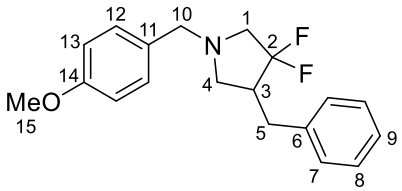

(*E*)-*N*-(2-Bromo-2,2-difluoroethyl)-*N*-(4-methoxybenzyl)-3-phenylprop-2-en-1-amine **42** (99.4 mg, 251 µmol) was subjected to General Procedure 6, stirring at room temperature for 16 hours. The resultant residue after concentration was purified by flash column chromatography (SiO_2, eluting with 5-7% diethyl ether in pentane) to give **63** (30.0 mg, 94.4 µmol, 38% yield) as a pale yellow oil.

R_f (90:10 petroleum ether: diethyl ether) = 0.26; **ν_{max}** (thin film)/cm^{-1} 3087, 3063, 3029, 3002, 2955, 2935, 2913, 2863, 2834, 2807, 2798, 1612, 1511; **δ_H** (400 MHz, $CDCl_3$) 7.42 – 7.09 (m, 7H, Ar*H*), 6.84 (d, *J* = 8.3 Hz, 2H, Ar*H*), 3.80 (s, 3H, *H*-15), 3.63 – 3.43 (m, 2H, *H*-10), 3.18 (ddd, *J* = 13.8, 10.7, 10.7 Hz, 1H, *H*-1), 3.04 (dd, *J* = 13.7, 5.0 Hz, 1H, *H*-5), 2.89 (dd, *J* = 9.3, 7.0 Hz, 1H, *H*-4), 2.80 – 2.65 (m, 2H, *H*-1 and *H*-3), 2.60 (dd, *J* = 13.8, 10.2 Hz, 1H, *H*-5), 2.30 (dd, *J* = 9.0, 9.0 Hz, 1H, *H*-4); **δ_C** (101 MHz, $CDCl_3$) 159.0 (*C*-14), 139.5 (*C*-6), 129.9 (Ar*C*H), 129.1 (dd, *J* = 250.3, 250.3 Hz, *C*-2), 128.8 (Ar*C*H), 128.7 (Ar*C*H), 128.1 (Ar*C*q), 126.43 (Ar*C*H), 113.9 (Ar*C*H), 62.0 (dd, *J* = 29.1, 29.1 Hz, *C*-1), 59.4 (*C*-10), 58.1 (d, *J* = 5.9, *C*-4), 55.4 (*C*-15), 47.8 (dd, *J* = 23.7, 20.4 Hz, *C*-3), 32.7 (d, *J* = 9.5 Hz, *C*-5); **δ_F** (376 MHz, $CDCl_3$) –93.12 (d, *J* = 230.0 Hz), –104.96 (d, *J* = 230.0 Hz); **HRMS** (ESI) m/z: $[M+H]^+$ calcd for $C_{19}H_{21}F_2NO$ 318.1664; found 318.1663 (+0.40 ppm).

3,3-Difluoro-1-(4-methoxybenzyl)-4-methylpyrrolidine 46

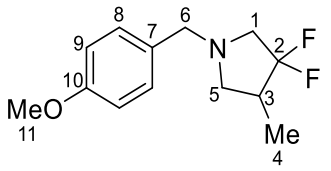

N-(2-Bromo-2,2-difluoroethyl)-*N*-(4-methoxybenzyl)prop-2-en-1-amine **41** (79.6 mg, 249 µmol) was subjected to General Procedure 6, stirring at room temperature for 16 hours. The resultant residue after concentration was purified by flash column chromatography (Al_2O_3, eluting with 5-20% ethyl acetate in pentane) to give **46** (47.3 mg, 196 µmol, 79% yield) as a yellow oil.

R_f (80:20 petroleum ether: ethyl acetate) = 0.53; **ν_{max}** (thin film)/cm^{-1} 3073, 3034, 2971, 2936, 2887, 2835, 2804, 2754; **δ_H** (400 MHz, $CDCl_3$) 7.25 – 7.17 (m, 2H, Ar*H*), 6.91 – 6.82 (m, 2H, Ar*H*), 3.81 (s, 3H, *H*-11), 3.61 – 3.46 (m, 2H, *H*-6), 3.17 (ddd, *J* = 18.4, 13.6, 10.7 Hz, 1H, *H*-1), 3.04 (dd, *J* = 9.2, 7.3 Hz, 1H, *H*-5), 2.66 (ddd, *J* = 18.4, 13.6, 11.3 Hz, 1H, *H*-1), 2.57 – 2.37 (m, 1H, *H*-3), 2.17 (dd, *J* = 9.1, 9.1 Hz, 1H, *H*-5), 1.06 (app dd, *J* = 7.1, 2.2 Hz, 3H, *H*-4); **δ_C** (101 MHz, $CDCl_3$) 159.0 (*C*-10), 130.0 (*C*-7), 130.0 (Ar*C*H), 129.5 (dd, *J* = 250.6, 250.6 Hz, *C*-2), 113.9 (Ar*C*H), 61.7 (dd, *J* = 29.3, 29.3 Hz, *C*-1), 59.9 (dd, *J* = 6.0, 1.3 Hz, *C*-5), 59.4 (*C*-11), 55.4 (*C*-6), 40.9 (dd, *J* = 24.3, 21.7 Hz, *C*-3), 10.9 (d, *J* = 10.3 Hz, *C*-4); **δ_F** (376 MHz, $CDCl_3$) –94.36 (d, *J* = 228.6 Hz), –106.63 (d, *J* = 228.6 Hz); **HRMS** (ESI) m/z: $[M+H]^+$ calcd for $C_{13}H_{17}F_2NO$ 242.1351; found 242.1350 (+0.30 ppm).

3,3-Difluoro-4-(2-(1,1,1,3,3,3-hexamethyl-2-(trimethylsilyl)trisilan-2-yl)ethyl)-1-(4-methoxybenzyl)pyrrolidine 68

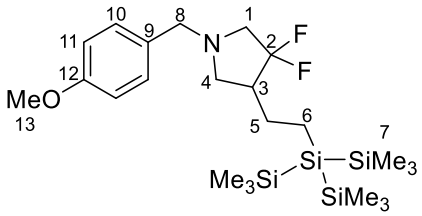

To a 50 mL culture tube was added *N*-(2-bromo-2,2-difluoroethyl)-*N*-(4-methoxybenzyl)buta-2,3-dien-1-amine **33** (83.5 mg, 251 mmol), $Ir(ppy)_3$ (1.64 mg, 2.50 µmol), DIPEA (0.44 mL, 2.50 mmol), TTMSS (390 µL, 1.25 mmol) and acetonitrile (25 mL). The culture tube was sealed and the mixture was sparged with Ar for 20 minutes. The blue LEDs were switched on and the reaction was stirred at room temperature for 16 hours. KF on alumina (40 wt%, 1.5 g) was added and the mixture was stirred for 20 minutes, then filtered and concentrated. The resultant residue was purified by flash column chromatography (SiO_2, eluting with 0-10% diethyl ether in pentane) to give **68** (43.0 mg, 85.7 µmol, 34% yield) as a colourless oil.

R_f (90:10 petroleum ether: diethyl ether) = 0.50; **ν_{max}** (thin film)/cm^{-1} 2998, 2947, 2893, 2834, 2808, 1613, 1512; **δ_H** (400 MHz, $CDCl_3$) 7.23 (d, *J* = 8.6 Hz, 2H, Ar*H*), 6.87 (d, *J* = 8.6 Hz, 2H, Ar*H*), 3.81 (s, 3H, *H*-13), 3.67 – 3.42 (m, 2H, *H*-8), 3.17 (ddd, *J* = 13.8, 11.2, 9.1 Hz, 1H, *H*-1), 3.07 (dd, *J* = 8.2, 8.2 Hz, 1H, *H*-4), 2.64 (ddd, *J* = 18.4, 13.9, 11.2 Hz, 1H, *H*-1), 2.47 – 2.24 (m, 1H, *H*-3), 2.15 (dd, *J* = 9.1, 9.1 Hz, 1H, *H*-4), 1.85 – 1.63 (m, 1H, *H*-5), 1.54 – 1.33 (m, 1H, *H*-5), 0.78 (m, 2H, *H*-6), 0.17 (s, 27H, *H*-7); **δ_C** (101 MHz, $CDCl_3$) 159.0 (*C*-12), 130.1 (*C*-9), 129.9 (Ar*C*H), 129.4 (dd, *J* = 250.9, 250.9 Hz, *C*-2), 113.9 (Ar*C*H), 62.3 (dd, *J* = 29.3, 29.3 Hz, *C*-1), 59.5 (*C*-8), 58.3 (d, *J* = 5.9 Hz, *C*-4), 55.4 (*C*-13), 49.8 (dd, *J* = 22.9, 20.8 Hz, *C*-3), 26.2 (d, *J* = 8.4 Hz, *C*-5), 6.0 (*C*-6), 1.3 (*C*-7); **δ_F** (376 MHz, $CDCl_3$) –91.02 (d, *J* = 230.2 Hz), –106.51 (d, *J* = 230.2 Hz); **HRMS** (ESI) m/z: $[M+H]^+$ calcd for $C_{23}H_{45}F_2NOSi_4$ 502.2619; found 502.2611 (+1.70 ppm).

4.4.4 Derivatisations

3,3-Difluoro-4-methylenepyrrolidine hydrochloride 64

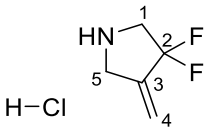

To a 0 °C solution of 3,3-difluoro-1-(4-methoxybenzyl)-4-methylenepyrrolidine **47** (121 mg, 500 µmol) in DCE (1.25 mL) was added 1-chloroethyl chloroformate (59 µL, 550 µmol) in DCE (0.5 mL) dropwise over 5 minutes. The mixture was stirred at 0 °C for 15 minutes, then warmed to room temperature and stirred for 30 minutes, then heated to 85 °C and stirred for 1 hour. The reaction was cooled to room temperature and concentrated. The residue was dissolved in MeOH (1 mL) and stirred at 75 °C for 1 hour. The reaction was cooled to room temperature and concentrated. The solid residue was filtered and washed with Et_2O (10 mL) to give **64** (54.7 mg, 0.352 mmol, 69%) as a colourless solid.

m.p. 152–155 °C; $\boldsymbol{\nu_{max}}$ (thin film)/cm^{-1} 2971, 2885, 2802, 2730, 2673, 2600, 2541, 2466, 2327; $\boldsymbol{\delta_H}$ (400 MHz, Methanol-*d*$_4$) 5.97 – 5.87 (m, 1H, *H*-4), 5.84 – 5.74 (m, 1H, *H*-4), 4.27 (t, *J* = 2.5 Hz, 2H, *H*-5), 3.89 (t, *J* = 10.9 Hz, 2H, *H*-1); $\boldsymbol{\delta_C}$ (101 MHz, Methanol-*d*$_4$) 137.5 (t, *J* = 21.9 Hz, *C*-3), 122.1 (t, *J* = 246.0 Hz, *C*-2), 117.4 (t, *J* = 2.9 Hz, *C*-4), 52.0 (t, *J* = 33.6 Hz, *C*-1), 48.4 (t, *J* = 2.7 Hz, *C*-5); $\boldsymbol{\delta_F}$ (376 MHz, Methanol-*d*$_4$) –100.68; **HRMS** (ESI) m/z: $[M+Na]^+$ calcd for $C_5H_7F_2N$ 142.0439; found 142.0435 (+2.50 ppm).

4,4-Difluoro-1-(4-methoxybenzyl)-3-methylpyrrolidin-3-ol 65

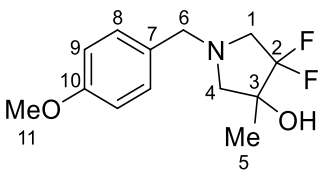

To a solution of 3,3-difluoro-1-(4-methoxybenzyl)-4-methylenepyrrolidine **47** (23.9 mg, 100 µmol) and Mn(dpm)$_3$ (3.02 mg, 5.00 µmol) in isopropanol (0.5 mL) under O_2 was added $PhSiH_3$ (25 µL, 200 µmol). The reaction mixture was stirred at room temperature for 24 hours, then

concentrated. The residue was purified by flash column chromatography (SiO_2, eluting with 10-20% ethyl acetate in pentane) to give **65** (17.3 mg, 67.0 µmol, 67% yield) as a pale yellow oil.

R_f (80:20 petroleum ether: ethyl acetate) = 0.19; **ν_{max}** (thin film)/cm^{-1} 3431, 2993, 2957, 2936, 2917, 2836, 2815, 1612, 1513; **δ_H** (400 MHz, $CDCl_3$) 7.23 – 7.16 (m, 2H, Ar*H*), 6.92 – 6.78 (m, 2H, Ar*H*), 3.80 (s, 3H, *H*-11), 3.60 (s, 2H, *H*-6), 3.18 (ddd, *J* = 15.3, 13.6, 11.5 Hz, 1H, *H*-1), 2.89 – 2.72 (m, 2H, *H*-1 and *H*-4), 2.63 – 2.53 (m, 1H, *H*-4), 1.33 (d, *J* = 3.1 Hz, 3H, *H*-5); **δ_C** (101 MHz, $CDCl_3$) 159.1 (*C*-10), 130.0 (Ar*C*H), 129.5 (*C*-7), 126.4 (dd, *J* = 258.8, 255.5 Hz, *C*-2), 114.0 (Ar*C*H), 77.0 (dd, *J* = 47.9, 27.8 Hz, *C*-3), 64.3 (dd, *J* = 1.5, 1.5 Hz, *C*-4), 59.7 (dd, *J* = 28.5, 28.5 Hz, *C*-1), 59.1 (*C*-6), 55.4 (*C*-11), 18.1 (d, *J* = 5.9 Hz, *C*-5); **δ_F** (376 MHz, $CDCl_3$) –105.33 (d, *J* = 231.2 Hz), –117.28 (d, *J* = 231.2 Hz); **HRMS** (ESI) m/z: $[M+H]^+$ calcd for $C_{13}H_{17}F_2NO_2$ 258.1300; found 258.1297 (+1.10 ppm).

4.4.5 Synthesis of Amide Starting Materials

_N_-Allyl-2-bromo-2,2-difluoroacetamide 99

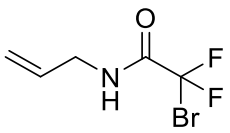

Allylamine (1.70 mL, 23.0 mmol) was subjected to General Procedure 1 to give **99** as a pale yellow oil (4.27 g, 20.0 mmol, 88% yield).

ν_{max} (thin film)/cm^{-1} 3300, 3083, 1698, 1536, 1431; **δ_H** (500 MHz, $CDCl_3$) 6.51 (s, 1H, N*H*), 5.85 (ddt, 1H, *J* = 17.2, 10.3, 6.0 Hz, H_2C=C*H*), 5.37 – 5.17 (m, 2H, *H*$_2$C=CH), 3.97 (dd, 2H, *J* = 6.0, 6.0 Hz, NC*H*$_2$); **δ_C** (126 MHz, $CDCl_3$) 160.0 (t, *J* = 27.5 Hz, *C*=O), 132.1 (H_2C=*C*H), 118.1 (H_2*C*=CH), 111.8 (t, *J* = 315.9 Hz, *C*F_2Br), 42.5 (N*C*H_2); **δ_F** (376 MHz, $CDCl_3$) –60.52; **HRMS** (ESI) m/z: $[M+H]^+$ calcd for $C_5H_7{}^{79}BrF_2NO$ 213.9674; found 213.9663 (+4.90 ppm).

Data are consistent with the literature.[127]

_N_-Allyl-_N_-benzyl-2-bromo-2,2-difluoroacetamide 71

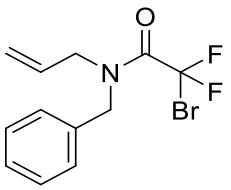

To a 0 °C suspension of NaH (672 mg, 16.8 mmol of a 60% dispersion in mineral oil) in DMF (15 mL) was added *N*-allyl-2-bromo-2,2-difluoroacetamide **99** (2.99 g, 14.0 mmol) in DMF (15 mL) dropwise over 5 minutes. The mixture was stirred at 0 °C for 30 minutes after which benzyl bromide (1.80 mL, 15.4 mmol) was added dropwise over 10 minutes. The reaction mixture was stirred at room temperature for 6 hours after which diethyl ether (20 mL), water (20 mL) and brine (10 mL of a sat. aq. solution) were added and the mixture was extracted with diethyl ether (2 × 20 mL). The combined organics were dried over magnesium sulfate and concentrated. The resulting residue was purified by flash column chromatography (SiO_2, eluting with 90:10 petroleum ether/ethyl acetate). The mixed fractions were purified twice by flash column chromatography (SiO_2, eluting with 90:10 petroleum ether/ethyl acetate). The residues were combined to give **71** (3.60 g, 11.8 mmol, 85% yield) as a pale yellow oil.

R_f (90:10 petroleum ether/ethyl acetate) = 0.50; **ν_{max}** (thin film)/cm^{-1} 3030, 1682, 1496, 1440, 1417, 1203; **δ_H** (500 MHz, $CDCl_3$) 7.41 – 7.29 (m, 3H, Ar*H*), 7.28 – 7.19 (m, 2H, Ar*H*), 5.87 – 5.68 (m, 1H, R*H*C=CH_2), 5.44 – 5.09 (m, 2H, RHC=CH_2), 4.72 (s, 1H, NC*H*Ar), 4.64 (s, 1H, NC*H*Ar), 4.03 (d, *J* = 5.9 Hz, 1H, C=CH(C*H*)), 3.93 (d, *J* = 5.9 Hz, 1H, C=CH(C*H*)); **δ_C** (126 MHz, $CDCl_3$) 159.89 (t, *J* = 26.5 Hz, *C*=O), 159.5 (t, *J* = 26.5 Hz, *C*=O), 135.6 (Ar*C*q), 134.9 (Ar*C*q), 131.7 (H*C*=CH_2), 130.7 (H*C*=CH_2), 129.1 (Ar*C*H), 129.0 (Ar*C*H), 128.2 (Ar*C*H), 128.1 (Ar*C*H), 127.3 (Ar*C*H), 119.6 (HC=*C*H_2), 118.9 (HC=*C*H_2), 111.1 (t, *J* = 315.0 Hz, *C*F_2Br), 111.1 (t, *J* = 315.0 Hz, *C*F_2Br), 50.9 (t, *J* = 3.8 Hz, N*C*H_2Ar), 49.8 (t, *J* = 3.8 Hz, C=CH(*C*H_2)), 48.9 (N*C*H_2Ar), 48.5 (C=CH(*C*H_2)) (Data listed for both rotamers); **δ_F** (376 MHz, $CDCl_3$) –53.73, –54.16; **HRMS** (ESI) m/z: $[M+H]^+$ calcd for $C_{12}H_{12}{}^{79}BrF_2NO$ 303.0070; found 303.0072 (+2.20 ppm).

Data are consistent with the literature.[31]

2-Bromo-2,2-difluoro-*N*-(prop-2-yn-1-yl)acetamide 100

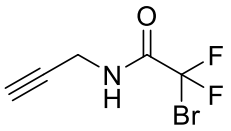

Propargylamine (190 µL, 3.00 mmol) was subjected to General Procedure 1 to give a residue was filtered through a pad of silica. The filtrate was concentrated to give **100** as a pale yellow oil (543 mg, 2.57 mmol, 86% yield).

$\boldsymbol{\nu}_{max}$ (thin film)/cm^{-1} 3301, 1699, 1532, 1426; $\boldsymbol{\delta}_H$ (400 MHz, $CDCl_3$) 6.54 (s, 1H, N*H*), 4.15 (dd, 2H, *J* = 5.4, 2.6 Hz, CH_2), 2.34 (t, 1H, *J* = 2.6 Hz, C*H,* alkyne); $\boldsymbol{\delta}_C$ (101 MHz, $CDCl_3$) 159.7 (t, *J* = 28.1 Hz, *C*=O), 111.4 (t, *J* = 315.7 Hz, *C*F_2Br), 77.3 (*C*q, alkyne), 73.4 (C≡*C*H), 30.2 (*C*H_2); $\boldsymbol{\delta}_F$ (376 MHz, $CDCl_3$) –60.84; **HRMS** (ESI) m/z: $[M+Na]^+$ calcd for $C_5H_4{}^{79}BrF_2NO$ 233.9337; found 233.9325 (+5.00 ppm).

***N*-Benzyl-2-bromo-2,2-difluoro-*N*-(prop-2-yn-1-yl)acetamide 101**

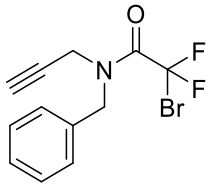

To a 0 °C suspension of NaH (114 mg, 2.84 mmol of a 60% dispersion in mineral oil) in DMF (14 mL) was added 2-bromo-2,2-difluoro-*N*-(prop-2-yn-1-yl)acetamide **100** (500 mg, 2.37 mmol) in DMF (14 mL) dropwise over 5 minutes. The mixture was stirred at 0 °C for 30 minutes after which benzyl bromide (330 µL, 2.84 mmol) was added dropwise over 5 minutes. The reaction mixture was stirred at room temperature for 5.5 hours after which diethyl ether (20 mL), water (30 mL) and brine (10 mL of a sat. aq. solution) were added and the mixture was extracted with diethyl ether (2 × 20 mL). The combined organics were dried over magnesium sulfate and concentrated. The resulting residue was purified by flash column chromatography (SiO_2, eluting with 0-5% ethyl acetate in petroleum ether). The mixed fractions were purified again by flash column chromatography (SiO_2, eluting with 0-5% ethyl acetate in petroleum

ether). The residues were combined to give **101** (667 mg, 2.21 mmol, 93% yield) as a pale yellow oil.

R_f (90:10 petroleum ether/ethyl acetate) = 0.50; **ν_{max}** (thin film)/cm^{-1} 3293, 3067, 3032, 2928, 1684; **δ_H** (400 MHz, $CDCl_3$) 7.43 – 7.27 (m, 10H, Ar*H*), 4.86 (s, 2H, NCH_2Ar), 4.80 (s, 2H, NCH_2Ar), 4.16 (d, *J* = 2.5 Hz, 2H, NCH_2), 4.12 (d, *J* = 2.5 Hz, 2H, NCH_2), 2.37 (t, *J* = 2.5 Hz, 1H, C*H,* alkyne), 2.29 (t, *J* = 2.5 Hz, 1H, C*H,* alkyne) (Data listed for both rotamers); **δ_C** (101 MHz, $CDCl_3$) 159.2 (t, *J* = 27.6 Hz, *C*=O), 159.2 (t, *J* = 27.6 Hz, *C*=O), 134.9 (Ar*C*q), 134.1 (Ar*C*q), 129.2 (Ar*C*H), 129.1 (Ar*C*H), 128.6 (Ar*C*H), 128.4 (Ar*C*H), 127.8 (Ar*C*H), 110.9 (t, *J* = 314.5 Hz, *C*F_2Br), 110.7 (t, *J* = 314.5 Hz, *C*F_2Br), 77.4 (*C*q*,* alkyne), 76.7 (*C*q*,* alkyne), 73.8 (*C*H, alkyne), 73.4 (*C*H, alkyne), 50.8 (t, *J* = 4.5 Hz, N*C*H_2), 49.2 (N*C*H_2), 37.0 (t, *J* = 4.5 Hz, N*C*H_2), 35.3 (N*C*H_2) (Data listed for both rotamers); **δ_F** (376 MHz, $CDCl_3$) –53.86, –54.37 (Data listed for both rotamers); **HRMS** (ESI) m/z: $[M+H]^+$ calcd for $C_{12}H_{10}{}^{79}BrF_2NO$ 301.9987; found 301.9988 (+0.40 ppm).

2-Bromo-2,2-difluoro-*N*,*N*-di(prop-2-yn-1-yl)acetamide 102

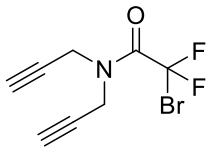

To a 0 °C suspension of NaH (274 mg, 6.84 mmol of a 60% dispersion in mineral oil) in DMF (12 mL) was added 2-bromo-2,2-difluoro-*N*-(prop-2-yn-1-yl)acetamide **100** (1.20 g, 5.70 mmol) in DMF (13 mL) dropwise over 5 minutes. The mixture was stirred at 0 °C for 30 minutes after which propargyl bromide (700 µL, 6.27 mmol of an 80% w/w solution in toluene) was added dropwise over 5 minutes. The reaction mixture was stirred at room temperature for 5 hours before ethyl acetate (40 mL) and water (40 mL) were added and the mixture was extracted with ethyl acetate (2 × 40 mL). The combined organics were dried over magnesium sulfate and concentrated. The resulting residue was purified by flash column chromatography (SiO_2, eluting with 0-10% ethyl acetate in petroleum ether) to give **102** (951 mg, 3.80 mmol, 67% yield) as a pale yellow oil.

R_f (90:10 petroleum ether/ethyl acetate) = 0.40; **ν_{max}** (thin film)/cm^{-1} 3297, 2985, 1685, 1436; **δ_H** (400 MHz, $CDCl_3$) 4.43 (app s, 4H, NC*H*$_2$), 4.40 (app s, 4H, NC*H*$_2$), 2.37 (app s, 2H, C*H*, alkyne), 2.33 (app s, 2H, C*H*, alkyne) (data listed as a mixture of rotamers); **δ_C** (101 MHz, $CDCl_3$) 158.3 (t, *J* = 27.8 Hz, *C*=O), 110.3 (t, *J* = 314.5 Hz, *C*F_2Br), 76.4 (*C*H, alkyne), 76.1 (*C*H, alkyne), 74.2 (*C*q, alkyne), 73.9 (*C*q, alkyne), 37.2 (t, *J* = 5.1 Hz, N*C*H_2), 35.6 (N*C*H_2) (data listed as a mixture of rotamers); **δ_F** (376 MHz, $CDCl_3$) –54.79; **HRMS** (ESI) m/z: $[M+H]^+$ calcd for $C_8H_6{}^{79}BrF_2NO$ 249.9674; found 249.9670 (+1.50 ppm).

***N*-Benzyl-2-bromo-*N*-(but-3-yn-1-yl)-2,2-difluoroacetamide 103**

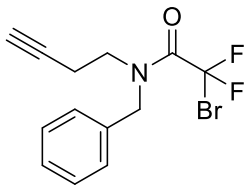

To a 0 °C suspension of **89** (501 mg, 3.14 mmol) and Et_3N (880 µL, 6.28 mmol) in dichloromethane (3 mL) was added a solution of bromodifluoroacetyl chloride (668 mg, 3.45 mmol) in dichloromethane (3 mL) at dropwise over 5 minutes under Ar. The reaction was stirred at room temperature for 16 hours after which dichloromethane (20 mL) and sat. aq. K_2CO_3 solution (20 mL) were added and the mixture was extracted with dichloromethane (2 × 20 mL). The organic fraction was washed with HCl (20 mL of a 1 N aq. solution) and brine (20 mL of a sat. aq. solution) and then dried over magnesium sulfate and concentrated. The resultant residue was purified by flash column chromatography (SiO_2, eluting with 99:1 petroleum ether/ethyl acetate) to give **103** (614 mg, 1.94 mmol, 62% yield) as an orange oil.

R_f (95:5 petroleum ether/ethyl acetate) = 0.35; **ν_{max}** (thin film)/cm^{-1} 3296, 3032, 2944, 1678; **δ_H** (400 MHz, $CDCl_3$) 7.42 – 7.29 (m, 3H, Ar*H*), 7.28 – 7.21 (m, 2H, Ar*H*), 4.75 (s, 2H, C*H*$_2$Ph), 3.62 (t, *J* = 7.3 Hz, 2H, NC*H*$_2$CH$_2$), 2.50 (m, 2H, NCH$_2$C*H*$_2$), 2.02 (t, *J* = 2.7 Hz, 1H, C*H*, alkyne) (data listed for major rotamer); **δ_C** (101 MHz, $CDCl_3$) 159.7 (t, *J* = 26.3 Hz, *C*=O), 134.9 (Ar*C*q), 129.2 (Ar*C*H), 128.4 (Ar*C*H), 127.4 (Ar*C*H), 110.9 (t, *J* = 314.7 Hz, *C*F_2Br), 80.9 (*C*q, alkyne), 70.5 (*C*H, alkyne), 52.8 (t, *J* = 3.9 Hz, N*C*H_2), 45.6 (N*C*H_2), 16.4 (NCH$_2$*C*H$_2$) (data listed for

major rotamer); **δ_F** (376 MHz, $CDCl_3$) –53.97 (data listed for major rotamer); **HRMS** (ESI) m/z: $[M+H]^+$ calcd for $C_{13}H_{12}{}^{79}BrF_2NO$ 316.0143; found 316.0144 (+0.20 ppm).

***N,N*-Diallyl-2-bromo-2,2-difluoroacetamide 104**

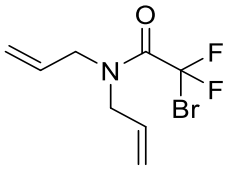

Diallylamine (270 µL, 2.20 mmol) was subjected to General Procedure 1 to give a residue which was filtered through a pad of silica. The filtrate was concentrated to give **104** as a pale yellow oil (296 mg, 1.21 mmol, 58% yield).

ν_{max} (thin film)/cm^{-1} 1681, 1463, 1442; **δ_H** (400 MHz, $CDCl_3$) 5.78 (ddt, *J* = 16.9, 10.1, 5.7 Hz, 2H, H_2C=C*H*), 5.38 – 5.14 (m, 4H, *H*$_2$C=CH), 4.09 (dt, *J* = 5.7, 1.5 Hz, 2H, NC*H*$_2$), 4.00 (dt, *J* = 5.7, 1.5 Hz, 2H, NC*H*$_2$); **δ_C** (101 MHz, $CDCl_3$) 159.2 (t, *J* = 26.5 Hz, *C*=O), 131.9 (H_2C=*C*H), 130.9 (H_2C=*C*H), 119.3 (H_2*C*=CH), 118.6 (H_2*C*=CH), 111.0 (t, *J* = 315.0 Hz, *C*F_2Br), 50.2 (t, J = 3.6 Hz, NCH_2), 48.6 (N*C*H_2); **δ_F** (376 MHz, $CDCl_3$) –54.26; **HRMS** (ESI) m/z: $[M+H]^+$ calcd for $C_8H_{11}{}^{79}BrF_2NO$ 253.9987; found 253.9980 (+2.50 ppm).

Data are consistent with the literature.[31]

2-Bromo-2,2-difluoro-*N*-(4-methoxyphenyl)-*N*-(prop-2-yn-1-yl)acetamide 105

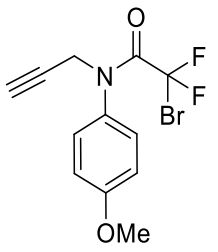

To a solution of 4-methoxyaniline (2.48 g, 20.0 mmol) and K_2CO_3 (2.76 g, 20.0 mmol) in DMF (28 mL) was added propargyl bromide (2.45 mL, 22.0 mmol of an 80% w/w solution in toluene) dropwise over 10 minutes. The mixture was stirred at room temperature for 18 hours. The

reaction mixture was poured into water (50 mL) and extracted with ethyl acetate (3 × 40 mL). The combined organics were washed with water (4 × 40 mL) then dried over magnesium sulfate and concentrated. The resultant residue was purified by flash column chromatography (SiO_2, eluting with 95:5 petroleum ether/ethyl acetate) to give 4-methoxy-*N*-(prop-2-yn-1-yl)aniline (1.57 g, 23.3 mol% purity) which was then dissolved in dichloromethane (2.3 mL) before a solution of Et_3N (640 µL, 4.56 mmol) in dichloromethane (2.3 mL) was added. A solution of bromodifluoroacetyl chloride (485 mg, 2.51 mmol) in dichloromethane (2.3 mL) was then added at 0 °C dropwise over 5 minutes under Ar and the reaction was stirred at room temperature for 16 hours. Dichloromethane (20 mL) and K_2CO_3 (20 mL of a sat. aq. solution) were added and the mixture was extracted with dichloromethane (2 × 20 mL). The organic fraction was washed with HCl (20 mL of a 1 N aq. solution) and brine (20 mL of a sat. aq. solution) and then dried over magnesium sulfate and concentrated. The resultant residue was purified by flash column chromatography (SiO_2, eluting with 0-10% ethyl acetate in petroleum ether) to give **105** (577 mg, 1.81 mmol, 9% yield) as a yellow oil.

R_f (95:5 petroleum ether/ethyl acetate) = 0.20; **ν_{max}** (thin film)/cm^{-1} 3296, 2965, 2937, 2840, 1688, 1509; **δ_H** (400 MHz, $CDCl_3$) 7.33 – 7.27 (m, 2H, Ar*H*), 6.95 – 6.90 (m, 2H, Ar*H*), 4.46 (d, *J* = 2.5 Hz, 2H, NCH_2), 3.84 (s, 3H, OCH_3), 2.30 (t, *J* = 2.5 Hz, 1H, C*H*, alkyne); **δ_C** (101 MHz, $CDCl_3$) 160.2 (Ar*C*(OMe)), 159.1 (t, *J* = 26.3 Hz, *C*=O), 131.6 (Ar*C*q), 130.1 (Ar*C*H), 114.4 (Ar*C*H), 111.3 (t, *J* = 317.2 Hz, *C*F_2Br), 77.3 (*C*q, alkyne) 73.9 (*C*H, alkyne), 55.6 (OCH_3), 42.2 (NCH_2); **δ_F** (376 MHz, $CDCl_3$) –52.29; **HRMS** (ESI) m/z: $[M+H]^+$ calcd for $C_{12}H_{10}{}^{79}BrF_2NO_2$ 317.9936; found 317.9937 (+0.50 ppm).

2-Bromo-2,2-difluoro-*N*-methyl-*N*-(prop-2-yn-1-yl)acetamide 106

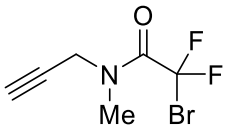

To a 0 °C suspension of NaH (120 mg, 3.00 mmol of a 60% dispersion in mineral oil) in DMF (15 mL) was added 2-bromo-2,2-difluoro-*N*-(prop-2-yn-1-yl)acetamide **100** (633 mg, 3.00 mmol) in DMF (15 mL) dropwise over 10 minutes. The mixture was stirred at 0 °C for 30

minutes before iodomethane (240 µL, 3.90 mmol) was added dropwise over 5 minutes. The reaction mixture was stirred at room temperature for 22 hours after which diethyl ether (20 mL), water (30 mL) and brine (10 mL of a sat. aq. solution) were added and the mixture was extracted with diethyl ether (2 × 20 mL). The combined organics were dried over magnesium sulfate and concentrated. The resulting residue was purified by flash column chromatography (SiO_2, eluting with 90:10 petroleum ether/ethyl acetate) to give **106** (549 mg, 2.43 mmol, 81% yield) as a pale yellow oil.

R_f (90:10 petroleum ether: ethyl acetate) = 0.40; **ν_{max}** (thin film)/cm^{-1} 3303, 3271, 2980, 2941, 2872, 1681; **δ_H** (400 MHz, $CDCl_3$) 4.27 (d, *J* = 2.5 Hz, 2H, NC*H*$_2$), 3.26 (s, 3H, NC*H*$_3$), 2.32 (t, *J* = 2.5 Hz, 1H, C*H*, alkyne) (data listed for major rotamer); **δ_C** (101 MHz, $CDCl_3$) 159.1 (t, *J* = 27.0 Hz, *C*=O), 110.9 (t, *J* = 314.5 Hz, *C*F_2Br), 76.7 (*C*q, alkyne), 73.6 (*C*H, alkyne), 38.8 (N*C*H_2), 35.4 (t, *J* = 4.7 Hz, N*C*H_3), (data listed for major rotamer); **δ_F** (376 MHz, $CDCl_3$) –54.90 (data listed for major rotamer); **HRMS** (ESI) m/z: $[M+H]^+$ calcd for $C_6H_6{}^{79}BrF_2NO$ 225.9674; found 225.9669 (+2.20 ppm).

2-Bromo-*N*-(but-3-en-1-yl)-2,2-difluoroacetamide 107

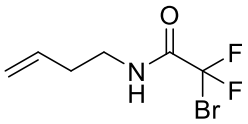

3-Buten-1-amine (1.70 mL, 23.0 mmol) was subjected to General Procedure 1 to give **107** as a colourless oil (956 mg, 4.19 mmol, 84% yield).

ν_{max} (thin film)/cm^{-1} 3303, 3082, 2983, 2946, 1698, 1540; **δ_H** (400 MHz, $CDCl_3$) 6.36 (s, 1H, N*H*), 5.85 – 5.69 (m, 1H, H_2C=C*H*), 5.18 – 5.15 (m, 1H, *H*$_2$C=CH), 5.14 – 5.12 (m, 1H, *H*$_2$C=CH), 3.44 (m, 2H, NHC*H*$_2$), 2.35 (app ddt, *J* = 13.5, 6.8, 1.3 Hz, 2H, NCH$_2$C*H*$_2$); **δ_C** (101 MHz, $CDCl_3$) 160.2 (t, *J* = 27.3 Hz, *C*=O), 134.1 (H_2C=*C*H), 118.5 (H_2*C*=CH), 111.9 (t, *J* = 315.9 Hz, *C*F_2Br), 39.1 (NH*C*H_2), 33.1 (NHCH$_2$*C*H_2); **δ_F** (376 MHz, $CDCl_3$) –60.53; **HRMS** (ESI) m/z: $[M+Na]^+$ calcd for $C_6H_8{}^{79}BrF_2NO$ 249.9650; found 249.9642 (+3.10 ppm).

_N_-Benzyl-2-bromo-_N_-(but-3-en-1-yl)-2,2-difluoroacetamide 108

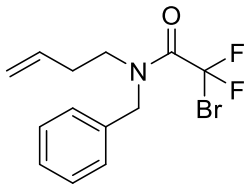

To a 0 °C suspension of NaH (84.0 mg, 2.10 mmol of a 60% dispersion in mineral oil) in DMF (5 mL) was added 2-bromo-*N*-(but-3-en-1-yl)-2,2-difluoroacetamide **107** (400 mg, 1.75 mmol) in DMF (5 mL) dropwise over 5 minutes. The mixture was stirred at 0 °C for 30 minutes before benzyl bromide (220 µL, 1.84 mmol) was added dropwise over 5 minutes. The reaction mixture was stirred at room temperature for 22 hours after which diethyl ether (20 mL), water (30 mL) and brine (10 mL of a sat. aq. solution) were added and the mixture was extracted with diethyl ether (2 × 20 mL). The combined organics were dried over magnesium sulfate and concentrated. The resulting residue was purified by flash column chromatography (SiO_2, eluting with 0-5% ethyl acetate in petroleum ether). The mixed fractions were purified again by flash column chromatography (SiO_2, eluting with 0-5% ethyl acetate in petroleum ether). The residues were combined to give **108** (431 mg, 1.36 mmol, 77% yield) as a pale yellow oil.

R_f (90:10 petroleum ether/ethyl acetate) = 0.46; **ν_{max}** (thin film)/cm^{-1} 3067, 3032, 2980, 2941, 1678; **δ_H** (400 MHz, $CDCl_3$) 7.42 – 7.19 (m, 10H, Ar*H*), 5.80 – 5.65 (m, 2H, *H*C=CH_2), 5.14 – 5.03 (m, 4H, HC=C*H*$_2$), 4.73 (s, 2H, NC*H*$_2$Ar), 4.68 (s, 2H, NC*H*$_2$Ar), 3.47 (t, *J* = 7.4 Hz, 2H, NC*H*$_2$), 3.39 (t, *J* = 7.4 Hz, 2H, NC*H*$_2$), 2.44 – 2.28 (m, 4H, NCH_2CH_2) (data listed for both rotamers); **δ_C** (101 MHz, $CDCl_3$) 159.9 (t, *J* = 26.4 Hz, *C*=O), 159.6 (t, *J* = 26.4 Hz, *C*=O), 135.7 (Ar*C*q), 135.1 (Ar*C*q), 134.4 (H*C*=CH_2), 133.6 (H*C*=CH_2), 129.1 (Ar*C*H), 129.0 (Ar*C*H), 128.2 (Ar*C*H), 128.1 (Ar*C*H), 128.0 (Ar*C*H), 127.3 (Ar*C*H), 118.1 (HC=*C*H_2), 117.8 (HC=*C*H_2), 111.3 (t, *J* = 315.0 Hz, *C*F_2Br), 111.1 (t, *J* = 315.0 Hz, *C*F_2Br), 52.0 (t, *J* = 3.9 Hz, N*C*H_2Ar), 50.0 (N*C*H_2Ar), 47.0 (t, *J* = 3.5 Hz, N*C*H_2), 46.3 (N*C*H_2), 32.7 (NCH_2CH_2), 31.0 (NCH_2CH_2) (data listed for both rotamers); **δ_F** (376 MHz, $CDCl_3$) –53.67, –54.02 (data listed for both rotamers); **HRMS** (ESI) m/z: $[M+H]^+$ calcd for $C_{13}H_{14}{}^{79}BrF_2NO$ 318.0300; found 318.0301 (+0.40 ppm).

2-Bromo-2,2-difluoro-*N*-(4-methoxybenzyl)-*N*-(prop-2-yn-1-yl)acetamide 109

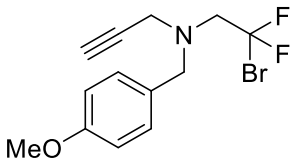

To a 0 °C suspension of NaH (227 mg, 5.69 mmol of a 60% dispersion in mineral oil) in DMF (14 mL) was added 2-bromo-2,2-difluoro-*N*-(prop-2-yn-1-yl)acetamide **100** (1.00 g, 4.74 mmol) in DMF (14 mL) dropwise over 5 minutes. The mixture was stirred at 0 °C for 30 minutes before 4-methoxybenzyl chloride (770 µL, 5.69 mmol) was added dropwise over 5 minutes. The reaction mixture was stirred at room temperature for 21 hours after which diethyl ether (40 mL), water (50 mL) and brine (15 mL of a sat. aq. solution) were added and the mixture was extracted with diethyl ether (2 × 40 mL). The combined organics were dried over magnesium sulfate and concentrated. The resulting residue was purified by flash column chromatography (SiO_2, eluting with 0-10% ethyl acetate in petroleum ether). The mixed fractions were purified again by flash column chromatography (SiO_2, eluting with 0-10% ethyl acetate in pentane). The residues were combined to give **109** (759 mg, 2.29 mmol, 48% yield) as a pale yellow oil.

R_f (90:10 petroleum ether/ethyl acetate) = 0.45; **ν_{max}** (thin film)/cm^{-1} 3288, 3002, 2958, 2936, 2915, 2838, 1682, 1612; **δ_H** (400 MHz, $CDCl_3$) 7.26 – 7.20 (m, 4H, Ar*H*), 6.93 – 6.85 (m, 4H, Ar*H*), 4.78 (s, 2H, NCH_2Ar), 4.72 (s, 2H, NCH_2Ar), 4.13 (d, *J* = 2.5 Hz, 2H, NCH_2), 4.09 (d, *J* = 2.5 Hz, 2H, NCH_2), 3.81 (s, 3H, OCH_3), 3.81 (s, 3H, OCH_3), 2.36 (t, *J* = 2.5 Hz, 1H, C*H*, alkyne), 2.29 (t, *J* = 2.5 Hz, 1H, C*H*, alkyne) (data listed for both rotamers); **δ_C** (101 MHz, $CDCl_3$) 159.8 (d, *J* = 12.2 Hz, *C*=O), 159.0 (t, *J* = 26.9 Hz, *C*=O), 130.1 (Ar*C*H), 129.3 (Ar*C*H), 126.8 (Ar*C*q), 125.8 (Ar*C*q), 114.5 (Ar*C*H), 114.4 (Ar*C*H), 110.9 (t, *J* = 315.2 Hz, *C*F_2Br), 110.8 (t, *J* = 315.2 Hz, *C*F_2Br), 73.7 (*C*H, alkyne), 73.3 (*C*q, alkyne), 55.4 (O*C*H_3), 55.4 (O*C*H_3), 50.2 (t, *J* = 3.7 Hz, N*C*H_2), 48.6 (N*C*H_2), 36.6 (t, *J* = 4.7 Hz, N*C*H_2), 34.8 (N*C*H_2) (data listed for both rotamers); **δ_F** (376 MHz, $CDCl_3$) –53.70, –54.33 (data listed for both rotamers); **HRMS** (ESI) m/z: $[M+H]^+$ calcd for $C_{13}H_{12}{}^{79}BrF_2NO_2$ 332.0092; found 332.0088 (+1.30 ppm).

4.4.6 Cyclised Amides

1-Benzyl-3,3-difluoro-4-methylpyrrolidin-2-one 72

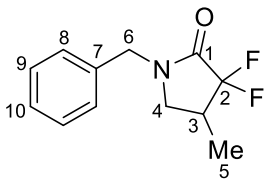

N-Allyl-*N*-benzyl-2-bromo-2,2-difluoroacetamide **71** (75.1 mg, 250 µmol) was subjected to General Procedure 4, stirring at room temperature for 2 hours. The resultant residue after concentration was purified by flash column chromatography (SiO_2, eluting with 80:20 petroleum ether/ethyl acetate) to give **72** (30.9 mg, 137 µmol, 56% yield) as a yellow oil.

R_f (80:20 petroleum ether/ethyl acetate) = 0.27; **ν_{max}** (thin film)/cm^{-1} 3032, 2925, 1718, 1453; **δ_H** (400 MHz, $CDCl_3$) 7.40 – 7.29 (m, 3H, Ar*H*), 7.25 – 7.21 (m, 2H, Ar*H*), 4.52 (s, 2H, *H*-6), 3.35 (ddd, *J* = 9.8, 7.9, 1.7 Hz, 1H, *H*-4), 2.96 – 2.81 (m, 1H, *H*-4), 2.71 – 2.43 (m, 1H, *H*-3), 1.16 (dd, *J* = 7.0, 1.7 Hz, 3H, *H*-5); **δ_C** (101 MHz, $CDCl_3$) 163.8 (dd, *J* = 31.2, 31.2, *C*-1), 134.7 (*C*-7), 129.1 (Ar*C*H), 128.4 (Ar*C*H), 128.3 (Ar*C*H), 118.3 (dd, *J* = 252.1, 252.1, *C*-2), 48.3 (d, *J* = 6.1, *C*-4), 47.3 (*C*-6), 35.2 (dd, *J* = 22.0, 22.0, *C*-3), 10.2 (d, *J* = 8.7, *C*-5); **δ_F** (376 MHz, $CDCl_3$) –111.70 (d, *J* = 266.3 Hz), –119.68 (d, *J* = 266.1 Hz); **HRMS** (ESI) m/z: $[M+H]^+$ calcd for $C_{12}H_{14}F_2NO$ 226.1038; found 226.1043 (+2.60 ppm).

1-Benzyl-3,3-difluoro-4-methylenepyrrolidin-2-one 73

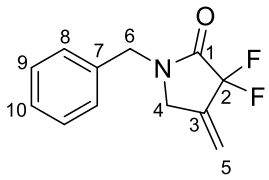

N-Benzyl-2-bromo-2,2-difluoro-*N*-(prop-2-yn-1-yl)acetamide **101** (75.5 mg, 250 µmol) was subjected to General Procedure 4, stirring at room temperature for 2.5 hours. The resultant residue after concentration was purified by flash column chromatography (SiO_2, eluting with

80:20 petroleum ether/ethyl acetate) to give **73** (29.6 mg, 133 µmol, 53% yield) as a yellow solid.

R_f (80:20 petroleum ether/ethyl acetate) = 0.23; **m.p.** 73–76 °C; **ν_{max}** (thin film)/cm^{-1} 3065, 3033, 2927, 2854, 1711; **δ_H** (400 MHz, $CDCl_3$) 7.40 – 7.30 (m, 3H, Ar*H*), 7.28 – 7.23 (m, 2H, Ar*H*), 5.95 (ttd, *J* = 3.3, 2.2, 1.0 Hz, 1H, *H*-5), 5.57 (ttd, *J* = 3.3, 2.2, 1.0 Hz, 1H, *H*-5), 4.59 (s, 2H, *H*-6), 3.88 (t, *J* = 2.2 Hz, 2H, *H*-4); **δ_C** (101 MHz, $CDCl_3$) 163.2 (t, *J* = 30.2 Hz, *C*-1), 134.3 (Ar*C*q), 133.6 (t, *J* = 20.0 Hz, *C*-3), 129.2 (Ar*C*H), 128.6 (Ar*C*H), 128.5 (Ar*C*H), 118.1 (t, *J* = 2.8 Hz, *C*-5), 111.2 (t, *J* = 247.2 Hz, *C*-2), 47.3 (*C*-6), 46.7 (t, *J* = 2.5 Hz, *C*-4); **δ_F** (376 MHz, $CDCl_3$) –103.52; **HRMS** (ESI) m/z: $[M+H]^+$ calcd for $C_{12}H_{14}F_2NO$ 226.1038; found 226.1043 (+2.60 ppm).

Data are consistent with the literature.[33]

3,3-Difluoro-4-methylene-1-(prop-2-yn-1-yl)pyrrolidin-2-one 74

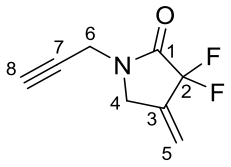

2-Bromo-2,2-difluoro-*N*,*N*-di(prop-2-yn-1-yl)acetamide **102** (62.1 mg, 250 µmol) was subjected to General Procedure 4, stirring at room temperature for 3 hours. The resultant residue after concentration was purified by flash column chromatography (SiO_2, eluting with 80:20 petroleum ether/ethyl acetate) to give **74** (37.2 mg, 217 µmol, 88% yield) as a yellow oil.

R_f (80:20 petroleum ether: ethyl acetate) = 0.20; **ν_{max}** (thin film)/cm^{-1} 3302, 3259, 2924, 2854, 1720; **δ_H** (400 MHz, $CDCl_3$) 6.00 – 5.95 (m, 1H, *H*-5), 5.71 – 5.65 (m, 1H, *H*-5), 4.25 – 4.23 (m, 2H, *H*-6), 4.15 – 4.13 (m, 2H, *H*-4), 2.34 (t, *J* = 2.6 Hz, 1H, *H*-8); **δ_C** (101 MHz, $CDCl_3$) 162.5 (t, *J* = 30.6 Hz, *C*-1), 133.2 (t, *J* = 20.0 Hz, *C*-3), 118.5 (t, *J* = 2.9 Hz, *C*-5), 110.9 (t, *J* = 247.5 Hz, *C*-2), 75.5 (*C*-7), 74.2 (*C*-8), 46.5 (t, *J* = 2.4 Hz, *C*-4), 32.6 (*C*-6); **δ_F** (376 MHz, $CDCl_3$) –103.54; **HRMS** (ESI) m/z: $[M+H]^+$ calcd for $C_8H_7F_2NO$ 172.0568; found 172.0569 (+0.40 ppm).

1-Benzyl-3,3-difluoro-4-methylenepiperidin-2-one 75

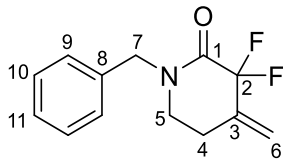

N-Benzyl-2-bromo-*N*-(but-3-yn-1-yl)-2,2-difluoroacetamide **103** (79.0 mg, 250 µmol) was subjected to General Procedure 4, stirring at room temperature for 22 hours. The resultant residue after concentration was purified by flash column chromatography (SiO_2, eluting with 85:15 petroleum ether/ethyl acetate) to give **75** (30.0 mg, 126 µmol, 51% yield) as a pale yellow oil.

R_f (80:20 petroleum ether: ethyl acetate) = 0.24; **ν_{max}** (thin film)/cm^{-1} 3088, 3064, 3032, 2926, 2872, 1679; **δ_H** (500 MHz, $CDCl_3$) 7.37 – 7.24 (m, 5H, Ar*H*), 5.72 – 5.64 (m, 1H, *H*-6), 5.35 (app t, *J* = 1.6 Hz, 1H, *H*-6), 4.63 (s, 2H, *H*-7), 3.29 (t, *J* = 6.2 Hz, 2H, *H*-5), 2.64 (tt, *J* = 6.3, 1.3 Hz, 2H, *H*-4); **δ_C** (126 MHz, $CDCl_3$) 162.1 (t, *J* = 30.4 Hz, *C*-1), 136.7 (t, *J* = 20.0 Hz, *C*-3), 135.7 (*C*-8), 129.0 (Ar*C*H), 128.4 (Ar*C*H), 128.1 (Ar*C*H), 115.9 (t, *J* = 6.8 Hz, *C*-6), 109.5 (t, *J* = 244.2 Hz, *C*-2), 50.7 (*C*-7), 45.9 (*C*-5), 28.3 (t, *J* = 2.6 Hz, *C*-4); **δ_F** (376 MHz, $CDCl_3$) -105.17; **HRMS** (ESI) m/z: $[M+H]^+$ calcd for $C_{13}H_{13}F_2NO$ 238.1038; found 238.1037 (+0.30 ppm).

1-Allyl-3,3-difluoro-4-methylpyrrolidin-2-one 76

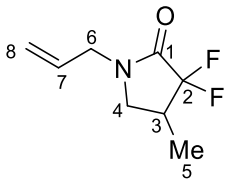

N,N-Diallyl-2-bromo-2,2-difluoroacetamide **104** (31.8 mg, 125 µmol) was subjected to General Procedure 4, stirring at room temperature for 4.5 hours. The resultant residue after concentration was purified by flash column chromatography (SiO_2, eluting with 80:20 petroleum ether/ethyl acetate) to give **76** (10.1 mg, 57.7 µmol, 46% yield) as a yellow oil.

R_f (80:20 petroleum ether/ethyl acetate) = 0.23; **ν_{max}** (thin film)/cm^{-1} 2958, 1721, 1492, 1457; **δ_H** (400 MHz, $CDCl_3$) 5.72 (m, 1H, *H*-7), 5.37 – 5.12 (2H, m, *H*-8), 3.96 (d, 2H, *J* = 6.2 Hz, *H*-6), 3.46 (ddd, 1H, *J* = 10.0, 7.9, 1.8 Hz, *H*-4), 3.09 – 2.90 (1H, m, *H*-4), 2.61 (1H, m, *H*-3), 1.21 (dd, 3H, *J* = 7.0, 1.8 Hz, *H*-5); **δ_C** (101 MHz, $CDCl_3$) 163.6 (dd, *J* = 31.2, 31.2 Hz, *C*-1), 130.8 (*C*-8), 119.6 (*C*-7), 118.2 (dd, *J* = 252.2 Hz, 252.2, *C*-2), 48.5 (d, *J* = 6.4 Hz, *C*-4), 46.0 (*C*-6), 35.3 (dd, *J* = 22.1, 22.1 Hz, *C*-3), 10.4 (d, *J* = 8.7 Hz, *C*-5); **δ_F** (376 MHz, $CDCl_3$) –111.54 (d, *J* = 266.3 Hz), –119.59 (d, *J* = 266.3 Hz); **HRMS** (ESI) m/z: $[M+H]^+$ calcd for $C_8H_{12}F_2NO$ 176.0881; found 176.0890 (+4.70 ppm).

3,3-Difluoro-1-(4-methoxyphenyl)-4-methylenepyrrolidin-2-one 77

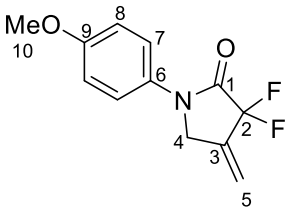

2-Bromo-2,2-difluoro-*N*-(4-methoxyphenyl)-*N*-(prop-2-yn-1-yl)acetamide **105** (80.2 mg, 250 µmol) was subjected to General Procedure 4, stirring at room temperature for 19 hours. The resultant residue after concentration was purified by flash column chromatography (SiO_2, eluting with 80:20 petroleum ether/ethyl acetate) to give **77** (38.2 mg, 160 µmol, 64% yield) as a yellow/brown solid.

R_f (80:20 petroleum ether: ethyl acetate) = 0.21; **m.p.** 111–114 °C (literature m.p 120–121 °C); **ν_{max}** (thin film)/cm^{-1} 3119, 2925, 2851, 1709, 1514; **δ_H** (400 MHz, $CDCl_3$) 7.62 – 7.58 (m, 2H, Ar*H*), 6.97 – 6.93 (m, 2H, Ar*H*), 6.07 – 6.03 (m, 1H, *H*-5), 5.76 – 5.72 (m, 1H, *H*-5), 4.45 (t, *J* = 2.2 Hz, 2H, *H*-4), 3.82 (s, 3H, *H*-10); **δ_C** (101 MHz, $CDCl_3$) 161.8 (t, *J* = 30.6 Hz, *C*-1), 158.0 (*C*-9), 133.0 (t, *J* = 20.0 Hz, *C*-3) 130.7 (*C*-5), 122.0 (Ar*C*H), 118.3 (t, *J* = 2.8 Hz, *C*-6), 114.6 (Ar*C*H), 111.1 (t, *J* = 246.3 Hz, *C*-2), 55.6 (*C*-10), 48.9 (t, *J* = 2.3 Hz, *C*-4); **δ_F** (376 MHz, $CDCl_3$) –102.81; **HRMS** (ESI) m/z: $[M+Na]^+$ calcd for $C_{12}H_{11}F_2NO_2$ 262.0650; found 262.0653 (+1.20 ppm).

Data are consistent with the literature.[102]

3,3-Difluoro-1-methyl-4-methylenepyrrolidin-2-one 78

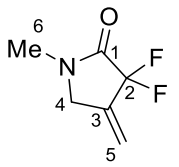

2-Bromo-2,2-difluoro-*N*-methyl-*N*-(prop-2-yn-1-yl)acetamide **106** (56.1 mg, 250 µmol) was subjected to General Procedure 4, stirring at room temperature for 5 hours. The resultant residue after concentration was purified by flash column chromatography (SiO_2, eluting with 30-50% ethyl acetate in petroleum ether) to give **78** (17.3 mg, 118 µmol, 47% yield) as a yellow oil.

R_f (50:50 petroleum ether: ethyl acetate) = 0.22; **ν_{max}** (thin film)/cm^{-1} 3236, 2971, 2932, 2874, 1719, 1640; **δ_H** (400 MHz, $CDCl_3$) 5.98 – 5.93 (m, 1H, *H*-5), 5.65 – 5.62 (m, 1H, *H*-5), 4.02 (t, *J* = 2.1 Hz, 2H, *H*-4), 3.00 (s, 3H, *H*-6); **δ_C** (101 MHz, $CDCl_3$) 163.2 (t, *J* = 30.3 Hz, *C*-1), 133.6 (t, *J* = 20.1 Hz, *C*-3), 117.9 (t, *J* = 2.8 Hz, *C*-5), 110.9 (t, *J* = 245.8 Hz, *C*-2), 49.4 (t, *J* = 2.6 Hz, *C*-4), 30.3 (*C*-6); **δ_F** (376 MHz, $CDCl_3$) –103.64; **HRMS** (ESI) m/z: $[M+H]^+$ calcd for $C_6H_7F_2NO$ 148.0568; found 148.0565 (+2.70 ppm).

1-Benzyl-3,3-difluoro-4-methylpiperidin-2-one 79

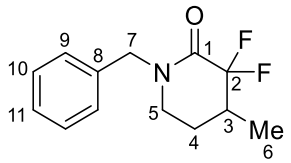

N-Benzyl-2-bromo-*N*-(but-3-en-1-yl)-2,2-difluoroacetamide **108** (79.5 mg, 250 µmol) was subjected to General Procedure 4, stirring at room temperature for 3 hours. The resultant residue after concentration was purified by flash column chromatography (SiO_2, eluting with 20-50% ethyl acetate in petroleum ether) to give **79** (13.8 mg, 57.7 µmol, 23% yield) as a yellow oil.

R_f (80:20 petroleum ether: ethyl acetate) = 0.19; **ν_{max}** (thin film)/cm^{-1} 3064, 3031, 2925, 2873, 1672, 1495; **δ_H** (400 MHz, $CDCl_3$) 7.41 – 7.24 (m, 5H, Ar*H*), 4.73 (d, *J* = 14.5 Hz, 1H, *H*-7), 4.53 (d, *J* = 14.5 Hz, 1H, *H*-7), 3.35 – 3.21 (m, 2H, *H*-5), 2.42 – 2.22 (m, 1H, *H*-3), 1.98 – 1.78 (m, 2H, *H*-4), 1.18 (d, *J* = 6.7 Hz, 3H, *H*-6); **δ_C** (101 MHz, $CDCl_3$) 162.0 (dd, *J* = 30.2, 30.2 Hz, *C*-1), 135.7 (Ar*C*q), 128.9 (Ar*C*H), 128.3 (Ar*C*H), 127.9 (Ar*C*H), 113. 7 (dd, *J* = 246.0, 246.0 Hz, *C*-2), 50.4 (*C*-7), 45.3 (*C*-5), 36.0 (dd, *J* = 21.8, 21.8 Hz, *C*-3), 26.0 (dd, *J* = 7.2, 1.8 Hz, *C*-4), 11.7 (dd, *J* = 6.2, 2.3 Hz, *C*-6); **δ_F** (376 MHz, $CDCl_3$) –108.62 (d, *J* = 278.7 Hz), –113.71 (d, *J* = 278.8 Hz); **HRMS** (ESI) m/z: $[M+Na]^+$ calcd for $C_{13}H_{15}F_2NO$ 262.1014; found 262.1015 (+0.50 ppm).

3,3-Difluoro-1-(4-methoxybenzyl)-4-methylenepyrrolidin-2-one 80

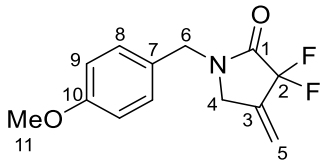

2-Bromo-2,2-difluoro-*N*-(4-methoxybenzyl)-*N*-(prop-2-yn-1-yl)acetamide **109** (83.0 mg, 250 µmol) was subjected to General Procedure 4, stirring at room temperature for 5 hours. The resultant residue after concentration was purified by flash column chromatography (SiO_2, eluting with 80:20 petroleum ether/ethyl acetate) to give **80** (30.8 mg, 122 µmol, 49% yield) as a yellow/brown solid.

R_f (80:20 petroleum ether/ethyl acetate) = 0.13; **m.p.** 83–86 °C; **ν_{max}** (thin film)/cm^{-1} 3302, 3011, 2927, 2840, 1707; **δ_H** (400 MHz, $CDCl_3$) 7.21 – 7.14 (m, 2H, Ar*H*), 6.92 – 6.84 (m, 2H, Ar*H*), 5.97 – 5.90 (m, 1H, *H*-5), 5.59 – 5.52 (m, 1H, *H*-5), 4.51 (s, 2H, *H*-6), 3.85 (t, *J* = 2.2 Hz, 2H, *H*-4), 3.79 (s, 3H, *H*-11); **δ_C** (101 MHz, $CDCl_3$) 163.0 (t, *J* = 30.2 Hz, *C*-1), 159.8 (*C-10*), 133.6 (t, *J* = 20.1 Hz, *C*-3), 123.0 (Ar*C*H), 126.3 (*C-7*), 118.0 (t, *J* = 2.8 Hz, *C-5*), 114.5 (ArCH), 111.3 (t, *J* = 247.2 Hz, *C-2*), 55.4 (*C*-11), 46.7 (*C-6*), 46.5 (t, *J* = 2.5 Hz, *C-4*); **δ_F** (376 MHz, $CDCl_3$) –103.49; **HRMS** (ESI) m/z: $[M+H]^+$ calcd for $C_{13}H_{14}F_2NO_2$ 254.0987; found 254.0985 (+1.00 ppm).

4.4.7 Synthesis of Photocatalysts

***fac*-Ir(ppy)$_3$ 110**

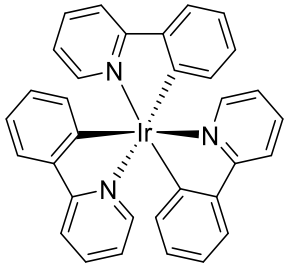

$IrCl_3.3H_2O$ (210 mg, 597 µmol) and 2-phenylpyridine (260 µL, 1.79 mmol) were suspended in 2-ethoxyethanol (12 mL) and water (4.2 mL). The mixture was heated at 150 °C for 7 hours. The precipitate was filtered and washed with ethanol (15 mL) and acetone (15 mL). The solid residue was dissolved in dichloromethane (30 mL), filtered and concentrated to give [μ-Cl Ir(ppy)$_2$]$_2$ as a yellow solid. To this solid was added potassium carbonate (309 mg, 2.34 mmol), 2-phenylpyridine (110 µL, 746 µmol) and glycerol (7.5 mL). The mixture was heated at 220 °C under Ar for 18 hours. The reaction was cooled to room temperature. Water (15 mL) was added and the precipitate was filtered and washed with methanol (15 mL), diethyl ether (15 mL) and hexane (15 mL). The solid residue was dissolved in dichloromethane (40 mL), filtered and concentrated to give a residue which was purified by flash column chromatography (SiO_2, eluting with dichloromethane) to give **110** (266 mg, 406 µmol, 68% yield) as a yellow solid.

ν_{max} (thin film)/cm^{-1} 3037, 2991, 2981, 2925, 2847, 1697, 1600, 1580, 1561; δ_H (400 MHz, DMSO-d$_6$) 8.13 (d, *J* = 8.2 Hz, 3H), 7.79 (t, *J* = 7.7 Hz, 3H), 7.75 (d, *J* = 7.7 Hz, 3H), 7.48 (d, *J* = 5.3 Hz, 3H), 7.13 (t, *J* = 6.4 Hz, 3H), 6.83 – 6.76 (m, 3H), 6.83 - 6.76 (m, 6H); δ_C (101 MHz, DMSO-d$_6$) 165.6, 160.8, 146.8, 143.8, 136.9, 136.3, 129.1, 124.2, 122.8, 119.6, 119.1.

Data are consistent with the literature.[128]

4CzIPN 111

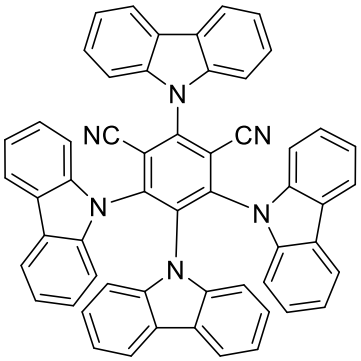

NaH (600 mg, 15.0 mmol of a 60% dispersion in mineral oil) was added portionwise to a stirred solution of carbazole (1.67 g, 10.0 mmol) in THF (40 mL) over 15 minutes under Ar. The mixture was stirred at room temperature for 30 minutes after which tetrafluoroisophthalonitrile (0.403 g, 2.00 mmol) was added and the mixture was stirred at room temperature for 20 hours. Water (2 mL) was added to the reaction mixture which was then concentrated under reduced pressure. The solid was filtered, washing with water (15 mL) and ethanol (15 mL). The resulting residue was purified by flash column chromatography (SiO_2, eluting with dichloromethane: petroleum ether 50:50). The resultant solid was triturated with ethanol to give **111** (1.25 g, 1.59 mmol, 79% yield) as a yellow solid.

$\mathbf{R_f}$ (50:50 DCM: petroleum ether) = 0.37; $\mathbf{\nu_{max}}$ (thin film)/cm^{-1} 3081, 3050, 3028, 2972, 2924; $\mathbf{\delta_H}$ (500 MHz, $CDCl_3$) 8.22 (dt, *J* = 7.7, 1.2 Hz, 2H), 7.76 – 7.65 (m, 8H), 7.49 (ddd, *J* = 8.2, 6.8, 1.4 Hz, 2H), 7.33 (dt, *J* = 7.7, 1.2 Hz, 2H), 7.24 – 7.19 (m, 4H), 7.13 – 7.03 (m, 8H), 6.87 – 6.78 (m, 4H), 6.63 (ddd, *J* = 8.2, 7.5, 1.2 Hz, 2H); $\mathbf{\delta_H}$ (400 MHz, DMSO) 8.37 (d, *J* = 7.7 Hz, 2H), 8.20 (d, *J* = 8.2 Hz, 2H), 7.87 (dd, *J* = 7.3, 1.5 Hz, 4H), 7.80 – 7.70 (m, 6H), 7.61 – 7.43 (m, 6H), 7.20 – 7.06 (m, 8H), 6.82 (t, *J* = 7.5 Hz, 2H), 6.71 (ddd, *J* = 8.2, 7.3, 1.5 Hz, 2H); $\mathbf{\delta_C}$ (126 MHz, $CDCl_3$) 145.4, 144.8, 140.1, 138.3, 137.1, 134.9, 127.1, 125.9, 125.1, 124.9, 124.7, 124.0, 122.5, 122.1, 121.5, 121.1, 120.6, 119.8, 116.5, 111.8, 110.1, 109.6, 109.6.

Data are consistent with the literature.[16,129]

4.5 Photoredox Set-up

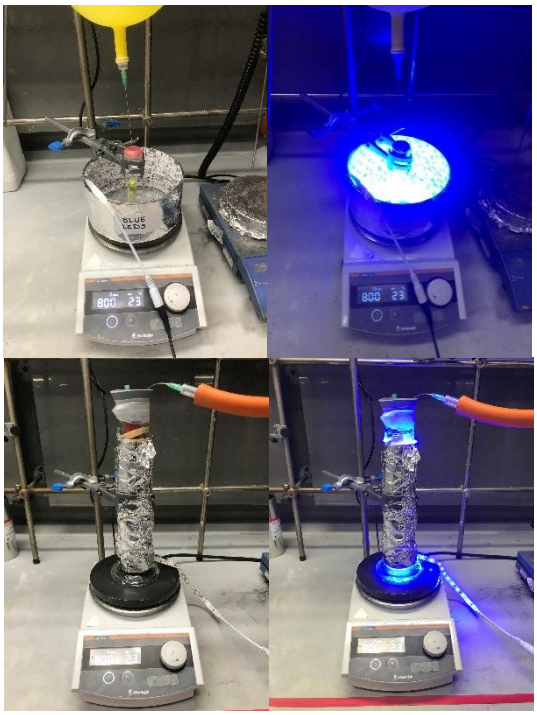

A culture tube placed inside a crystallising dish wrapped in LEDs and foil, or a 250 mL borosilicate glass measuring cylinder wrapped in blue LEDs and foil.

4.6 Computational Investigations

Amine cyclisation:

Quantum chemical calculations were carried out using the Macintosh version of Spartan 2018.[130] Equilibrium geometries and transition structures were confirmed by either the absence or presence of an imaginary frequency respectively. Starting points for equilibrium geometry calculations were obtained by performing a molecular mechanics equilibrium conformer search also implemented in Spartan 2018. The theoretical model chosen was wB97X-D/6-31G* (unrestricted) and Figure 2.3 summarises the relative free energies obtained with this method at 298 K *in vacuo*. Other theoretical models were explored for comparison and the M06-2X/6-31+G* model gave a barrier of 8.2 kcal/mol for the 5-*exo*-*dig* cyclisation – essentially the same as the less expensive wB97X-D/6-31G* method.

Amide cyclisation:

Quantum chemical calculations were carried out using the Windows version of Spartan 2008.[130] Equilibrium geometries and transition structures were confirmed by either the absence or presence of an imaginary frequency respectively. Starting points for equilibrium geometry calculations were obtained by performing a molecular mechanics equilibrium conformer search also implemented in Spartan 2008. The theoretical model chosen was B3LYP/6-31G* (unrestricted) and Figure 3.4 summarises the relative free energies obtained with this method at 298 K *in vacuo*. The energies are relative uncorrected electronic energies expressed in kcal/mol.

4.7 X-ray Crystallography

The structure is disordered over a mirror plane where the ring carbon atoms lie on the plane and the nitrogen and fluorine lie above it. For clarity only one structure from the mirror plane is depicted in Scheme 2.10.

Crystal data and structure refinement for 64:

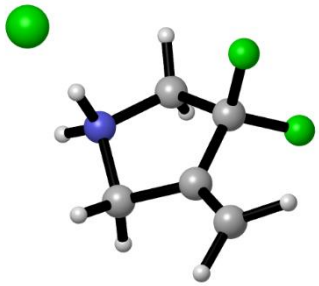

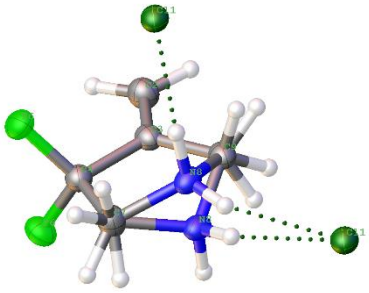

Empirical formula	$C_5H_8ClF_2N$
Formula weight	155.57
Temperature/K	120(2)
Crystal system	orthorhombic
Space group	Pnma
a/Å	10.0074(7)
b/Å	7.0673(5)
c/Å	9.5009(6)
α/°	90
β/°	90
γ/°	90
Volume/Å^3	671.95(8)
Z	4
ρ_{calc}g/cm^3	1.538
μ/mm^{-1}	4.681
F(000)	320.0
Crystal size/mm^3	0.24 × 0.04 × 0.023
Radiation	Cu Kα (λ = 1.54184)
2Θ range for data collection/°	12.848 to 145.26
Index ranges	-12 ≤ h ≤ 12, -7 ≤ k ≤ 8, -11 ≤ l ≤ 11
Reflections collected	4429
Independent reflections	714 [R_{int} = 0.0526, R_{sigma} = 0.0265]
Data/restraints/parameters	714/2/61
Goodness-of-fit on F^2	1.084
Final R indexes [I>=2σ (I)]	R_1 = 0.0318, wR_2 = 0.0811
Final R indexes [all data]	R_1 = 0.0331, wR_2 = 0.0819
Largest diff. peak/hole / e Å^{-3}	0.34/-0.26

References

(1) Nicewicz, D. A.; MacMillan, D. W. C. Merging Photoredox Catalysis with Organocatalysis: The Direct Asymmetric Alkylation of Aldehydes. *Science,* **2008**, *322* (5898), 77–80.

(2) Ischay, M. A.; Anzovino, M. E.; Du, J.; Yoon, T. P. Efficient Visible Light Photocatalysis of [2+2] Enone Cycloadditions. *J. Am. Chem. Soc.* **2008**, *130* (39), 12886–12887.

(3) Narayanam, J. M. R. R.; Tucker, J. W.; Stephenson, C. R. J. J. Electron-Transfer Photoredox Catalysis: Development of a Tin-Free Reductive Dehalogenation Reaction. *J. Am. Chem. Soc.* **2009**, *131* (25), 8756–8757.

(4) Kalyanasundaram, K.; Grätzel, M. Applications of Functionalized Transition Metal Complexes in Photonic and Optoelectronic Devices. *Coord. Chem. Rev.* **1998**, *177* (1), 347–414.

(5) Takeda, H.; Ishitani, O. Development of Efficient Photocatalytic Systems for CO_2 Reduction Using Mononuclear and Multinuclear Metal Complexes Based on Mechanistic Studies. *Coord. Chem. Rev.* **2010**, *254* (3), 346–354.

(6) Sumino, S.; Uno, M.; Fukuyama, T.; Ryu, I.; Matsuura, M.; Yamamoto, A.; Kishikawa, Y. Photoredox-Catalyzed Hydrodifluoroalkylation of Alkenes Using Difluorohaloalkyl Compounds and a Hantzsch Ester. *J. Org. Chem.* **2017**, *82* (10), 5469–5474.

(7) Nguyen, J. D.; D'Amato, E. M.; Narayanam, J. M. R. R.; Stephenson, C. R. J. J. Engaging Unactivated Alkyl, Alkenyl and Aryl Iodides in Visible-Light-Mediated Free Radical Reactions. *Nat. Chem.* **2012**, *4* (10), 854–859.

(8) Prier, C. K.; Rankic, D. A.; MacMillan, D. W. C. Visible Light Photoredox Catalysis with Transition Metal Complexes: Applications in Organic Synthesis. *Chem. Rev.* **2013**, *113* (7), 5322–5363.

(9) Romero, N. A.; Nicewicz, D. A. Organic Photoredox Catalysis. *Chem. Rev.* **2016**, *116* (17), 10075–10166.

(10) Graham, M. A.; Noonan, G.; Cherryman, J. H.; Douglas, J. J.; Gonzalez, M.; Jackson, L. V; Leslie, K.; Liu, Z.; McKinney, D.; Munday, R. H.; Parsons, C. D.; Whittaker, D. T. E.; Zhang, E.; Zhang, J. Development and Proof of Concept for a Large-Scale Photoredox Additive-Free Minisci Reaction. *Org. Process Res. Dev.* **2021**, *25* (1), 57–67.

(11) Hara, M.; Waraksa, C. C.; Lean, J. T.; Lewis, B. A.; Mallouk, T. E. Photocatalytic Water Oxidation in a Buffered Tris(2,2‘-Bipyridyl)Ruthenium Complex-Colloidal IrO2 System. *J. Phys. Chem. A* **2000**, *104* (22), 5275–5280.

(12) Orellana, G.; García-Fresnadillo, D. Environmental and Industrial Optosensing with Tailored Luminescent Ru(II) Polypyridyl Complexes BT - Optical Sensors: Industrial Environmental and Diagnostic Applications; Narayanaswamy, R., Wolfbeis, O. S., Eds.; Springer Berlin Heidelberg: Berlin, Heidelberg, 2004; pp 309–357.

(13) Campagna, S.; Puntoriero, F.; Nastasi, F.; Bergamini, G.; Balzani, V. Photochemistry and Photophysics of Coordination Compounds: Ruthenium BT - Photochemistry and Photophysics of Coordination Compounds I; Balzani, V., Campagna, S., Eds.; Springer Berlin Heidelberg: Berlin, Heidelberg, 2007; pp 117–214.

(14) Spiccia, L.; Deacon, G. B.; Kepert, C. M. Synthetic Routes to Homoleptic and Heteroleptic Ruthenium(II) Complexes Incorporating Bidentate Imine Ligands. *Coord. Chem. Rev.* **2004**, *248* (13), 1329–1341.

(15) Alkan-Zambada, M.; Hu, X. Cu Photoredox Catalysts Supported by a 4,6-Disubstituted 2,2′-Bipyridine Ligand: Application in Chlorotrifluoromethylation of Alkenes. *Organometallics* **2018**, *37* (21), 3928–3935.

(16) Luo, J.; Zhang, J. Donor–Acceptor Fluorophores for Visible-Light-Promoted Organic Synthesis: Photoredox/Ni Dual Catalytic C(Sp3)–C(Sp2) Cross-Coupling. *ACS Catal.*

2016, *6* (2), 873–877.

(17) Arias-Rotondo, D. M.; McCusker, J. K. The Photophysics of Photoredox Catalysis: A Roadmap for Catalyst Design. *Chem. Soc. Rev.* **2016**, *45* (21), 5803–5820.

(18) Neumann, M.; Füldner, S.; König, B.; Zeitler, K. Metal-Free, Cooperative Asymmetric Organophotoredox Catalysis with Visible Light. *Angew. Chem. Int. Ed.* **2011**, *50* (4), 951–954.

(19) Condie, A. G.; González-Gómez, J. C.; Stephenson, C. R. J. Visible-Light Photoredox Catalysis: Aza-Henry Reactions via C−H Functionalization. *J. Am. Chem. Soc.* **2010**, *132* (5), 1464–1465.

(20) Pan, Y.; Kee, C. W.; Chen, L.; Tan, C.-H. Dehydrogenative Coupling Reactions Catalysed by Rose Bengal Using Visible Light Irradiation. *Green Chem.* **2011**, *13* (10), 2682–2685.

(21) Pan, Y.; Wang, S.; Kee, C. W.; Dubuisson, E.; Yang, Y.; Loh, K. P.; Tan, C.-H. Graphene Oxide and Rose Bengal: Oxidative C–H Functionalisation of Tertiary Amines Using Visible Light. *Green Chem.* **2011**, *13* (12), 3341–3344.

(22) Liu, Q.; Li, Y.-N.; Zhang, H.-H.; Chen, B.; Tung, C.-H.; Wu, L.-Z. Reactivity and Mechanistic Insight into Visible-Light-Induced Aerobic Cross-Dehydrogenative Coupling Reaction by Organophotocatalysts. *Chem. Eur. J* **2012**, *18* (2), 620–627.

(23) McNally, A.; Prier, C. K.; MacMillan, D. W. C. Discovery of an α-Amino C–H Arylation Reaction Using the Strategy of Accelerated Serendipity. *Science,* **2011**, *334* (6059), 1114–1117.

(24) Musacchio, A. J.; Lainhart, B. C.; Zhang, X.; Naguib, S. G.; Sherwood, T. C.; Knowles, R. R. Catalytic Intermolecular Hydroaminations of Unactivated Olefins with Secondary Alkyl Amines. *Science,* **2017**, *355* (6326), 727–730.

(25) Bordwell, F. G.; Cheng, J.; Ji, G. Z.; Satish, A. V; Zhang, X. Bond Dissociation Energies

in DMSO Related to the Gas Phase Values. *J. Am. Chem. Soc.* **1991**, *113* (26), 9790–9795.

(26) Ganley, J. M.; Murray, P. R. D.; Knowles, R. R. Photocatalytic Generation of Aminium Radical Cations for C–N Bond Formation. *ACS Catal.* **2020**, *10* (20), 11712–11738.

(27) Baldwin, J. E. Rules for Ring Closure. *J. Chem. Soc. Chem. Commun.* **1976**, 18, 734–736.

(28) Beckwith, A. L. J.; Easton, C. J.; Serelis, A. K. Some Guidelines for Radical Reactions. *J. Chem. Soc. Chem. Commun.* **1980**, *11*, 482–483.

(29) Ghelfi, F.; Stevens, C. V.; Laureyn, I.; Van Meenen, E.; Rogge, T. M.; De Buyck, L.; Nikitin, K. V.; Grandi, R.; Libertini, E.; Pagnoni, U. M.; Schenetti, L. Synthesis of 5-Methoxylated 3-Pyrrolin-2-ones via the Rearrangement of Chlorinated Pyrrolidin-2-Ones. *Tetrahedron* **2003**, *59*, 1147–1157.

(30) Hiorns, R. Polymer Handbook, 4th Edn, Edited by J Brandup, EH Immergut and EA Grulke, Associate Editors A Abe and DR Bloch, John Wiley and Sons, New York, 1999. *Polym. Int.* **2000**, *49* (7), 807.

(31) Nagashima, H.; Isono, Y.; Iwamatsu, S. I. Copper-Catalyzed Cyclization of *N*-Allylhalodifluoroacetamides: An Efficient Synthesis of α,α-Difluorinated γ-Lactams. *J. Org. Chem.* **2001**, *66* (1), 315–319.

(32) Motoyama, Y.; Kamo, K.; Yuasa, A.; Nagashima, H. Catalytic Atom-Transfer Radical Cyclization by Copper/Bipyridine Species Encapsulated in Polysiloxane Gel. *Chem. Commun.* **2010**, *46*, 2256–2258.

(33) Uneyama, K.; Yanagiguchi, T.; Asai, H. Generation and Intramolecular Cyclization of Difluoroalkyl Radicals via Single Electron Transfer from the Benzeneselemolate Anion: Synthesis of α,α-Difluoro-γ-Lactams. *Tetrahedron Lett.* **1997**, *38* (44), 7763–7764.

(34) Kim, H.; Lee, C. Visible-Light-Induced Photocatalytic Reductive Transformations of

Organohalides. *Angew. Chem. Int. Ed.* **2012**, *51* (49), 12303–12306.

(35) Devery, J. J.; Nguyen, J. D.; Dai, C.; Stephenson, C. R. J. Light-Mediated Reductive Debromination of Unactivated Alkyl and Aryl Bromides. *ACS Catal.* **2016**, *6* (9), 5962–5967.

(36) Zhang, Z.; Tang, X.; Thomoson, C. S.; Dolbier, W. R. Photoredox-Catalyzed Intramolecular Aminodifluoromethylation of Unactivated Alkenes. *Org. Lett.* **2015**, *17* (14), 3528–3531.

(37) Musacchio, A. J.; Nguyen, L. Q.; Beard, G. H.; Knowles, R. R. Catalytic Olefin Hydroamination with Aminium Radical Cations: A Photoredox Method for Direct C–N Bond Formation. *J. Am. Chem. Soc.* **2014**, *136* (35), 12217–12220.

(38) Nguyen, T. M.; Nicewicz, D. A. Anti-Markovnikov Hydroamination of Alkenes Catalyzed by an Organic Photoredox System. *J. Am. Chem. Soc.* **2013**, *135* (26), 9588–9591.

(39) Nguyen, T. M.; Manohar, N.; Nicewicz, D. A. Anti-Markovnikov Hydroamination of Alkenes Catalyzed by a Two-Component Organic Photoredox System: Direct Access to Phenethylamine Derivatives. *Angew. Chem. Int. Ed.* **2014**, *53* (24), 6198–6201.

(40) Mei, H.; Han, J.; Fustero, S.; Medio-Simon, M.; Sedgwick, D. M.; Santi, C.; Ruzziconi, R.; Soloshonok, V. A. Fluorine-Containing Drugs Approved by the FDA in 2018. *Chem. Eur. J* **2019**, *25* (51), 11797–11819.

(41) de la Torre, B. G.; Albericio, F. The Pharmaceutical Industry in 2019. An Analysis of FDA Drug Approvals from the Perspective of Molecules. *Molecules* **2020**, *25* (3), 745–758.

(42) Meanwell, N. A. Fluorine and Fluorinated Motifs in the Design and Application of Bioisosteres for Drug Design. *J. Med. Chem.* **2018**, *61* (14), 5822–5880.

(43) Chernykh, A. V.; Melnykov, K. P.; Tolmacheva, N. A.; Kondratov, I. S.; Radchenko, D. S.; Daniliuc, C. G.; Volochnyuk, D. M.; Ryabukhin, S. V.; Kuchkovska, Y. O.;

Grygorenko, O. O. Last of the Gem-Difluorocycloalkanes: Synthesis and Characterization of 2,2-Difluorocyclobutyl-Substituted Building Blocks. *J. Org. Chem.* **2019**, *84* (13), 8487–8496.

(44) O'Hagan, D. Fluorine in Health Care: Organofluorine Containing Blockbuster Drugs. *J. Fluor. Chem.* **2010**, *131* (11), 1071–1081.

(45) Gillis, E. P.; Eastman, K. J.; Hill, M. D.; Donnelly, D. J.; Meanwell, N. A. Applications of Fluorine in Medicinal Chemistry. *J. Med. Chem.* **2015**, *58* (21), 8315–8359.

(46) Jeffries, B.; Wang, Z.; Felstead, H. R.; Le Questel, J. Y.; Scott, J. S.; Chiarparin, E.; Graton, J.; Linclau, B. Systematic Investigation of Lipophilicity Modulation by Aliphatic Fluorination Motifs. *J. Med. Chem.* **2020**, *63* (3), 1002–1031.

(47) Huchet, Q. A.; Kuhn, B.; Wagner, B.; Fischer, H.; Kansy, M.; Zimmerli, D.; Carreira, E. M.; Müller, K. On the Polarity of Partially Fluorinated Methyl Groups. *J. Fluor. Chem.* **2013**, *152*, 119–128.

(48) Morgenthaler, M.; Schweizer, E.; Hoffmann-Röder, A.; Benini, F.; Martin, R. E.; Jaeschke, G.; Wagner, B.; Fischer, H.; Bendels, S.; Zimmerli, D.; Schneider, J.; Diederich, F.; Kansy, M.; Müller, K. Predicting and Tuning Physicochemical Properties in Lead Optimization: Amine Basicities. *ChemMedChem* **2007**, *2* (8), 1100–1115.

(49) Shah, P.; Westwell, A. D. The Role of Fluorine in Medicinal Chemistry. *J. Enzyme Inhib. Med. Chem.* **2007**, *22* (5), 527–540.

(50) Rosenblum, S. B.; Huynh, T.; Afonso, A.; Davis, H. R.; Yumibe, N.; Clader, J. W.; Burnett, D. A. Discovery of 1-(4-Fluorophenyl)-(3R)-[3-(4-Fluorophenyl)-(3S)-Hydroxypropyl]-(4S)-(4-Hydroxyphenyl)-2-Azetidinone (SCH 58235): A Designed, Potent, Orally Active Inhibitor of Cholesterol Absorption. *J. Med. Chem.* **1998**, *41* (6), 973–980.

(51) Popovici-Muller, J.; Lemieux, R. M.; Artin, E.; Saunders, J. O.; Salituro, F. G.; Travins,

J.; Cianchetta, G.; Cai, Z.; Zhou, D.; Cui, D.; Chen, P.; Straley, K.; Tobin, E.; Wang, F.; David, M. D.; Penard-Lacronique, V.; Quivoron, C.; Saada, V.; De Botton, S.; Gross, S.; Dang, L.; Yang, H.; Utley, L.; Chen, Y.; Kim, H.; Jin, S.; Gu, Z.; Yao, G.; Luo, Z.; Lv, X.; Fang, C.; Yan, L.; Olaharski, A.; Silverman, L.; Biller, S.; Su, S. S. M.; Yen, K. Discovery of AG-120 (Ivosidenib): A First-in-Class Mutant IDH1 Inhibitor for the Treatment of IDH1 Mutant Cancers. *ACS Med. Chem. Lett.* **2018**, *9* (4), 300–305.

(52) Hu, X. G.; Thomas, D. S.; Griffith, R.; Hunter, L. Stereoselective Fluorination Alters the Geometry of a Cyclic Peptide: Exploration of Backbone-Fluorinated Analogues of Unguisin A. *Angew. Chem. Int. Ed.* **2014**, *53*, 6176–6179.

(53) Peddie, V.; Butcher, R. J.; Robinson, W. T.; Wilce, M. C. J.; Traore, D. A. K.; Abell, A. D. Synthesis and Conformation of Fluorinated β-Peptidic Compounds. *Chem. Eur. J* **2012**, *18* (21), 6655–6662.

(54) Olsen, J. A.; Banner, D. W.; Seiler, P.; Sander, U. O.; D'Arcy, A.; Stihle, M.; Müller, K.; Diederich, F. A Fluorine Scan of Thrombin Inhibitors to Map the Fluorophilicity/Fluorophobicity of an Enzyme Active Site: Evidence for C-F···C=O Interactions. *Angew. Chem. Int. Ed.* **2003**, *42* (22), 2507–2511.

(55) Jeschke, P. The Unique Role of Fluorine in the Design of Active Ingredients for Modern Crop Protection. *ChemBioChem* **2004**, *5* (5), 570–589.

(56) Abbate, F.; Casini, A.; Scozzafava, A.; Supuran, C. T. Carbonic Anhydrase Inhibitors: X-Ray Crystallographic Structure of the Adduct of Human Isozyme II with the Perfluorobenzoyl Analogue of Methazolamide. Implications for the Drug Design of Fluorinated Inhibitors. *J. Enzyme Inhib. Med. Chem.* **2003**, *18* (4), 303–308.

(57) Wang, J.; Sánchez-Roselló, M.; Aceña, J. L.; del Pozo, C.; Sorochinsky, A. E.; Fustero, S.; Soloshonok, V. A.; Liu, H. Fluorine in Pharmaceutical Industry: Fluorine-Containing Drugs Introduced to the Market in the Last Decade (2001–2011). *Chem. Rev.* **2014**, *114* (4), 2432–2506.

(58) Adler, P.; Teskey, C. J.; Kaiser, D.; Holy, M.; Sitte, H. H.; Maulide, N. α-Fluorination of Carbonyls with Nucleophilic Fluorine. *Nat. Chem.* **2019**, *11* (4), 329–334.

(59) Takebe, T.; Imai, R.; Ono, S. The Current Status of Drug Discovery and Development as Originated in United States Academia: The Influence of Industrial and Academic Collaboration on Drug Discovery and Development. *Clin. Transl. Sci.* **2018**, *11* (6), 597–606.

(60) Downes, T. D.; Jones, S. P.; Klein, H. F.; Wheldon, M. C.; Atobe, M.; Bond, P. S.; Firth, J. D.; Chan, N. S.; Waddelove, L.; Hubbard, R. E.; Blakemore, D. C.; De Fusco, C.; Roughley, S. D.; Vidler, L. R.; Whatton, M. A.; Woolford, A. J.-A.; Wrigley, G. L.; O'Brien, P. Design and Synthesis of 56 Shape-Diverse 3D Fragments. *Chem. Eur. J* **2020**, *26* (41), 8969–8975.

(61) Stepan, A. F.; Subramanyam, C.; Efremov, I. V.; Dutra, J. K.; O'Sullivan, T. J.; Dirico, K. J.; McDonald, W. S.; Won, A.; Dorff, P. H.; Nolan, C. E.; Becker, S. L.; Pustilnik, L. R.; Riddell, D. R.; Kauffman, G. W.; Kormos, B. L.; Zhang, L.; Lu, Y.; Capetta, S. H.; Green, M. E.; Karki, K.; Sibley, E.; Atchison, K. P.; Hallgren, A. J.; Oborski, C. E.; Robshaw, A. E.; Sneed, B.; O'Donnell, C. J. Application of the Bicyclo[1.1.1]Pentane Motif as a Nonclassical Phenyl Ring Bioisostere in the Design of a Potent and Orally Active γ-Secretase Inhibitor. *J. Med. Chem.* **2012**, *55* (7), 3414–3424.

(62) Bychek, R. M.; Hutskalova, V.; Bas, Y. P.; Zaporozhets, O. A.; Zozulya, S.; Levterov, V. V.; Mykhailiuk, P. K. Difluoro-Substituted Bicyclo[1.1.1]Pentanes for Medicinal Chemistry: Design, Synthesis, and Characterization. *J. Org. Chem.* **2019**, *84* (23), 15106–15117.

(63) Lovering, F.; Bikker, J.; Humblet, C. Escape from Flatland: Increasing Saturation as an Approach to Improving Clinical Success. *J. Med. Chem.* **2009**, *52* (21), 6752–6756.

(64) Troelsen, N. S.; Shanina, E.; Gonzalez-Romero, D.; Danková, D.; Jensen, I. S. A.; Śniady, K. J.; Nami, F.; Zhang, H.; Rademacher, C.; Cuenda, A.; Gotfredsen, C. H.;

Clausen, M. H. The 3F Library: Fluorinated Fsp^3-Rich Fragments for Expeditious 19F NMR Based Screening. *Angew. Chem. Int. Ed.* **2020**, *59* (6), 2204–2210.

(65) Colomer, I.; Empson, C. J.; Craven, P.; Owen, Z.; Doveston, R. G.; Churcher, I.; Marsden, S. P.; Nelson, A. A Divergent Synthetic Approach to Diverse Molecular Scaffolds: Assessment of Lead-Likeness Using LLAMA, an Open-Access Computational Tool. *Chem. Commun.* **2016**, *52* (45), 7209–7212.

(66) Morley, A. D.; Pugliese, A.; Birchall, K.; Bower, J.; Brennan, P.; Brown, N.; Chapman, T.; Drysdale, M.; Gilbert, I. H.; Hoelder, S.; Jordan, A.; Ley, S. V.; Merritt, A.; Miller, D.; Swarbrick, M. E.; Wyatt, P. G. Fragment-Based Hit Identification: Thinking in 3D. *Drug Discov. Today* **2013**, *18* (23), 1221–1227.

(67) Kim, D. W.; Song, C. E.; Chi, D. Y. New Method of Fluorination Using Potassium Fluoride in Ionic Liquid: Significantly Enhanced Reactivity of Fluoride and Improved Selectivity. *J. Am. Chem. Soc.* **2002**, *124* (35), 10278–10279.

(68) Gertsch, J. C.; Cano, A. M.; Bright, V. M.; George, S. M. SF_4 as the Fluorination Reactant for Al2O3 and VO2 Thermal Atomic Layer Etching. *Chem. Mater.* **2019**, *31* (10), 3624–3635.

(69) Miao, J.; Yang, K.; Kurek, M.; Ge, H. Palladium-Catalyzed Site-Selective Fluorination of Unactivated $C(Sp^3)$–H Bonds. *Org. Lett.* **2015**, *17* (15), 3738–3741.

(70) Meyer, D.; Jangra, H.; Walther, F.; Zipse, H.; Renaud, P. A Third Generation of Radical Fluorinating Agents Based on *N*-Fluoro-*N*-Arylsulfonamides. *Nat. Commun.* **2018**, *9* (1), 1–10.

(71) Marcus, Y. Thermodynamics of Solvation of Ions. Part 5. - Gibbs Free Energy of Hydration at 298.15 K. *J. Chem. Soc. Faraday Trans.* **1991**, *87* (18), 2995–2999.

(72) Hollingworth, C.; Gouverneur, V. Transition Metal Catalysis and Nucleophilic Fluorination. *Chem. Commun.* **2012**, *48* (24), 2929–2942.

(73) Lee, J. W.; Oliveira, M. T.; Jang, H. Bin; Lee, S.; Chi, D. Y.; Kim, D. W.; Song, C. E. Hydrogen-Bond Promoted Nucleophilic Fluorination: Concept, Mechanism and Applications in Positron Emission Tomography. *Chem. Soc. Rev.* **2016**, *45* (17), 4638–4650.

(74) Liang, S.; Hammond, G. B.; Xu, B. Hydrogen Bonding: Regulator for Nucleophilic Fluorination. *Chem. Eur. J* **2017**, *23* (71), 17850–17861.

(75) Champagne, P. A.; Desroches, J.; Hamel, J. D.; Vandamme, M.; Paquin, J. F. Monofluorination of Organic Compounds: 10 Years of Innovation. *Chem. Rev.* **2015**, *115* (17), 9073–9174.

(76) Charpentier, J.; Früh, N.; Togni, A. Electrophilic Trifluoromethylation by Use of Hypervalent Iodine Reagents. *Chem. Rev.* **2015**, *115* (2), 650–682.

(77) Zhang, C. Recent Advances in Trifluoromethylation of Organic Compounds Using Umemoto's Reagents. *Org. Biomol. Chem.* **2014**, *12* (34), 6580–6589.

(78) Azaindazole Compounds As Inhibitors Of T790m Containing Egfr Mutants. WO2014210354, 2014.

(79) Nielsen, M. K.; Ugaz, C. R.; Li, W.; Doyle, A. G. PyFluor: A Low-Cost, Stable, and Selective Deoxyfluorination Reagent. *J. Am. Chem. Soc.* **2015**, *137* (30), 9571–9574.

(80) Mohammadkhani, L.; Heravi, M. M. XtalFluor-E: A Useful and Versatile Reagent in Organic Transformations. *J. Fluor. Chem.* **2019**, *225*, 11–20.

(81) Messina, P. A.; Mange, K. C.; Middleton, W. J. Aminosulfur Trifluorides: Relative Thermal Stability [1]. *J. Fluor. Chem.* **1989**, *42* (1), 137–143.

(82) Beeler, A. B.; Gadepalli, R. S. V. S.; Steyn, S.; Castagnoli, N.; Rimoldi, J. M. Synthesis and in Vitro Biological Evaluation of Fluoro-Substituted-4- Phenyl-1,2,3,6-Tetrahydropyridines as Monoamine Oxidase B Substrates. *Bioorg. Med. Chem.* **2003**, *11* (23), 5229–5234.

(83) Ni, C.; Hu, J. Recent Advances in the Synthetic Application of Difluorocarbene. *Synthesis (Stuttg).* **2014**, *46* (7), 842–863.

(84) Kubyshkin, V.; Kheylik, Y.; Mykhailiuk, P. K. Synthesis and Studies on Gem-Fluorinated 2-Azabicyclo[n.1.0]Alkanes. *J. Fluor. Chem.* **2015**, *175*, 73–83.

(85) Measom, N. D.; Down, K. D.; Hirst, D. J.; Jamieson, C.; Manas, E. S.; Patel, V. K.; Somers, D. O. Investigation of a Bicyclo[1.1.1]Pentane as a Phenyl Replacement within an LpPLA2 Inhibitor. *ACS Med. Chem. Lett.* **2017**, *8* (1), 43–48.

(86) Hall, H. K.; Smith, C. D.; Blanchard, E. P.; Cherkofsky, S. C.; Sieja, J. B. Synthesis and Polymerization of Bridgehead-Substituted Bicyclobutanes. *J. Am. Chem. Soc.* **1971**, *93* (1), 121–130.

(87) Michurin, O. M.; Radchenko, D. S.; Komarov, I. V. Direct Nucleophilic Difluoromethylation of Enolizable Ketones with CHF_2TMS/HMPA. *Tetrahedron* **2016**, *72* (10), 1351–1356.

(88) Mykhailiuk, P. K.; Koenigs, R. M. Difluorodiazoethane (CF_2HCHN_2): A New Reagent for the Introduction of the Difluoromethyl Group. *Chem. Eur. J* **2019**, *25* (24), 6053–6063.

(89) Zheng, Y.; Yu, X.; Lv, S.; Mykhailiuk, P. K.; Ma, Q.; Hai, L.; Wu, Y. Synthesis of CHF_2-Substituted 3-Azabicyclo[3.1.0]-Hexanes by Photochemical Decomposition of CHF_2-Pyrazolines. *RSC Adv.* **2018**, *8* (10), 5114–5118.

(90) Hock, K. J.; Mertens, L.; Koenigs, R. M. Rhodium Catalyzed Synthesis of Difluoromethyl Cyclopropanes. *Chem. Commun.* **2016**, *52* (95), 13783–13786.

(91) Peng, S. Q.; Zhang, X. W.; Zhang, L.; Hu, X. G. Esterification of Carboxylic Acids with Difluoromethyl Diazomethane and Interrupted Esterification with Trifluoromethyl Diazomethane: A Fluorine Effect. *Org. Lett.* **2017**, *19* (20), 5689–5692.

(92) Taylor, R. D.; Maccoss, M.; Lawson, A. D. G. Rings in Drugs. *J. Med. Chem.* **2014**, *57*

(14), 5845–5859.

(93) Roughley, S. D.; Jordan, A. M. The Medicinal Chemist's Toolbox: An Analysis of Reactions Used in the Pursuit of Drug Candidates. *J. Med. Chem.* **2011**, *54* (10), 3451–3479.

(94) Vitaku, E.; Smith, D. T.; Njardarson, J. T. Analysis of the Structural Diversity, Substitution Patterns, and Frequency of Nitrogen Heterocycles among U.S. FDA Approved Pharmaceuticals. *J. Med. Chem.* **2014**, *57* (24), 10257–10274.

(95) He, Y.; Zheng, Z.; Yang, J.; Zhang, X.; Fan, X. Recent Advances in the Functionalization of Saturated Cyclic Amines. *Org. Chem. Front.* **2021**.

(96) Majumdar, R.; Barchi, B.; Turlapati, S. A.; Gagne, M.; Minocha, R.; Long, S.; Minocha, S. C. Glutamate, Ornithine, Arginine, Proline, and Polyamine Metabolic Interactions: The Pathway Is Regulated at the Post-Transcriptional Level. *Front. Plant Sci.* **2016**, *7*, 78.

(97) Knutsen, H. K.; Alexander, J.; Barregård, L.; Bignami, M.; Brüschweiler, B.; Ceccatelli, S.; Cottrill, B.; Dinovi, M.; Edler, L.; Grasl-Kraupp, B.; Hogstrand, C.; Hoogenboom, L. (Ron); Nebbia, C. S.; Oswald, I. P.; Petersen, A.; Rose, M.; Roudot, A.-C.; Schwerdtle, T.; Vollmer, G.; Wallace, H.; Benford, D.; Calò, G.; Dahan, A.; Dusemund, B.; Mulder, P.; Németh-Zámboriné, É.; Arcella, D.; Baert, K.; Cascio, C.; Levorato, S.; Schutte, M.; Vleminckx, C. Update of the Scientific Opinion on Opium Alkaloids in Poppy Seeds. *EFSA Journal.* **2018**, *16* (5), 5243.

(98) Andrews, K. G.; Faizova, R.; Denton, R. M. A Practical and Catalyst-Free Trifluoroethylation Reaction of Amines Using Trifluoroacetic Acid. *Nat. Commun.* **2017**, *8*, 15913.

(99) Shi, L.; Xia, W. Photoredox Functionalization of C–H Bonds Adjacent to a Nitrogen Atom. *Chem. Soc. Rev.* **2012**, *41* (23), 7687–7697.

(100) Fava, E.; Nakajima, M.; Tabak, M. B.; Rueping, M. Tin-Free Visible Light Photoredox Catalysed Cyclisation of Enamides as a Mild Procedure for the Synthesis of γ-Lactams. *Green Chem.* **2016**, *18*, 4531–4535.

(101) Sato, T.; Wada, Y.; Nishimoto, M.; Ishibashi, H.; Ikeda, M. Synthesis of Five-Membered Lactams by a-Carbamoyl Radical Cyclisations. *J. Chem. Soc. Perkin Trans. I* **1989**, No. Id, 879–886.

(102) Sun, K.; Wang, S.; Feng, R.; Zhang, Y.; Wang, X.; Zhang, Z.; Zhang, B. Copper-Catalyzed Radical Selenodifluoromethylation of Alkenes: Access to CF_2-Containing γ-Lactams. *Org. Lett.* **2019**, *21* (7), 2052–2055.

(103) Zhuang, X.; Shi, X.; Zhu, R.; Sun, B.; Su, W.; Jin, C. Photocatalytic Intramolecular Radical Cyclization Involved Synergistic SET and HAT: Synthesis of 3,3-Difluoro-γ-Lactams. *Org. Chem. Front.* **2021**, *8* (4), 736–742.

(104) Kim, H. Y.; Wiles, J. A.; Wang, Q.; Pais, G. C. G.; Lucien, E.; Hashimoto, A.; Nelson, D. M.; Thanassi, J. A.; Podos, S. D.; Deshpande, M.; Pucci, M. J.; Bradbury, B. J. Exploration of the Activity of 7-Pyrrolidino-8-Methoxyisothiazoloquinolones against Methicillin-Resistant Staphylococcus Aureus (MRSA). *J. Med. Chem.* **2011**, *54* (9), 3268–3282.

(105) Wong, J. C.; Tang, G.; Wu, X.; Liang, C.; Zhang, Z.; Guo, L.; Peng, Z.; Zhang, W.; Lin, X.; Wang, Z.; Mei, J.; Chen, J.; Pan, S.; Zhang, N.; Liu, Y.; Zhou, M.; Feng, L.; Zhao, W.; Li, S.; Zhang, C.; Zhang, M.; Rong, Y.; Jin, T.-G.; Zhang, X.; Ren, S.; Ji, Y.; Zhao, R.; She, J.; Ren, Y.; Xu, C.; Chen, D.; Cai, J.; Shan, S.; Pan, D.; Ning, Z.; Lu, X.; Chen, T.; He, Y.; Chen, L. Pharmacokinetic Optimization of Class-Selective Histone Deacetylase Inhibitors and Identification of Associated Candidate Predictive Biomarkers of Hepatocellular Carcinoma Tumor Response. *J. Med. Chem.* **2012**, *55* (20), 8903–8925.

(106) Tucker, J. W.; Zhang, Y.; Jamison, T. F.; Stephenson, C. R. J. Visible-Light Photoredox

Catalysis in Flow. *Angew. Chem. Int. Ed.* **2012**, *51*, 4144–4147.

(107) Bou-Hamdan, F. R.; Seeberger, P. H. Visible-Light-Mediated Photochemistry: Accelerating $Ru(Bpy)_3^{2+}$-Catalyzed Reactions in Continuous Flow. *Chem. Sci.* **2012**, *3* (5), 1612.

(108) Wei, X.-J. J.; Boon, W.; Hessel, V.; Noël, T. Visible-Light Photocatalytic Decarboxylation of α,β-Unsaturated Carboxylic Acids: Facile Access to Stereoselective Difluoromethylated Styrenes in Batch and Flow. *ACS Catal.* **2017**, *7* (10), 7136–7140.

(109) Daina, A.; Michielin, O.; Zoete, V. SwissADME: A Free Web Tool to Evaluate Pharmacokinetics, Drug-Likeness and Medicinal Chemistry Friendliness of Small Molecules. *Sci. Rep.* **2017**, *7* (1), 42717.

(110) Sharma, G. V. M.; Chary, D. H.; Chandramouli, N.; Achrainer, F.; Patrudu, S.; Zipse, H. Free Radical 5-Exo-Dig Cyclization as the Key Step in the Synthesis of Bis-Butyrolactone Natural Products: Experimental and Theoretical Studies. *Org. Biomol. Chem.* **2011**, *9* (11), 4079–4084.

(111) Wang, X.; Lei, J.; Li, G.; Meng, J.; Li, C.; Li, J.; Sun, K. Synthetic Methods for Compounds Containing Fluoro-Lactam Units. *Org. Biomol. Chem.* **2020**, *18* (48), 9762–9774.

(112) Wang, Q.; Qu, Y.; Xia, Q.; Song, H.; Song, H.; Liu, Y.; Wang, Q. Visible-Light-Mediated Dearomatization/Cyanation Cascade Reaction of Indoles: Access to Highly Functionalized Spiro-γ-Lactam Indolines with Two Contiguous Sterically Congested Quaternary Carbon Stereocenters. *Adv. Synth. Catal.* **2018**, *360* (15), 2879–2884.

(113) Zhang, M.; Li, W.; Duan, Y.; Xu, P.; Zhang, S.; Zhu, C. Cascade Photoredox/Iodide Catalysis: Access to Difluoro-γ-Lactams via Aminodifluoroalkylation of Alkenes. *Org. Lett.* **2016**, *18* (13), 3266–3269.

(114) Singh, R. P.; Majumder, U.; Shreeve, J. M. Nucleophilic Di- and Tetrafluorination of

Dicarbonyl Compounds. *J. Org. Chem.* **2001**, *66* (19), 6263–6267.

(115) Li, B. H.; Li, K. L.; Chen, Q. Y. Rational and Practical Synthesis of α,α-Difluoro-γ-Lactams. *J. Fluor. Chem.* **2012**, *133*, 163–166.

(116) Chen, H.; Wang, X.; Guo, M.; Zhao, W.; Tang, X.; Wang, G. Highly Efficient and Versatile Synthesis of α,α-Difluoro-γ-Lactams: Via Aminodifluoroalkylation of Alkenes. *Org. Chem. Front.* **2017**, *4* (12), 2403–2407.

(117) Lv, Y.; Pu, W.; Wang, Q.; Chen, Q.; Niu, J.; Zhang, Q. Copper-Catalyzed Aminodifluoroalkylation of Alkenes with α-Bromodifluoroacetamides: Synthesis of 3,3-Difluoropyrrolidin-2-ones. *Adv. Synth. Catal.* **2017**, *359* (18), 3114–3119.

(118) Mai, W. P.; Wang, F.; Zhang, X. F.; Wang, S. M.; Duan, Q. P.; Lu, K. Nickel-Catalysed Radical Tandem Cyclisation/Arylation: Practical Synthesis of 4-Benzyl-3,3-Difluoro-γ-Lactams. *Org. Biomol. Chem.* **2018**, *16* (35), 6491–6498.

(119) Sun, K.; Wang, S.; Feng, R.; Zhang, Y.; Wang, X.; Zhang, Z.; Zhang, B. Copper-Catalyzed Radical Selenodifluoromethylation of Alkenes: Access to CF_2 -Containing γ-Lactams. *Org. Lett.* **2019**, *21* (7), 2052–2055.

(120) Chen, D.-F.; Chu, J. C. K.; Rovis, T. Directed γ-C(Sp^3)–H Alkylation of Carboxylic Acid Derivatives through Visible Light Photoredox Catalysis. *J. Am. Chem. Soc.* **2017**, *139*, 14897–14900.

(121) Stoll, E. L.; Tongue, T.; Andrews, K. G.; Valette, D.; Hirst, D. J.; Denton, R. M. A Practical Catalytic Reductive Amination of Carboxylic Acids. *Chem. Sci.* **2020**, *11* (35), 9494–9500.

(122) Azuma, M.; Yoshikawa, T.; Kogure, N.; Kitajima, M.; Takayama, H. Biogenetically Inspired Total Syntheses of Lycopodium Alkaloids, (+)-Flabellidine and (−)-Lycodine. *J. Am. Chem. Soc.* **2014**, *136* (33), 11618–11621.

(123) Efthymiou, T. C.; Huynh, V.; Oentoro, J.; Peel, B.; Desaulniers, J.-P. Efficient Synthesis

and Cell-Based Silencing Activity of SiRNAS That Contain Triazole Backbone Linkages. *Bioorg. Med. Chem. Lett.* **2012**, *22* (4), 1722–1726.

(124) Crick, P. J.; Simpkins, N. S.; Highton, A. Synthesis of the Asperparaline Core by a Radical Cascade. *Org. Lett.* **2011**, *13* (24), 6472–6475.

(125) Sekine, K.; Kobayashi, R.; Yamada, T. Silver-Catalyzed Three-Component Reaction of Propargylic Amines, Carbon Dioxide, and N-Iodosuccinimide for Stereoselective Preparation of (E)-Iodovinyloxazolidinones. *Chem. Lett.* **2015**, *44* (10), 1407–1409.

(126) Buzzetti, L.; Puriņš, M.; Greenwood, P. D. G.; Waser, J. Enantioselective Carboetherification/Hydrogenation for the Synthesis of Amino Alcohols via a Catalytically Formed Chiral Auxiliary. *J. Am. Chem. Soc.* **2020**, *142* (41), 17334–17339.

(127) Nishida, H.; Fujimori, I.; Arikawa, Y.; Hirase, K.; Ono, K.; Nakai, K.; Inatomi, N.; Hori, Y.; Matsukawa, J.; Fujioka, Y.; Imanishi, A.; Fukui, H.; Itoh, F. Exploration of Pyrrole Derivatives to Find an Effective Potassium-Competitive Acid Blocker with Moderately Long-Lasting Suppression of Gastric Acid Secretion. *Bioorg. Med. Chem.* **2017**, *25* (13), 3447–3460.

(128) Zhang, J.; Li, Y.; Zhang, F.; Hu, C.; Chen, Y. Generation of Alkoxyl Radicals by Photoredox Catalysis Enables Selective C(Sp^3)-H Functionalization under Mild Reaction Conditions. *Angew. Chem. Int. Ed.* **2016**, *55* (5), 1872–1875.

(129) Lévêque, C.; Chenneberg, L.; Corcé, V.; Ollivier, C.; Fensterbank, L. Organic Photoredox Catalysis for the Oxidation of Silicates: Applications in Radical Synthesis and Dual Catalysis. *Chem. Commun.* **2016**, *52* (64), 9877–9880.

(130) Shao, Y.; Molnar, L. F.; Jung, Y.; Kussmann, J.; Ochsenfeld, C.; Brown, S. T.; Gilbert, A. T. B.; Slipchenko, L. V; Levchenko, S. V; O'Neill, D. P.; DiStasio Jr, R. A.; Lochan, R. C.; Wang, T.; Beran, G. J. O.; Besley, N. A.; Herbert, J. M.; Yeh Lin, C.; Van Voorhis, T.; Hung Chien, S.; Sodt, A.; Steele, R. P.; Rassolov, V. A.; Maslen, P. E.; Korambath, P. P.; Adamson, R. D.; Austin, B.; Baker, J.; Byrd, E. F. C.; Dachsel, H.; Doerksen, R.

J.; Dreuw, A.; Dunietz, B. D.; Dutoi, A. D.; Furlani, T. R.; Gwaltney, S. R.; Heyden, A.; Hirata, S.; Hsu, C.-P.; Kedziora, G.; Khalliulin, R. Z.; Klunzinger, P.; Lee, A. M.; Lee, M. S.; Liang, W.; Lotan, I.; Nair, N.; Peters, B.; Proynov, E. I.; Pieniazek, P. A.; Min Rhee, Y.; Ritchie, J.; Rosta, E.; David Sherrill, C.; Simmonett, A. C.; Subotnik, J. E.; Lee Woodcock III, H.; Zhang, W.; Bell, A. T.; Chakraborty, A. K.; Chipman, D. M.; Keil, F. J.; Warshel, A.; Hehre, W. J.; Schaefer III, H. F.; Kong, J.; Krylov, A. I.; Gill, P. M. W.; Head-Gordon, M. Advances in Methods and Algorithms in a Modern Quantum Chemistry Program Package. *Phys. Chem. Chem. Phys.* **2006**, *8* (27), 3172–3191.